

For Reference

NOT TO BE TAKEN FROM THIS ROOM

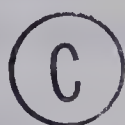
Ex LIBRIS
UNIVERSITATIS
ALBERTAENSIS



THE UNIVERSITY OF ALBERTA

MODEL REFERENCE ADAPTIVE CONTROL:
HYBRID COMPUTER SIMULATION AND EXPERIMENTAL VERIFICATION

BY



W. KENT OLIVER

A THESIS

SUBMITTED TO THE FACULTY OF GRADUATE STUDIES AND RESEARCH
IN PARTIAL FULFILMENT OF THE REQUIREMENTS FOR THE DEGREE
OF MASTER OF SCIENCE IN CHEMICAL ENGINEERING

DEPARTMENT OF CHEMICAL AND PETROLEUM ENGINEERING

EDMONTON, ALBERTA

SPRING, 1972



Digitized by the Internet Archive
in 2019 with funding from
University of Alberta Libraries

<https://archive.org/details/Oliver1972>

1972
113

UNIVERSITY OF ALBERTA
FACULTY OF GRADUATE STUDIES AND RESEARCH

The undersigned certify that they have read, and recommend to the Faculty of Graduate Studies and Research, for acceptance, a thesis entitled MODEL REFERENCE ADAPTIVE CONTROL: HYBRID COMPUTER SIMULATION AND EXPERIMENTAL VERIFICATION submitted by W. Kent Oliver, B.Sc., in partial fulfilment of the requirements for the degree of Master of Science.

DECLARATION

STATE OF NEW YORK

I, the undersigned, do hereby certify that the foregoing is a true and correct copy of the original as the same appears in the records of the Department of the State.

IN WITNESS WHEREOF, I have hereunto set my hand and the seal of the Department of the State at Albany, New York, this _____ day of _____, 19____.

Secretary of the Department of the State

ABSTRACT

This thesis presents the design of a model reference adaptive control system for a double effect evaporator. Liapunov's second or direct method of stability analysis is used in the design approach to ensure a stable system response. Hybrid computer simulation runs were performed in order to test the effect of several design parameters on the control scheme. Experimental runs were also conducted using an IBM 1800 process control computer and the pilot plant process.

A literature survey of hybrid computer applications in the chemical engineering field is included. An EAI 590 hybrid computer system was recently installed in the Department of Chemical and Petroleum Engineering and the literature survey reveals several possible applications for this hybrid computer system. The literature survey is accompanied by several example problems that demonstrate hybrid computer techniques.

The existing theory for model reference adaptive control designed by Liapunov's second method is presented for a linear time-invariant process with a basic feedforward, feedback control configuration. Extensions to the basic theory for adaptive integral and setpoint control are also included. The basic feedback control design is then applied to a fifth-order linear state-space model of a double effect evaporator using an optimal feedback reference model.

Hybrid simulation results demonstrate the ability of model reference adaptive control to improve upon the initial control policy and eventually attain the same response as the reference model. The control scheme is able to survive unmeasured disturbances, poor

initial control policies, and physically impossible reference models. The effect of other design parameters on control is also demonstrated. The control scheme demonstrates the ability to adjust and improve control with continuing process disturbances. However, numerical problems, associated with the discrete approximation to the continuous adaptive control law, develop with large adaptive loop gains or large control intervals. Low adaptive loop gains and a well-tuned multiloop initial control policy produce excellent control and model following for major process disturbances.

The experimental runs that test the model reference adaptive control system verify the simulation results and demonstrate the industrial feasibility of this control scheme.

ACKNOWLEDGEMENTS

The author wishes to thank his thesis supervisor, Dr. D.E. Seborg, for his guidance and assistance in this project.

Thanks also go to Dr. D.G. Fisher for his helpful suggestions and the Data Acquisition, Control, and Simulation Center staff for their assistance in the use of their computing facilities.

The author also acknowledges his fellow control students, past and present, whose efforts made the completion of this study much simpler.

Financial support was generously given by the National Research Council.

Finally, the author expresses great appreciation for the support and encouragement of his wife, Janice.

TABLE OF CONTENTS

	<u>Page</u>
CHAPTER ONE, INTRODUCTION	
1.1 Objectives of the Study	3
1.2 Structure of the Thesis	4
CHAPTER TWO, HYBRID COMPUTER APPLICATIONS IN CHEMICAL ENGINEERING	
2.1 Introduction	6
2.2 Hybrid Computer Structure	7
2.3 Literature Survey	10
2.3.1 Analog-oriented Problems	10
2.3.2 Digitally Generated Functions	11
2.3.3 Sampled-Data Systems	13
2.3.4 Control	15
2.3.5 Real-Time Applications	17
2.3.6 Optimization and Parameter Estimation	17
2.3.7 Simulation of Staged Processes	18
2.3.8 Partial Differential Equations	20
2.4 Illustrative Examples	23
2.4.1 Digital Initiation and Check of an Analog Simulation	24
2.4.2 Reconstruction of Sampled Signals	30
2.4.3 Simulation of Time Delays	31
2.4.4 Nonisothermal Batch Reactor	40
2.4.5 Construction of a Digital Controller	45
2.4.6 Hybrid Optimization of the Sutro Weir Control System	49

TABLE OF CONTENTS (continued)

	<u>Page</u>
2.4.7 Hybrid Solution of Partial Differential Equations	55
CHAPTER THREE, MODEL REFERENCE ADAPTIVE CONTROL BY LIAPUNOV'S DIRECT METHOD: LITERATURE SURVEY AND BASIC EQUATIONS	
3.1 Introduction	63
3.2 Literature Survey	63
3.3 Theory	68
3.4 Extensions to the Existing Theory: Adaptive Integral and Setpoint Control	74
3.4.1 Adaptive Integral Control	74
3.4.2 Adaptive Setpoint Control	76
3.5 Application of MRAC to a Pilot Plant Evaporator	79
CHAPTER FOUR, HYBRID SIMULATION OF A MODEL REFERENCE ADAPTIVE CONTROL SYSTEM FOR THE EVAPORATOR	
4.1 Introduction	85
4.2 Analog Evaporator Model	85
4.3 Digital Computer Control Programs	86
4.4 Results	86
4.4.1 Improvements in Control	88
4.4.2 Effect of ξ_{ij} on MRAC	88
4.4.3 Number of Adapting Elements of $\underline{\Gamma}$	91
4.4.4 Effect of Initial Control Policy, $\underline{\Gamma}(0)$	97
4.4.5 Effect of Unseen Disturbances	100
4.4.6 MRAC with a Physically Impossible Reference Model	100

TABLE OF CONTENTS (continued)

	<u>Page</u>
4.4.7 Adaptive Control in the Presence of a Continual Disturbance	105
4.4.8 State Weighting	105
4.4.9 Final Process Response and Final Feedback Matrix	109
4.5 Conclusions	113
CHAPTER FIVE, MODEL REFERENCE ADAPTIVE CONTROL APPLIED TO A DOUBLE EFFECT EVAPORATOR: EXPERIMENTAL RESULTS	
5.1 Introduction	115
5.2 Control System	115
5.3 Experimental Results	119
5.3.1 Improvement in Control	120
5.3.2 Effect of Adaptive Loop Gain	127
5.3.3 State Weighting	127
5.3.4 Effect of Repeated Disturbances	131
5.3.5 Initial Control Policy	132
5.3.6 Number of Adapting Elements of \underline{r}	132
5.3.7 Effect of Unseen Disturbances	132
5.3.8 Violation of Control Constraints	135
5.3.9 Change in Operating Conditions	135
5.4 Conclusions	138
CHAPTER SIX, CONCLUSIONS	
6.1 Industrial Applications of Model Reference Adaptive Control	141
6.2 Future Work	146

TABLE OF CONTENTS (continued)

	<u>Page</u>
6.2.1 Feedforward, Integral, and Setpoint Adaptive Control	146
6.2.2 Selection of Adaptive Loop Gains	147
6.2.3 Selection of Reference Model	147
6.2.4 Constrained State and Control Variables	148
6.2.5 Selection of the \underline{P} Matrix Used in the Adaptive Control Law	149
6.3 Conclusions	149
NOMENCLATURE	
Chapter Two	151
Chapter Three	153
Chapter Four	156
Chapter Five	158
Chapter Six	160
BIBLIOGRAPHY	
Chapter One	161
Chapter Two	162
Chapter Three	165
Chapter Four	167
Chapter Five	168
Chapter Six	169
APPENDICES	
Chapter Three	170
Chapter Four	174

LIST OF TABLES

	<u>Page</u>
CHAPTER TWO	
TABLE 2.1 EAI 590 Hybrid Computer System	8
CHAPTER FOUR	
TABLE 4.1 Model and Process Feedback Matrices	110
CHAPTER SIX	
TABLE 6.1 Summary of Design Considerations in MRAC by Liapunov's Direct Method	142

LIST OF FIGURES

	<u>Page</u>
 CHAPTER TWO	
FIGURE 2.1 Hybrid Computing System Block Diagram	7
FIGURE 2.2 Sampled-Data Control System	14
FIGURE 2.3 Hybrid Computers in Multivariable Control System Design	16
FIGURE 2.4 Sutro Weir Experiment	24
FIGURE 2.5 Block Diagram of Two Tank Control System	25
FIGURE 2.6 Simulated Response of the Sutro Weir to Load and Setpoint Changes	27
FIGURE 2.7 HOI and CSMP Dynamic Checks of Sutro Weir Simulation	29
FIGURE 2.8 Sine Wave, 25 Samples per Second	32
FIGURE 2.9 Sine Wave, 2 Samples per Second	33
FIGURE 2.10 Hybrid Generated Time Delayed Function $Y = 2 \sin .786 (t - 2)$	35
FIGURE 2.11 CSDAP Generated Time Delay, Second Order Pade Approximation for $Y = 2 \sin$ $.786 (t - 2)$	36
FIGURE 2.12 Hybrid Time Delayed Response of Sutro Weir	38
FIGURE 2.13 CSDAP Time Delayed Response of Sutro Weir, Second Order Pade Approximation	39
FIGURE 2.14 CSMP vs Hybrid Simulation of a Nonlinear Batch Reactor	42

LIST OF FIGURES (continued)

	<u>Page</u>
FIGURE 2.15 CSMP vs Hybrid Simulation of a Nonlinear Batch Reactor	43
FIGURE 2.16 Nonisothermal Batch Reactor	44
FIGURE 2.17 Comparison of HOI and FORTRAN Digital Deadbeat Controllers	47
FIGURE 2.18 Sampled-Data Control System	48
FIGURE 2.19 Optimization of Rise Time Overshoot Criterion, Setpoint Change .5 Feet	51
FIGURE 2.20 Optimization with ITSE Criterion, Setpoint Change of 0.5 feet in H_2	52
FIGURE 2.21 Optimization with ITSE Criterion Load Change of 0.7 Cubic Feet per Minute	53
FIGURE 2.22 Optimization with ISE Criterion Setpoint Change of 0.5 feet	54
FIGURE 2.23 Tube Fluid Temperature Profile	57
FIGURE 2.24 Tube Wall Temperature Profile	58
FIGURE 2.25 Tube Fluid Temperature Profile, 100°C Step in Inlet Temperature	59
FIGURE 2.26 Single Pass Heat Exchanger	60
 CHAPTER THREE	
FIGURE 3.1 Block Diagram of Model Reference Adaptive Control	64
FIGURE 3.2 Block Diagram of MRAC via Liapunov's Direct Method	73

LIST OF FIGURES (continued)

	<u>Page</u>
FIGURE 3.3 Schematic Diagram of the Double Effect Evaporator	80
CHAPTER FOUR	
FIGURE 4.1 Analog Simulation of the Linear, Fifth-Order Evaporator Model	87
FIGURE 4.2 Simulated Responses Comparing Open-loop, Optimal Feedback Reference Model, and Model Reference Adaptive Control ($\xi_{ij} = 10$)	89
FIGURE 4.3 Simulated Results Demonstrating the Effect of Adaptive Loop Gain, ξ_{ij} , on MRAC	90
FIGURE 4.4 Simulated Effect of ξ_{ij} on $e_1 = x_{m1} - x_{p1}$	92
FIGURE 4.5 Simulated Effect of ξ_{ij} on Rate of Adapting for γ_{51}	93
FIGURE 4.6 Simulated Results Demonstrating Inherent Stability of MRAC Designed via Liapunov's Direct Method	94
FIGURE 4.7 Simulated Results for Only Some Elements of $\underline{\Gamma}$ Adapting, $\xi_{ij} = 10$	95
FIGURE 4.8 Simulated Results, Four Elements of $\underline{\Gamma}$ Adapting, $\xi_{ij} = 100$	96
FIGURE 4.9 Simulated Effect of Adaptive Loop Gains with Few Elements of $\underline{\Gamma}$ Adapting	98

LIST OF FIGURES (continued)

	<u>Page</u>
FIGURE 4.10 Simulated Effect of the Initial Control Policy on MRAC, $\xi_{ij} = 10$ (+ 50% Feed Flow)	99
FIGURE 4.11 Simulated Multiloop Control as an Initial Control Policy $\xi_{ij} = 10$ (+ 50% Feed Flow)	101
FIGURE 4.12 Simulated Comparison of Multiloop and Multivariable MRAC (+ 50% Feed Flow)	102
FIGURE 4.13 Simulated Effect of Unseen Disturbances on MRAC (+ 20% Feed Flow, + 10% Feed Composition)	103
FIGURE 4.14 Simulated Effect of a Physically Impossible Reference Model, $\underline{x}_m = \underline{0}$	104
FIGURE 4.15 Simulated Results of the Effect of a Continuing Disturbance on MRAC, $\xi_{ij} = 10$, $t = 0$ to 150 minutes	106
FIGURE 4.16 Simulated Effect of a Continuous Disturbance on MRAC, $t \rightarrow \infty$	107
FIGURE 4.17 Simulated Effect of State Weighting with Adaptive Loop Gains	108
 CHAPTER FIVE	
FIGURE 5.1 Schematic Diagram of Model Reference Adaptive Control	116
FIGURE 5.2 Pilot Plant Double Effect Evaporator with a Conventional Multiloop Control System	117

LIST OF FIGURES (continued)

	<u>Page</u>
FIGURE 5.3 Experimental Results of MRAC, Adaptive Loop Gain $\xi_{ij} = 1$	121
FIGURE 5.4 Experimental MRAC and Reference Model ($\xi_{i3} = 0.25$, $\xi_{i5} = 10$, $\xi_{ij} = 1$ for all other i,j)	122
FIGURE 5.5 Experimental vs Hybrid Simulation Results, $\xi_{ij} = 1$	123
FIGURE 5.6 Experimental vs Hybrid Simulation Results ($\xi_{i3} = 0.25$, $\xi_{i5} = 10$, $\xi_{ij} = 1$ for all other i,j)	124
FIGURE 5.7 Experimental W_1 Error vs Simulated W_1 Error ($\xi_{i3} = 0.25$, $\xi_{i5} = 10$, all other $\xi_{ij} = 1$)	125
FIGURE 5.8 Experimental γ_{51} Element vs Simulated γ_{51} Element ($\xi_{i3} = 0.25$, $\xi_{i5} = 10$, all other $\xi_{ij} = 1$)	126
FIGURE 5.9 Experimental MRAC, $\xi_{ij} = 10$	128
FIGURE 5.10 Experimental MRAC, Second Disturbance for $\xi_{ij} = 10$	129
FIGURE 5.11 Experimental Effects of State Weighting and Repeated Disturbances ($\xi_{i3} = 0.25$, $\xi_{i5} = 10$ all other $\xi_{ij} = 1$)	130
FIGURE 5.12 Experimental MRAC with Multiloop Initial Control vs Multiloop Control ($\xi_{i3} = .25$, $\xi_{i5} = 10$ all other $\xi_{ij} = 1$)	133

LIST OF FIGURES (continued)

	<u>Page</u>
FIGURE 5.13 Experimental MRAC, 11 Elements Adapting, $\xi_{ij} = 10$	134
FIGURE 5.14 Experimental MRAC, Effect of Unseen Disturbances ($\xi_{ij} = 1$, -10% Feed Composition Unobserved)	136
FIGURE 5.15 Experimental MRAC, Violation of Steam Constraint ($\xi_{i3} = 0.25$, $\xi_{i5} = 10$, all other $\xi_{ij} = 1$)	137
FIGURE 5.16 Experimental MRAC at Low Feed Rates, $\xi_{ij} = 1$	139
CHAPTER SIX	
FIGURE 6.1 Fixed Parameter Control Derived From MRAC (MRAC for 45 minutes, $\xi_{ij} = 10$, Open-Loop Initial Control, + 20% Feed Flow)	145

CHAPTER ONE

INTRODUCTION

Automatic control systems inevitably require on-line tuning to achieve a satisfactory degree of control. Furthermore, frequent readjustment of controller constants may be required if process conditions change significantly. An adaptive control system is one in which the control parameters or control configuration changes automatically during process operation to compensate for changing process conditions. In the model reference approach to adaptive control, the control parameters are adapted so that the process response approaches that of a reference model when both are subjected to the same inputs.

Modern multivariable control systems often rely heavily on model accuracy for their success. However, in many industrial situations a process model may not be readily available. Two adaptive control approaches reduce the requirements for model accuracy: model reference adaptive control (MRAC) and optimal adaptive control. The reference model in MRAC represents the desired closed-loop plant dynamics rather than the actual plant dynamics and thus does not require the availability of an accurate process model. Optimal adaptive control combines process identification with optimization of the continually updated process model. MRAC has the advantage of not requiring process identification and time consuming optimization calculations and would seem to be more applicable to industrial situations. Only MRAC is dealt with in this thesis.

MRAC schemes have found extensive use in the aerospace industries both in single-input, single-output and multivariable control systems. However, the process industries have only applied MRAC to

single variable systems. This thesis is concerned with the application of multivariable MRAC to a pilot plant double effect evaporator.

The pilot plant double effect evaporator in the Department of Chemical and Petroleum Engineering at the University of Alberta has been the subject of several studies in modelling and control [1 - 4]. The experimental verification of many conventional and advanced control schemes has been made possible by interfacing the evaporator to an IBM 1800 process control computer.

Early studies in the Department have investigated multiloop Direct Digital Control (DDC) including inferential and feedforward control configurations [2,3]. Recent work has dealt with optimal regulatory multivariable control [4] and control techniques for making optimal setpoint changes [5]. These control techniques proved much more successful than conventional schemes. Current research [6] deals with control techniques using reduced order state-space models. Studies are also being conducted on multivariable control techniques [7,8] which consider various conditions (noise, time-delays) that are not significant problems for the evaporator but can be important in other processes. However, in all these studies an approximate dynamic model of the evaporator was required.

Work on a nine inch, eight tray distillation column in the Department [9] has illustrated the difficulty and time involved in obtaining an adequate state-space model for some systems. Part of the motivation for this study was to evaluate an adaptive control technique that relies less heavily on an accurate model of the process being controlled.

This thesis presents a study of a MRAC technique designed via

Liapunov's direct method of stability analysis. The MRAC technique, based on an approach developed by Winsor and Roy [11] and Porter and Tatnall [10], was first evaluated by using a hybrid simulation of the IBM 1800/evaporator configuration. The simulation results were then experimentally verified on the pilot plant system. Since this thesis research was the first project in the Department of Chemical and Petroleum Engineering to use the recently installed EAI 590 hybrid computer system, several hybrid programs demonstrating various aspects of hybrid computation were developed in order to become familiar with the system.

1.1 OBJECTIVES OF THE STUDY

The intent of this thesis is to experimentally verify a model reference adaptive control technique designed via Liapunov's direct method. The theory for this adaptive control design approach was developed in the late 1960's [10,11] and has been investigated in several mathematical and simulation studies. However, the only experimental verification of the simulation results has been conducted on a simple hydromechanical process modelled as a first-order system [12].

The following steps were taken to achieve the completion of this project:

- i) Develop familiarity with the new hybrid computing system through the solution of typical problems taken from the literature.
- ii) Design a MRAC system for the evaporator using Liapunov's direct method.
- iii) Simulate the evaporator control system using the EAI 590

hybrid system and use the hybrid simulation to investigate the critical design features of this method.

- iv) Experimentally verify the simulation results using the actual double effect evaporator and the IBM 1800 computer.

1.2 STRUCTURE OF THE THESIS

The thesis involves two distinct sections: the first section presented in the next chapter includes a literature survey of representative hybrid computer applications in chemical engineering and illustrates some of the applications on the EAI 590 system in a series of sample problems. The problems were used to test the capabilities of the analog, digital, and interface sections of the hybrid system. They also provided insight into which programming language would be best for the model reference adaptive control simulation to follow.

The second section of the thesis involves MRAC. Chapter Three presents a literature survey of MRAC techniques that have developed over the last ten to fifteen years. The theory of the MRAC design approach via Liapunov's direct method and the specific application to the double effect evaporator are then presented.

The hybrid simulation results are given in Chapter Four and conclusions regarding the usefulness of MRAC are drawn from these results. Chapter Five presents the experimental verification of the simulation results for the actual evaporator using the IBM 1800 process control computer. The experimental runs also produced some unexpected problems not encountered in the simulation studies. The computer programs used to obtain the simulation and experimental results are given in detail in research reports and user's manuals that are referenced in

each chapter.

Chapter Six summarizes the overall conclusions drawn from the study.

CHAPTER TWO

HYBRID COMPUTER APPLICATIONS IN CHEMICAL ENGINEERING

2.1 INTRODUCTION

Hybrid computers have found increasing use in chemical engineering simulations since the early 1960's. Many problems in the fields of process dynamics, process control, and optimization are best suited to a hybrid computer because a hybrid system combines the high speed integration capabilities of an analog computer with the arithmetic and logic capabilities of a digital machine. The improvements in digital software and interface hardware in the last ten years have helped to increase the popularity of hybrid computation and have led to highly complex simulations of large systems [1].

With the recent purchase of an EAI 590 hybrid computer system by the Department of Chemical and Petroleum Engineering of the University of Alberta, an investigation was undertaken in order to determine the capabilities and possible applications of the system. This investigation took the form of a literature survey and a series of example problems solved on the EAI 590 system. The objectives of this investigation were as follows:

- i) To determine the type of problems applicable to hybrid solutions in the fields of chemical engineering and process control.
- ii) To test the level of problem complexity that could be solved on the relatively small EAI 590 system.
- iii) To investigate the types of software languages available on the EAI 590 and determine which language would be most useful in later research.

- iv) To provide familiarity with the new computer by "debugging" sample problems.

This chapter briefly reviews the structure of a hybrid computer system followed by a literature survey of hybrid computer applications in chemical engineering. Finally, seven hybrid sample problems are presented in order to illustrate some of the applications discovered in the literature survey.

2.2 HYBRID COMPUTER STRUCTURE

Figure 2.1 presents a block diagram of a typical hybrid computing system.

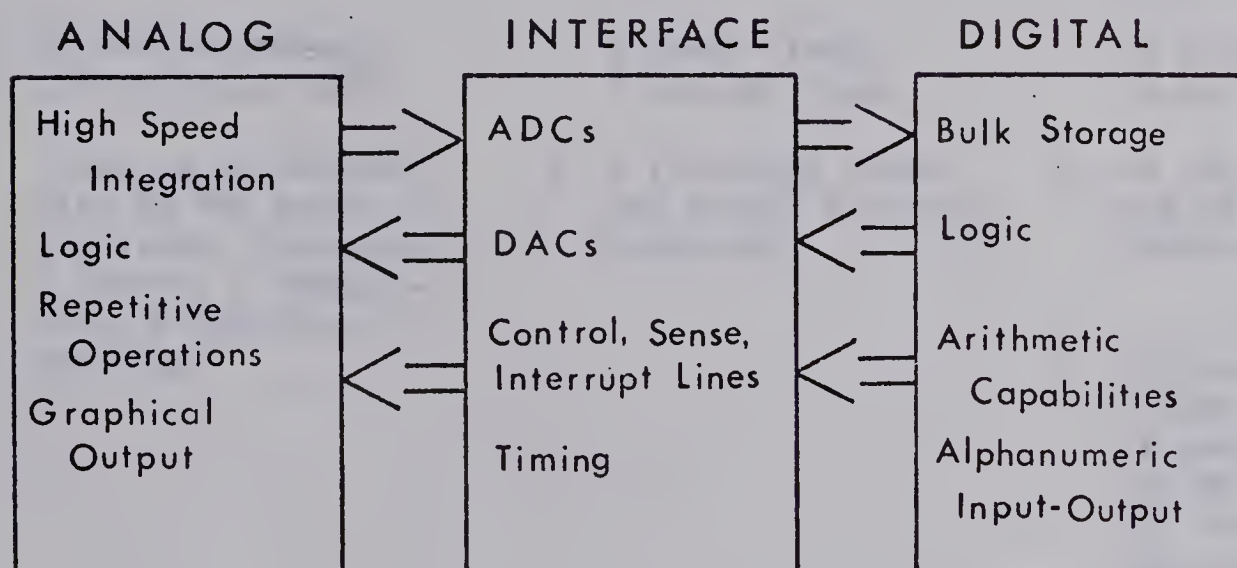


FIGURE 2.1 HYBRID COMPUTING SYSTEM BLOCK DIAGRAM

The specifications for the present EAI 590 configuration at the University of Alberta are presented in Table 2.1. As the table indicates, the hybrid computer includes an EAI 640 digital computer with 16 K of

TABLE 2.1
EAI 590 HYBRID COMPUTING SYSTEM
(October 1971)

ANALOG (580)	INTERFACE (693)	DIGITAL (640)
1. 36 High gain amplifiers (12 integrators).	1. 12 Analog to Digital Converters (ADC) 13 bit conversion (33 μ sec.).	1. 16K, 1.65 μ sec. core cycle time.
2. Repetitive operation capabilities to .2 Msec.	2. 4 Digital to Analog Multipliers (DAM) (zero order hold) 14 bit accuracy, 9.0 μ sec. conversion.	2. Teletype, cassette and high speed paper tape input-output systems. Expansion to line printer and card reader possible.
3. 33 Potentiometers (25 digitally set).	3. 4 sense lines, 4 control lines.	3. 12 hardware, 16 bit registers.
4. 1 Analog logic panel with 16 AND gates, 2 registers, 1 counter, 2 timers, 4 comparators, 2 function switches.	4. 2 interrupt lines and an ADC finished interrupt.	4. 64 instructions and 64 external interrupts.
		5. Software includes FORTRAN IV compiler, ASSEMBLER and HOI, Hytran Operations Interpreter.
For more details see E.A.I. 590 ANALOG/HYBRID Computing System, Pub. No. 008002055.0 March 1968.	See E.A.I. 693 II INTERFACE SYSTEM, Pub. No. 008003052-0, October 1970.	See E.A.I. 640 Reference Handbook, Pub. No. 8009118-0, June 1969.

core storage and without high speed bulk storage devices (e.g. disks) or high speed input-output devices. Because of the small core storage and the slow peripherals, the EAI 640 can be classified as a "mini-computer". The EAI 580 analog computer is relatively small and is limited by a shortage of operational amplifiers. The functions usually associated with each of the hybrid sections will now be outlined.

i) Analog

The basic function of the analog computer in hybrid simulations is to solve the dynamic equations that arise in modelling a chemical process by integrating with electronic analog components. Other operations in addition to integration may be performed such as summation, multiplication, function generation, and limited logic operations; however, the main advantage of analog simulation is high speed, accurate, continuous integration.

ii) Digital

The digital computer performs the arithmetic and logic functions in hybrid simulations. It also has far greater storage and data playback capabilities than does the analog. Most of the input-output is done through the digital peripherals.

iii) Interface

The interface controls the communications between the discrete digital section and the continuous analog section. Analog to digital converters (ADCs) allow the digital computer to monitor analog voltages. Digital to analog converters (DACs) transform a digital number into a voltage. Also, logic control lines provide communication of logic signals between the analog and digital sections allowing interrupt handling, timing control, mode control, contact closures, potentiometer settings,

etc. The interface conversion times are often crucial to successful hybrid simulations and rapid, accurate components are needed.

2.3 LITERATURE SURVEY

Hybrid computer solutions can be classified according to the requirements placed on the analog and digital sections during the solution. The category -- analog-oriented, balanced, or digital-oriented -- a problem falls into is governed by the type of problem and the capabilities of the specific hybrid system. Analog-oriented problems can use the digital computer to check and initiate a pure analog simulation and to monitor the analog voltages for later analysis. Balanced problems usually utilize the analog's integration capabilities and the digital's arithmetic capacity to generate functions not easily programmed on the analog computer. Digital-oriented problems use the digital computer's ability for mode and timing control to utilize the analog essentially as a subroutine to solve dynamic equations.

The following hybrid literature survey begins with analog-oriented problems, demonstrates many balanced applications and concludes with digitally-oriented problems. The emphasis is on chemical engineering applications, although many similar examples of hybrid simulations in other fields (bio-medical, aerospace, communications, nuclear, etc.) can be readily discovered in the literature.

2.3.1 Analog-oriented Problems

The first stage beyond pure analog computation in hybrid simulations is the digital set-up and check of analog circuits. Greenberg [2] uses computer checkout and analog debugging as the first part of a four part program to teach hybrid computation to undergraduates.

Babushkin, Kogan and Rybashov [3] indicate the digital program used to aid in analog set-up may be able to perform several functions. They outline programs that are able to reduce the dynamic equations to a series of first-order differential equations, provide the optimal scale factors for the analog simulation, and automatically set the potentiometers from these results.

The checkout facility usually includes a static check, i.e. checking the analog patchboard by placing voltages at various locations in the patch panel and checking component outputs. The digital computer can also perform a dynamic check of the analog solution by solving the differential equations numerically. Hambury [4] states that simple interpretive languages are ideal for this type of hybrid application since the ability to easily change the digital program is more important than the need for rapid digital execution. The first illustrative example in section 2.4 demonstrates the use of a low level interpretive language, the Hytran Operations Interpreter (HOI) [5], in checking the analog simulation of the Sutro Weir experiment used in the undergraduate laboratory at the University of Alberta.

2.3.2 Digitally Generated Functions

Hybrid computers have found extensive use in solving nonlinear ordinary differential equations that often arise when modelling the dynamics of a chemical process. Analog nonlinear elements are expensive and inaccurate, and because of this, many analog simulations involve linearized models. Digital computers have the arithmetic capabilities to generate highly nonlinear functions; thus digital simulations for nonlinear problems are popular. The digital computer in a hybrid

simulation performs the nonlinear function generation and the analog integrators eliminate some of the problems (round-off error, truncation error, and computation time) that can develop with pure digital simulations. However, the synchronization of the analog and digital computers and conversion errors (analog to digital and digital to analog conversions) add extra problems to hybrid simulations.

The major drawbacks to digitally generated functions in hybrid simulations arise from sampling a continuous analog function. The analog is sampled at a time, t , and the function generated at a time, $t + \Delta t$, where Δt is the time required to calculate the function and complete the conversions required. This causes the function to be in error by the amount of time required to complete the function generation. Rapid ADCs and DACs can make this error negligible in most real-time and moderately time-scaled (accelerated) simulations. When the analog is operating in the repetitive operation mode or simulating a rapidly changing process, these errors can become critical. The text by Bekey and Karplus [6] presents a complete chapter (Chapter 5) on errors caused by these conversions. Methods of predicting the value of a function at time, $t + \Delta t$, from an input at time, t , have been extensively investigated [6,7]. Vansteenkiste [8] has summarized some of these compensating formulae for both zero-order and first-order hold circuits that are present in the DACs of most hybrid systems. Methods of testing these formulae have also been developed [9,10]. The hybrid example problem in section 2.4 demonstrates the accuracy of digitally generated functions by comparing a digitally generated sine wave to an analog sine wave for different sampling frequencies.

Many examples of digitally generated functions can be found in

hybrid simulations of process systems. Severe nonlinearities occur in simulations of chemical reactor systems where the reaction rate involves the Arrhenius relationship, $\exp(-E/RT)$, and is not suitable for linearization. Sharpe [11], Dahlin and Nelson [12], and Ruzskay and Mitchell [13] all demonstrated the use of a digital computer in nonlinear function generation for hybrid solution of reaction problems. An example of the hybrid simulation of a nonlinear batch reactor is presented in the example problem section. Sharpe's article [11] contains a comparison of the time and cost for a hybrid simulation and a digital simulation of space vehicle dynamics. A similar comparison is made in the reactor problem presented in the next section. Both simulations incurred large savings on the hybrid computer.

A mathematical function ideally suited to digital generation is a time delay. Pure analog simulation of time delays involves a series approximation (Pade, Stubbs-Single etc.) that requires many operational amplifiers and often yields good results for only certain types of simulations. By contrast, simulating time delays on a digital machine is very accurate. Fox, Parsons and Dutcher [14] simulate time delays digitally in the hybrid simulation of a polymerization process. Nilson [15] has demonstrated a technique for generating delayed functions, $f(t-\tau)$, from a variety of functions, $f(t)$. Section 2.4 presents examples of time delay programs.

2.3.3 Sampled-Data Systems

The sampling problems inherent in hybrid simulations of continuous systems can be put to advantage in analysing sampled-data systems. As Figure 2.2 indicates, the analysis of sampled-data systems

allows for a sample and hold device present in the system.

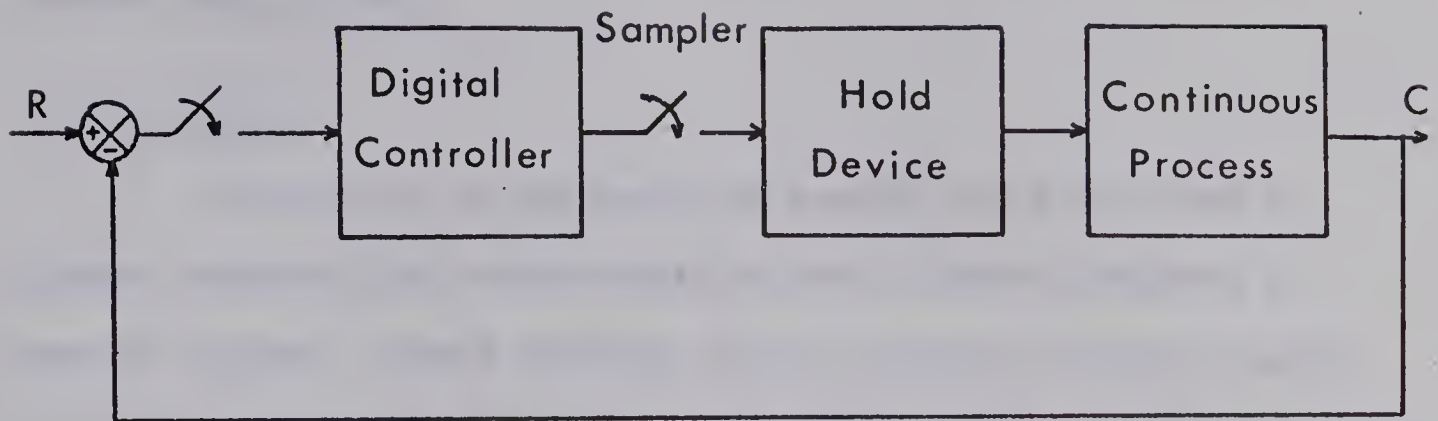


FIGURE 2.2 SAMPLED-DATA CONTROL SYSTEM

For sampled-data problems analysed in the Z-domain [16], the digital computer acts as the digital controller, the interface components represent the sample and hold device, and the analog computer simulates the continuous process. A digital controller designed to give a dead-beat response [17] is demonstrated in section 2.4.

Digital control of a process always requires sampling. Often the effect of sampling is ignored and the controlled process is analysed as a continuous system. Many digital simulations do not allow for errors that can arise because of sampling. However, if the analog simulates the actual process and the digital controls this process, sampling errors may be discovered at the time of the simulation, not when the control scheme is being implemented. Fox et al [14] used a hybrid computer to simulate Direct Digital Control (DDC) of a polymerization process and investigated the effect of sampling frequency. Lawrence et al [18] used the similarity between hybrid simulation and control of an actual plant to investigate DDC control algorithms on control loops

that existed at a nuclear power station. More examples of hybrid digital control simulations will be reviewed in the next section on control applications.

2.3.4 Control

The ability of the analog to provide rapid solutions to dynamic equations has caused extensive use of hybrid computers in control studies. Single variable control problems have been studied on hybrid computers to obtain optimal control settings for conventional controllers. Sharpe [11] describes a hybrid simulation of a tubular chemical reactor used to optimize the controller constants for a PID controller. Ung [20] designed a three mode controller for a heat exchanger control system by minimizing the integral of the absolute error performance criterion. A similar optimization problem for the Sutro Weir experiment is presented in section 2.4.

Multivariable control studies have been popular hybrid computer applications because the implementation of multivariable schemes depends on a simultaneous knowledge of all the controlled variables (available because of the analog parallel integration capabilities) and on matrix operations (available from the arithmetic capabilities of the digital). Bekey [21] has used hybrid computers in the dynamic optimization of multivariable systems. As Figure 2.3 illustrates, the analog simulates the process represented by vector-matrix differential equations. The digital evaluates the criterion to be minimized from the analog results (controlled variables, \underline{x}) and calculates the control action, \underline{u} , from a control algorithm depending on the criterion, the controlled variables, and the control action.

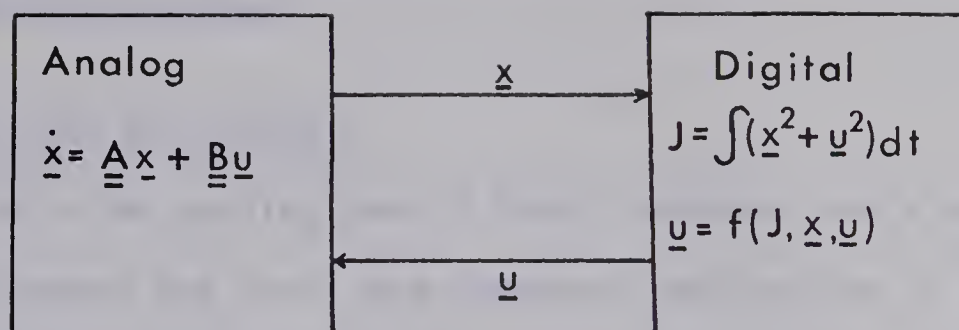


FIGURE 2.3 HYBRID COMPUTERS IN MULTIVARIABLE CONTROL SYSTEM DESIGN

Gonzalez [22] has used the same hybrid approach to calculate the minimum time optimal control of hypothetical second-and third-order processes with constrained control variables.

Hybrid computers have found extensive use in the study of adaptive control techniques. Sandoz and Swanick [23] conducted a hybrid simulation of a model reference adaptive control system in which the error between the analog "process" and digitally generated model was minimized by adapting the control of the system at each interval. They reported excellent results for a second-order system with feedback control. Godebole and Smith [24] tested another adaptive control technique using both digital and hybrid simulations. The control scheme greatly improved control for systems modelled with transfer functions. Furthermore, they maintain the hybrid simulation to be the most realistic because the analog process simulation and the digital control calculations are working in parallel; therefore sampling errors that would occur in actual process control also occur in the simulation. By contrast, digital simulation suspends process dynamics until the control calculations are complete. The later chapters of this thesis

illustrate a model reference adaptive control technique simulated on the EAI 590 hybrid system.

2.3.5 Real-Time Applications

Real-time applications of hybrid computers are a relatively recent development but could have important applications in the future. Mellichamp [25,26] demonstrated this application when he optimized a second-order process with [25] and without [26] time delays. He optimized a process model on the analog in "fast-time" and returned the optimal control values to the process in real-time. Then, the process states were read by the digital control computer and used to update the analog model for the next optimization iteration. Mellichamp reported excellent results. With process control computers becoming more commonplace, this type of hybrid real-time application should become more popular.

2.3.6 Optimization and Parameter Estimation

Optimization and parameter estimation problems rely heavily on the rapid solution of an analog model. Andrews and Moore [19] used a hybrid simulation to optimize the cost of the catalytic dehydrogenation of normal butane. The analog computer simulated the reactor section of the plant and contained an optimization routine to minimize the reactor operating cost. The digital computer updated the optimization parameters in the analog section, calculated the distillation costs from the reactor outlet composition, and from the combined total cost (reactor and distillation) optimized the entire process by varying reactor conditions (feed rates, temperatures, recycle rate, etc.).

In parameter estimation, the digital stores the actual process

response and the analog produces a model response. The parameters of the model are then updated until the desired "goodness of fit" between the process and model are attained. Carlson [27] outlines the procedure for parameter estimation in kinetic reaction equations. His paper is typical in that it uses the rapid analog solution of the model equations to quickly obtain the best parameters (rate constants) for the kinetic rate equations.

2.3.7 Simulation of Staged Processes

The simulation of staged processes is a major digital-oriented hybrid application. In the hybrid simulation of staged processes, the process being simulated is divided into identical stages and the differential equations describing the dynamics of the stage are programmed on the analog. The digital then links the simulation together by transferring the boundary conditions between stages. The stages may be real, as in a plate distillation column, or contrived, as in a packed column or tubular reactor. For some processes, a large number of stages are required for an accurate model. Therefore, an excessive number of components would be required in pure analog simulation. Furthermore, accuracy and computation time problems could arise in digital simulations. Many examples of large scale, staged process, hybrid simulations are available in the literature.

Dahlin and Nelson [12] used a hybrid computer to study the cooling of a tubular chemical reactor by countercurrent flow. They modelled the tubular reactor as a series of backmix reactors with backflow between adjacent stages. Two first-order consecutive reactions were considered involving three dynamic component balances and a heat

balance for each stage. A single stage analog circuit used 12 operational amplifiers, and if 20 stages were needed to model the reactor, then over 200 operational amplifiers would be required. Few analog computers have this capacity. With the hybrid solution, each stage was solved separately and the solution of that stage was read into the digital via ADC channels. These values were then used to calculate the boundary conditions for the next stage. Therefore, all the identical stages used the same analog solution. The countercurrent cooling of the reactor led to a split-boundary value problem and an iterative solution was required. The outlet coolant temperature had to be assumed in order to solve the problem and the resulting solution for the inlet cooling temperature was compared to a known inlet condition. The simulation had to be repeated if the temperatures were not within reasonable agreement. Because of the iterative nature of the solution, the rapid single stage analog solution made the hybrid calculation time much less than the digital solution time.

Frank and Lapidus [28] used this technique to simulate a seven stage, five component distillation column and a fixed bed catalytic reactor modelled as eight continuous stirred tank reactors. Ruszkay and Mitchell [13] simulated a twenty-five stage reacting distillation column using the single analog stage technique. This method of solution is equivalent to solving a partial differential equation in length and time coordinates by the discrete-space-discrete-time (DSDT) method. Indeed, the hybrid solution of partial differential equations is an extremely popular hybrid application.

2.3.8 Partial Differential Equations

Partial differential equations (PDE) often arise when modelling chemical processes. When analytic solutions are not available, the PDE can be solved using numerical techniques on digital computers, however, large amounts of computer time are involved in multidimensional integrations. In the past few years, several hybrid techniques for solving PDE have been investigated; continuous-time-discrete-space(CTDS), continuous-space-discrete-time (CSDT), and discrete-space-discrete-time (DSDT). These methods are presented in detail in Bekey and Karplus [6] (Chapter 8). Essentially all the methods involve solving one dimension of the differential equation (time or space) continuously on the analog and the other dimension by discrete methods on the digital. The dynamics of many systems are best described by a PDE and many hybrid solution techniques have been discussed in the literature.

Carling [29] developed equations for the hybrid simulation of a counterflow heat exchanger with thermal capacity in both fluids and the tube wall. He was unable to achieve a complete hybrid solution because of hybrid hardware difficulties on his computer. Carling did verify his technique on a digital hybrid simulator. Poulsen [30] solved a similar problem for the dynamics of steam loss from a tube. Owen and Kistler [31] and Vichnevetsky and Tomalesky [32] have developed two different techniques to obtain the heat exchanger solution. The same heat exchanger problem described by Owen and Kistler is solved in the next section using the standard CSDT method.

A PDE similar to those arising from heat exchanger modelling is found in fixed bed adsorption models and has been solved by Eteson and Zwiebel [33] on a hybrid computer.

Second-order partial differential equations in the spatial coordinates often occur when diffusion in mass transfer or conduction in heat transfer is important. Bryant, Amiot, et al [42] have solved the two dimensional heat transfer differential equation of the form

$$\frac{1}{x} \frac{\partial}{\partial x} \left(x \frac{\partial \xi}{\partial x} \right) = g(x) \frac{\partial \xi}{\partial z} \quad (2.1)$$

where x is radial distance, z is axial distance and ξ is temperature. This equation results from a steady-state laminar flow heat balance around a double pipe heat exchanger. Equation (2.1) is a form of the Sturm-Liouville equation and often occurs with split-boundary values. The application of numerical techniques to the hybrid solution of this type of PDE has made use of high speed analog integration to reduce solution time.

The diffusion equation

$$\frac{\partial^2}{\partial x^2} C_A = \frac{1}{\alpha} \frac{\partial C_A}{\partial t} \quad (2.2)$$

has been solved many times in the literature [34-36]. Many approaches to solving this equation have been discussed because at high solution speeds, sampling errors can be significant. Also, difficulties are encountered in finding a value of the time increment (CSDT method) that yields an acceptable compromise between the effect of round-off error (in analog to digital and digital to analog conversions) and the truncation error associated with time-discretization.

One of the most complex PDE problems solved by hybrid techniques to date deals with river pollution [37] and takes the form

$$\frac{\partial C}{\partial t} = \frac{\partial}{\partial x} k \frac{\partial C}{\partial x} - \frac{\partial (v.C)}{\partial x} - D(x) + f(x,t) \quad (2.3)$$

where v = river velocity

$D(x)$ = pollutant degradation

C = pollutant concentration

k = diffusion constant

and $f(x,t)$ = pollutant source function

Third-order and higher partial differential equations are rarely solved on hybrid computers, mainly because they seldom occur in process modelling. Multidimensional (more than two dimensions) simulations also do not occur because the synchronization of two analog machines would be required for the solution unless all but one dimension was solved for numerically.

The papers just reviewed cover all the major areas of hybrid computer problems in chemical engineering and are representative of work in this field. From the literature survey, some applications of the University of Alberta EAI 590 hybrid system can be suggested. These are:

i) **Evaluation of Control Techniques:** The ability to adjust the time scale and the close correlation of hybrid simulation and process operating conditions under computer control make hybrid computers ideal for testing computer control techniques before actual process implementation. The following chapters present the first such research performed using the department's EAI 590 hybrid computer.

ii) **Simulation of Staged Processes:** The solution of models of present equipment at the University of Alberta, such as the 8 tray,

9 inch distillation column could be attempted on the hybrid computer.

iii) Solution of Partial Differential Equations: The partial differential equations describing heat exchangers and mass transfer operations could be solved on the EAI 590 computer.

iv) Process Identification and Kinetic Parameter Estimation

v) Undergraduate Teaching Aid: Hybrid computers are becoming more commonplace and undergraduate courses in hybrid computer techniques are being taught at some universities [2].

2.4 ILLUSTRATIVE EXAMPLES

To demonstrate some of the hybrid applications mentioned in the literature survey, several sample problems were solved on the EAI 590 hybrid computer. The seven example problems are the following:

2.4.1 Digital Initiation and Check of an Analog Simulation

2.4.2 Reconstruction of Sampled Signals

2.4.3 Simulation of Time Delays

2.4.4 Nonisothermal Batch Reactor

2.4.5 Construction of a Digital Controller

2.4.6 Hybrid Optimization of the Sutro Weir Control System

2.4.7 Hybrid Solution of Partial Differential Equations

For each problem, a brief introduction is presented outlining the nature and scope of the simulation. Next, the function of the analog and digital portions of the simulation are outlined. Some examples include a brief description of the theory associated with the problem. Finally, simulation results are presented and conclusions are drawn. More information on the simulation programs (flowcharts, analog diagrams, program listings, execution instructions, etc.) may be

found in a research report which describes the examples in detail [38].

2.4.1 Digital Initiation and Check of an Analog Simulation

PURPOSE

To demonstrate the capability of a hybrid computer and specifically the Hytran Operations Interpreter (HOI) digital language in assisting with analog computer set-up and check out. The analog simulation involves the two tank Sutro Weir experiment used in the undergraduate laboratories.

DESCRIPTION

The Sutro Weir experiment is shown schematically in Figure 2.4

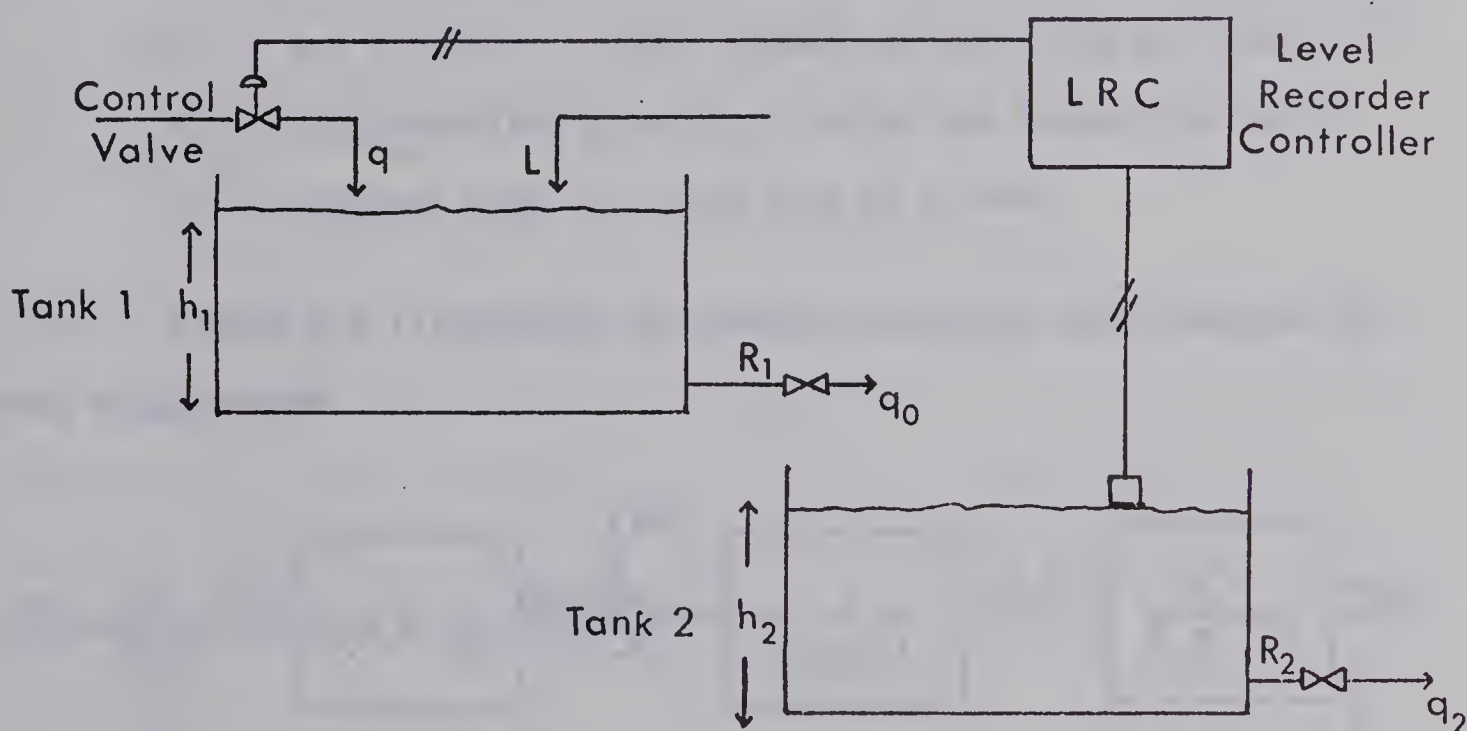


FIGURE 2.4 SUTRO WEIR EXPERIMENT

The process consists of a single feedback control system used to control the level in the second tank, h_2 , by manipulating the flow to the first tank, q . A pneumatic proportional plus integral controller is used in the laboratory. The process is easily modelled with simple mass balances

about each tank and controller yielding the following transfer function relationships between levels and flow [38]:

$$H_1(s) = \frac{Q(s)}{A_1 R_1 s + 1} + \frac{L(s)}{A_1 R_1 s + 1} \quad (2.4)$$

$$H_2(s) = \frac{H_1(s) R_1}{A_2 R_2 s + 1} \quad (2.5)$$

$$Q(s) = (R(s) - H_2(s))(K_c K_v (1 + \frac{1}{\tau_I s})) \quad (2.6)$$

where s is the Laplace transform variable

Q, L, H, R are variables in the s -domain as described by Figure 2.4

K_c is the controller gain, K_v is valve and transmitter gain

τ_I is integral time, A is the area of a tank

Figure 2.5 illustrates the transfer function relationships in block diagram form

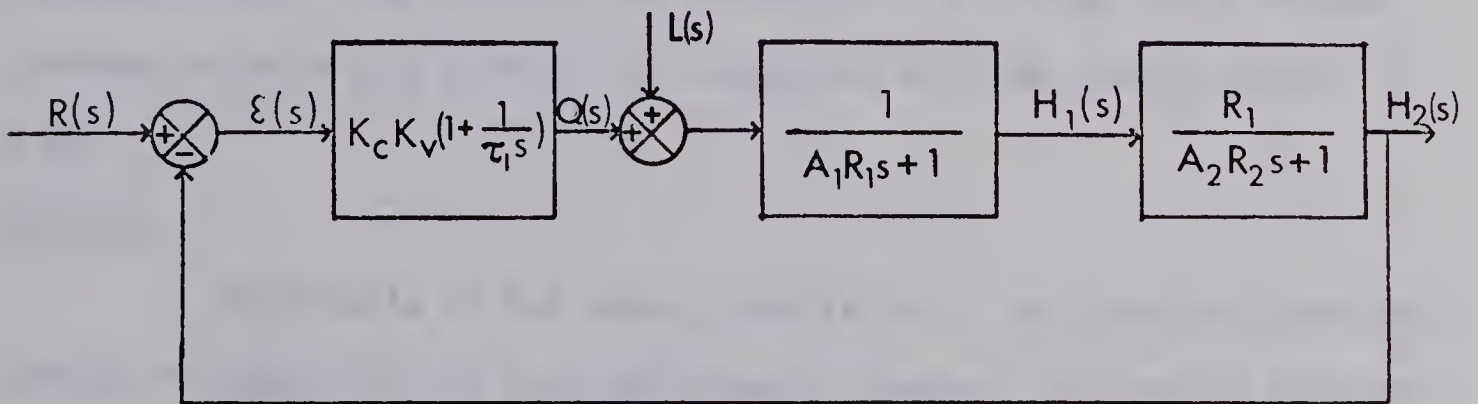


FIGURE 2.5 BLOCK DIAGRAM OF TWO TANK CONTROL SYSTEM

ANALOG FUNCTION

To simulate the Sutro Weir experiment by solving the dynamic equations (2.4), (2.5) and (2.6).

DIGITAL FUNCTION

To use the HOI language to calculate and set potentiometers, to make a static check of the analog patch panel, and to make a dynamic check of the analog solution of the differential equations. The HOI language is an interpretive language that has many capabilities for digitally initiating and checking analog simulations [5]. In setting up the analog simulation, the digital program calculated and set potentiometers from parameter values (controller constants) entered from the teletype. This saved time and eliminated human error.

The static check was automatically performed by the digital computer (i.e. HOI). The equations describing the system were entered and a voltage check around each component was made against the equations. This effectively checked the patching and the components in the analog simulation [38].

The dynamic check involved a numerical solution of the differential equations. The equations describing the Sutro Weir experiment used in the static check were solved numerically using finite-difference approximations. The solution was converted to a voltage via a DAM and plotted on the analog plotter for comparison with the analog results [38].

RESULTS

The results of the analog simulation of the Sutro Weir are presented in Figure 2.6 for load and setpoint changes. The analog solution was obtained after a static check of the analog circuit was completed. The static check involved two parts; the first section was programmed to describe the analog patching and checked the analog circuit against the dynamic equations. The second part of the static check put the analog in

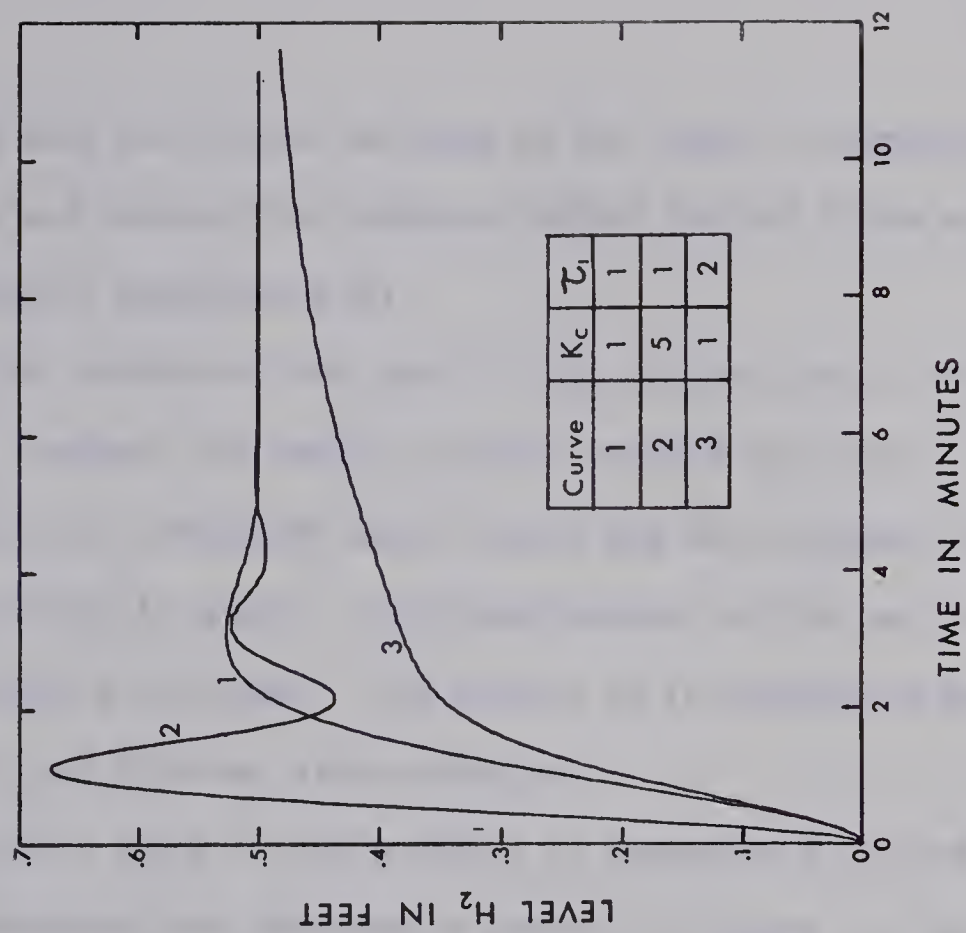
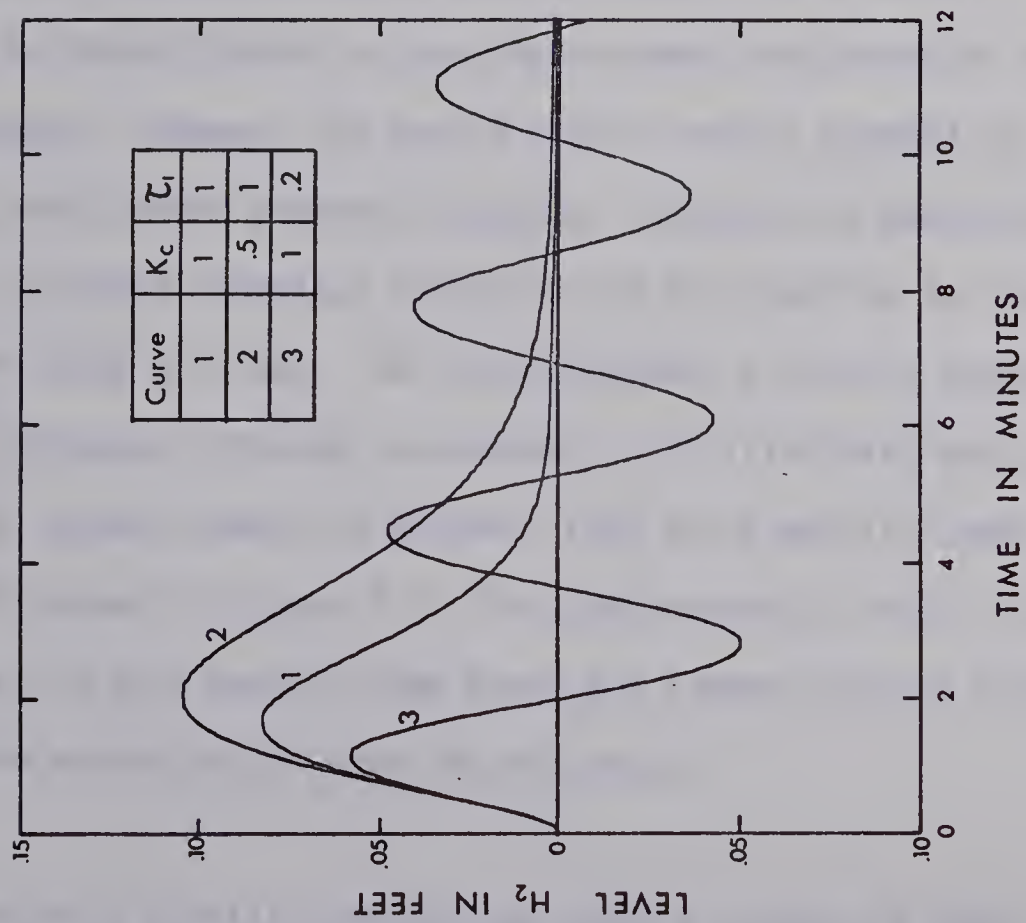


FIGURE 2.6 SIMULATED RESPONSE OF THE SUTRO WEIR EXPERIMENT TO LOAD AND SETPOINT CHANGES

the Static Check mode and placed voltages at the input to components in the patch panel; and checked the component output against those expected from the differential equations [38].

The first section of the static check gave no errors in the analog patching; however, the second section revealed two errors. A derivative input to an integrator was in error and the voltages around a potentiometer failed to check. The potentiometer setting was in error and was manually corrected. The balance on an integrator amplifier was also in error and this was also corrected.

The dynamic check of the response is presented in Figure 2.7. The controller constants are the same as curve 1 in Figure 2.6 for a setpoint change. The dynamic check uses a numerical integration (trapezoidal rule) and numerical errors could arise. The calculation time required to produce this solution was large using the HOI interpreter because this language executes source coding. As a result, execution time is several orders of magnitude slower than compiler or assembler languages. However, the source code is easily changed on-line, providing very simple program debugging. Because the execution is slow, highly accurate numerical solutions are not feasible for the dynamic check of large problems. For large problems a digital machine using an analog simulator program is advisable. To illustrate this, a CSMP (Continuous Systems Modelling Program) [39] check was also made and the result is shown in Figure 2.7. The CSMP numerical check is the more accurate for it uses smaller time steps and a more accurate second order integration approximation than the HOI check.

CONCLUSIONS

The use of a digital computer can greatly reduce the time

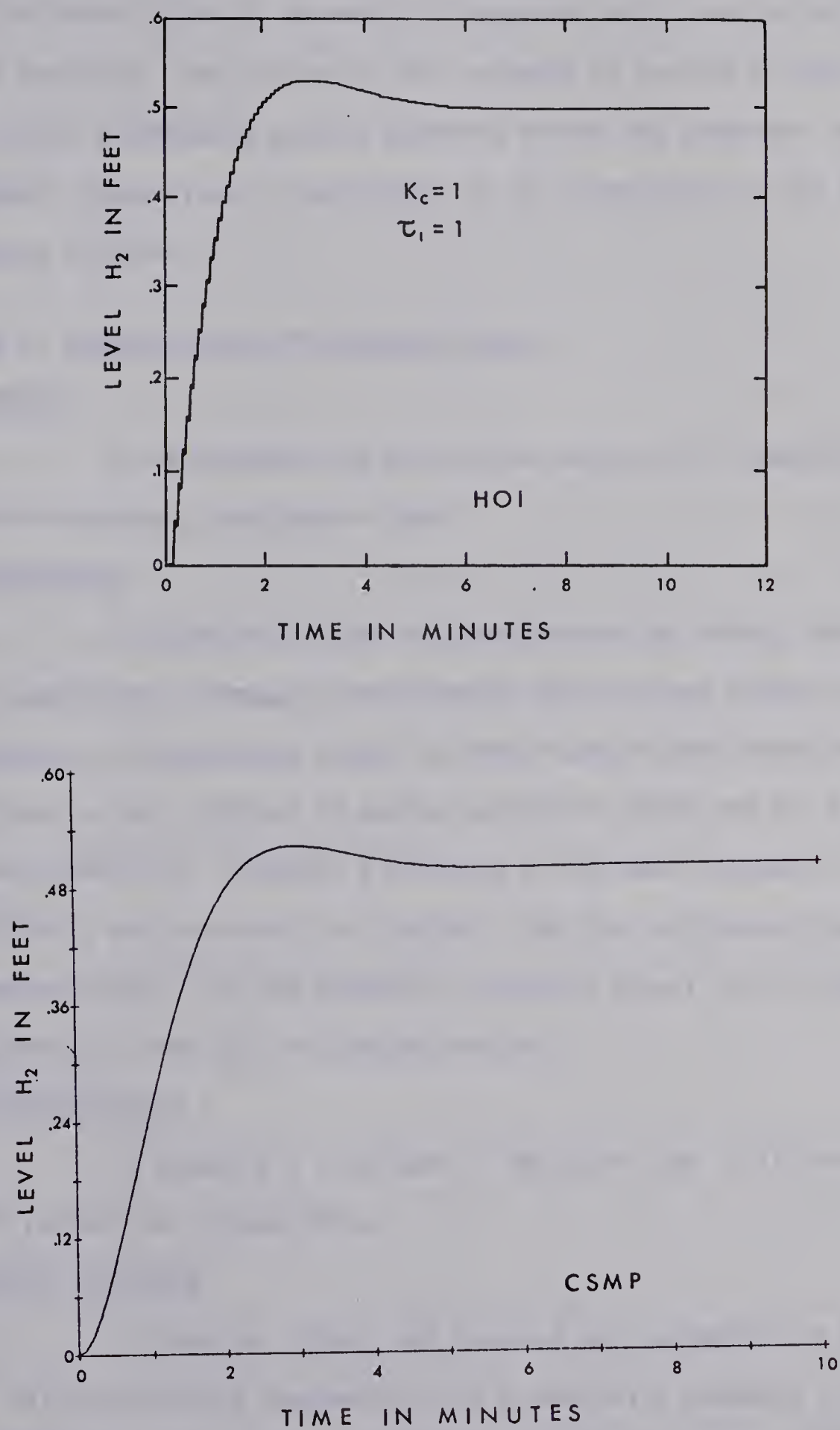


FIGURE 2.7 HOI AND CSMP DYNAMIC CHECKS OF SUTRO WEIR SIMULATION

required to check an analog simulation. A simple interpretive language is desirable since it is easily changed and high speed calculations are not required. The ability of the language to provide a static check provides a safeguard against patching errors and component failure. A dynamic check gives an indication of the correctness of the final analog solution.

2.4.2 Reconstruction of Sampled Signals

PURPOSE

To demonstrate the errors that may arise in sampling and reconstructing a continuous signal.

DESCRIPTION

A sinusoidal signal is generated on the analog computer. It is sampled at a frequency specified by the user and stored in the digital computer. A continuous signal is then reconstructed from the stored values, using a digital to analog multiplier (DAM) and its associated zero order hold. Finally, a sinusoid of the same frequency is calculated digitally and outputted via the DAM. Then the continuous signal, the sampled signal, and the digitally generated signal can be compared graphically from the X-Y plotter results.

ANALOG FUNCTION

To generate a sine wave of amplitude two volts and frequency $\pi/4$ radians per second [38].

DIGITAL FUNCTION

To acquire, store, and playback data generated on the analog at various sampling frequencies and to digitally generate $A \sin \omega t$. A FORTRAN program is used with timing controlled by core cycle time. The digital program also controls the analog modes necessary to plot the

sinusoidal functions on the X-Y plotter with the DAM. This involves synchronizing the X-axis sweep (via analog integration) with the start of the DAM output [38].

RESULTS

Typical results are illustrated in Figures 2.8 and 2.9. As expected, the analog sine wave is more accurately reproduced at higher sampling frequencies. At two samples per second, the output still gives a good approximation of a sine wave. Above 25 samples per second the digitally generated function appears almost continuous.

Care must be taken to ensure that the sampling frequency is more than double the highest frequency of the sampled signal (Shannon's rule) if the sampled signal is to be recovered completely. For example, this sine wave would have to be sampled at least once every four seconds (natural period of 8 seconds) to recover the sine wave form.

2.4.3 Simulation of Time Delays

PURPOSE

To demonstrate the simulation of time delays on a hybrid computer.

DESCRIPTION

Time delays (or transport lags) occur frequently in process models. Analog simulation of transport lags requires an approximate representation which often uses many operational amplifiers and gives "good" results only for a process which acts as a low pass filter. Even then, undesirable harmonics caused by the approximation to the time delay may appear in the simulated process response. Hybrid computers can use the digital section to control the duration of time delays precisely.

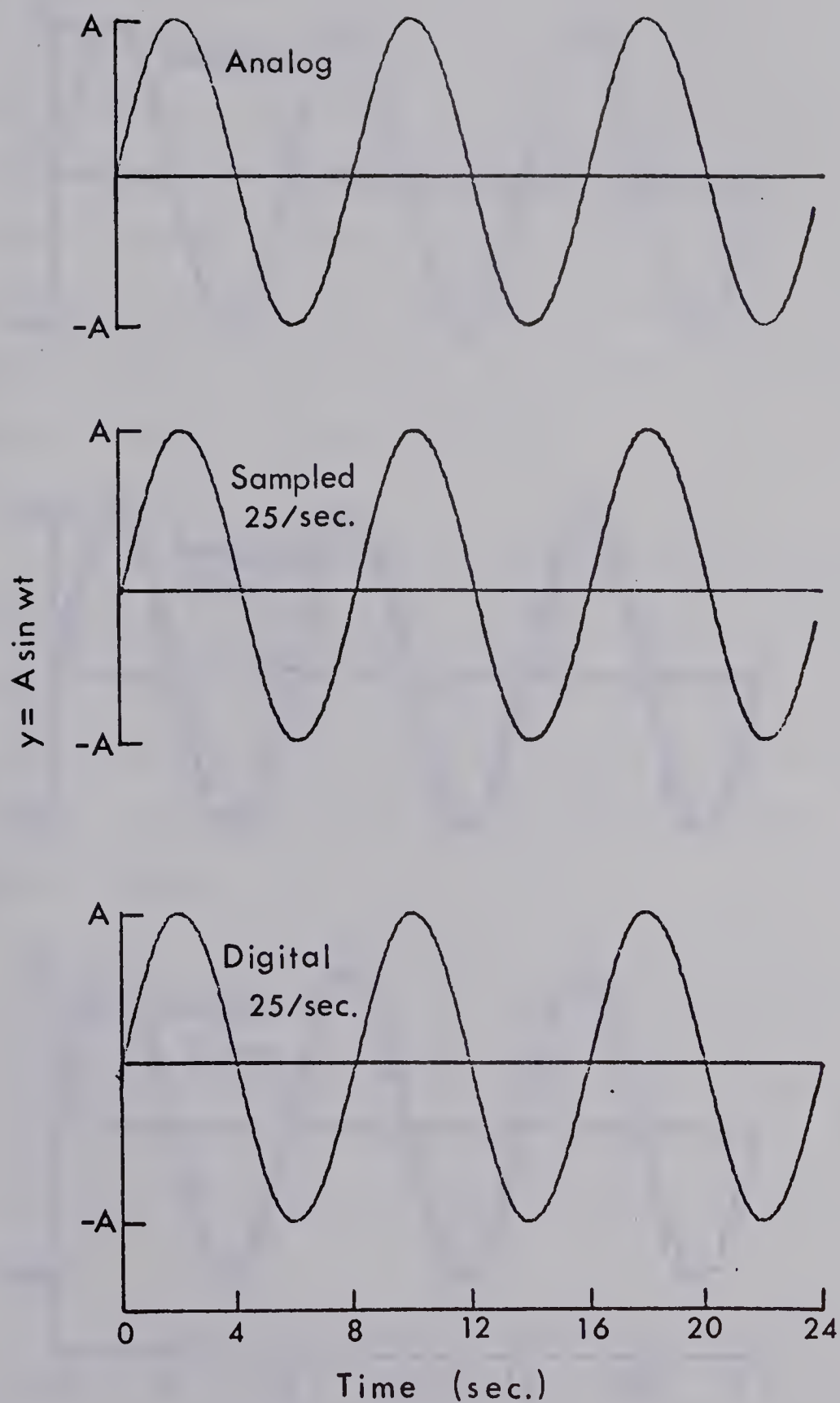


FIGURE 2.8 SINE WAVE, 25 SAMPLES PER SECOND

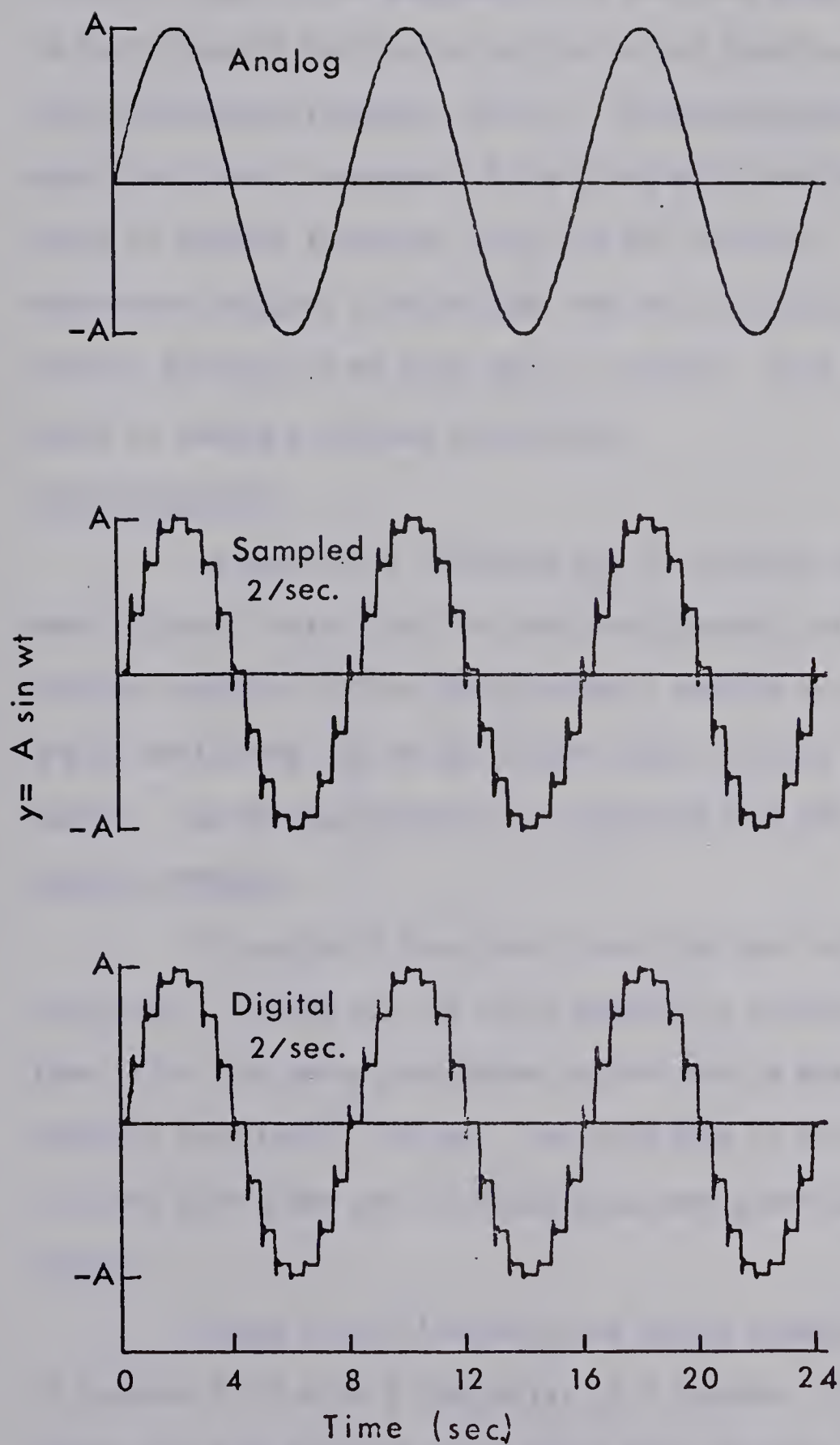


FIGURE 2.9 SINE WAVE, 2 SAMPLES PER SECOND

Two problems of this type are demonstrated. The first problem generates a time delay of τ seconds in the original function, $A \sin \omega t$. The FORTRAN subroutine for the time delay was written to be quite general and can be applied to any function, $f(t)$, to produce the time-delayed function, $f(t-\tau)$. The second problem simulates the open loop dynamic response of the Sutro Weir experiment for several types of forcing functions using the HOI language. The Sutro Weir experiment contains a fictitious time delay causing the results of the forcing function to be seen after τ seconds. Both sections are compared to analog simulated time delays.

ANALOG FUNCTION

To generate a sine wave and to simulate the Sutro Weir experiment (without controller) for open loop dynamic testing [38]. Timing for the transport lag in the Sutro Weir problem is controlled by integrator monitoring via an ADC channel [38], and has a resolution of .1 second. The forcing function is outputted by a DAM.

DIGITAL FUNCTION

To provide a time delay in a sine wave and the Sutro Weir simulation. Timing for the first example is controlled by core cycle time. The time delay subroutine can be used to delay any analog function to within $\pm .01$ sec. The sine wave in this example is reconstructed with a DAM and its associated zero order hold.

RESULTS

Figure 2.10 illustrates the hybrid output for the sine wave of example 2.4.2 with a time delay of 2 seconds. Figure 2.11 illustrates the same function using CSDAP [40] (Control System Design and Analysis Program), a digital continuous process simulator that uses a

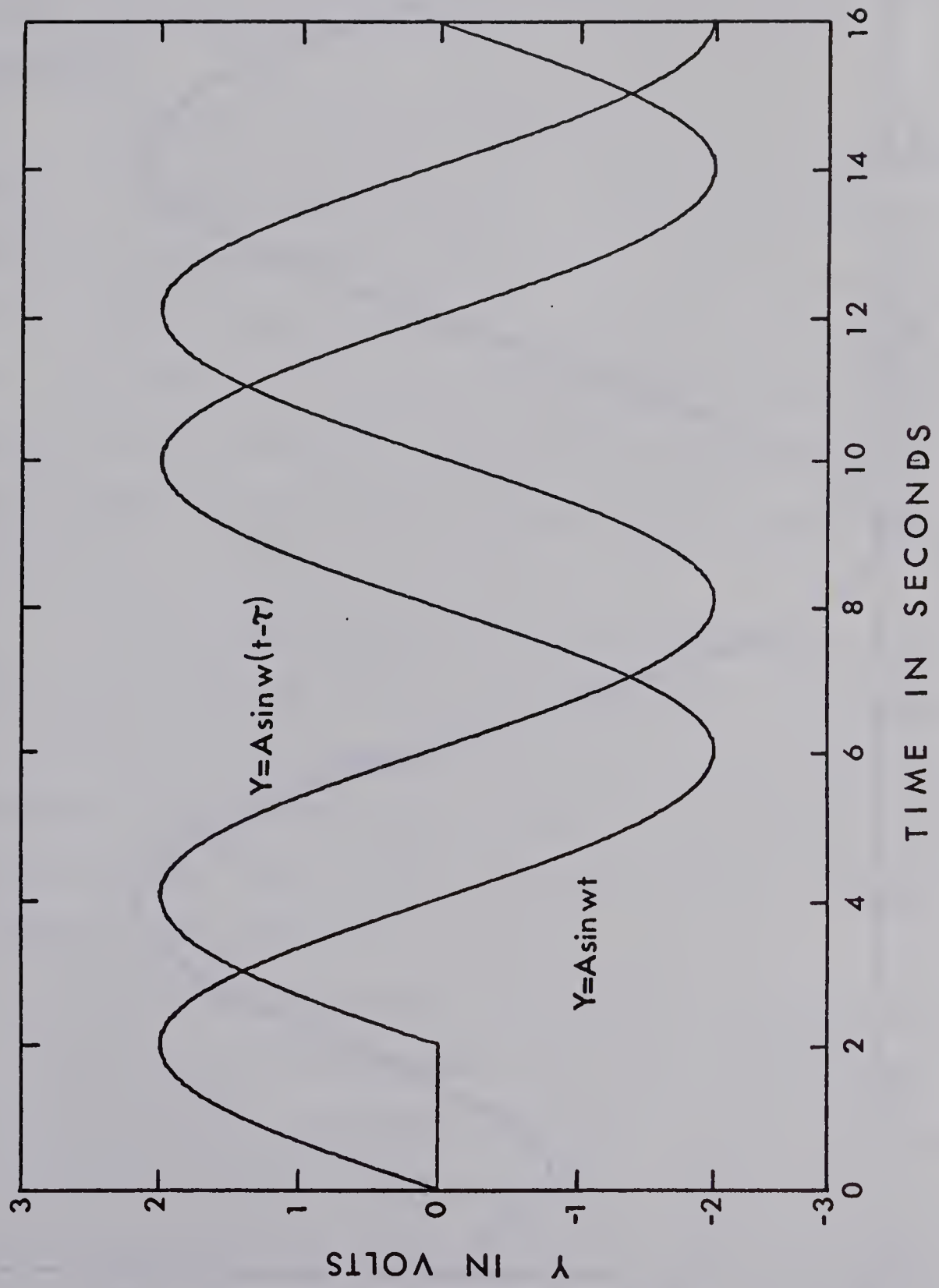


FIGURE 2.10 HYBRID GENERATED TIME DELAYED FUNCTION $Y = 2 \sin .786 (t - 2)$

TRANSIENT RESPONSE CSDAP TIME DELAY 2ND ORDER PADE

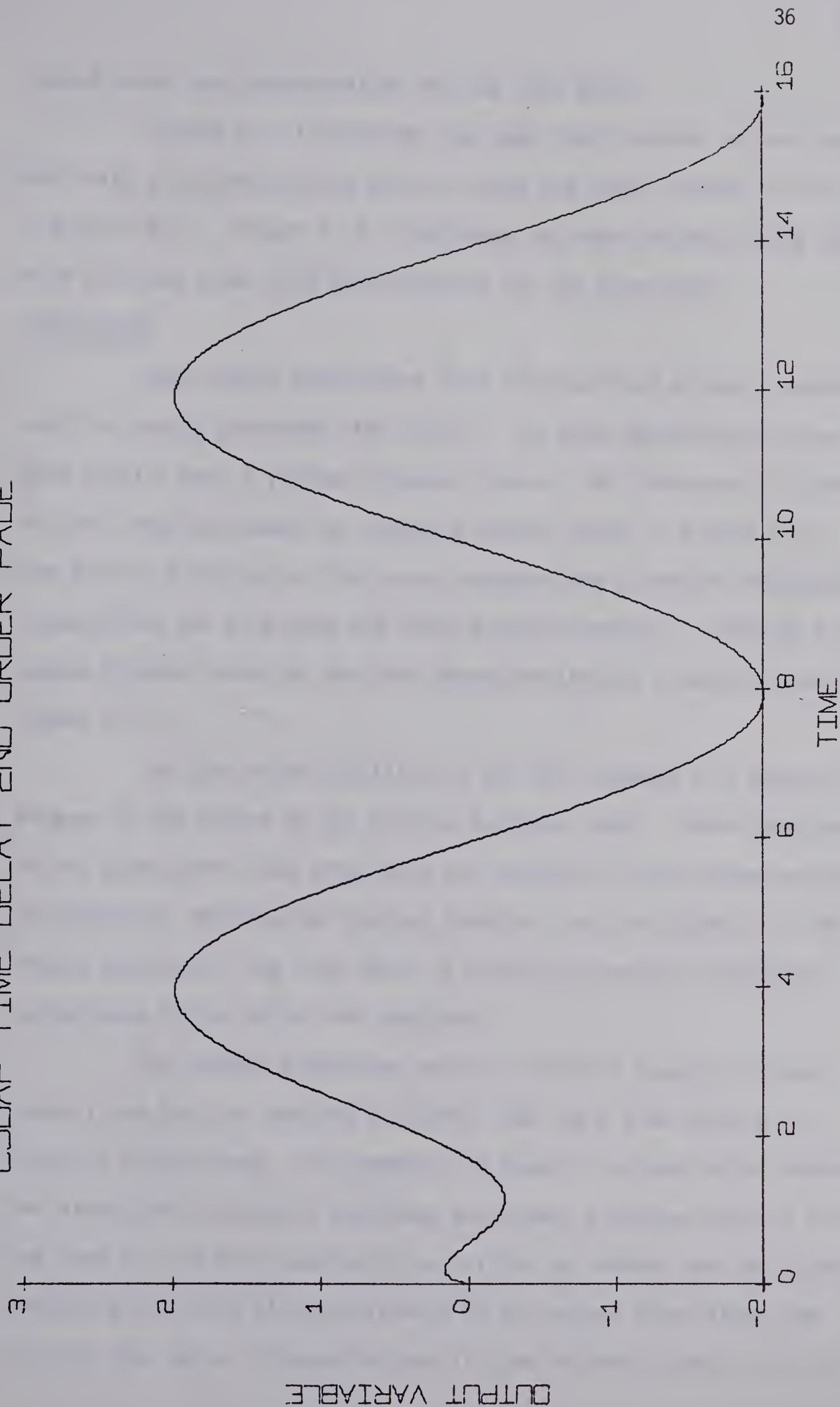


FIGURE 2.11 CSDAP GENERATED TIME DELAY SECOND ORDER PADE APPROXIMATION FOR
 $Y = 2 \sin .786 (t - 2)$

second order Padé approximation for the time delay.

Figure 2.12 illustrates the open loop response of the Sutro Weir with a two minute time delay to step and pulse changes in flow to the first tank. Figure 2.13 illustrates the same response using CSDAP with a second order Padé approximation for the time delay.

CONCLUSIONS

Both hybrid simulations show improved time delayed responses over the analog simulated time delays. The Padé approximation gives good results over a limited frequency range. The sine wave is closer to this range and hence the adequate results shown in Figure 2.11. The forcing functions of the second program have a greater frequency content than the sine wave and exhibit poorer results. The high frequency ripples caused by the Padé approximation are clearly evident in Figure 2.13.

The time delay simulated in the HOI language is a special type because of the nature of the forcing functions used. These functions do not change with time after they are inputted to the system and can be delayed by delaying the forcing function into the system. In the second simulation, the time delay is fictitious and has no physical equivalence in the Sutro Weir equipment.

The FORTRAN subroutine used in the first example is more general and could be applied to plants that had a time delay with physical significance. For example, if there is a time delay between two plants whose transfer functions are known, a program similar to the one used for the sine wave could be written to connect the two plants, inputting the first plant's variable to the second plant after the desired time delay. Reconstruction of time delayed signals with HOI is

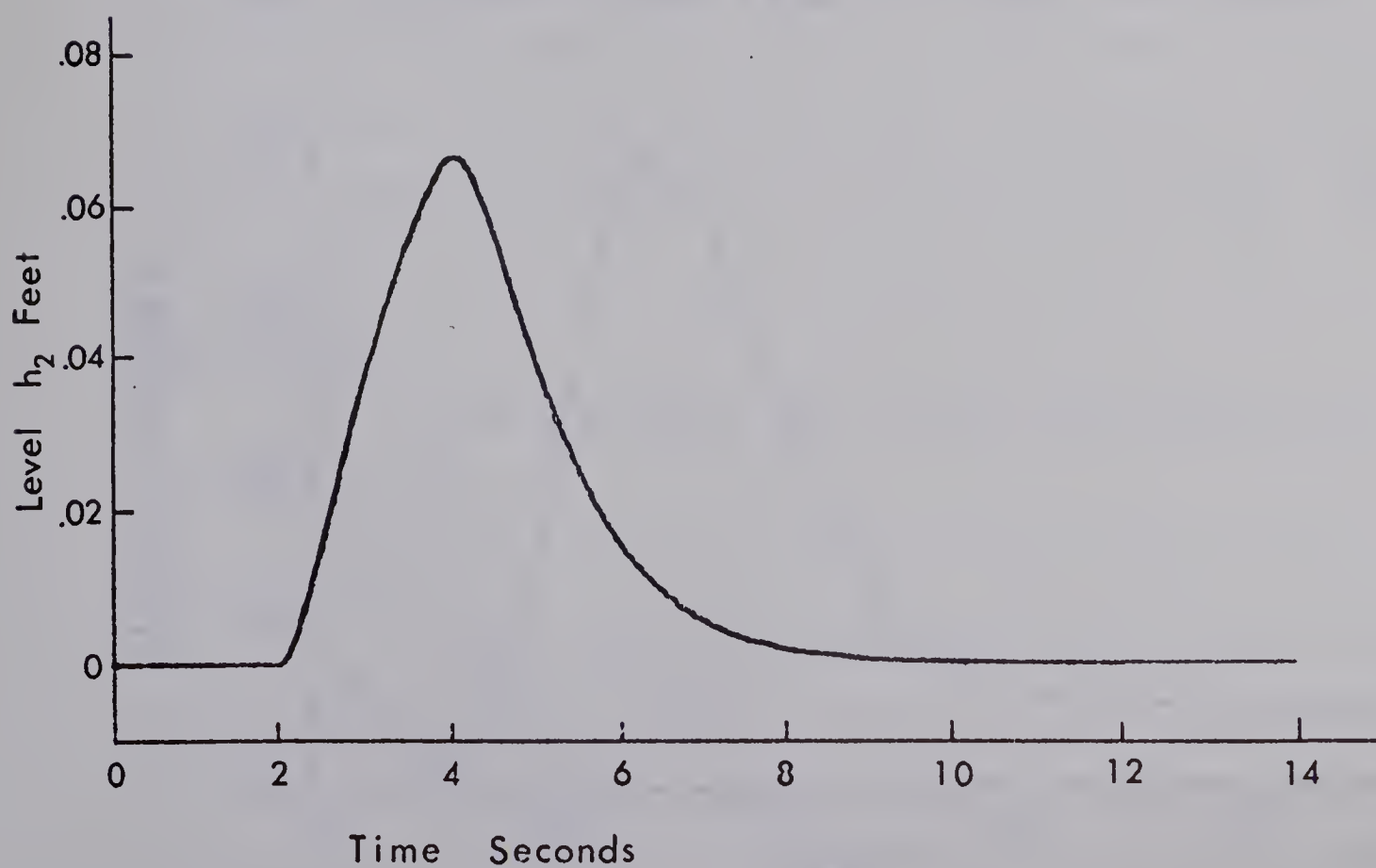
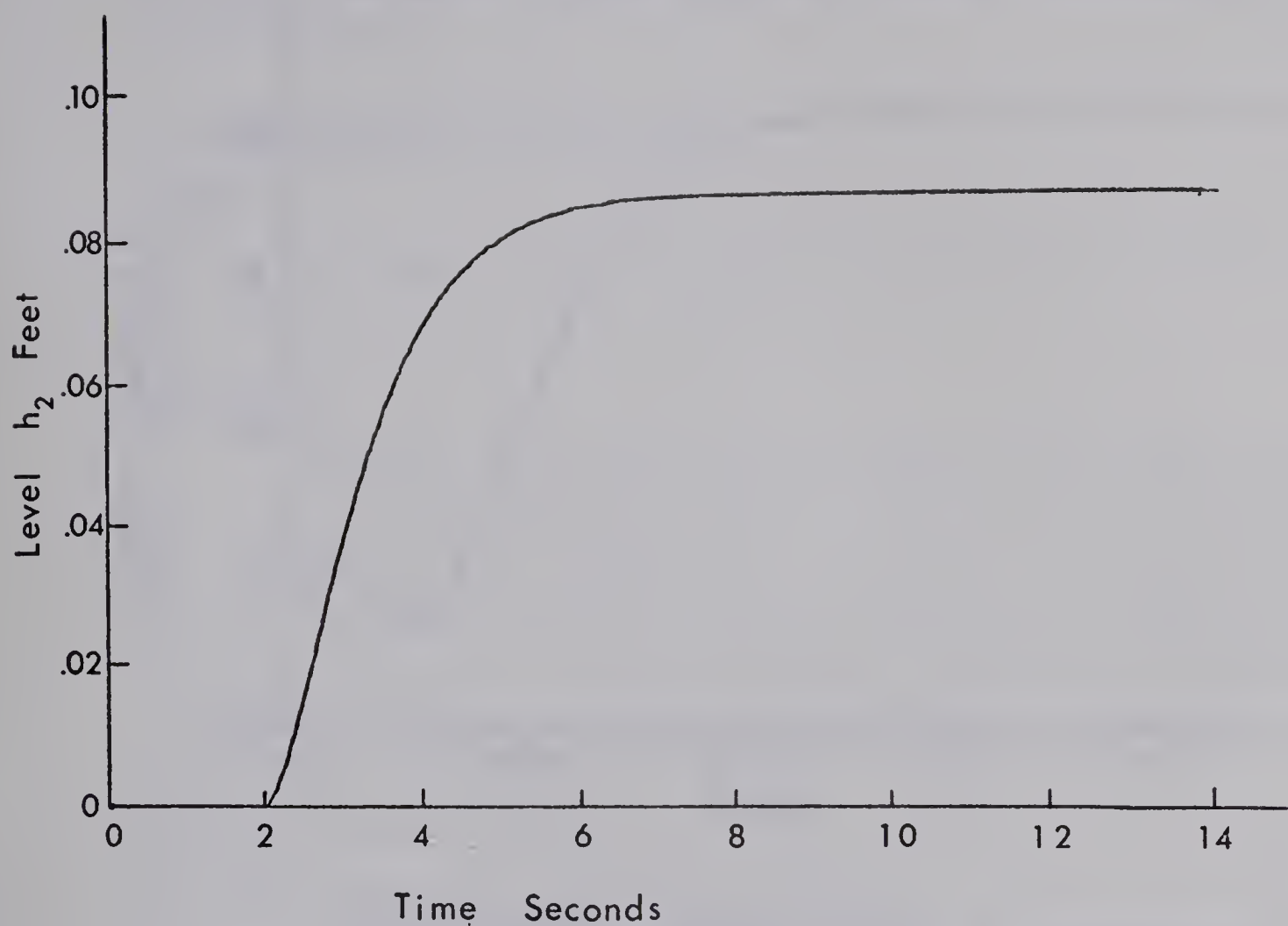


FIGURE 2.12 HYBRID TIME DELAYED RESPONSE OF SUTRO WEIR

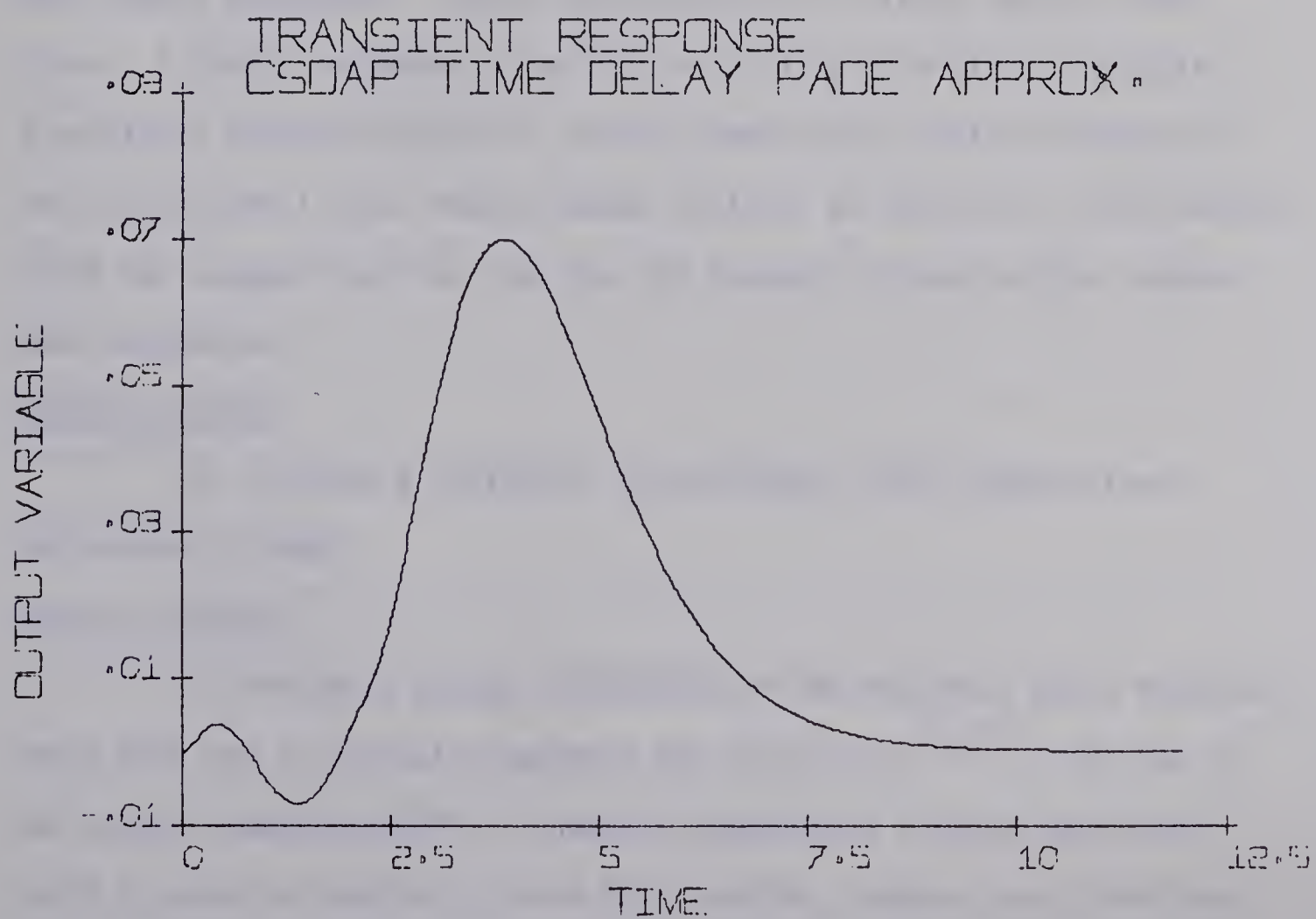
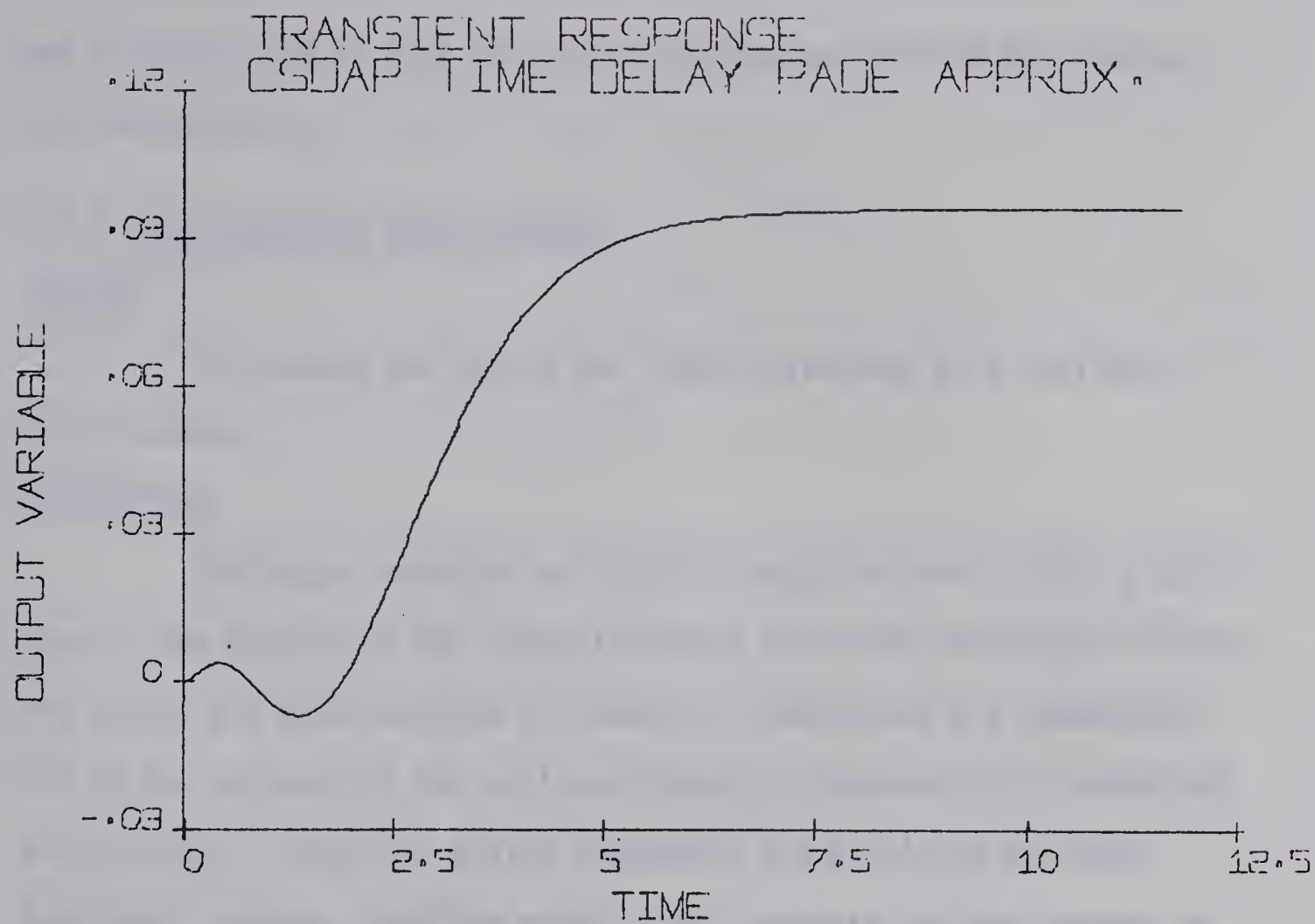


FIGURE 2.13 CSDAP TIME DELAYED RESPONSE OF SUTRO WEIR, SECOND ORDER PADE APPROXIMATION

not practical due to slow HOI execution time and present HOI timing considerations.

2.4.4 Nonisothermal Batch Reactor

PURPOSE

To compare the hybrid and CSMP simulations of a nonlinear batch reactor.

DESCRIPTION

The major advantage of digital simulation over analog simulation is the ability of the digital machine to handle nonlinear functions. The errors and time involved in numerical integration are compensated for by the accuracy of the nonlinear model as compared to a linearized analog model. Nonlinear analog components are available for many functions, however, they are usually less accurate and more expensive than linear components. Hence the popularity of linear analog simulations. A hybrid computer system has the ability of digitally generate a nonlinear function and still use the speed of the analog integrators. The nonisothermal batch reactor model contains an exponential nonlinearity since the assumed reaction rate has the standard Arrhenius-type temperature dependence.

ANALOG FUNCTION

To simulate a nonlinear, nonisothermal batch reactor (see Derivation of Model).

DIGITAL FUNCTION

To provide a digital simulation of the nonlinear batch reaction using CSMP and to digitally generate the function, $e^{(-E/RT)}$, for use in the analog simulation [38]. An analog exponential function generator could be used to completely solve this problem, however, many functions

cannot be adequately described by analog components. FORTRAN is used as the program language because speed is essential if the nonlinear function which is calculated and outputted to the analog, is to closely approximate the correct continuous function. H0I, because of its interpretive nature, has a slower execution speed and hence the results using this language would be less accurate.

RESULTS

Figure 2.14 compares the hybrid simulation for reactor temperature with the CSMP simulation. Figure 2.15 compares hybrid and CSMP simulations for reactor concentration. The computer time required for 10 hours batch reactor simulation time is 30 to 282 seconds (depending on the accuracy desired) using CSMP (IBM 1800 version) and 10 seconds on the EAI 590 hybrid computer.

CONCLUSIONS

Hybrid simulation, although initially more time consuming to set up (patching, magnitude and time scaling), can have substantial time and cost savings over digital simulation if multiple runs are expected (e.g. optimizing batch reactor temperature control). Both CSMP and hybrid simulations can easily generate arbitrary nonlinear functions. However, the time involved getting accurate numerical results (small integration interval) may prohibit many digital simulations.

DERIVATION OF MODEL

The problem chosen for simulation is an ideal first order gas reaction carried out in a nonisothermal batch reactor.

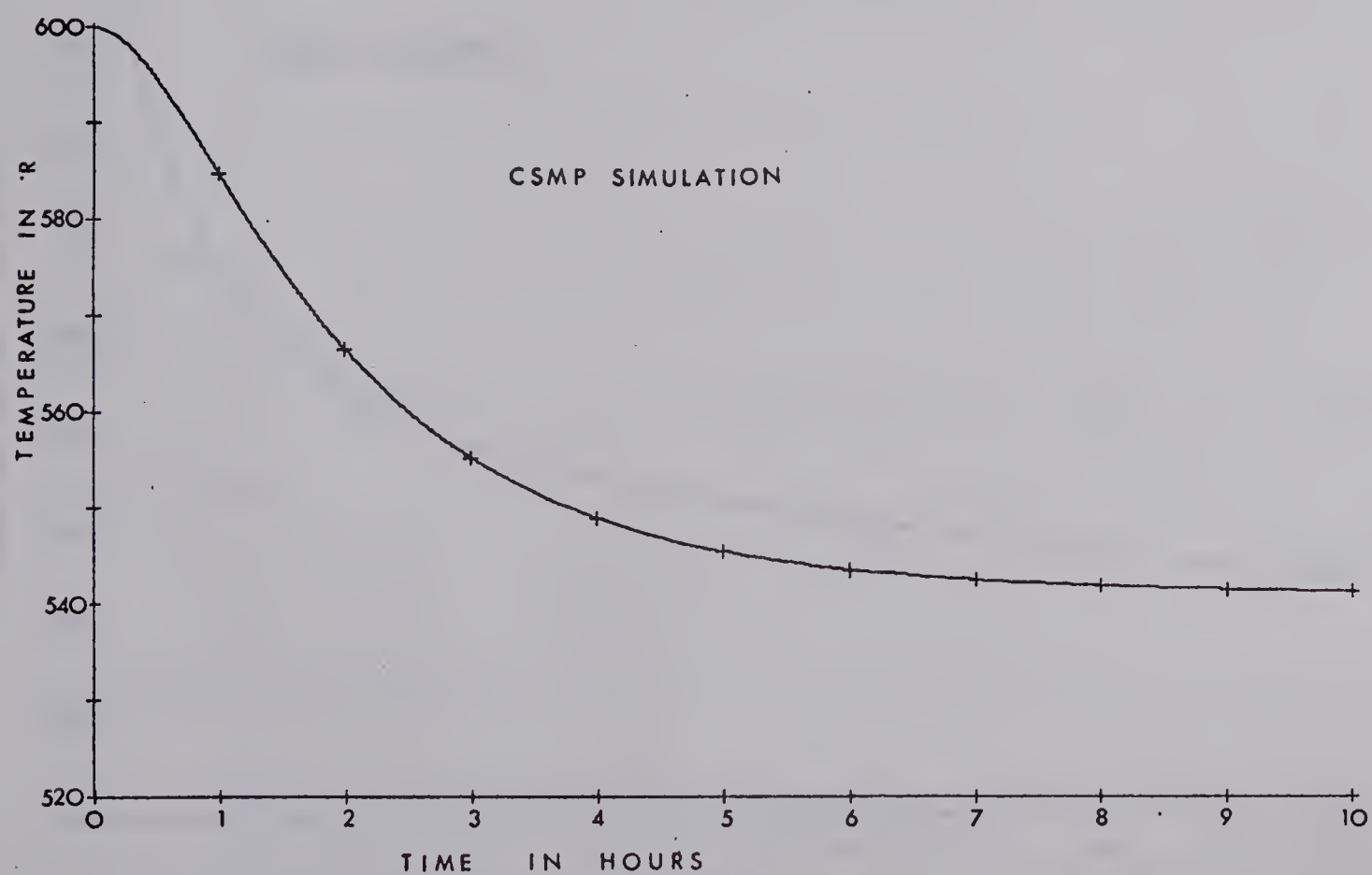
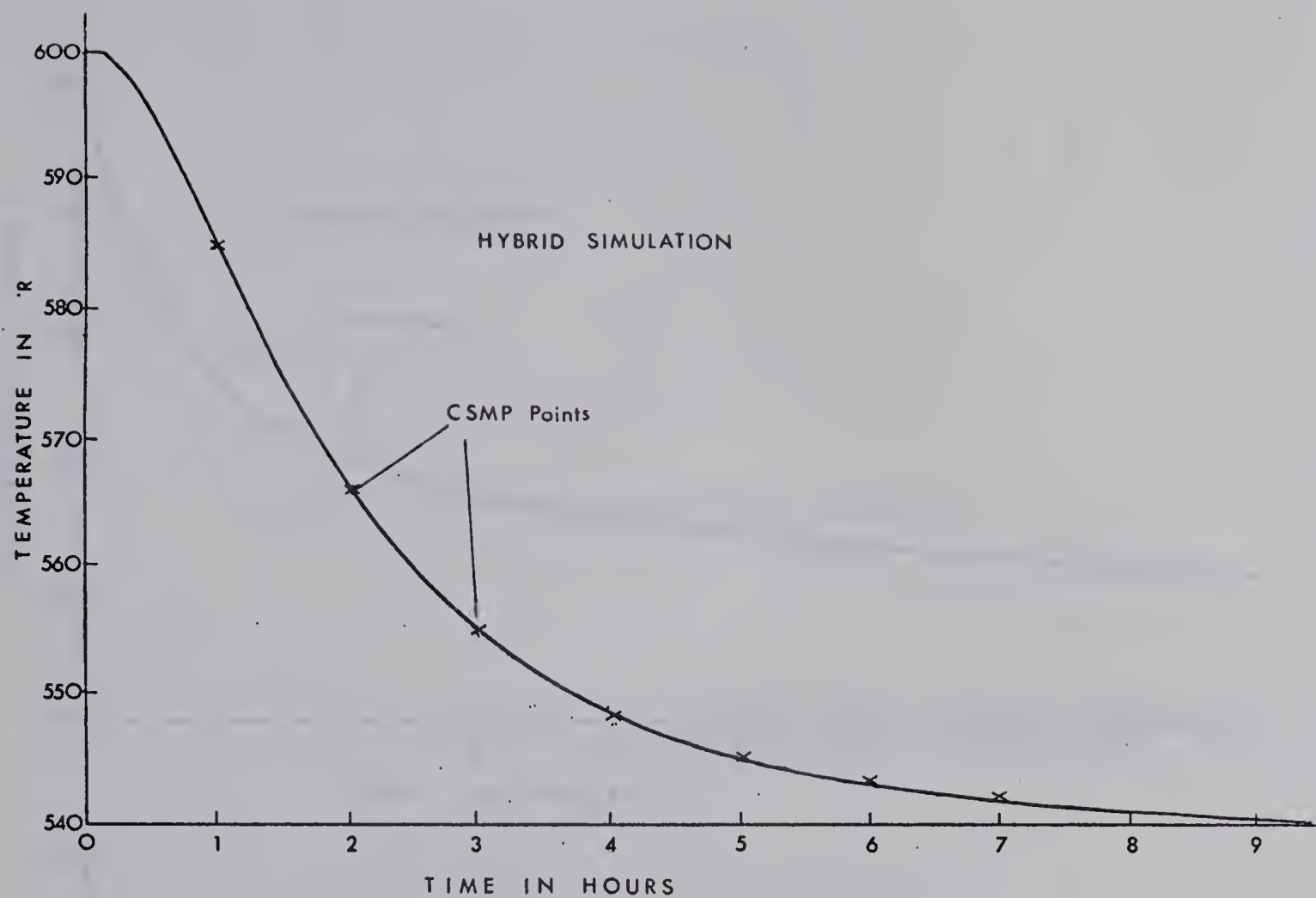


FIGURE 2.14 CSMP VS HYBRID SIMULATION OF A NONLINEAR BATCH REACTOR

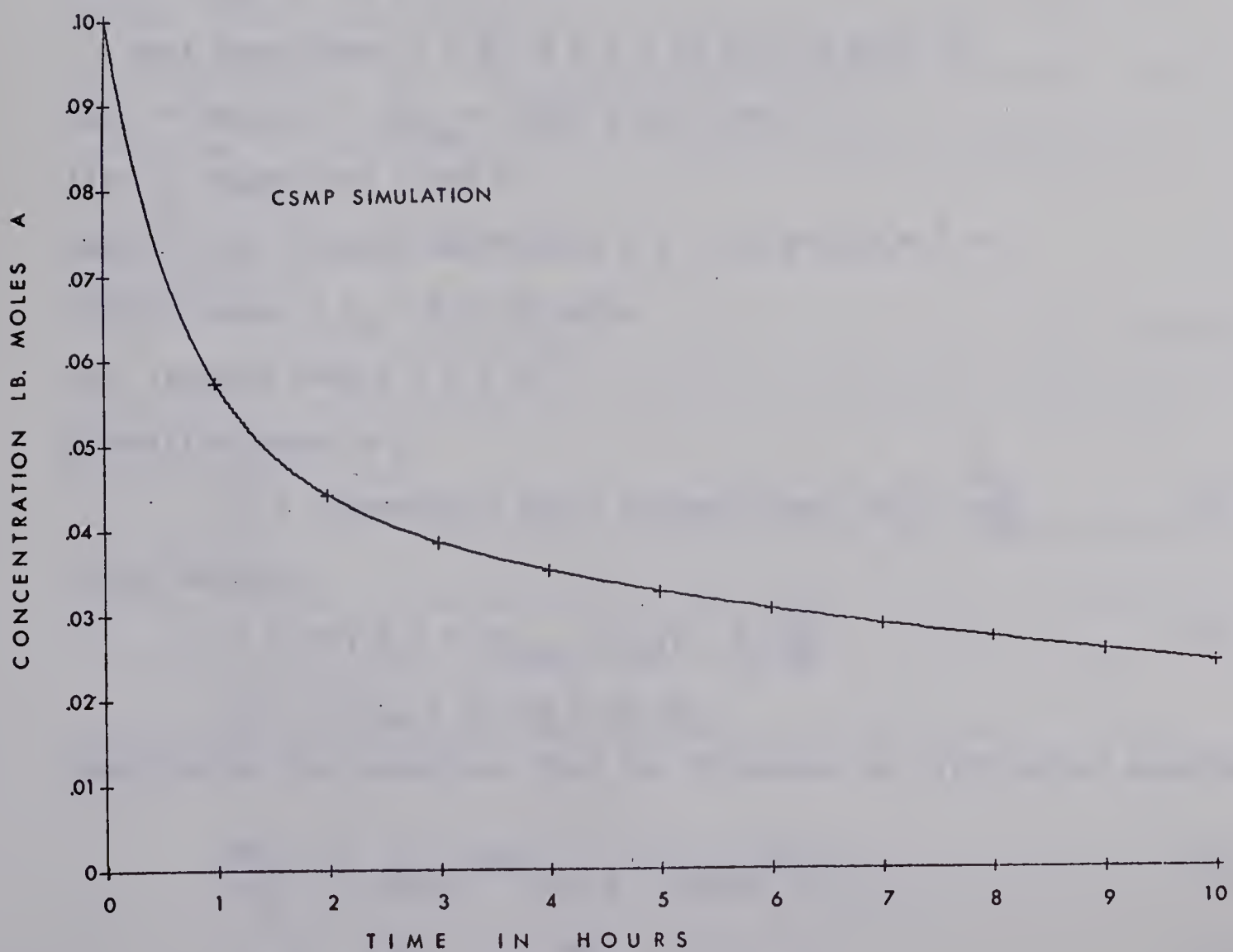
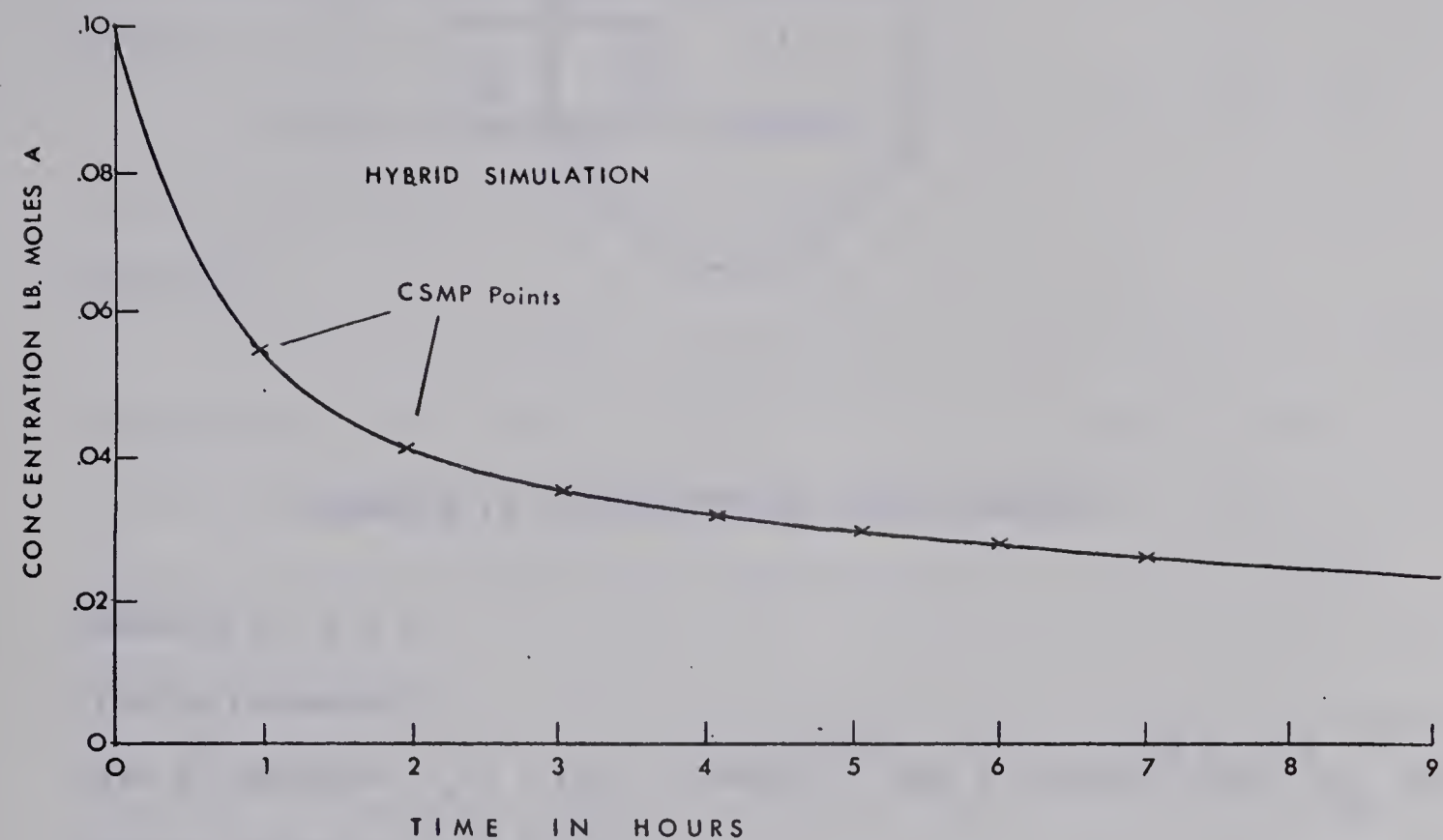


FIGURE 2.15 CSMP VS HYBRID SIMULATION OF A NONLINEAR BATCH REACTOR

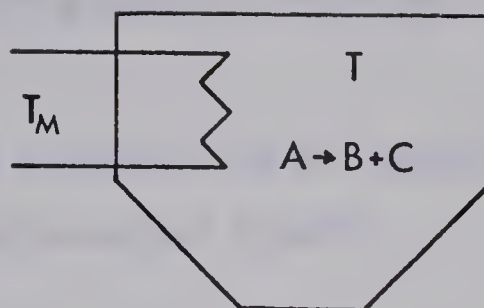


FIGURE 2.16 NONISOTHERMAL BATCH REACTOR

Reaction $A \rightarrow B + C$

Problem Parameters:

Rate of Reaction $r_A = -k n_A = -.856 \times 10^{-10} \exp(-1.394 \times 10^4/T) \text{ hr}^{-1} n_A$ (2.7)

Reactor Volume = $V = 8.75 \text{ ft}^3$

C_v , Heat Capacities: $A = 30$, $B \text{ \& } C = 25 \text{ BTU./lb.mole } ^\circ\text{F}$

Heat of Reaction = $\Delta H_{\text{rxn}} = -2500 \text{ BTU/(lb mole A)}$

Initial Temperature = $600 ^\circ\text{R}$

Overall Heat Transfer Coefficient = $U = 3.0 \text{ BTU/hr.ft}^2 ^\circ\text{R}$

Initial Charge = $n_A = 0.10 \text{ lb moles}$

Heat Transfer Area = $A = 1 \text{ ft}^2$

Material Balance on A:

$$\text{In} + \text{Generation} = \text{Out} + \text{Accumulation}, -k n_A = \frac{dn_A}{dt} \quad (2.8)$$

Energy Balance:

$$0 = UA(T - T_m) + \Delta H_{\text{rxn}} (-k n_A V) + \bar{C}_v \frac{dT}{dt} \quad (2.9)$$

$$\bar{C}_v = n_A C_{vA} + n_B C_{vB} + n_C C_{vC}$$

Substituting the parameters gives the following two differential equations:

$$\frac{dn_A}{dt} = [-.856 \times 10^{-10} \exp(-1.394 \times 10^4/T)] n_A \quad (2.10)$$

$$(5-20 n_A) \frac{dT}{dt} = 2500 \frac{dn_A}{dt} - 3.0(T-540) \quad (2.11)$$

2.4.5 Construction of a Digital Controller

PURPOSE

To program a general digital controller on a hybrid computer for use in sampled-data control studies.

DESCRIPTION

A digital controller is constructed for the analysis of control problems which result when the controller input is a sampled signal obtained from a continuous process. The analysis of such sampled-data systems is usually achieved using Z-transforms [16]. In this example the coefficients of the Z-domain digital controller are specified by the user and are inputted to the digital program. The controller is designed to provide a "deadbeat" system response [17] for a first order plant, however, the controller is general enough for use in other types of sampled-data control problems. An introduction to sampled-data control systems may be found in Chapter 13, Automatic Control Engineering, by F. H. Raven [41].

ANALOG FUNCTION

The continuous first order plant $G(s) = 1/(\tau s + 1)$ is simulated on the analog and the controlled variable is sampled by an ADC channel.

DIGITAL FUNCTION

To act as a digital controller (see DIGITAL CONTROLLER THEORY section). Direct programming [7] was used in the controller simulation. The digital computer also controls the sampling of the plant output, computes the control action, and outputs this control action to the plant.

Both HOI and FORTRAN programs are used with FORTRAN sampling being controlled digitally by core cycle time with resolution to 1

millisecond. The HOI sampling is controlled by integrator monitoring with resolution to 0.1 seconds. The time required for calculating the control action upon receiving the plant error and implementing the control action should be only a small fraction of the sampling period. Again, the interpreter (HOI) execution time can prove prohibitive for small sampling periods [38].

RESULTS

Results for the first order plant designed for a deadbeat response to a step input with a sampling period of 1 second are shown in Figure 2.17. This figure shows the different responses for the FORTRAN controller and the HOI controller. Deadbeat controllers are extremely sensitive to controller parameters and timing inaccuracies [17], and hence the slightly inaccurate deadbeat response found in the HOI program (due to timing inaccuracies and significant HOI execution time). The HOI program could be used in less critical applications with larger sampling periods.

CONCLUSIONS

Because of the presence of the zero-order hold in the DAM circuit of the EAI 693 hybrid interface, the hybrid computer is ideally suited for the study of sampled-data control problems. Care should be taken when accurate results are dependent on calculation time and in these instances FORTRAN Integer Subroutines or Assembler language programs should be considered.

DIGITAL CONTROLLER THEORY

The pulse transfer function form a digital controller takes is

$$D(z) = \frac{a_0 + a_1 z^{-1} + a_2 z^{-2} + \dots + a_n z^{-n}}{b_0 + b_1 z^{-1} + b_2 z^{-2} + \dots + b_m z^{-m}} \quad (2.12)$$

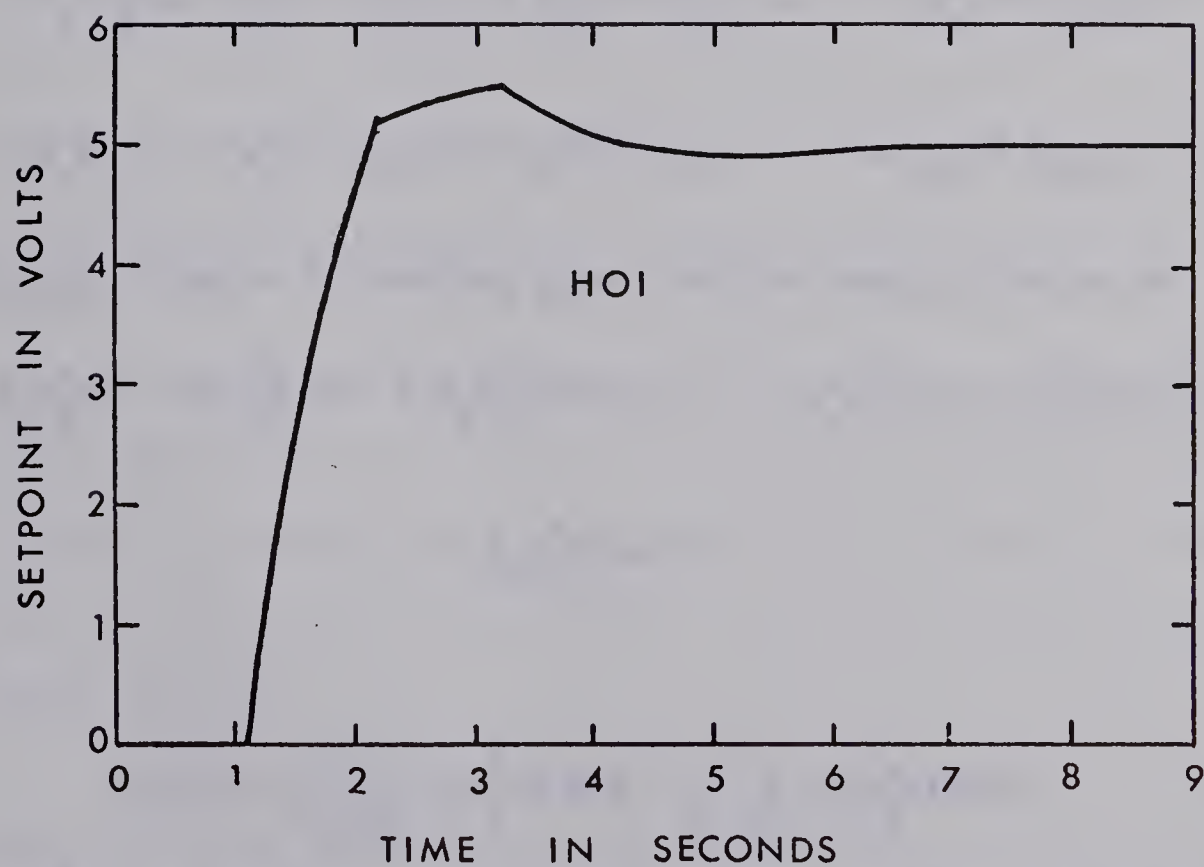
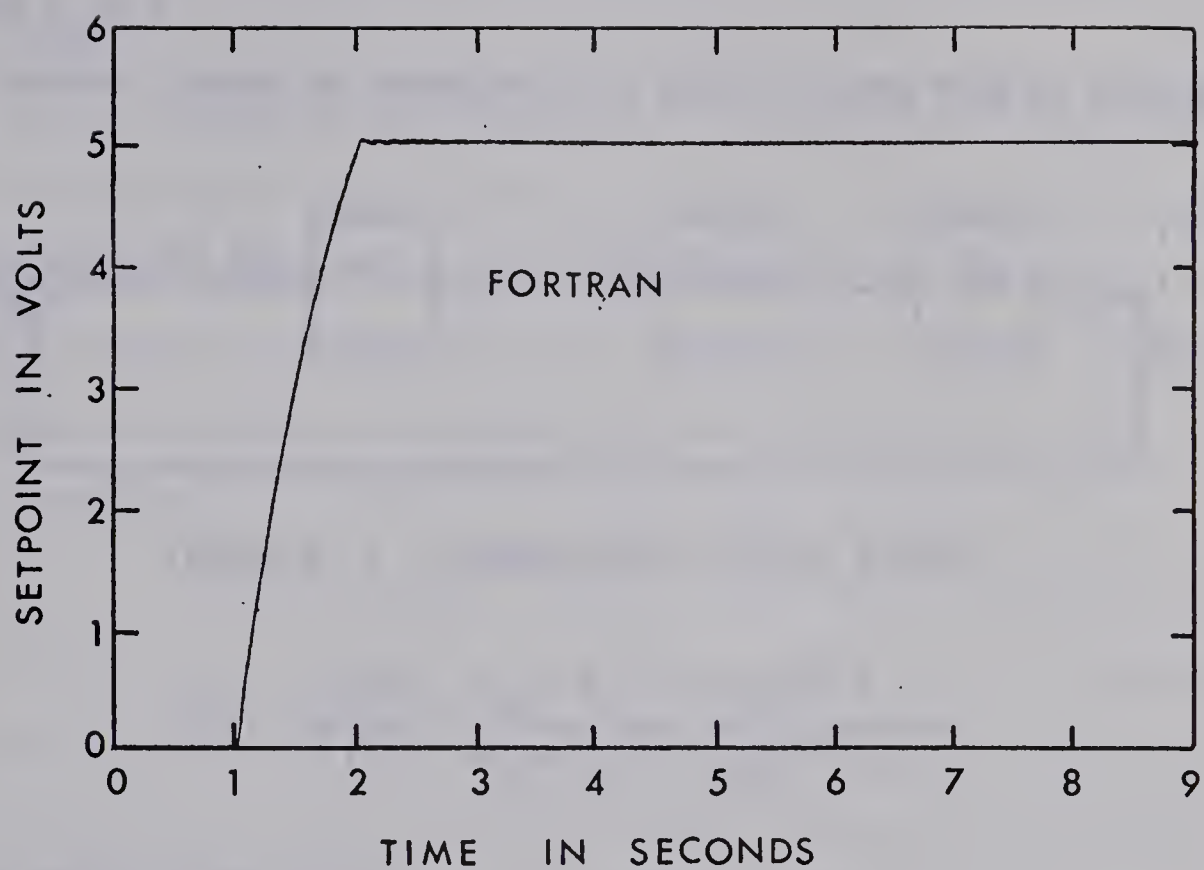


FIGURE 2.17 COMPARISON OF HOI AND FORTRAN DIGITAL DEADBEAT CONTROLLERS

where $b_0 \neq 0$

The control system is represented in block diagram form by Figure 2.18

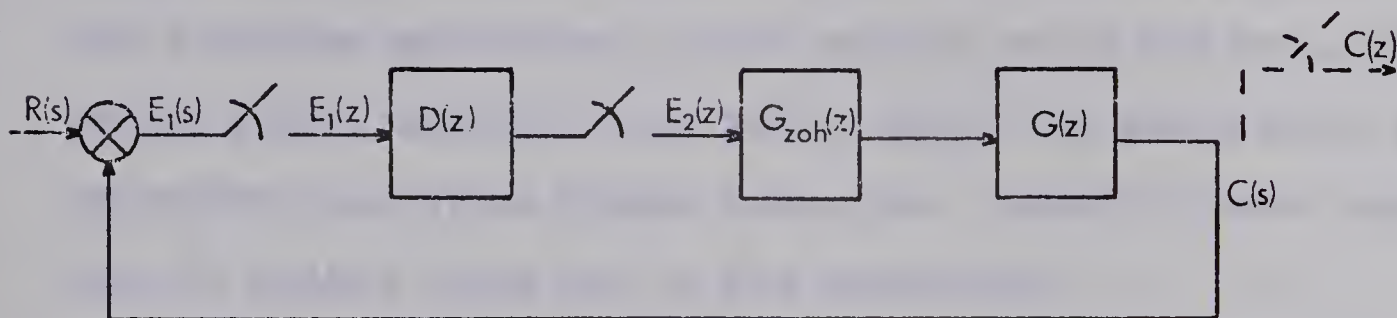


FIGURE 2.18 SAMPLED-DATA CONTROL SYSTEM

$$D(z) = \frac{E_2(z)}{E_1(z)} = \frac{a_0 + a_1 z^{-1} + a_2 z^{-2} + \dots}{b_0 + b_1 z^{-1} + b_2 z^{-2} + \dots} \quad (2.13)$$

Cross multiplying yields

$$b_0 E_2(z) + b_1 z^{-1} E_2(z) + b_2 z^{-2} E_2(z) + \dots + b_m z^{-m} E_2(z) = a_0 E_1(z) + a_1 z^{-1} E_1(z) + a_2 z^{-2} E_1(z) + \dots + a_n z^{-n} E_1(z) \quad (2.14)$$

Taking the inverse Z-transform gives the time domain solution as

$$b_0 e_2^*(t) + b_1 e_2^*(t-T) + b_2 e_2^*(t-2T) + \dots = a_0 e_1^*(t) + a_1 e_1^*(t-T) + \dots + a_n e_1^*(t-nT) \quad (2.15)$$

or

$$e_2^*(t) = \frac{1}{b_0} \sum_{k=0}^n a_k e_1^*(t-kT) - \frac{1}{b_0} \sum_{k=1}^m b_k e_2^*(t-kT) \quad (2.16)$$

where $e_2^*(t)$ is the control action at the present sampling instant

$e_1^*(t)$ is the plant error at the present sampling instant

T is the sampling period

2.4.6 Hybrid Optimization of the Sutro Weir Control System

PURPOSE

An optimization problem is used to illustrate a class of hybrid computer applications in which multiple analog runs are performed and the digital computer is used both to monitor the analog during a run and perform calculations between analog runs. Automatic plotter operation for multiple analog runs is also demonstrated.

DESCRIPTION

In this example, "optimum" controller constants are calculated for the Sutro Weir control system described in 2.4.1. Optimization techniques are used to determine controller settings for a $P + I$ controller which produce "optimal" process responses according to three different performance indices. The first performance index is minimum rise time subject to the constraint that the maximum overshoot be less than 20%. This criterion is often used when it is desired to drive a process to within specified limits in the shortest possible time. A simple exhaustive search is carried out in order to determine the optimum values of the controller constants, K_C and τ_I .

The second and third criteria, the integral time squared error (ITSE) and the integral squared error (ISE), are common in many control schemes. A systematic, one dimensional search is used to discover the values of the proportional gain, K_C , that minimize these criteria.

ANALOG FUNCTION

To simulate the Sutro Weir equipment (Section 2.4.1) with the analog output h_2 being monitored by an ADC channel. In the first program (minimum time criterion) timing is controlled by monitoring an integrator via an ADC channel. In the second program (ISE and ITSE)

timing is controlled by a "high" signal into a sense line. The high signal is generated by the analog counter [38].

DIGITAL FUNCTION

To input initial controller constants, to control the analog plotter operation, to monitor the analog during a simulation run in order to evaluate a performance criterion, to calculate new controller constants between analog runs, and to use the calculated controller constants to set potentiometers for another analog run [38].

RESULTS

Figure 2.19 shows the output of one of the six runs incrementing τ_I but holding K_C constant in the rise time, overshoot optimization program. From the results of the runs, a value of $K_C = 2.75$ and $\tau_I = 1.1$ minutes gives a minimum rise time with an overshoot of 18.75% [38]. Better resolution can be obtained in the rise time calculations if time scaling on the analog circuit is decreased.

Figure 2.20 shows the effect of K_C on the ITSE criterion for a step change in setpoint with a τ_I value of 1 minute. A final K_C value of 3.7 was found to minimize the ITSE criterion for a setpoint change of 6 inches. Figure 2.21 shows the automatic plotter output for a load change of 0.7 cu. ft. per minute. A controller gain of 14.5 (the gain limit of the physical controller) minimized the ITSE criterion for this load change and a τ_I of 1 minute.

Figure 2.22 illustrates the plotter output for the minimization of the ISE criterion for a setpoint change of 6 inches and an integral time of 1 minute. An optimum gain of 6.9 was discovered in this case.

CONCLUSIONS

The preceeding results illustrate the general method for using the hybrid computer to solve an optimization problem. The number of runs

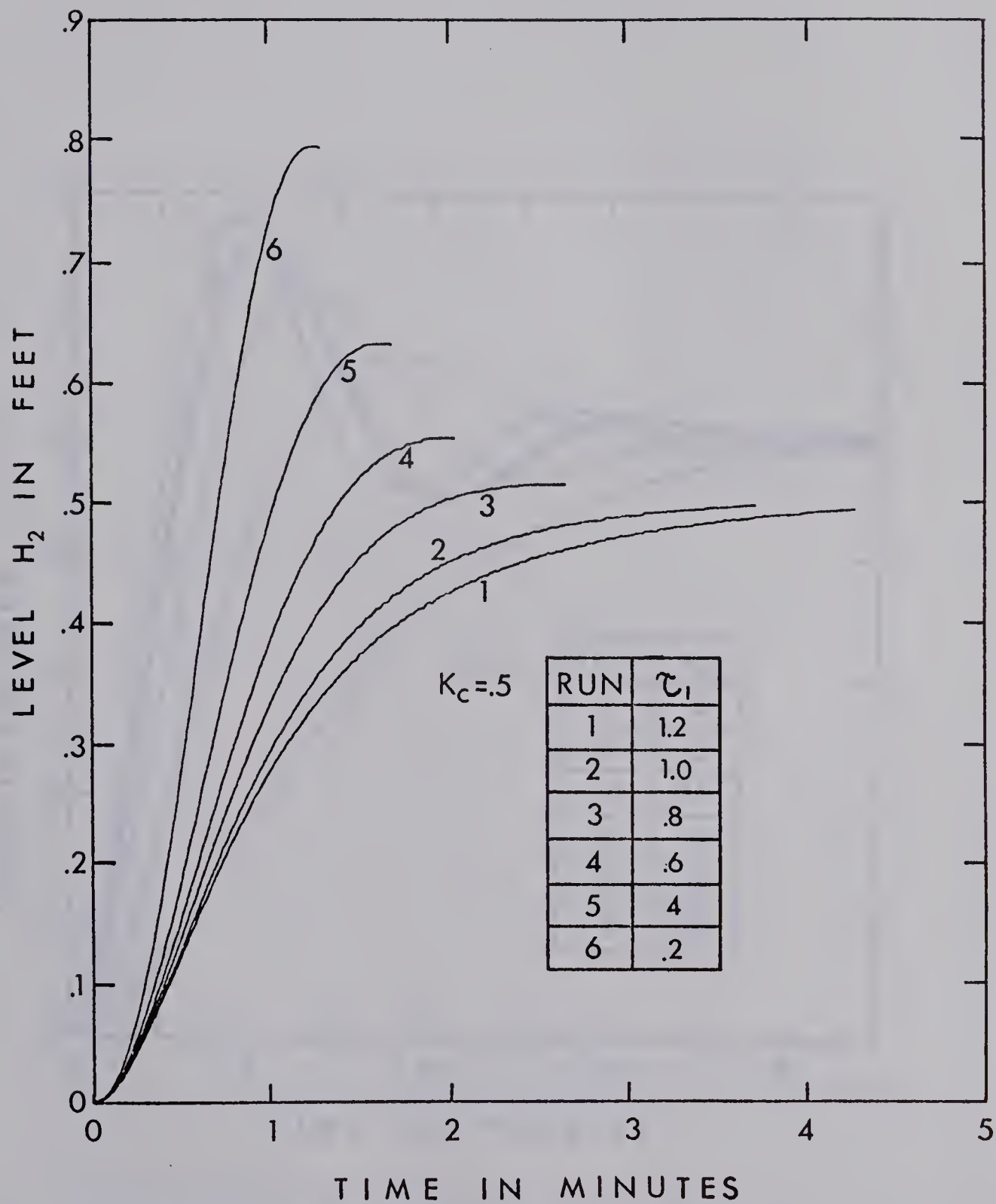


FIGURE 2.19 OPTIMIZATION OF RISE TIME OVERSHOOT CRITERION
SETPOINT CHANGE .5 FEET

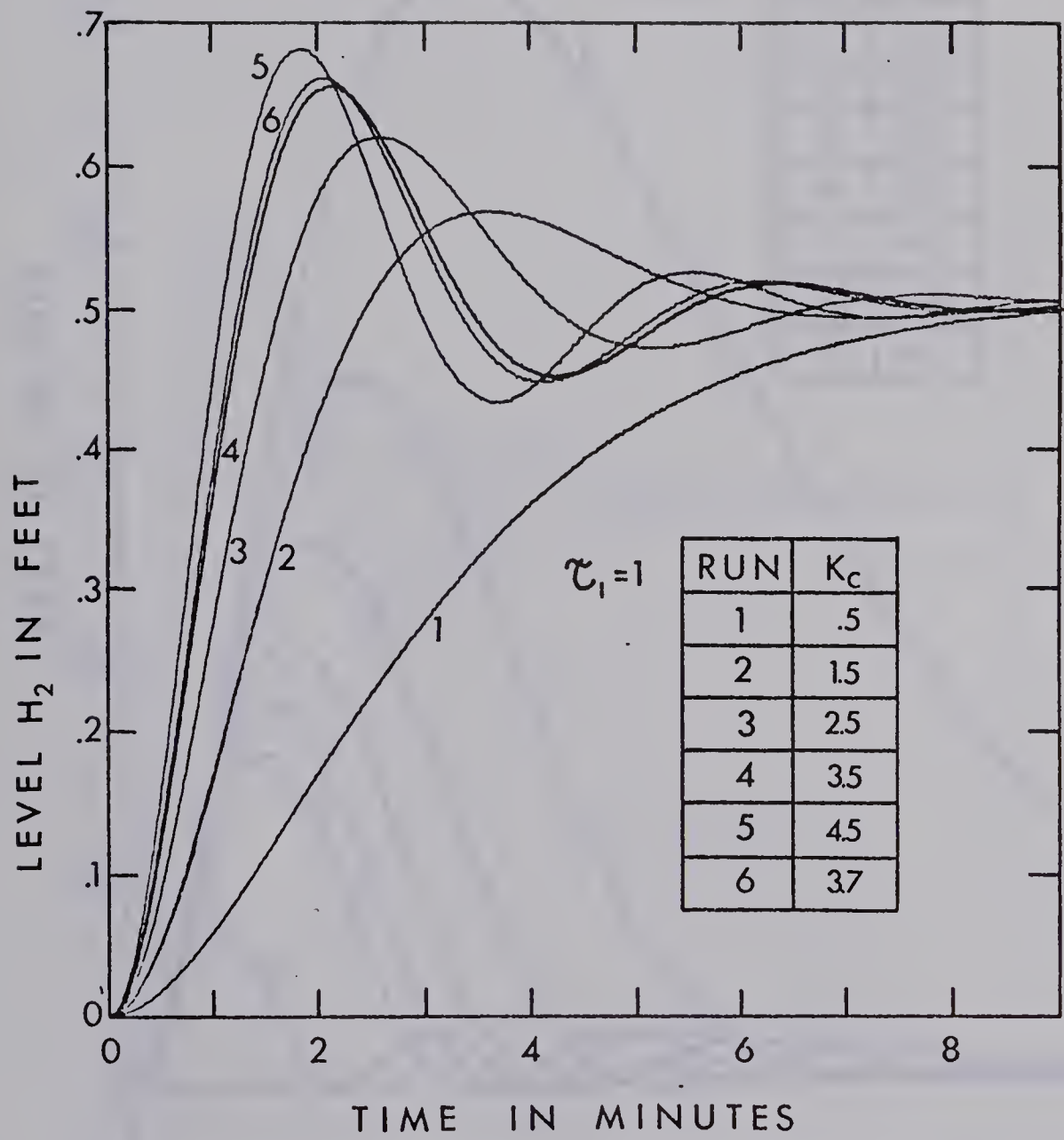


FIGURE 2.20 OPTIMIZATION WITH ITSE CRITERION
SETPOINT CHANGE OF 0.5 FEET IN H_2

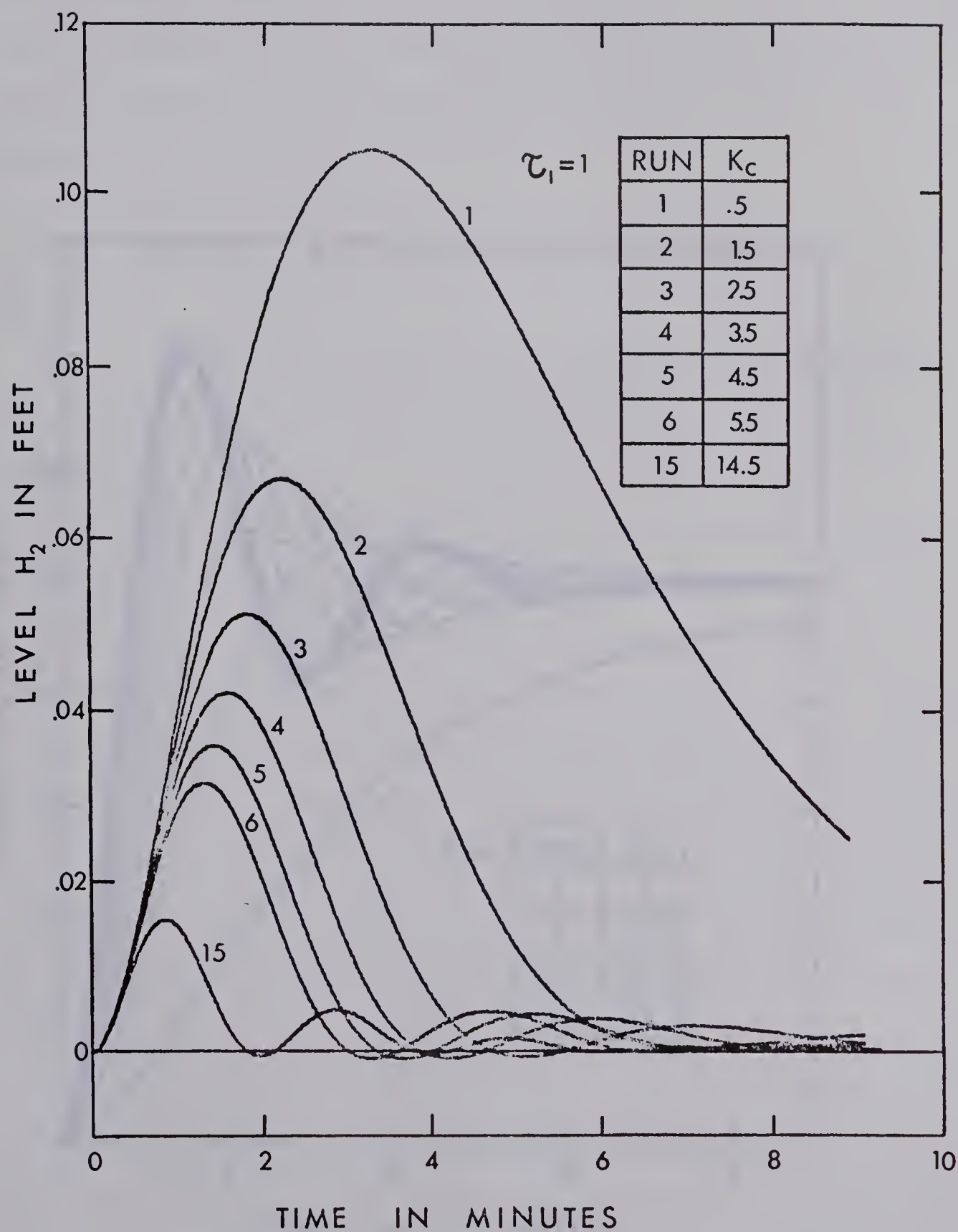


FIGURE 2.21 OPTIMIZATION WITH ITSE CRITERION
LOAD CHANGE OF 0.7 CU. FEET PER MINUTE

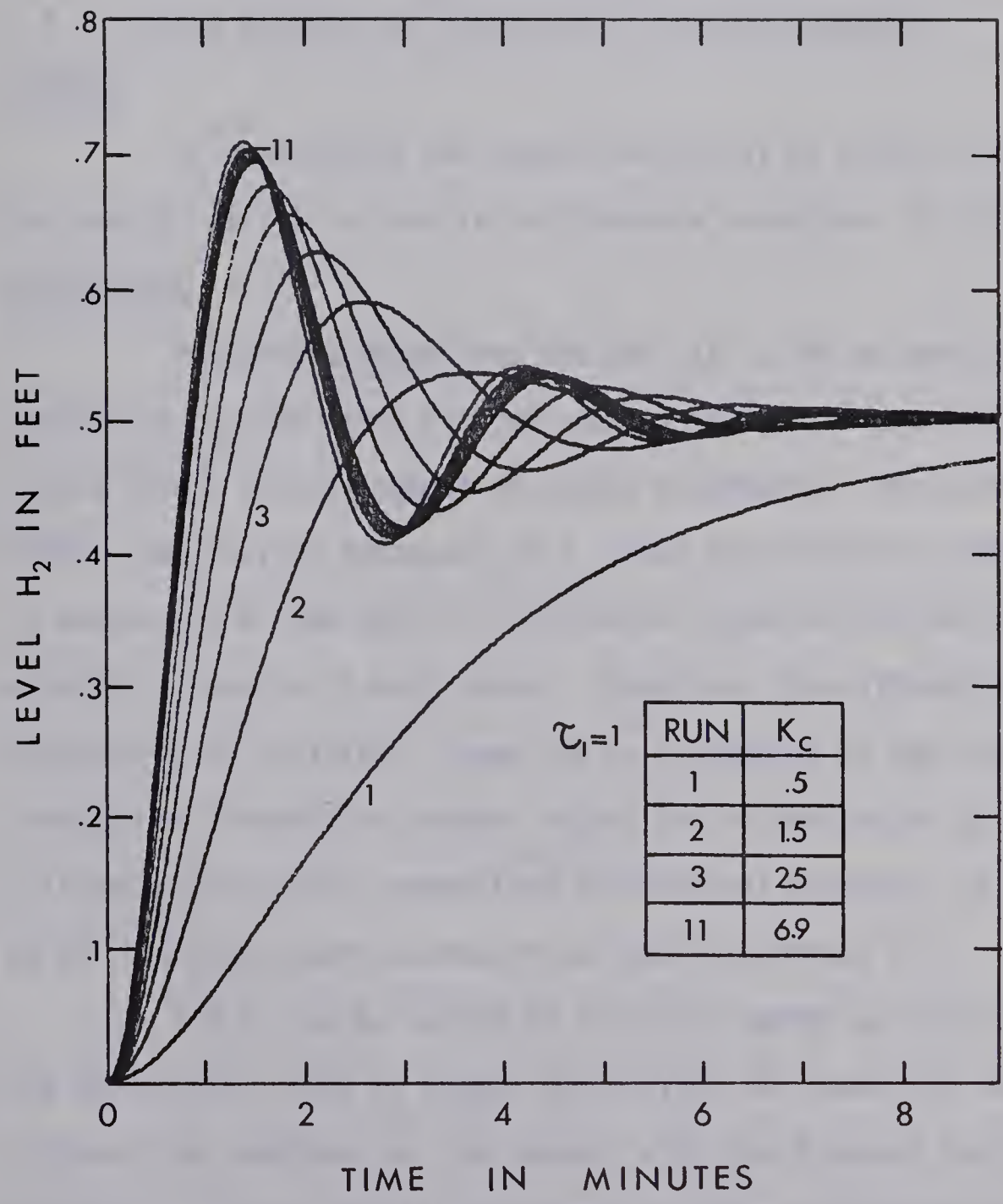


FIGURE 2.22 OPTIMIZATION WITH ISE CRITERION
SETPOINT CHANGE OF 0.5 FEET

for a given length of time may be increased by operating the analog in the repetitive operation mode or by increasing integrator speed. Other, more efficient, optimization techniques (e.g. golden section and gradient) could be used; however, the procedure is generally the same. The analog simulates the system to be optimized, while the digital monitors the analog, evaluates the performance criterion and makes the necessary optimization calculations.

2.4.7 Hybrid Solution of Partial Differential Equations

PURPOSE

To demonstrate the repetitive use of an analog integrator in the hybrid solution of partial differential equations (P.D.E.).

DESCRIPTION

A hybrid computer has the ability to use an analog integrator repeatedly in order that problems containing many integrations may be solved with a limited number of analog components. For naturally discrete, time varying processes (e.g. plate distillation columns, reactors in series), the same type of differential equation may describe the physical situation of each stage. Therefore, the differential equation describing the individual stage can be programmed on the analog and the transfer of information between stages can be controlled by the digital. This method of solving repetitive differential equations is referred to as the discrete-space-discrete-time (DSDT) technique [6].

P.D.E. may be solved in a similar manner by discretizing one of the derivatives (time or space) and solving the resulting set of ordinary differential equations on the analog, with the discrete portion solved digitally. If the spatial coordinate is solved continuously and time is incremented digitally, the method of solution is referred to as the

continuous-space-discrete-time (CSDT) technique. The CSDT method is illustrated in this example by solving the P.D.E. that results from heat balances on a tubular heat exchanger (see DERIVATION OF PROCESS MODEL).

ANALOG FUNCTION

To solve the spatial differential equation that arises when modelling a tubular heat exchanger [38].

DIGITAL FUNCTION

To increment time and to accumulate, store and replay data gathered from the analog in order to numerically solve the time discretized differential equation. The temperature data at the j^{th} sampling instant, T_1^j and T_2^j , are sampled every 0.01 feet along the length of the exchanger to give a close approximation to a continuous function in the spatial direction [38]. This data is returned to the analog as T_1^{j-1} and T_2^{j-1} in the next time increment (see DERIVATION OF PROCESS MODEL).

RESULTS

The temperature profile for tube fluid temperature is illustrated in Figure 2.23 (0.2 second plotting interval). The temperature profile for tube wall temperature is shown in Figure 2.24. Figure 2.25 illustrates the response of the tube fluid temperature to a step change of +100°F in the tube inlet temperature.

CONCLUSIONS

Figure 2.23 compares the theoretical steady state results with the hybrid results after 5 seconds. The agreement is excellent.

The solution of P.D.E. on a hybrid computer has been studied in great detail. At very rapid solution speeds, sampling error can be significant and many published papers have dealt with this problem. Also,

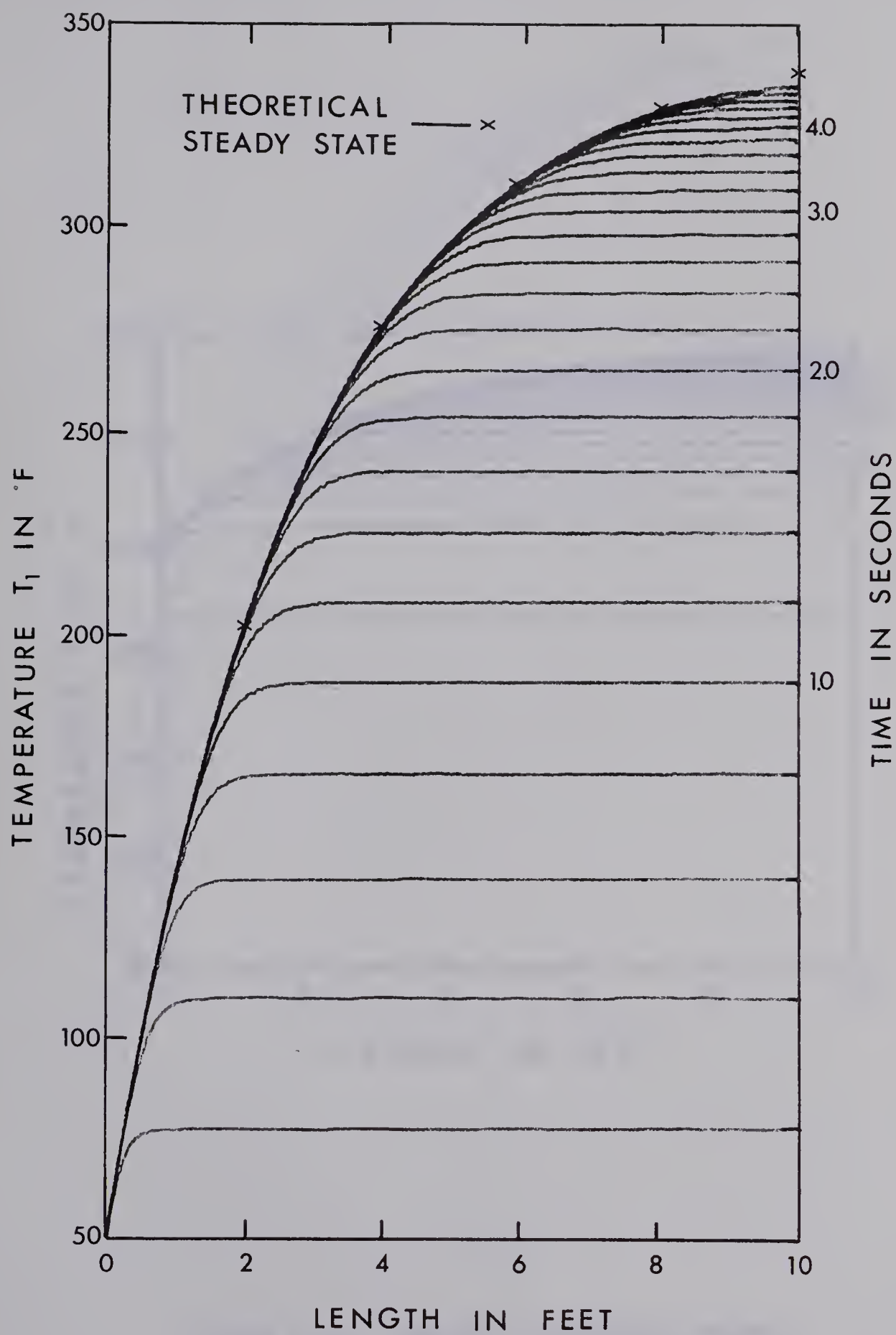


FIGURE 2.23 TUBE FLUID TEMPERATURE PROFILE

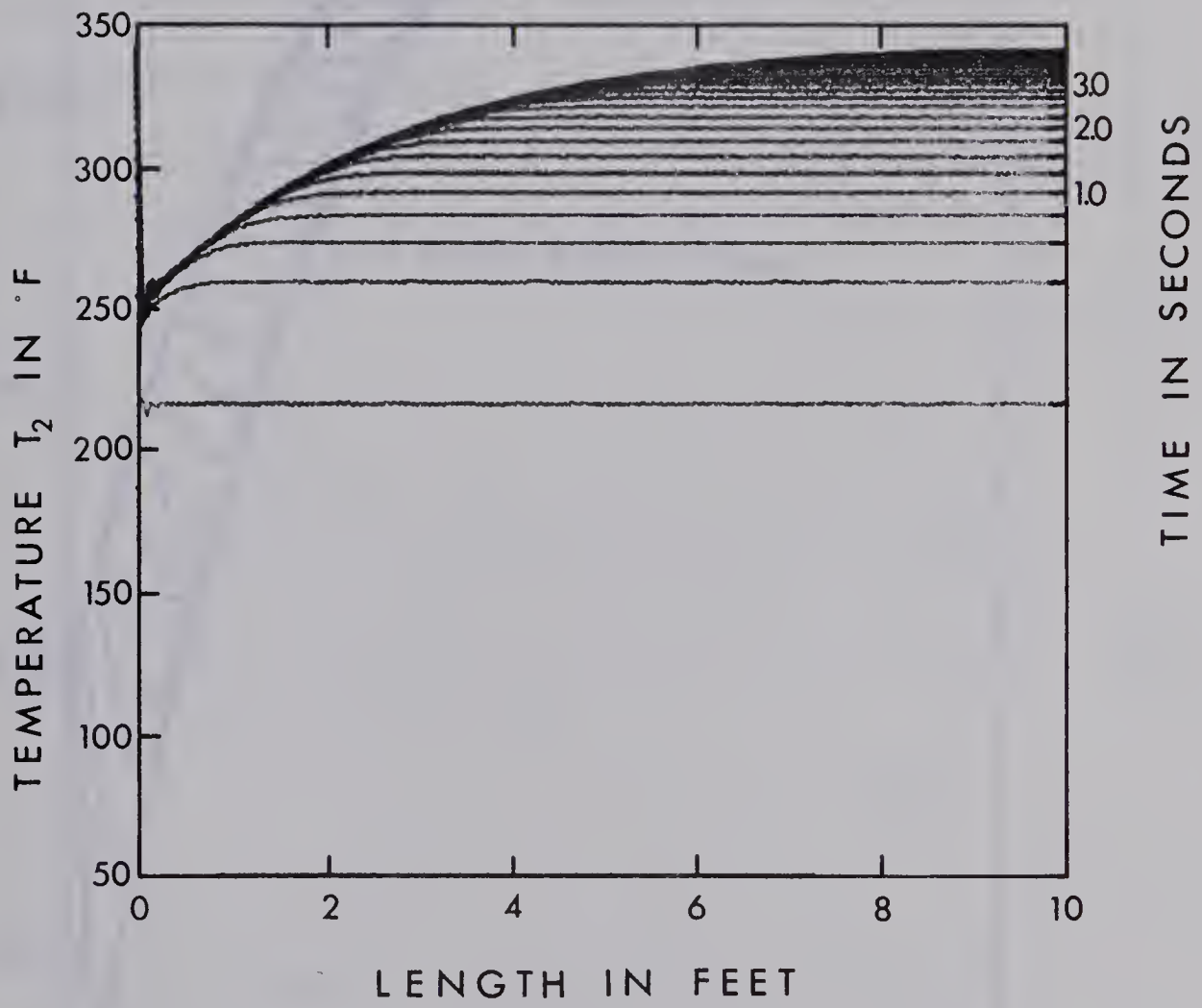


FIGURE 2.24 TUBE WALL TEMPERATURE PROFILE

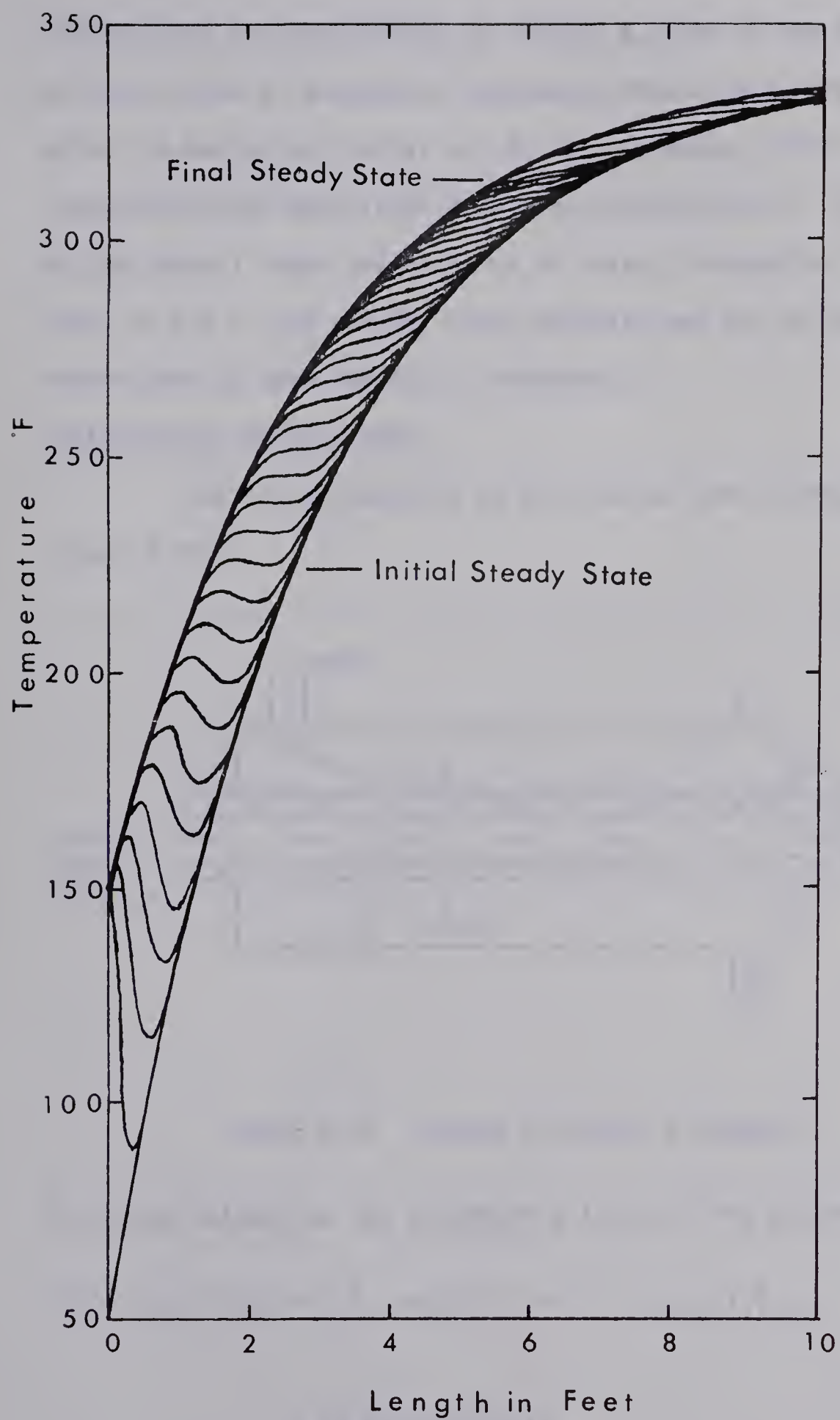


FIGURE 2.25 TUBE FLUID TEMPERATURE PROFILE,
100°F STEP IN INLET TEMPERATURE

difficulties are encountered in finding a value of the time increment Δt that yields an acceptable compromise between the effect of roundoff error (in analog to digital and digital to analog conversion) and the truncation error associated with time discretization. However, because of the overall speed and accuracy of analog integration, hybrid solutions to P.D.E. are usually quite accurate and can be obtained much faster than by pure numerical techniques.

DERIVATION OF PROCESS MODEL

The system modelled is the tubular heat exchanger described in Figure 2.26.

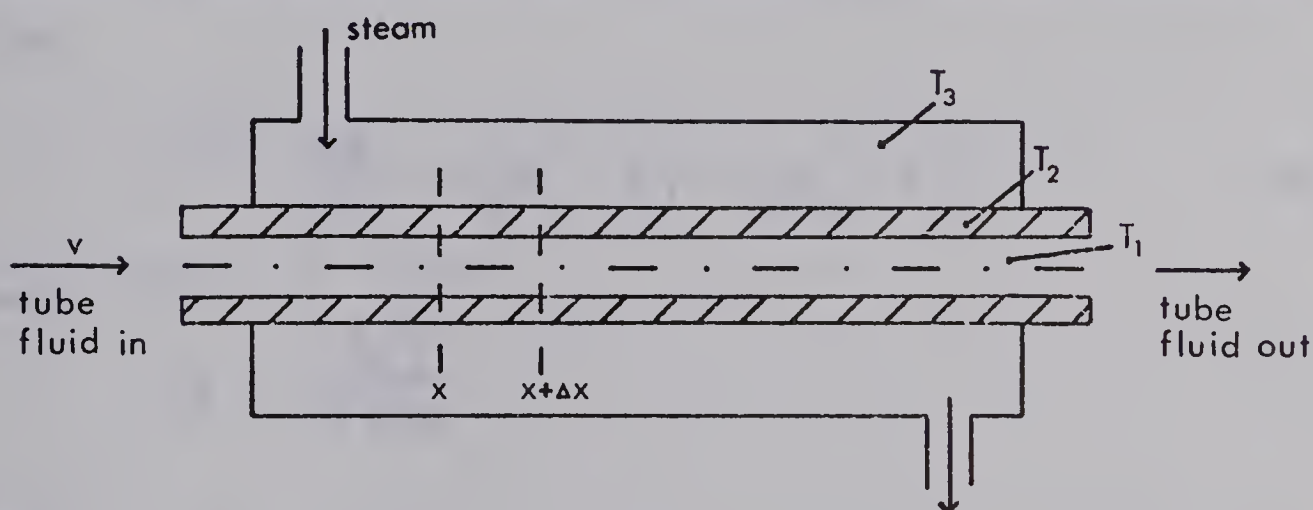


FIGURE 2.26 SINGLE PASS HEAT EXCHANGER

An energy balance on the increment x to Δx of the exchanger yields

$$\begin{aligned} (A_1 v \rho_1 C_{p1} T_1)|_x + h_1 P_1 \Delta x (T_2 - T_1) &= (A_1 v \rho_1 C_{p1} T_1)|_{x+\Delta x} \\ &+ \frac{\partial}{\partial t} \{ \Delta x A_1 \rho_1 C_{p1} T_1 \} \end{aligned} \quad (2.17)$$

Assume the physical parameters; A_1 = area of tube, ρ_1 = density of tube fluid, C_{p1} = heat capacity of tube fluid, P_1 = perimeter of tube available

for heat transfer; are constant. Divide by Δx and take the limit as $\Delta x \rightarrow 0$

$$A_1 \rho_1 C_{p1} \frac{\partial T_1}{\partial t} + A_1 \rho_1 C_{p1} v \frac{\partial T_1}{\partial x} = h_1 P_1 (T_2 - T_1) \quad (2.18)$$

Rearranging

$$\frac{\partial T_1}{\partial t} + v \frac{\partial T_1}{\partial x} = K_1 (T_2 - T_1) \quad (2.19)$$

where

$$K_1 = \frac{h_1 P_1}{A_1 \rho_1 C_{p1}}$$

A similar balance on the tube wall assuming T_2 to be independent of x gives

$$\frac{\partial T_2}{\partial t} = K_2 (T_3 - T_2) - K_3 (T_2 - T_1) \quad (2.20)$$

where

$$K_2 = \frac{h_2 P_2}{A_2 \rho_2 C_{p2}}$$

and

$$K_3 = \frac{h_1 P_1}{A_2 \rho_2 C_{p2}}$$

T_3 is the temperature of the saturated steam and therefore is constant with time and length. The parameter values are those used by Vichnevetsky and Tomalesky [32]:

$$\begin{array}{lll} L = 10 \text{ ft} & K_1 = 1 \text{ sec}^{-1} & K_3 = 5 \text{ sec}^{-1} \\ v = 2 \text{ ft/sec} & K_2 = 10 \text{ sec}^{-1} & \end{array}$$

A numerical backwards difference formula is used to approximate the time

derivatives. Equations (2.19) and (2.20) become

$$\frac{T_1^j - T_1^{j-1}}{\Delta t} + v \frac{dT_1^j}{dx} = K_1(T_2^j - T_1^j) \quad (2.21)$$

and

$$\frac{T_2^j - T_2^{j-1}}{\Delta t} = K_2(T_3^j - T_2^j) - K_3(T_2^j - T_1^j) \quad (2.22)$$

Rearranging (2.21) and (2.22) gives the equations solved on the analog

$$\begin{aligned} \frac{dT_1^j}{dx} &= \frac{K_1}{v} T_2^j - \left(\frac{K_1}{v} + \frac{1}{\Delta t v} \right) T_1^j + \frac{T_1^{j-1}}{\Delta t v} \\ T_2^j &= \frac{T_2^{j-1}}{(1 + \Delta t K_2 + \Delta t K_3)} + \frac{\Delta t K_2 T_3^j}{(1 + \Delta t K_2 + \Delta t K_3)} + \frac{K_3 \Delta t}{(1 + \Delta t K_2 + \Delta t K_3)} T_1^j \end{aligned}$$

Δt was chosen as .05 seconds.

CHAPTER THREE

MODEL REFERENCE ADAPTIVE CONTROL BY LIAPUNOV'S DIRECT METHOD:

LITERATURE SURVEY AND BASIC EQUATIONS

3.1 INTRODUCTION

A fixed parameter control scheme cannot maintain "good" control in industrial processes which are highly nonlinear, time varying, operate over a wide range of process specifications, or have control systems designed on the basis of approximate mathematical models. Consequently, frequent tuning of control loops is required as the process operating conditions change. Model reference adaptive control (MRAC) is a control technique that changes the control policy to partially compensate for varying process conditions. A reference model of the desired closed-loop process dynamics is postulated; the adaptive control scheme then attempts to minimize the error between the process response and the reference model response when both are subjected to the same inputs. This chapter presents a brief historical survey of MRAC schemes, from single variable gradient techniques to the multivariable scheme based on Liapunov stability theorems that is used later in this study. The theory of multivariable model reference adaptive control designed by Liapunov's direct method is then presented. Extensions to existing theory are given for multivariable adaptive integral and setpoint control. Finally, the theory is applied to the design of a MRAC system for a pilot plant double effect evaporator.

3.2 LITERATURE SURVEY

Model reference adaptive control systems were developed in the late 1950's and early 1960's in the aircraft and aerospace industries for

applications where adequate control could not be achieved with a fixed parameter control design [1]. In many applications, because of model inaccuracy and process nonlinearities, the control scheme had to change as the process changed. Eveleigh ([1], Chapter 13) and Bristol [2] present summaries of early practical applications of adaptive control techniques including MRAC. Bristol also outlines the early single-input, single-output process applications using conventional analog controllers. He reported that adaptive control for nonlinear systems subjected to large setpoint changes "works in a trouble-free and insensitive manner independent of process, initial settings, disturbances, or set-point magnitude." ([2], page 561).

The early model reference adaptive control systems had the same objective as the later multivariable techniques: to minimize the error (or difference) between the outputs of the model and the physical process (see Figure 3.1).

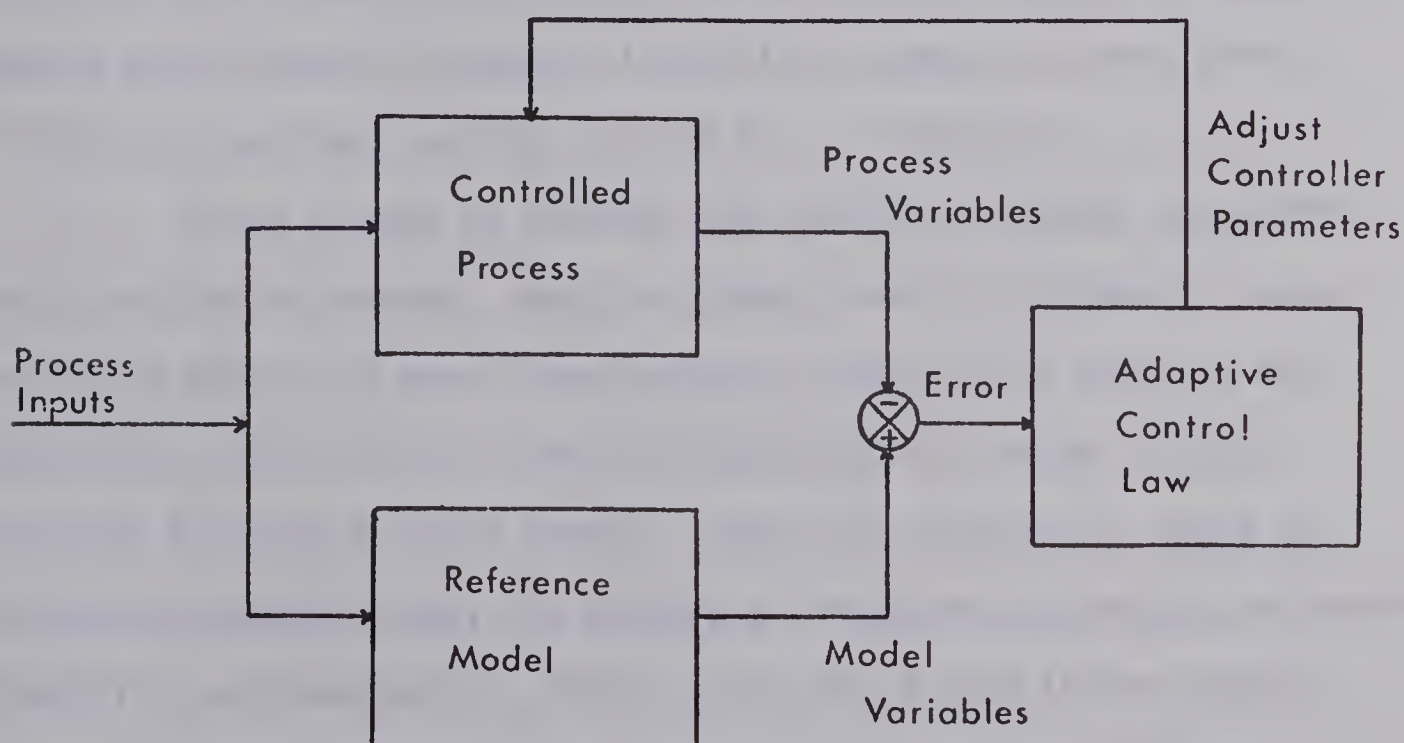


FIGURE 3.1 BLOCK DIAGRAM OF MODEL REFERENCE ADAPTIVE CONTROL

The early techniques used sensitivity functions and gradient-like searches to minimize a function of this error [1]. For example in the "M.I.T. technique" [23], the design objective is to minimize the integral of the error squared, $\int e^2 dt$, where e is defined as the error between the model response and the process response for the same input. A differential equation for adapting the controller parameters is obtained based on the gradient of the error with respect to the adapting parameters:

$$\frac{d\mathbf{g}}{dt} = -b e \nabla_{\mathbf{g}} e$$

where \mathbf{g} is the vector of parameters being adapted, $\nabla_{\mathbf{g}}$ denotes the gradient with respect to \mathbf{g} , and b is a positive constant. However, these gradient techniques fail to guarantee stability for even simple systems and are difficult to apply to multivariable systems [3]. Eveleigh ([1], Chapter 8) describes these gradient methods in greater detail while Parks [3] presents informative examples showing instability arising from adapting with the M.I.T. technique.

In an attempt to overcome the stability problems associated with gradient techniques, adaptive schemes based on Liapunov's second or direct method [4] were investigated by Grayson [4], Butchart and Shackcloth [5], Parks [3], and Shackcloth [6] for simple, single-variable transfer function models. Since this approach is based on stability considerations, the resulting closed-loop system has guaranteed stability and consequently, higher gains can be used in the adapting loops. Simulation studies [5] and a theoretical analysis [3] demonstrated that the Liapunov approach solves the stability problems

encountered using the gradient methods. Winsor and Roy [7] and Porter and Tatnall [8] extended the Liapunov analysis to multivariable, time-invariant systems presented as differential equation (state-space) models. Porter and Tatnall's simulation studies [8] demonstrated a dramatic improvement over fixed parameter control schemes with the Liapunov design method for second and third order systems.

The "dual problem" of process identification using a reference model has also made extensive use of Liapunov stability considerations. In the process identification problem, the error between the process and the reference model is minimized by changing the model parameters to obtain a more accurate representation of the physical process. Apparently, Rang [9] first developed the Liapunov model reference approach for process identification. Grayson [4] presents a good review of Rang's technique and related methods. Pazdera and Pottinger [10] demonstrated the effectiveness of the Liapunov method in simulation studies and were able to identify the process parameters using only process noise combined with large adaptive loop gains.

More recently, Porter and Tatnall [11] have extended their adaptive control analysis to time-varying systems and have provided an experimental demonstration of this technique for a hydraulic servo-mechanism modelled as a first-order system with time-varying gain [12]. Their experimental results tended to verify the simulation studies and showed greatly improved control over a fixed parameter scheme because of large variations in process parameters. No other experimental applications of MRAC systems designed by Liapunov's direct method have been reported.

Some interesting questions related to MRAC have yet to be

answered. One of these is discussed by Schooley and Pazdera [13] and Gromyko and Sankovskii [24] and involves the proper choice of the adaptive loop gains. Since the controlled system is guaranteed to be stable, all values of the adaptive loop gains can be used; however, in practice some stable responses are more desirable than others. Schooley and Pazdera [13] have investigated this problem and have attempted to eliminate loop gain sensitivity by adding feedforward control. Gromyko and Sankovskii [24] have optimized the values of adaptive loop gain using Pontryagin's Maximum Principle. Their work illustrates the improved control resulting from optimum loop gains in simulation studies. This problem is also extensively dealt with in succeeding chapters.

A few applications of MRAC to process control problems have been reported but deal exclusively with single-input, single-output systems which are presented as transfer function models, controlled using conventional PID controllers, and adapted using gradient techniques. Furthermore, experimental studies have only been reported on the earliest and simplest techniques [2]. Simulation results for nonlinear continuous stirred tank reactors [14,15,16] have shown great improvement in control when process operating conditions vary greatly (e.g. start-up, setpoint changes); however, no experimental confirmation of the simulation results has been reported.

Crandall and Stevens [14] investigated MRAC of a single chemical reaction occurring in a continuous stirred tank reactor (CSTR). They used a gradient technique to adapt the gain of a temperature control loop; their simulation studies demonstrated a large improvement over a fixed gain feedback control scheme. Casciano and Staffin [15] controlled reactor temperature by adapting the integral time of a

standard proportional-integral controller. Again improved control was reported. Ahlgren and Stevens [16] applied the gradient technique to all three modes of a PID controller for the same reactor example used by Crandall and Stevens. They also simultaneously adapted the parameters of two single variable controllers for reactor temperature and composition respectively. Excellent control was achieved over a wide range of process operating conditions. They also demonstrated their system was stable for certain large process disturbances but did not attempt a theoretical investigation of system stability.

The next section develops a MRAC system for a general multi-variable process using the Liapunov design procedure of Porter and Tatnall [8] to guarantee stability. The theory is then modified for an actual process in order that experimental verification of this method can be attempted.

3.3 THEORY

The dynamic behavior of many plants, including the double effect evaporator in the Department of Chemical and Petroleum Engineering, can be adequately approximated by a state-space model of the form

$$\dot{\underline{x}}_p = \underline{A}\underline{x}_p + \underline{B}\underline{u} + \underline{D}\underline{d} \quad (3.1)$$

where \underline{x}_p represents the n state variables

\underline{d} represents the p disturbances

\underline{u} represents the r controls

and \underline{A} , \underline{B} and \underline{D} are constant matrices of the appropriate dimensions.

Assuming multivariable feedforward-feedback control of the form

$$\underline{u} = \underline{K}_{FB} \underline{x}_p + \underline{K}_{FF} \underline{d} \quad (3.2)$$

yields a closed-loop process model

$$\dot{\underline{x}}_p = (\underline{A} + \underline{B} \underline{K}_{FB}) \underline{x}_p + (\underline{D} + \underline{B} \underline{K}_{FF}) \underline{d} \quad (3.3a)$$

or using the closed-loop process matrices \underline{A}_p and \underline{D}_p gives

$$\dot{\underline{x}}_p = \underline{A}_p \underline{x}_p + \underline{D}_p \underline{d}. \quad (3.3b)$$

For future reference, define the control matrices $\underline{\Gamma}$ and $\underline{\Omega}$ as

$$\underline{\Gamma} = \underline{B} \underline{K}_{FB} \quad (3.4)$$

$$\underline{\Omega} = \underline{B} \underline{K}_{FF}$$

A linear, asymptotically stable, n^{th} -order model of the desired closed-loop plant behavior is postulated as

$$\dot{\underline{x}}_m = \underline{A}_m \underline{x}_m + \underline{D}_m \underline{d} \quad (3.5)$$

where \underline{x}_m is the n -dimensional state vector for the reference model and \underline{A}_m and \underline{D}_m are specified to provide the desired transient and steady state behavior. The error, \underline{e} , between the model and the process is defined as

$$\underline{e} = \underline{x}_m - \underline{x}_p \quad (3.6)$$

The intent of this adaptive control technique is to make the plant and model behavior identical by changing the control matrices $\underline{\Gamma}$ and $\underline{\Omega}$. The technique for changing elements in $\underline{\Gamma}$ and $\underline{\Omega}$ develops from Liapunov's direct method of stability analysis [4,8].

Subtracting Equation (3.3b) from Equation (3.5) yields

$$\dot{\underline{e}} = \underline{A_m} \underline{e} + (\underline{A_m} - \underline{A_p}) \underline{x_p} + (\underline{D_m} - \underline{D_p}) \underline{d} \quad (3.7)$$

Consider the reduced system:

$$\dot{\underline{e}} = \underline{A_m} \underline{e} \quad (3.8)$$

This system is asymptotically stable since the model in Equation (3.5) is asymptotically stable. A Liapunov stability theorem states that for any asymptotically stable linear system, such as that described by Equation (3.8), there exists a positive-definite matrix \underline{P} that is the unique solution of

$$\underline{A_m}^T \underline{P} + \underline{P} \underline{A_m} = -\underline{Q} \quad (3.9)$$

where \underline{Q} is an arbitrary symmetric positive-definite matrix. The Liapunov function is then chosen as

$$V = \underline{e}^T \underline{P} \underline{e} \quad (3.10)$$

since \underline{P} is positive-definite. The total time derivative of the Liapunov function reduces to

$$\dot{V} = -\underline{e}^T \underline{Q} \underline{e} \quad (3.11)$$

which is negative-definite since \underline{Q} is assumed to be positive-definite.

For the system described by Equation (3.7) define

$$\underline{A_m} - \underline{A_p} = \underline{A} = [\alpha_{ij}] \quad (i, j = 1, 2, \dots, n) \quad (3.12)$$

and

$$\underline{D_m} - \underline{D_p} = \underline{\Lambda} = [\lambda_{ij}] \quad (i=1, 2, \dots, n; j=1, 2, \dots, p) \quad (3.13)$$

Following Porter and Tatnall [8], choose the Liapunov function to be the positive-definite quadratic form

$$V = \underline{e}^T \underline{P} \underline{e} + \sum_{i=1}^n \sum_{j=1}^n \frac{1}{\xi_{ij}} \alpha_{ij}^2 + \sum_{i=1}^n \sum_{j=1}^p \frac{1}{v_{ij}} \lambda_{ij}^2 \quad (3.14)$$

with $\xi_{ij} > 0$, $v_{ij} > 0$; ξ_{ij} and v_{ij} are adaptive loop gains, design parameters to be specified.

The Liapunov function defined by Equation (3.14) will be zero if, and only if,

$$\underline{e} = \underline{0}$$

$$\underline{A}_p = \underline{A}_m \quad (3.15)$$

$$\underline{D}_p = \underline{D}_m$$

The total time derivative of Equation (3.14) is given by

$$\dot{V} = \dot{\underline{e}}^T \underline{P} \underline{e} + \underline{e}^T \underline{P} \dot{\underline{e}} + \sum_{i=1}^n \sum_{j=1}^n \frac{2}{\xi_{ij}} \alpha_{ij} \dot{\alpha}_{ij} + \sum_{i=1}^n \sum_{j=1}^p \frac{2}{v_{ij}} \lambda_{ij} \dot{\lambda}_{ij} \quad (3.16)$$

Substituting Equation (3.7) for $\dot{\underline{e}}$, and using Equation (3.9) with $\underline{Q} = \underline{I}$ yields

$$\begin{aligned} \dot{V} = & - \underline{e}^T \underline{e} + 2 \sum_{i=1}^n \sum_{j=1}^n \left(\frac{1}{\xi_{ij}} \dot{\alpha}_{ij} + x_{pj} \underline{e}^T \underline{P}_{-i} \right) \alpha_{ij} \\ & + 2 \sum_{i=1}^n \sum_{j=1}^p \left(\frac{1}{v_{ij}} \dot{\lambda}_{ij} + d_j \underline{e}^T \underline{P}_{-i} \right) \lambda_{ij} \end{aligned} \quad (3.17)$$

where \underline{P}_{-i} denotes the i^{th} column of matrix \underline{P} . For stability, \dot{V} must be negative-semidefinite which requires that the last two terms of Equation (3.17) be identically equal to zero. This will only occur if $\alpha_{ij} = 0$

and $\lambda_{ij} = 0$ (i.e. the model and the process are identical) or if

$$\frac{1}{\xi_{ij}} \dot{\alpha}_{ij} + x_{pj} \underline{e}_{-i}^T = 0 \quad (i, j = 1, \dots, n) \quad (3.18)$$

and

$$\frac{1}{v_{ij}} \dot{\lambda}_{ij} + d_j \underline{e}_{-i}^T = 0 \quad (i = 1, \dots, n; j = 1, \dots, p) \quad (3.19)$$

leaving

$$\dot{V} = - \underline{e}^T \underline{e}$$

which is negative-semidefinite in \underline{e} , α_{ij} and λ_{ij} . Since $\dot{V} = 0$ if, and only if, $\underline{e} = \underline{0}$ and since V is positive-definite, it follows that V will decrease monotonically with time until V either equals zero or some positive constant. If $V = 0$ then $\underline{e} = \underline{0}$ and $\alpha_{ij} = 0$ and $\lambda_{ij} = 0$; alternatively, if V eventually attains a positive value, then $\underline{e} = \underline{0}$ but $\alpha_{ij} \neq 0$ and/or $\lambda_{ij} \neq 0$. If the latter case occurs, $\underline{A}_m - \underline{A}_p = [\alpha_{ij}] \neq \underline{0}$ and/or $\underline{D}_m - \underline{D}_p = [\lambda_{ij}] \neq \underline{0}$. Consequently, the closed-loop model and process matrices do not have to be equal for the error between the process and model states to be zero. This point is emphasized because it arises in the evaporator application.

Equations (3.18) and (3.19) can be rearranged to give

$$\dot{\alpha}_{ij} = - x_{pj} \underline{e}_{-i}^T \xi_{ij} \quad (3.20)$$

and

$$\dot{\lambda}_{ij} = - d_j \underline{e}_{-i}^T v_{ij} \quad (3.21)$$

Equations (3.20) and (3.21) define how the elements of the matrices

$\underline{A}_m - \underline{A}_p$ and $\underline{D}_m - \underline{D}_p$ should adapt. However, the elements which can be physically manipulated are \underline{r} and \underline{u} as defined by Equation (3.4). The

corresponding equations for the elements of these matrices are readily derived by differentiating Equations (3.12) and (3.13) using the assumption that the open-loop plant and model matrices are time-invariant.

$$[\dot{\alpha}_{ij}] = \dot{\underline{A}}_m - \dot{\underline{A}}_p = -\dot{\underline{A}}_p = -(\dot{\underline{A}} + \dot{\underline{\Gamma}}) = -\dot{\underline{\Gamma}} = -[\dot{\gamma}_{ij}] \quad (3.22)$$

$$[\dot{\lambda}_{ij}] = \dot{\underline{D}}_m - \dot{\underline{D}}_p = -\dot{\underline{D}}_p = -(\dot{\underline{D}} + \dot{\underline{\Omega}}) = -\dot{\underline{\Omega}} = -[\dot{\omega}_{ij}] \quad (3.23)$$

Therefore, Equations (3.22) and (3.23) combined with Equations (3.20) and (3.21) yield the following two adaptive control laws for changing the elements of $\underline{\Gamma}$ and $\underline{\Omega}$.

$$\dot{\gamma}_{ij} = x_{pj} e^T \underline{P}_i \xi_{ij} \quad (3.24)$$

$$\dot{\omega}_{ij} = d_j e^T \underline{P}_i v_{ij} \quad (3.25)$$

The block diagram in Figure 3.2 reviews the interrelations of the equations in this adaptive control scheme.

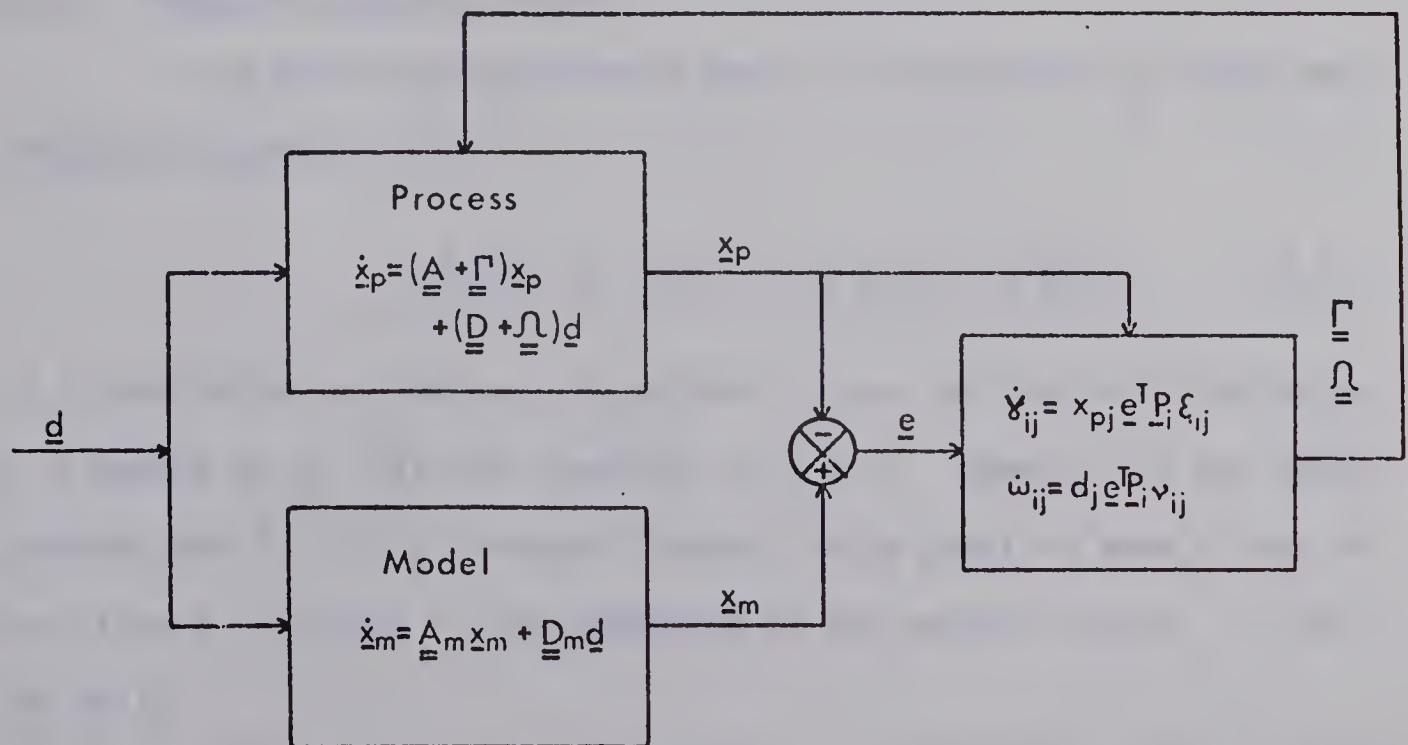


FIGURE 3.2 BLOCK DIAGRAM OF MRAC VIA LIAPUNOV'S DIRECT METHOD

The MRAC scheme based on Liapunov's direct method can be considered to be nonlinear due to the adapting algorithms given by Equations (3.24) and (3.25). The method requires measurements or estimates of all the process states, \underline{x}_p , and disturbances, and also the ability to change the elements of $\underline{r}(t)$ and $\underline{\Omega}(t)$.

3.4 EXTENSIONS TO THE EXISTING THEORY: ADAPTIVE INTEGRAL AND SETPOINT CONTROL

The control theory just presented considers feedforward and proportional feedback control. For many processes, integral control action is desirable in order that offset in some of the variables may be eliminated. Also, setpoint changes cause the process conditions to change and thus require the parameters in the linear process model to be updated. The theory for adding adaptive integral and setpoint control is now developed as an extension of the feedforward-feedback theory just presented.

3.4.1 Adaptive Integral Control

The open-loop state-space model of the process is again described by Equation (3.1)

$$\dot{\underline{x}}_p(t) = \underline{A} \underline{x}_p(t) + \underline{B} \underline{u}(t) + \underline{D} \underline{d}(t) \quad (3.1)$$

It is desirable to eliminate the offset in some of the state variables, \underline{y} , a subset of \underline{x}_p . Let the dimension of \underline{y} be q . Newell [17] has demonstrated that for all q "integral states" to be equal to zero, q must be less than or equal to r , the dimension of the control vector, \underline{u} . We can write

$$\underline{y} = \underline{C} \underline{x}_p \quad (3.26)$$

where \underline{C} is specified to make \underline{y} the desired subset of \underline{x}_p .

Define a new set of state variables \underline{z} as

$$\underline{z} = \int_0^t \underline{y} \, dt \quad (3.27)$$

or

$$\dot{\underline{z}} = \underline{y} \quad (3.28)$$

Equations (3.28) and (3.26) give

$$\dot{\underline{z}} = \underline{C} \underline{x}_p \quad (3.29)$$

Augment the state vector, \underline{x}_p , with the new states \underline{z} by using Equations (3.29) and (3.1)

$$\begin{bmatrix} \dot{\underline{x}}_p \\ \dot{\underline{z}} \end{bmatrix} = \begin{bmatrix} \underline{A} & \underline{0} \\ \underline{C} & \underline{0} \end{bmatrix} \begin{bmatrix} \underline{x}_p \\ \underline{z} \end{bmatrix} + \begin{bmatrix} \underline{B} \\ \underline{0} \end{bmatrix} \underline{u} + \begin{bmatrix} \underline{D} \\ \underline{0} \end{bmatrix} \underline{d} \quad (3.30)$$

Define

$$\underline{x}'_p = \begin{bmatrix} \underline{x}_p \\ \underline{z} \end{bmatrix}; \quad \underline{A}' = \begin{bmatrix} \underline{A} & \underline{0} \\ \underline{C} & \underline{0} \end{bmatrix}; \quad \underline{B}' = \begin{bmatrix} \underline{B} \\ \underline{0} \end{bmatrix}; \quad \underline{D}' = \begin{bmatrix} \underline{D} \\ \underline{0} \end{bmatrix} \quad (3.31)$$

A feedback control law is now used for the augmented system

$$\underline{u}(t) = \underline{K}' \underline{x}'_p(t) \quad (3.32)$$

Define

$$\underline{K}' = [\underline{K}_{FB}, \underline{K}_I] \quad (3.33)$$

Expanding Equation (3.32) using Equations (3.31), (3.28) and (3.27) yields the proportional integral control action

$$\underline{u} = \underline{K}_{FB} \underline{x}_p + \underline{K}_I \int_0^t y \, dt \quad (3.34)$$

Substituting Equation (3.32) into Equation (3.30) yields

$$\dot{\underline{x}}'_p = [\underline{A}' + \underline{B}' \underline{K}'] \underline{x}'_p + \underline{D}' \underline{d} \quad (3.35)$$

Equation (3.35) is now in the form of Equation (3.3a) (without feed-forward control) and the adaptive control law defined by Equation (3.24) can be used to generate the elements of \underline{K}' and hence \underline{K}_{FB} and \underline{K}_I .

The addition of integral control adds more elements to be calculated by the adaptive control law. The number of adaptive control calculations increases as the square of the augmented state vector so integral action can greatly increase the adaptive control calculation time. The dimension of \underline{K}' is $n+q \times r$ instead of $n \times r$ for \underline{K}_{FB} . The matrices for the augmented reference model

$$\dot{\underline{x}}'_m = \underline{A}'_m \underline{x}'_m + \underline{D}'_m \underline{d} \quad (3.36)$$

can be obtained from optimal control applied to the augmented state vector [17] or by other techniques.

3.4.2 Adaptive Setpoint Control

Setpoint changes are an important adaptive control application because when a setpoint change is made to a nonlinear system, the control action should adapt in order to maintain the best control at the new process operating conditions. A control law that has been derived from an open-loop linear model at one set of operating conditions cannot be expected to work as well at conditions far from where the linear model was obtained.

The open-loop dynamics of the system can again be described by Equation (3.1)

$$\dot{\underline{x}}_p = \underline{A} \underline{x}_p + \underline{B} \underline{u} + \underline{D} \underline{d} \quad (3.1)$$

Let the state variables that are subjected to setpoint changes be defined by

$$\underline{y} = \underline{C} \underline{x}_p \quad (3.37)$$

Again \underline{y} is a subset of \underline{x}_p as defined by matrix \underline{C} . The maximum dimension of \underline{y} is r , the dimension of the controls [17,25]. In other words, only a subset of the state variables equal to the number of control variables can have their setpoints arbitrarily specified and have the remaining states stay at their original setpoint.

A control law that accounts for setpoint changes is of the form

$$\underline{u}(t) = \underline{K}_{FB} \underline{x}_p(t) + \underline{K}_{FF} \underline{d}(t) + \underline{K}_{sp} \underline{y}_{sp}(t) \quad (3.38)$$

where \underline{y}_{sp} is the desired value of \underline{y} and can be time-varying. Using the setpoint vector to augment the disturbance vector

$$\underline{u}(t) = \underline{K}_{FB} \underline{x}_p(t) + \underline{K}_{FF}' \underline{d}'(t) \quad (3.39)$$

where

$$\underline{K}_{FF}' = [\underline{K}_{FF} \quad \underline{K}_{sp}] \quad (3.40)$$

$$\underline{d}' = \begin{bmatrix} \underline{d} \\ \underline{y}_{sp} \end{bmatrix} \quad (3.41)$$

Substituting Equation (3.38) into Equation (3.1) yields

$$\dot{\underline{x}}_p = (\underline{A} + \underline{B} \underline{K}_{FB}) \underline{x}_p + (\underline{D} + \underline{B} \underline{K}_{FF}) \underline{d} + \underline{B} \underline{K}_{sp} \underline{y}_{sp} \quad (3.42)$$

Define

$$\underline{D}' = [\underline{D}, \underline{0}] \quad (3.43)$$

Substituting Equations (3.43), (3.41) and (3.40) into Equation (3.42) yields

$$\dot{\underline{x}}_p = (\underline{A} + \underline{B} \underline{K}_{FB}) \underline{x}_p + (\underline{D}' + \underline{B} \underline{K}_{FF}') \underline{d}' \quad (3.44)$$

This is in the standard form of Equation (3.3a) and the adaptive control law for adapting the feedforward matrix as described by Equation (3.25) can be used. The resulting control configuration, feedback feedforward setpoint control, again has the disadvantage of requiring additional adaptive control calculations. The increase in time required is proportional to the square of the dimension of the \underline{y} vector.

The model matrices in the closed-loop model equation

$$\dot{\underline{x}}_m = \underline{A}_m \underline{x}_m + \underline{D}'_m \underline{d}' \quad (3.45)$$

can be determined from a modification of the optimal control problem [17,25] or from other considerations such as state driving.

Both integral and setpoint adaptive control can be used simultaneously by augmenting the state vector for integral control and the disturbance vector for setpoint control. Newell [17,25] has considered these extensions to the standard optimal regulator problem. The resulting control scheme contains feedforward and setpoint modes as well as proportional plus integral feedback control. That is a control law results of the form

$$\underline{u}(t) = \underline{K}_{FB} \underline{x}_p(t) + \underline{K}_I \int_0^t \underline{y}(t) dt + \underline{K}_{FF} \underline{d}(t) + \underline{K}_{sp} \underline{y}_{sp}(t) \quad (3.46)$$

3.5 APPLICATION OF MRAC TO A PILOT PLANT EVAPORATOR

This section demonstrates how the theory described in the previous section can be applied to the double effect evaporator in the Department of Chemical and Petroleum Engineering of the University of Alberta. A schematic diagram of the pilot plant evaporator is shown in Figure 3.3. The first effect is a calandria type unit with 32 eighteen inch long, 3/4 inch O.D. tubes. The feed to this three gallon unit is 5 pounds per minute of 3 percent by weight triethylene glycol and this feed is heated by 2 pounds per minute of 250°F saturated steam. The second effect has externally forced circulation through three 6 feet long, one inch O.D. tubes fed by the first effect product and heated by the first effect vapour. The second effect vapour is totally condensed. Vacuum control maintains the necessary pressure differential between effects. The product is about 1.5 pounds per minute of 10% glycol. A more detailed description of the evaporator can be found in a thesis by Newell [17, Chapter 4] or a paper by Andre and Ritter [19].

The evaporator has been extensively modelled by Newell [17], Wilson [18], and Andre and Ritter [19]. The model used here is due to Wilson [18] and is a five state, linear, time-invariant model in the form of Equation (3.1) or

$$\dot{\underline{x}}_p = \underline{A} \underline{x}_p + \underline{B} \underline{u} + \underline{D} \underline{d}$$

The following definitions for the state, disturbance, and control vectors \underline{x}_p , \underline{d} , and \underline{u} , were used:

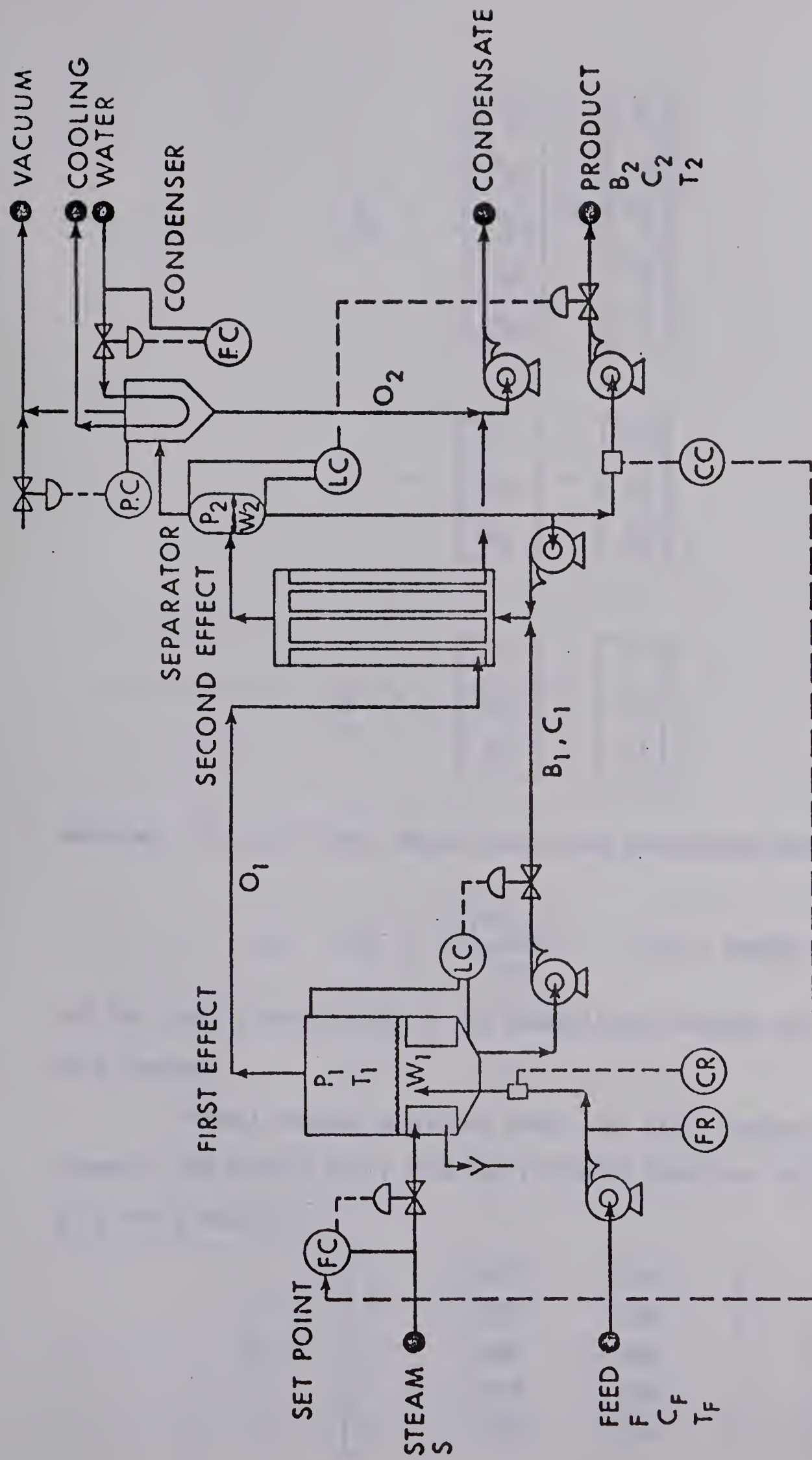


FIGURE 3.3 SCHEMATIC DIAGRAM OF DOUBLE EFFECT EVAPORATOR

$$\underline{x}_p = \begin{bmatrix} x_{p1} \\ x_{p2} \\ x_{p3} \\ x_{p4} \\ x_{p5} \end{bmatrix} = \begin{bmatrix} W_1' \\ C_1' \\ h_1' \\ W_2' \\ C_2' \end{bmatrix}$$

$$\underline{u} = \begin{bmatrix} u_1 \\ u_2 \\ u_3 \end{bmatrix} = \begin{bmatrix} S' \\ B_1' \\ B_2' \end{bmatrix}$$

$$\underline{d} = \begin{bmatrix} d_1 \\ d_2 \\ d_3 \end{bmatrix} = \begin{bmatrix} F' \\ C_F' \\ h_F' \end{bmatrix}$$

where W_1' , C_1' , S' , F' etc. denote normalized perturbed variables

$$\text{i.e. } W_1' = \frac{(W_1 - W_{1ss})}{W_{1ss}} \quad (\text{ss - steady state})$$

and the symbols are defined in the Nomenclature section associated with this Chapter.

Normal process operating conditions [18] (presented in the Appendix for Chapter Four) gave the following numerical values for the \underline{A} , \underline{B} and \underline{C} matrices.

$$\underline{A} = \begin{bmatrix} 0 & -.0011 & -.1255 & 0 & 0 \\ 0 & -.0755 & .1255 & 0 & 0 \\ 0 & -.0060 & -.7741 & 0 & 0 \\ 0 & -.0012 & -.1448 & 0 & .0001 \\ 0 & .0393 & .1448 & 0 & -.0380 \end{bmatrix}$$

$$\underline{B} = \begin{bmatrix} 0 & -.0766 & 0 \\ 0 & 0 & 0 \\ .2160 & 0 & 0 \\ 0 & .0795 & -.0381 \\ 0 & -.0414 & 0 \end{bmatrix}$$

$$\underline{D} = \begin{bmatrix} .1098 & 0 & 0 \\ -.0333 & .0766 & 0 \\ -.0188 & 0 & .0911 \\ 0 & 0 & 0 \\ 0 & 0 & 0 \end{bmatrix}$$

For implementation on the evaporator, only multivariable proportional feedback control was considered since previous studies [17] have demonstrated that this configuration gives excellent control. Therefore, in Equations (3.3) and (3.4), $\underline{K}_{FF} = \underline{0}$ and $\underline{\Omega} = \underline{0}$. The \underline{r} matrix generated by the adaptive control law in Equation (3.24) consists of 25 elements. However, only 15 elements of \underline{K}_{FB} can be adapted since \underline{B} is fixed by the physical process (note that $\underline{r} = \underline{B} \underline{K}_{FB}$ in Equation (3.4)). Consequently, the pseudo-inverse approach [20] was used to generate the following "solution" to Equation (3.4);

$$\underline{K}_{FB}(t) = (\underline{B}^T \underline{B})^{-1} \underline{B}^T \underline{r}(t) \quad (3.47)$$

Equation (3.47) provides a least squares solution for $\underline{K}_{FB}(t)$ that is only approximate since the 15 unknown elements of \underline{K}_{FB} are generated from 25 scalar equations involving the elements of $\underline{r}(t)$ and \underline{B} .

The model of the desired closed-loop behavior is chosen to be the open-loop model plus the optimal feedback control law for a quadratic performance index. This optimal feedback matrix is derived using

dynamic programming and minimizes the quadratic performance index used by Newell [17, Chapter 5].

The $\underline{r}(t)$ matrix is calculated from Equation (3.24) using a backwards difference approximation. This yields

$$\gamma_{ij}(k) = x_{pj}(k) \underline{e}(k)^T \underline{p}_i \varepsilon_{ij} \Delta t + \gamma_{ij}(k-1) \quad (3.48)$$

The initial conditions for Equation (3.48), $\gamma_{ij}(0)$, are related to the initial control matrix, $\underline{K}_{FB}(0)$, and must be specified. The importance of the initial control is investigated in Chapters Four and Five.

The values of \underline{x}_p are sampled from the continuous process and the model states are calculated from

$$\underline{x}_m(k+1) = \underline{\phi}_m \underline{x}_m(k) + \underline{\theta}_m \underline{d}(k) \quad (3.49)$$

which is Equation (3.5) in discrete form. The numerical values of the discrete matrices $\underline{\phi}_m$ and $\underline{\theta}_m$ are:

$$\underline{\phi}_m = \begin{bmatrix} .4341 & -.0110 & -.0785 & 0 & -.7874 \\ .1248 & .9037 & .0313 & 0 & -.2266 \\ 1.692 & -.2564 & -.3186 & 0 & -3.071 \\ 0 & 0 & 0 & -.0001 & -.0003 \\ -.0835 & .0015 & .0150 & 0 & .1515 \end{bmatrix}$$

$$\underline{\theta}_m = \begin{bmatrix} .1182 & 0 & -.0050 \\ -.0351 & .0785 & .0049 \\ -.0136 & -.0002 & .0662 \\ .0012 & 0 & -.0058 \\ -.0019 & .0016 & .0058 \end{bmatrix}$$

Details on the derivation of these matrices are given in the Appendix for

this chapter.

A review of the theory presented above suggests the following procedure for the implementation of multivariable model reference adaptive control. At each sampling instant:

- a) Sample the plant state, $\underline{x}_p(k)$, from the continuous process.
- b) Calculate the model state for the optimal feedback model, $\underline{x}_m(k)$, from the discrete closed-loop model in Equation (3.49).
- c) Compare these states and from the error, $\underline{e}(k) = \underline{x}_m(k) - \underline{x}_p(k)$, calculate the control matrices $\underline{\Gamma}(k)$ and $\underline{K}_{FB}(k)$ from Equations (3.47) and (3.48).
- d) Calculate the control variables $\underline{u}(k)$ from $\underline{u}(k) = \underline{K}_{FB}(k) \underline{x}_p(k)$ and send these signals to the process.

CHAPTER FOUR

HYBRID SIMULATION OF A MODEL REFERENCE ADAPTIVE
CONTROL SYSTEM FOR THE EVAPORATOR4.1 INTRODUCTION

The model reference adaptive control (MRAC) scheme described in the previous chapter was simulated on the EAI 590 hybrid computer system in the Department of Chemical and Petroleum Engineering at the University of Alberta. The EAI 580 analog computer was used to simulate the dynamic behavior of the double effect evaporator, as represented by the fifth-order linear evaporator model of Wilson [2]. The reference model response and the adaptive control matrices were generated on the EAI 640 digital computer. The hybrid simulation was ideal for evaluating this computer control technique because the analog model provided an intuitive feel for the behavior of the actual evaporator, while the digital computer provided an authentic simulation of the process control computer required for actual implementation. Furthermore, the digital control programs used in the simulation were easily transferred to the IBM 1800 computer for experimental verification of the technique.

4.2 ANALOG EVAPORATOR MODEL

The analog simulation of the evaporator was essentially the same as the one used by Newell [7] with modifications in the disturbance, control, and data monitoring sections for control by the EAI 640 digital computer. The state-space evaporator model chosen was in normalized perturbation form making all the states, controls, and disturbances vary about the steady state value of zero and generally stay within the range of ± 1.0 [3]. This model was ideal for analog simulation because

magnitude scaling was not required unless extremely large disturbances or inadequate control schemes were to be considered. Figure 4.1 shows the analog circuit used for the evaporator simulation. The nonlinear evaporator model [5] would have provided more accurate process dynamics; however, a lack of nonlinear elements prevented this simulation.

Communication with the digital computer was achieved through analog to digital converters (ADCs) to access the process states as required by the MRAC algorithm. The analog simulation was time scaled by a factor of 60, i.e. one second of simulation time represented one minute of real time. Also, data were acquired automatically for later analysis and plotting by the IBM 1800 computer for 5 minutes of simulation time. More details on the analog simulation and the data accumulation programs can be found in a hybrid user's manual by Oliver and Seborg [4].

4.3 DIGITAL COMPUTER CONTROL PROGRAMS

The digital computer program controlled sampling of the evaporator states from the analog and calculated the model states from the discrete form of the reference model (Chapter Three). These states were compared and the resulting errors and acquired process states were used to generate the adaptive control matrix, $\underline{\Gamma}(t)$. This matrix was then used to calculate the feedback matrix, \underline{K}_{FB} , and subsequently the controls, $\underline{u}(t)$. These controls were then sent to the analog evaporator model via digital to analog multipliers (DAMs). The logic flowchart for these calculations and complete program listings can be found in a research report [4].

4.4 RESULTS

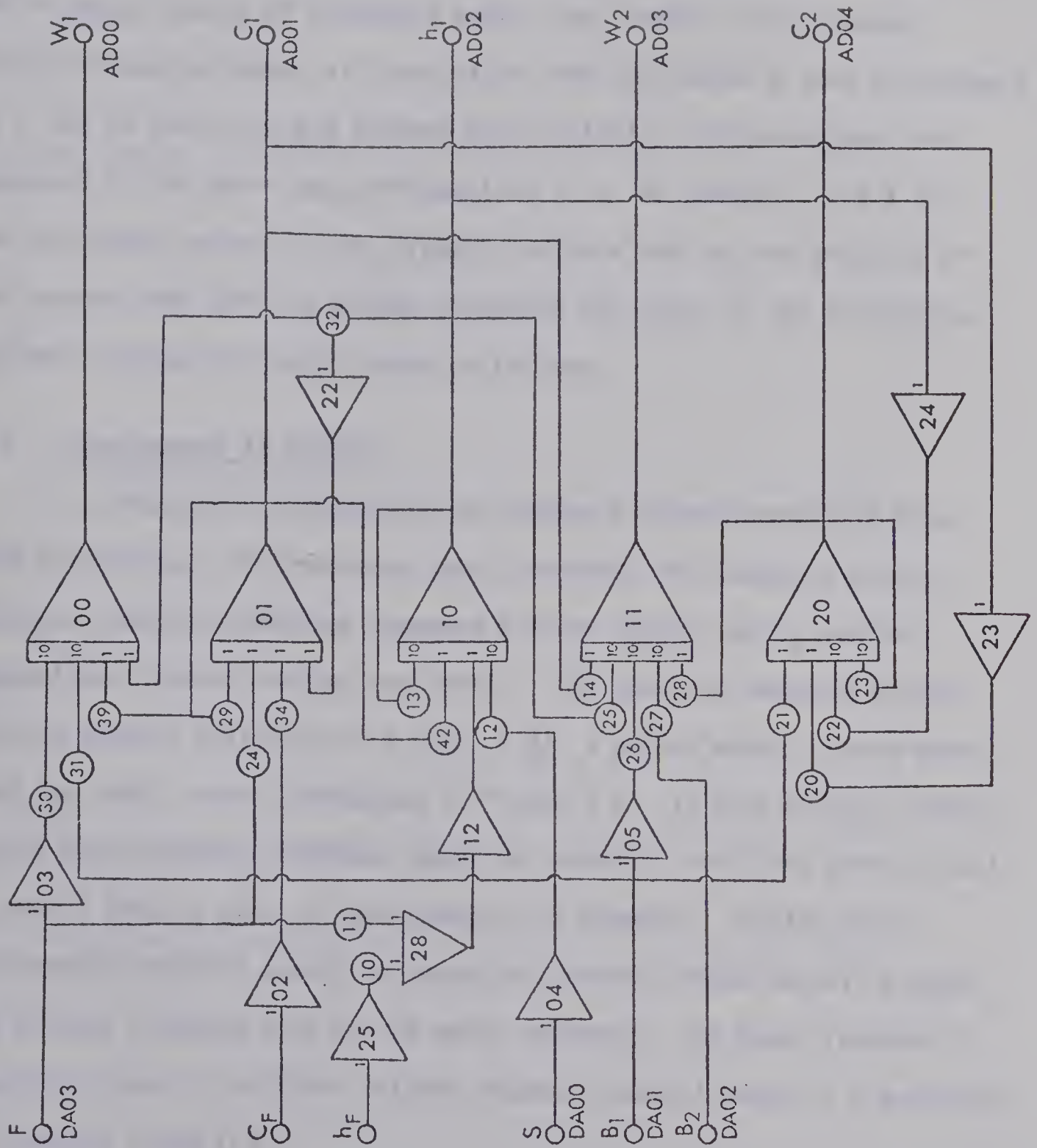


FIGURE 4.1 ANALOG SIMULATION OF THE LINEAR, FIFTH-ORDER EVAPORATOR MODEL

Simulation runs were made to investigate several factors which affect the performance of the adaptive control system including: initial control policy, adaptive loop gains, number of elements of $\underline{\Gamma}$ which adapt, choice of reference model, and "unseen" disturbances. Unless otherwise noted, all simulation runs considered a step disturbance of + 20% in feed flow and assumed that initially, the evaporator was operated in the open-loop configuration (i.e. no control, $\underline{r}(0) = \underline{0}$). The horizontal arrows on the figures indicate the desired setpoint of the system; the vertical arrows represent the start of the disturbance. The most noteworthy results were as follows:

4.4.1 Improvement in Control

Figure 4.2 illustrates the improved control resulting from MRAC and displays the reference model response, the adaptive control response, and the open-loop response with no control of C_2 and only proportional control of the two levels. The adaptive response starts with no control initially (i.e. $\underline{r}(0) = \underline{0}$), a policy which is even worse than the level control presented in Figure 4.2. If this initial control policy were continued (without adaptive control), the first effect level, W_1 , would drop to zero in approximately 45 minutes. Despite this unfavorable starting point, the adaptive control scheme quickly brought the process response back to the model response. The model response is excellent since it utilizes optimal feedback control based on a quadratic performance index [5].

4.4.2 Effect of ξ_{ij} on MRAC

The effect of the adaptive loop gains, ξ_{ij} , is demonstrated in Figure 4.3 where values of 1, 10 and 100 for all elements of $\underline{\Xi}$ were

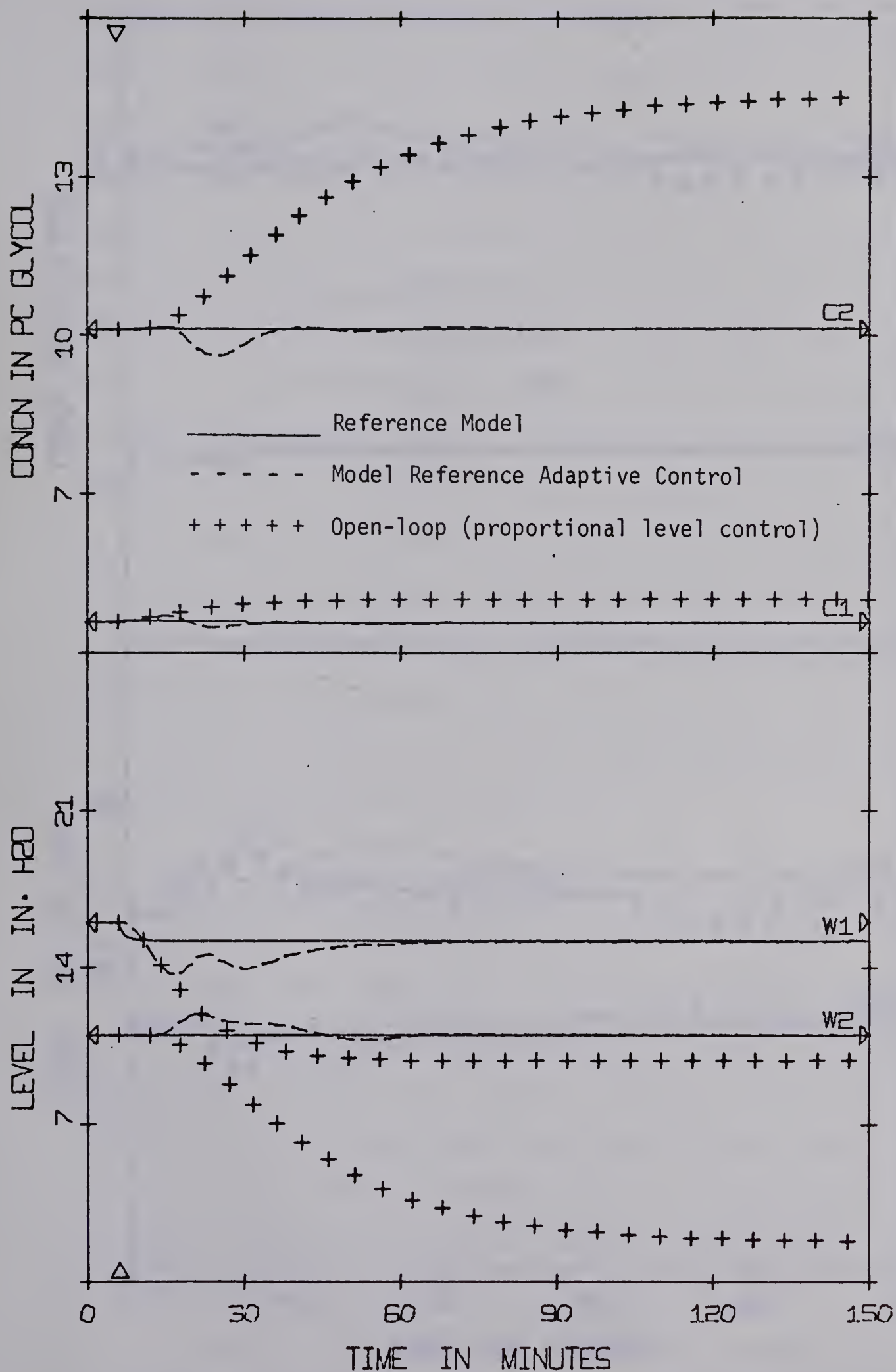


FIGURE 4.2 SIMULATED RESPONSES COMPARING OPEN-LOOP, OPTIMAL FEEDBACK REFERENCE MODEL, AND MODEL REFERENCE ADAPTIVE CONTROL ($\xi_{ij} = 10$, -20% FEED FLOW)

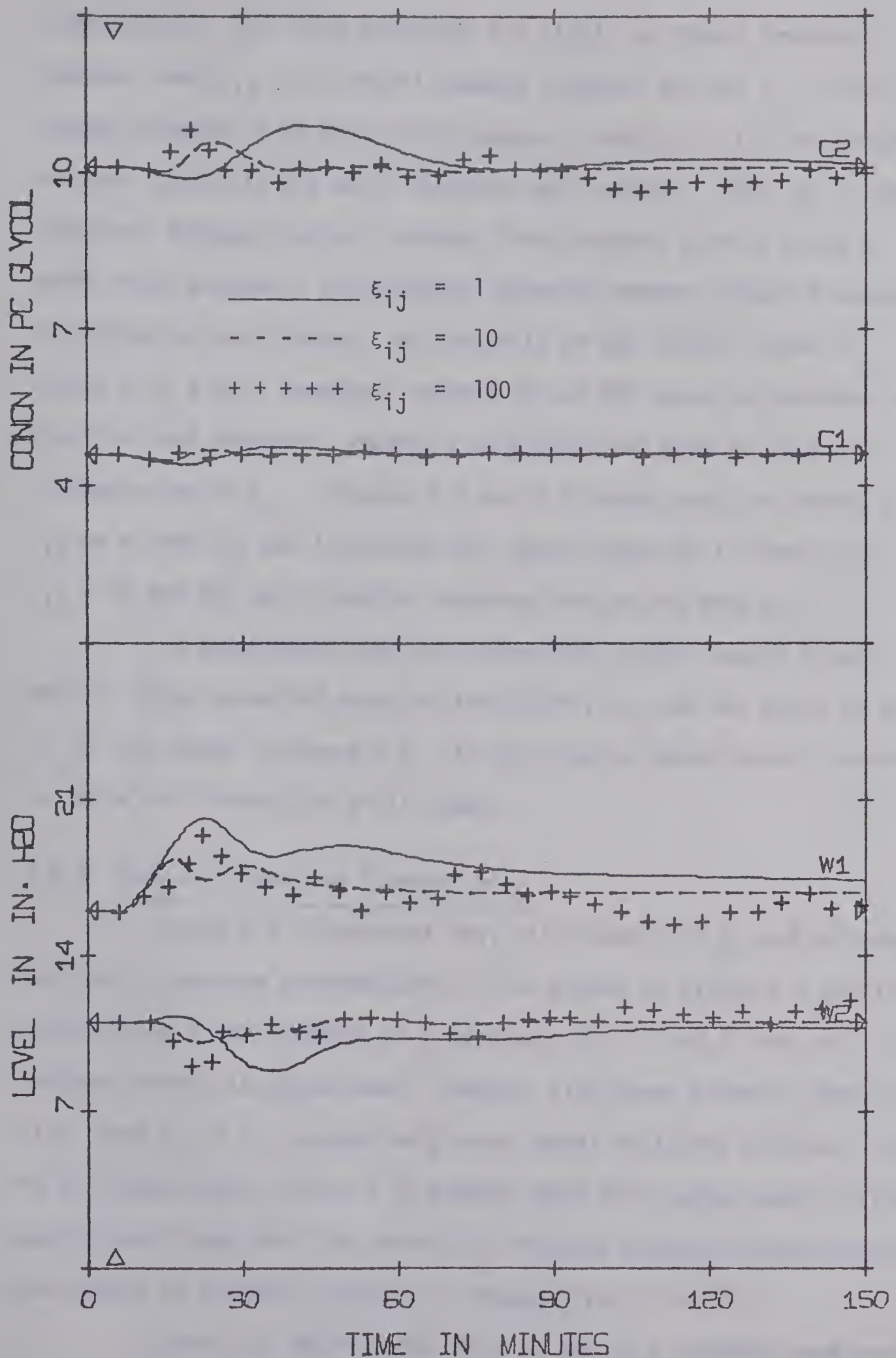


FIGURE 4.3 SIMULATED RESULTS DEMONSTRATING THE EFFECT OF ADAPTIVE LOOP GAIN, ξ_{ij} , ON MRAC

investigated. All three responses are stable as theory predicts; however, when $\xi_{ij} = 1$, control appears sluggish and for $\xi_{ij} = 100$, the system responds in an oscillatory manner. When $\xi_{ij} = 10$, the process response adapts to the model response most rapidly. Thus, as in conventional feedback control systems, there appears to be a range of gains which provide a satisfactory trade-off between speed of response and degree of oscillation. On the basis of the results shown in Figure 4.3, a gain somewhere between 10 and 100 would be expected to give the best response. However, no attempt was made to find the optimum value of ξ_{ij} . Figures 4.4 and 4.5 demonstrate the effect of ξ_{ij} on e_1 and γ_{51} and illustrate the rapid reduction in error for $\xi_{ij} = 10$ and the more sluggish adapting that occurs when $\xi_{ij} = 1$.

To demonstrate that the controlled system remains stable despite large values of adaptive loop gains, ξ_{ij} was set equal to 10,000 in the run shown in Figure 4.6. As this figure demonstrates, the control is quite oscillatory but still stable.

4.4.3 Number of Adapting Elements of $\underline{\Gamma}$

Figure 4.7 illustrates that all elements of $\underline{\Gamma}$ need not adapt for MRAC to perform satisfactorily. The curves in Figure 4.7 are for successively fewer elements of $\underline{\Gamma}$ adapting (21, 11 and 7) and still satisfactory control is maintained. However, with fewer elements adapting (i.e. some $\xi_{ij} = 0$), successively worse model following results. Also, it is increasingly difficult to predict what will happen when a disturbance occurs (note that the initial C_2 response changes direction when the number of elements adapting is changed from 11 to 7).

Figure 4.8 demonstrates that as few as 4 elements need adapt for adequate control to be maintained. However, the elements of $\underline{\Gamma}$ which

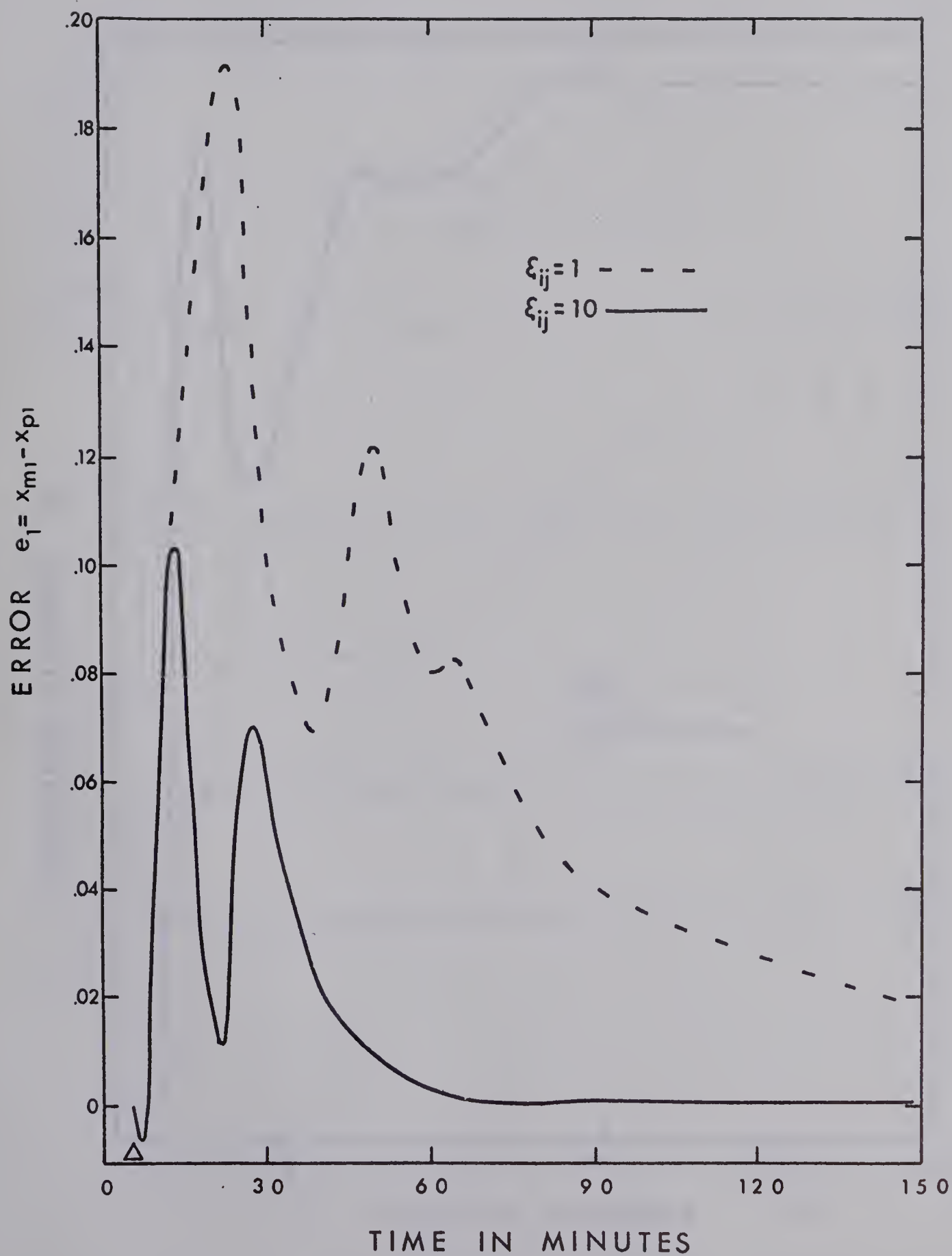


FIGURE 4.4 SIMULATED EFFECT OF ξ_{ij} ON $e_1 = x_{m1} - x_{p1}$

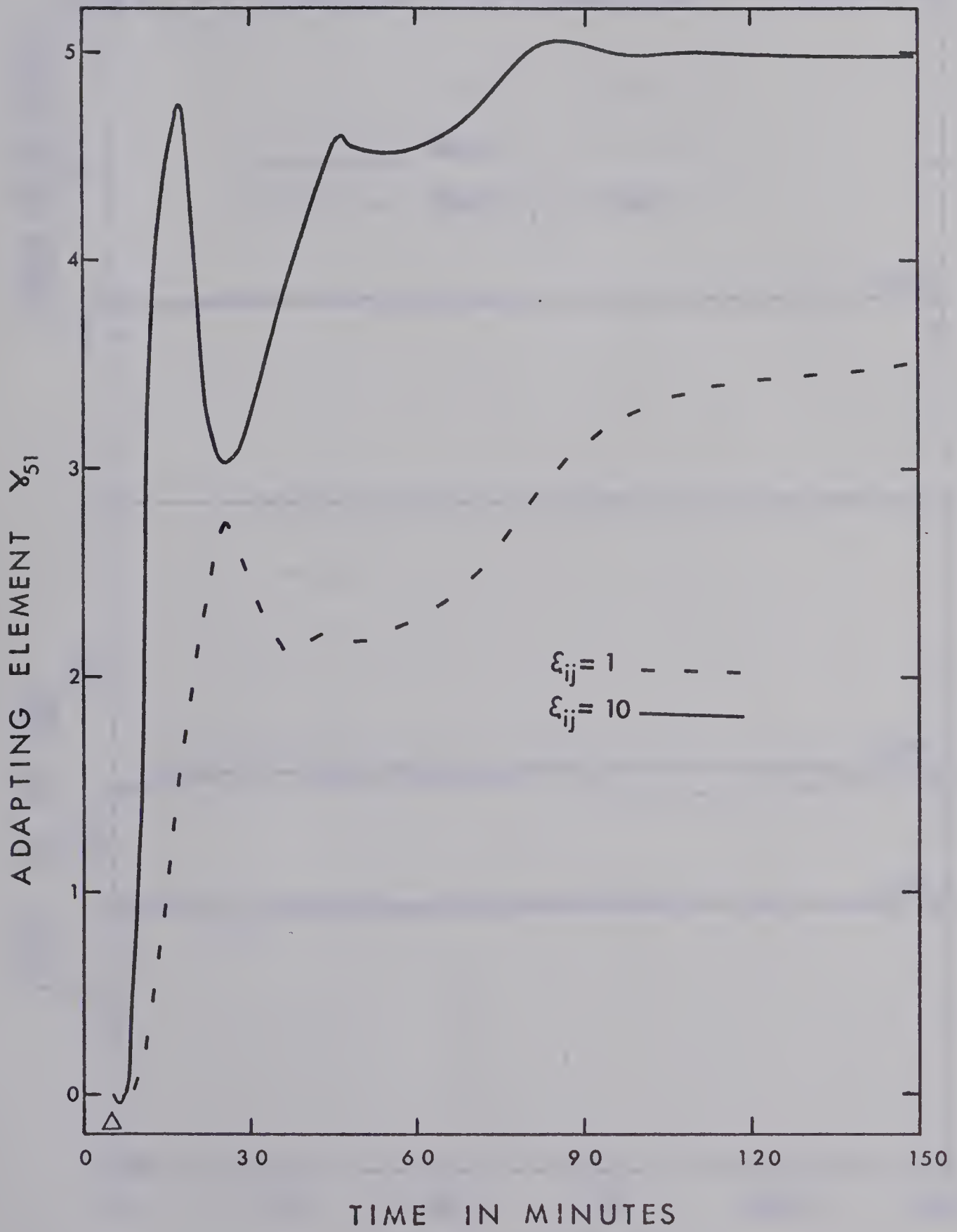


FIGURE 4.5 SIMULATED EFFECT OF ξ_{ij} ON RATE OF ADAPTING FOR γ_{51}

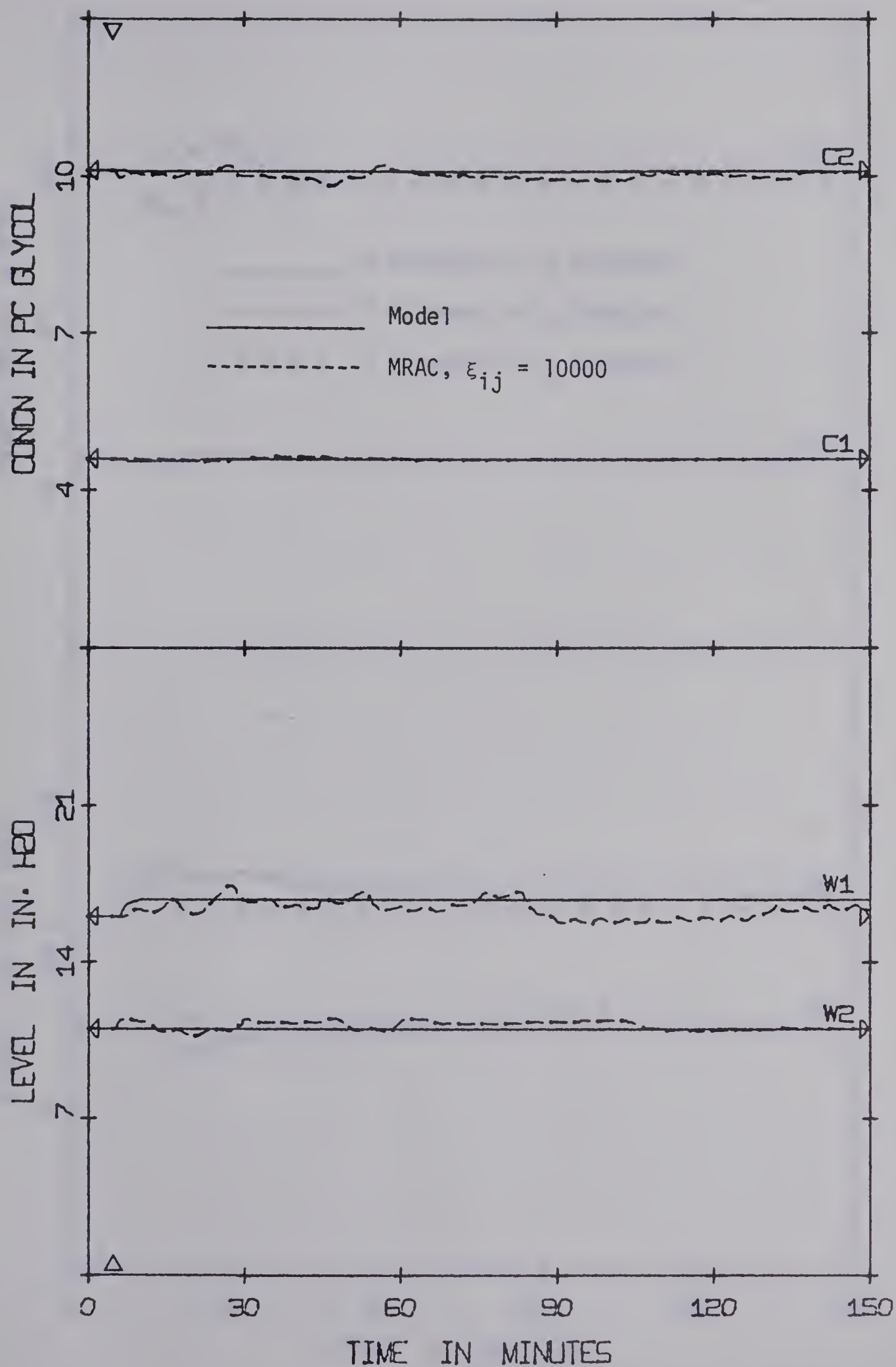


FIGURE 4.6 SIMULATED RESULTS DEMONSTRATING INHERENT STABILITY OF MRAC DESIGNED VIA LIAPUNOV'S DIRECT METHOD

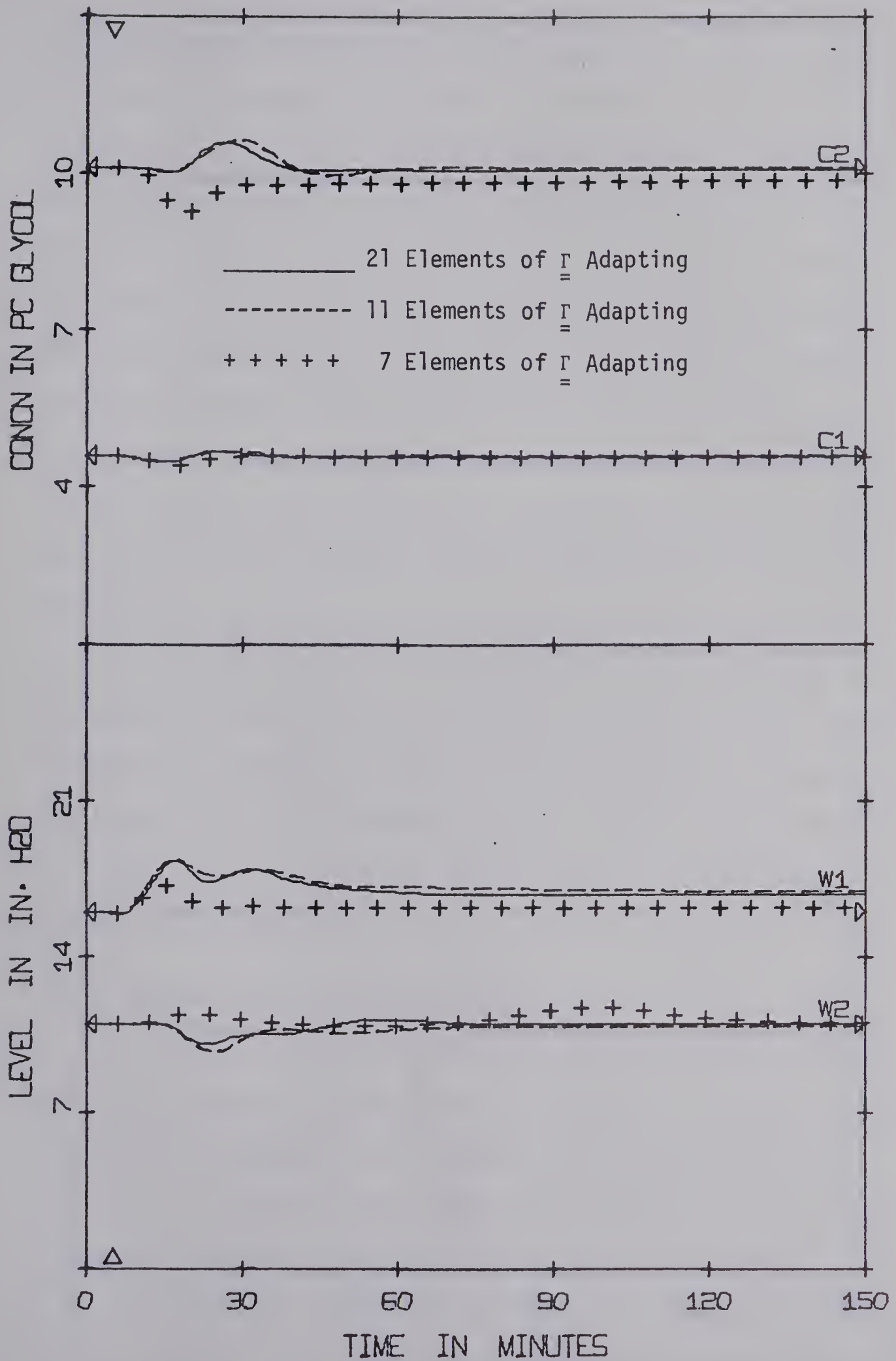


FIGURE 4.7 SIMULATED RESULTS FOR ONLY SOME ELEMENTS OF Γ ADAPTING, $\xi_{ij} = 10$

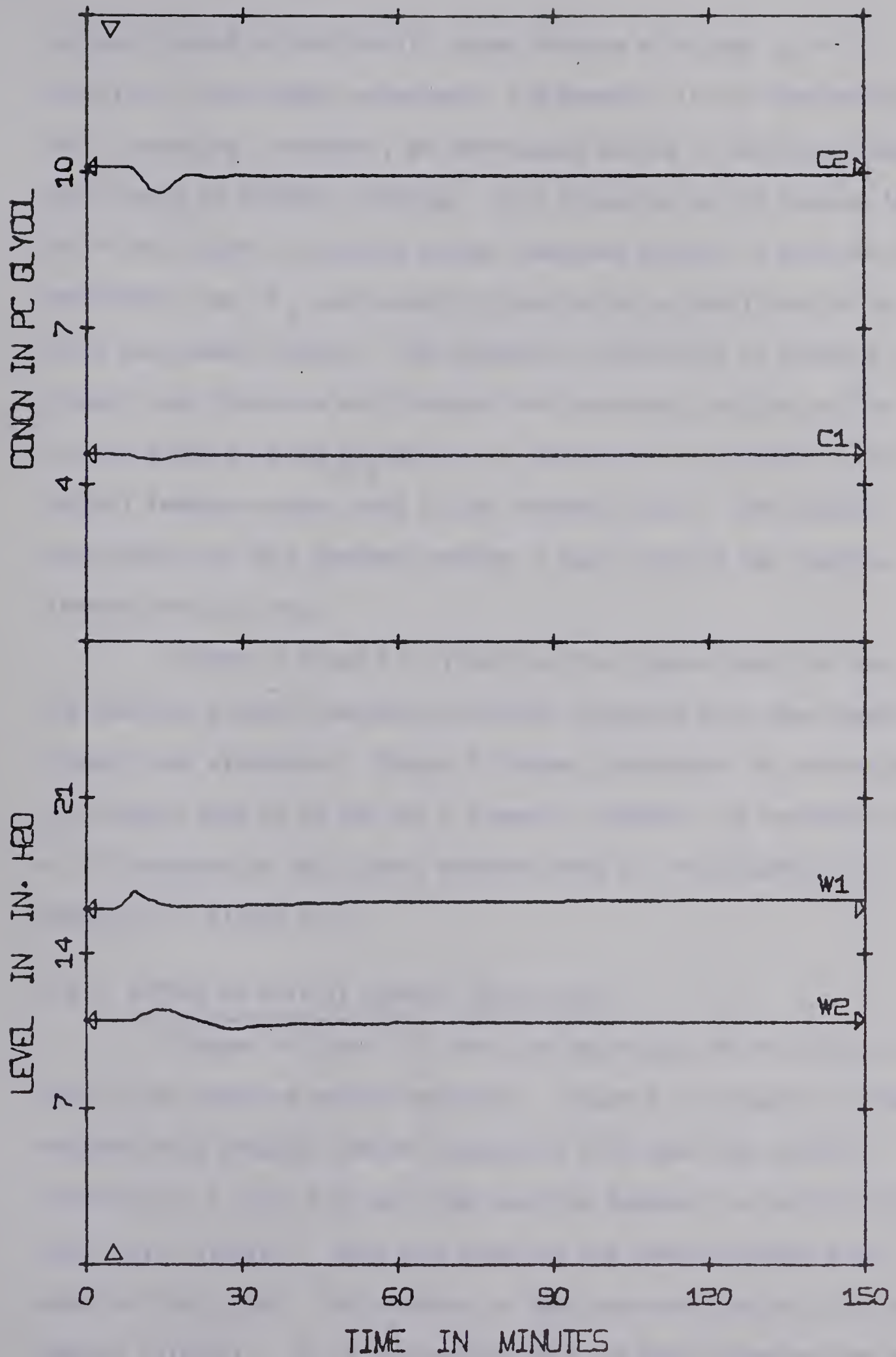


FIGURE 4.8 SIMULATED RESULTS, FOUR ELEMENTS OF Γ ADAPTING,
 $\xi_{ij} = 100$

do adapt cannot be arbitrarily chosen because with some $\xi_{ij} = 0$, stability is no longer guaranteed. For example, it was observed that with 6 adapting $\underline{\Gamma}$ elements, an unfortunate choice of adapting elements would cause an unstable response. This situation occurs because the open-loop system is unstable and at least one element in both the first and fourth rows of $\underline{\Gamma}$ must adapt if there is to be level control for the first and second effects. The successive elimination of adapting $\underline{\Gamma}$ elements was chosen so as to retain the subsequent adapting of the largest element of the \underline{K}_{FB} matrix, as determined from examining the optimal feedback matrix used in the reference model. The Appendix associated with this chapter presents a table showing the adapting elements for each run.

Figures 4.8 and 4.9 illustrate that higher adaptive loop gains are possible without causing oscillatory responses when some adapting elements are eliminated. Figure 4.9 shows improvement in control when ξ_{ij} changes from 10 to 100 for 7 elements adapting. By contrast, a gain of 100 produced an oscillatory response when all the elements of $\underline{\Gamma}$ adapted (cf. Figure 4.3).

4.4.4 Effect of Initial Control Policy, $\underline{\Gamma}(0)$

Figures 4.10 and 4.11 show the importance of the initial control on the adaptive control response. Figure 4.10 compares the model response with adaptive control responses, with open-loop control initially (i.e. $\underline{\Gamma}(0) = \underline{0}$) and with positive feedback on the first effect level, W_1 , initially. Both runs were for the same disturbance and adaptive loop gains. The response is much more satisfactory with no control initially. It is encouraging that the MRAC technique can recover from a disastrous initial control policy such as one involving positive

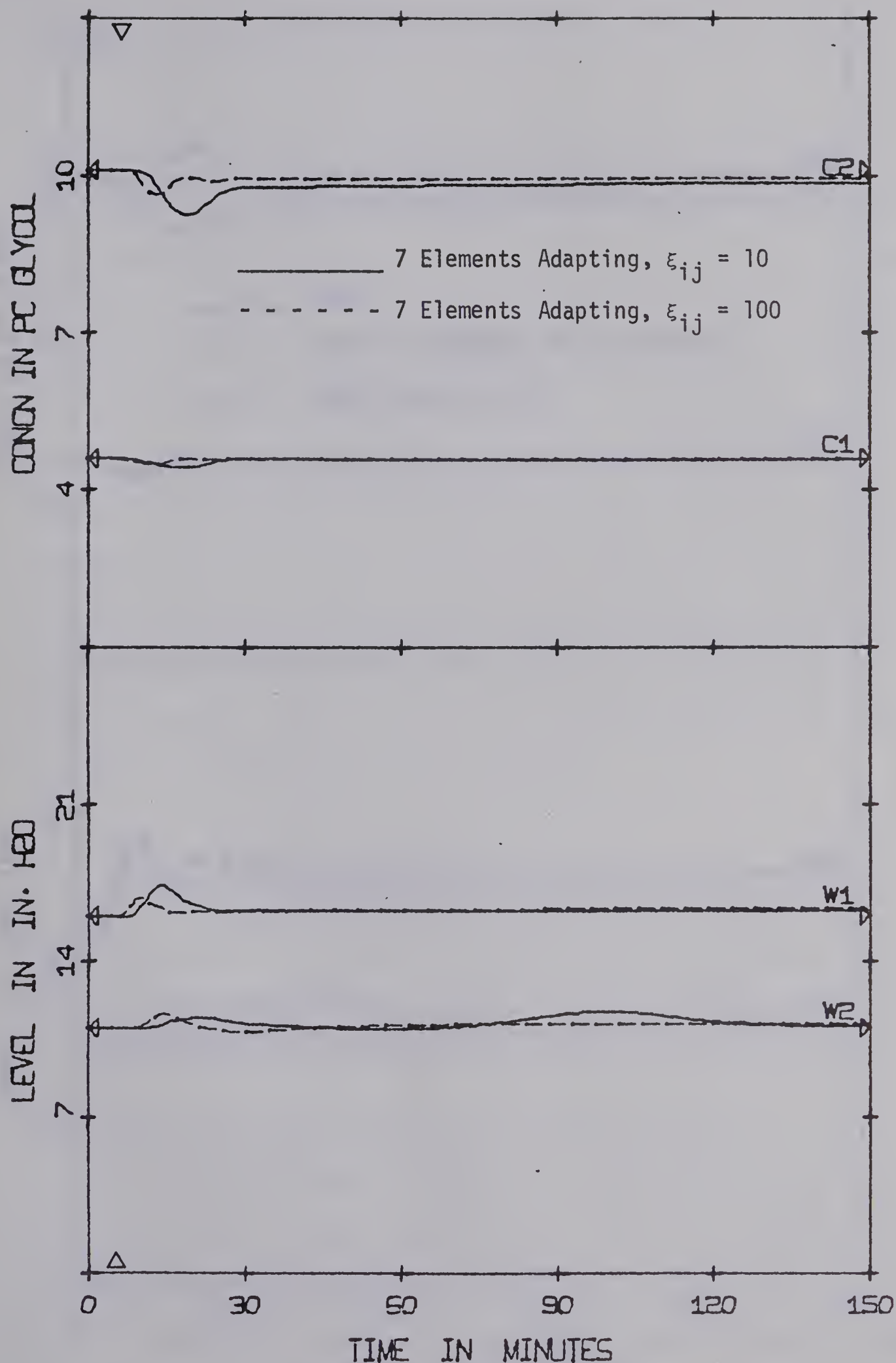


FIGURE 4.9 SIMULATED EFFECT OF ADAPTIVE LOOP GAINS WITH FEW ELEMENTS OF \underline{T} ADAPTING

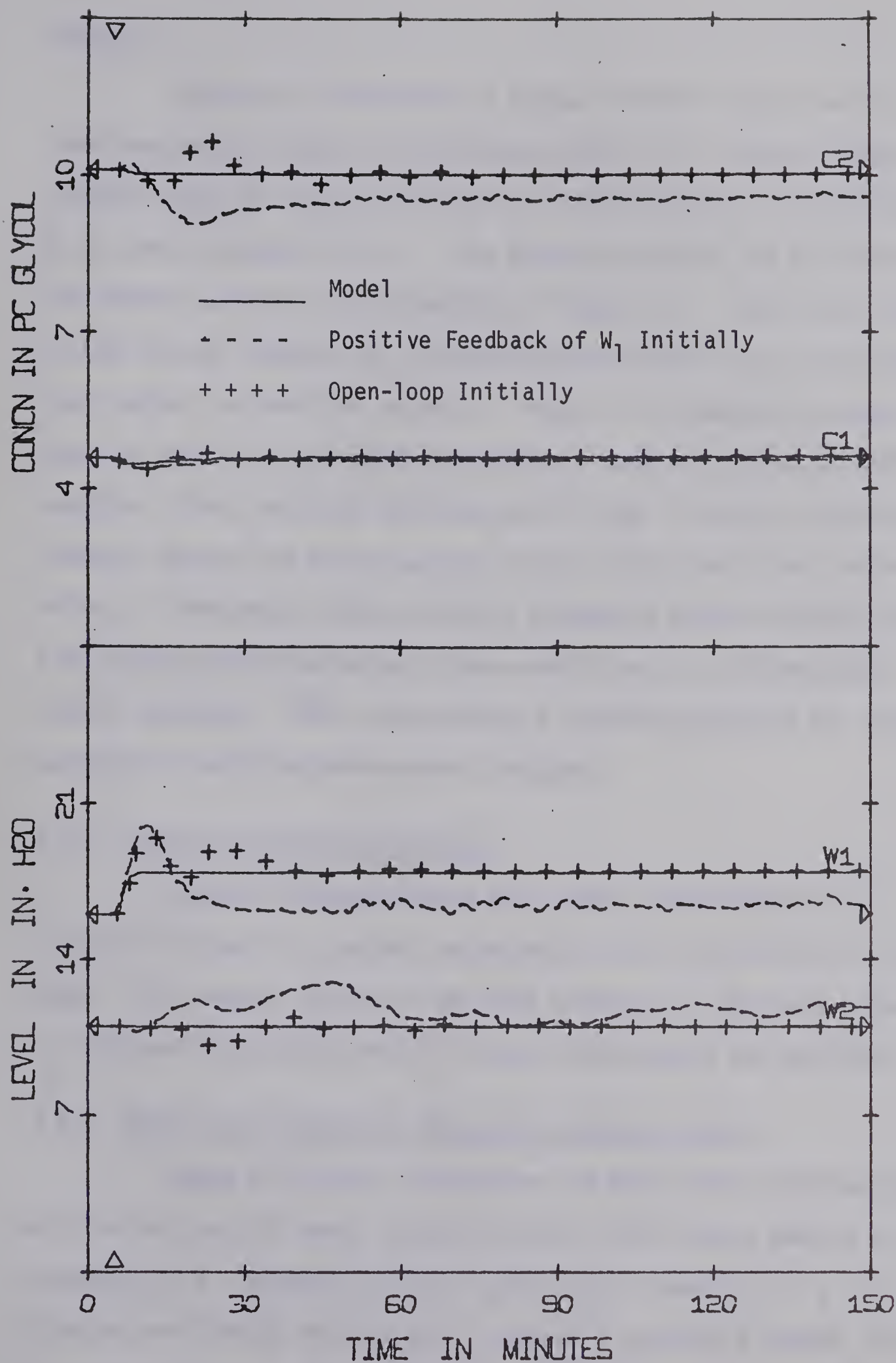


FIGURE 4.10 SIMULATED EFFECT OF THE INITIAL CONTROL POLICY ON MRAC, $\xi_{ij} = 10$ (+50% FEED FLOW)

feedback.

Figure 4.11 illustrates a logical initial control policy, well-tuned proportional gains for multiloop control (i.e. several single variable loops [5, Chapter 4]) with W_1 controlled by B_1 , W_2 controlled by B_2 , and C_2 controlled by S . The Appendix presents the multiloop control matrix used for initial control in Figure 4.11. Multiloop control as the initial condition on \underline{r} shows improved control over initial open-loop control, as would be expected. Figure 4.12 favourably compares adaptive control to multiloop proportional feedback control without adapting. Thus, the MRAC technique can be used to evolve a multivariable feedback control law which improves on the initial multiloop control policy. Furthermore, MRAC provides a systematic method for the transition (during normal operation) from a multiloop to a multivariable control technique. MRAC also provides a promising approach for tuning multiloop or multivariable control constants.

4.4.5 Effect of Unseen Disturbances

Figure 4.13 demonstrates that control deteriorates only slightly if there is a process disturbance that is not observed by the model. This robust feature of the MRAC technique is desirable since, in practical situations, not all process disturbances are monitored.

4.4.6 MRAC with a Physically Impossible Reference Model

Figure 4.14 shows a simulation run that used a reference model which maintained all model states at their initial value despite disturbances (i.e. "perfect control", $\underline{x}_m(t) = \underline{0}$). The gain of $\xi_{ij} = 10$ displays oscillatory results, but a gain of 1 exhibits a smooth, although sluggish, response. This indicates that the larger the model error, the

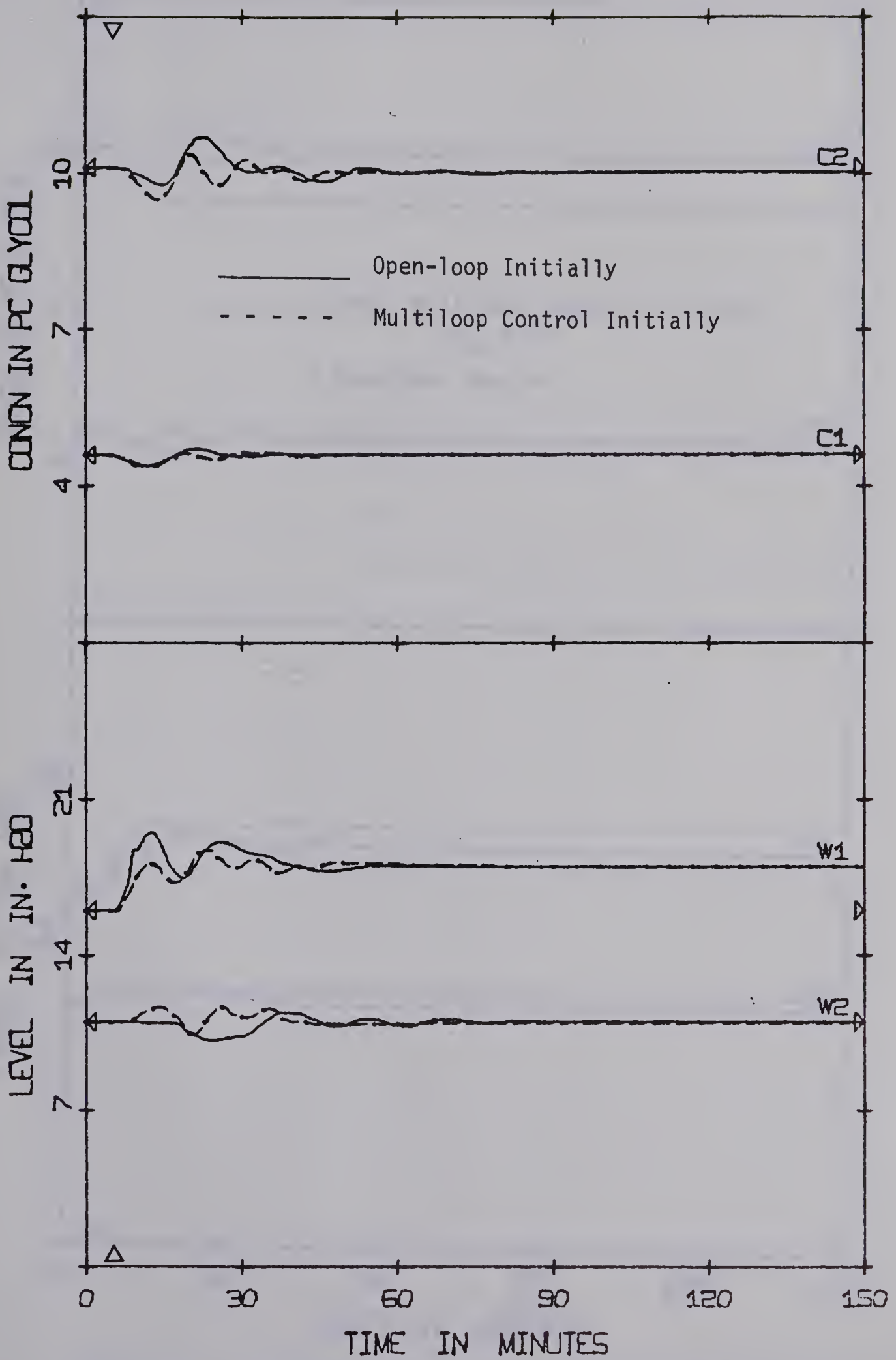


FIGURE 4.11. SIMULATED MULTILoop CONTROL AS AN INITIAL CONTROL POLICY $\xi_{ij} = 10$ (+50% FEED FLOW).

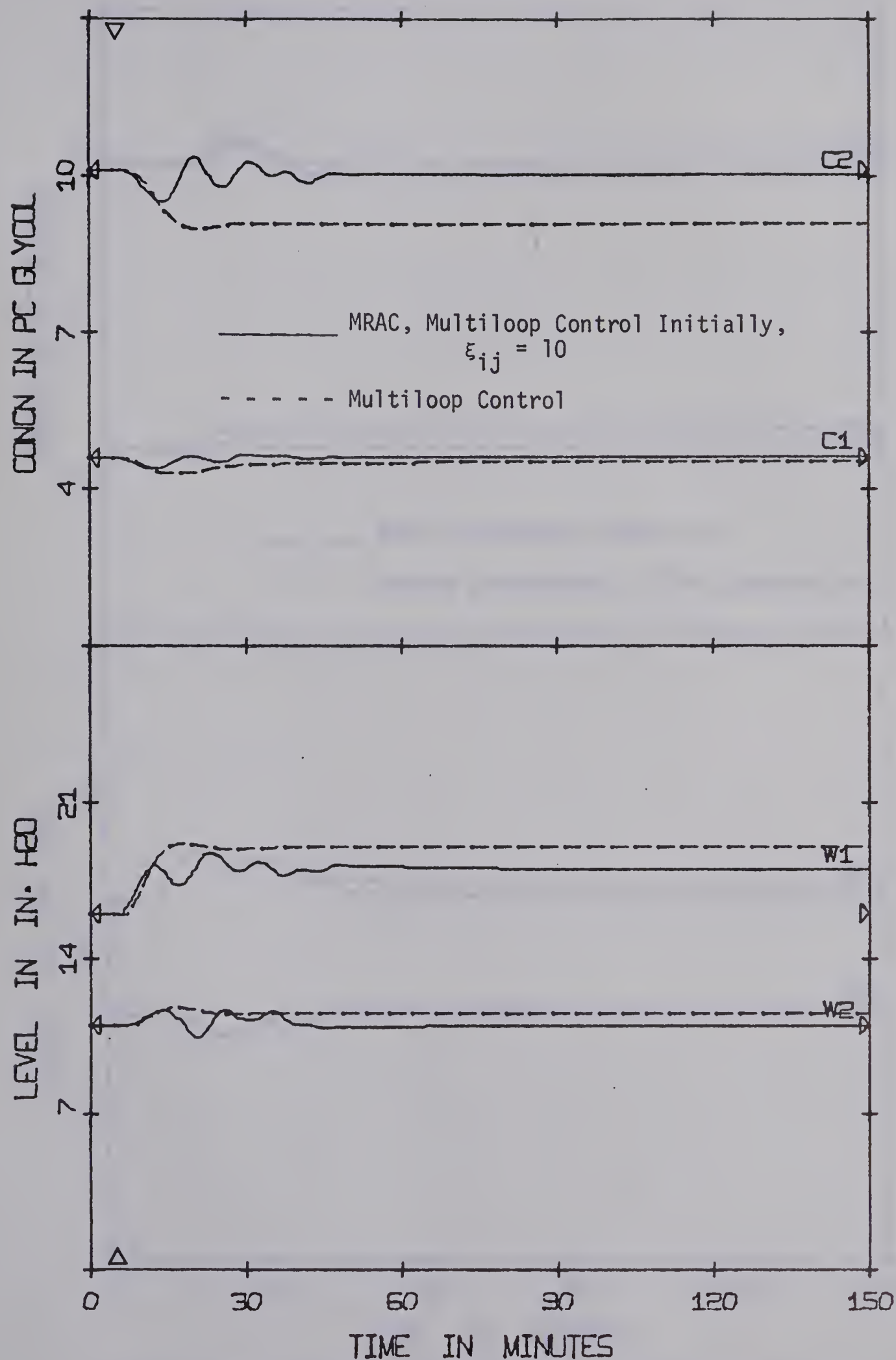


FIGURE 4.12 SIMULATED COMPARISON OF MULTILoop AND MULTIVARIABLE MRAC (+50% FEED FLOW)

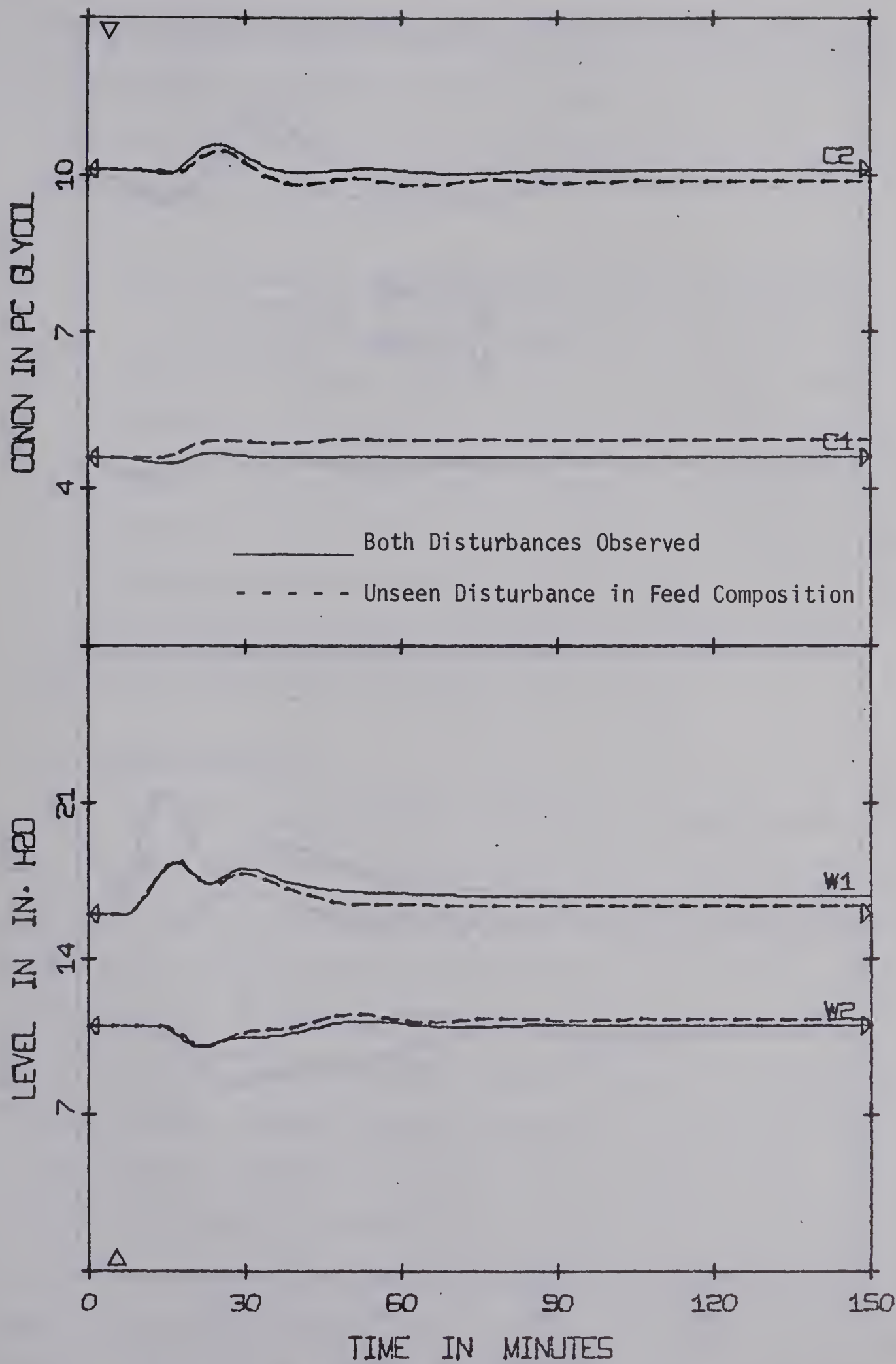


FIGURE 4.13 SIMULATED EFFECT OF UNSEEN DISTURBANCE ON MRAC (+20% FEED FLOW, +10% FEED COMPOSITION)

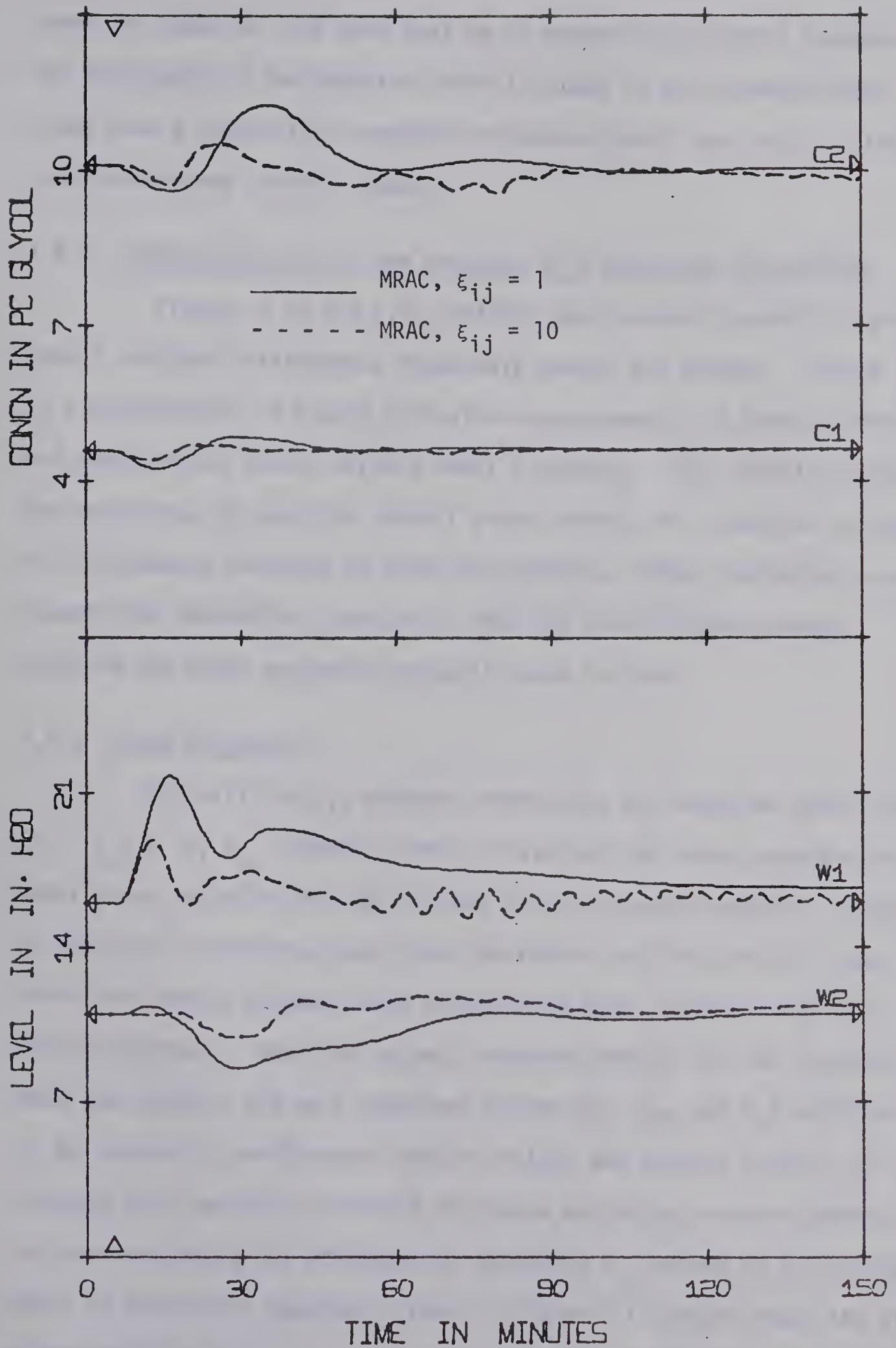


FIGURE 4.14 SIMULATED EFFECT OF PHYSICALLY IMPOSSIBLE REFERENCE MODEL, $x_m = 0$

lower the adaptive loop gain must be to prevent oscillatory responses. The robustness of the adaptive control scheme is again demonstrated since even a physically impossible reference model resulted in a less than disastrous control scheme.

4.4.7 Adaptive Control in the Presence of a Continual Disturbance

Figures 4.15 and 4.16 indicate that control gradually improves when a continual disturbance repeatedly upsets the process. Figure 4.16 is a continuation of Figure 4.15 after approximately 75 hours on MRAC and demonstrates almost perfect model following. This greatly increases the usefulness of adaptive control since control will continue to improve as disturbances continue to upset the process. These simulation results support the theoretical conclusion that the error between process response and model response eventually goes to zero.

4.4.8 State Weighting

With all the ξ_{ij} elements identical, the adaptive control law, $\dot{\gamma}_{ij} = x_{pj} e^T p_i \xi_{ij}$ (Chapter Three), minimizes the errors between the model state variables and the process state variables equally. However, in practical situations, some state variables are less critical than others and errors between these process and model states can be more easily tolerated. When the optimal feedback control for the reference model was chosen, the more important states (W_1 , W_2 , and C_2) were weighted in the quadratic performance index to obtain the optimal control law [5]. Although this partially provided for state weighting, another approach to state weighting was attempted by selecting ξ_{ij} values on an individual basis to stress the important states. Figure 4.17 demonstrates the effect of weighting C_2 (i.e. x_{p5}) more heavily by increasing the values of the

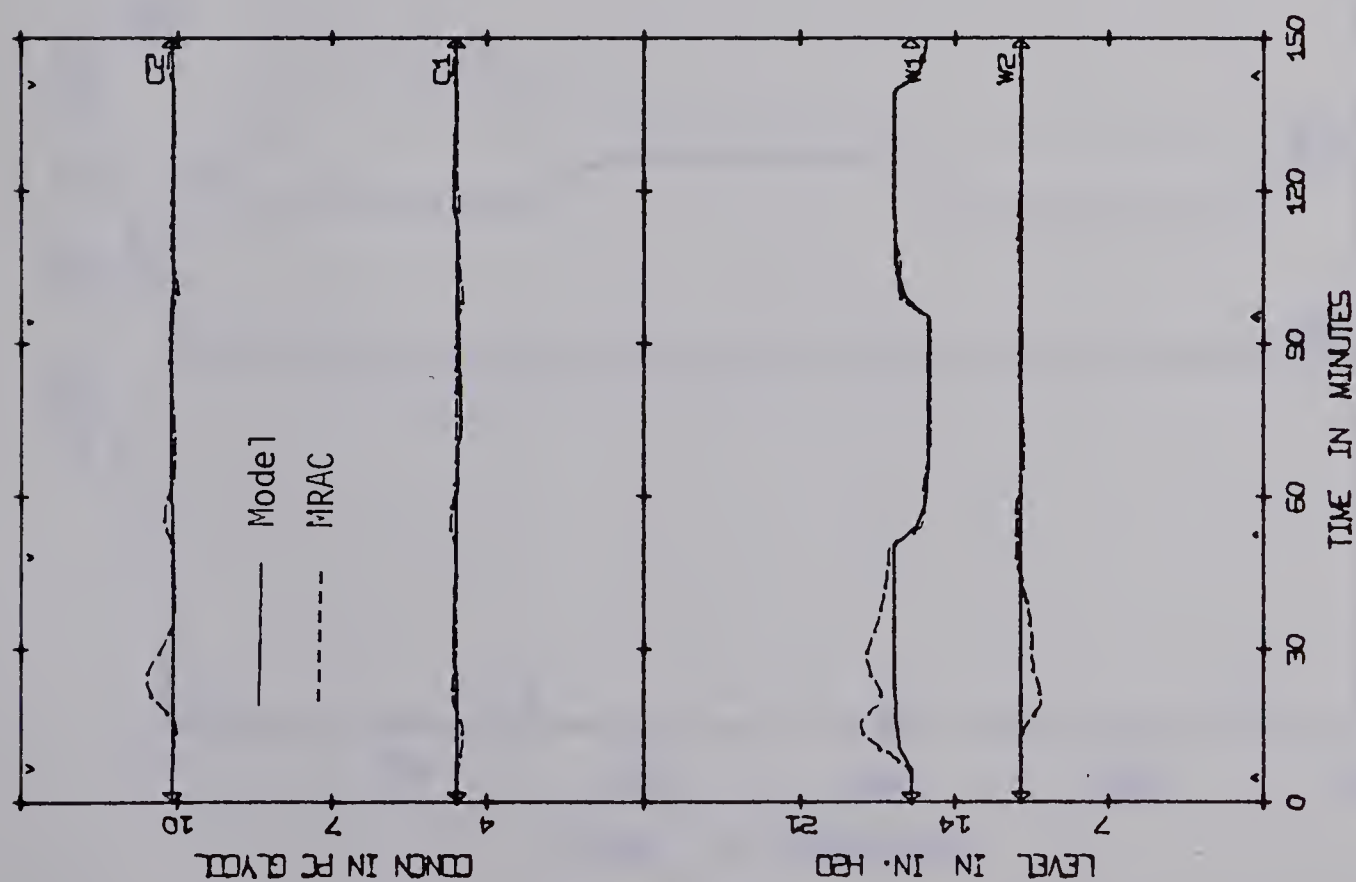
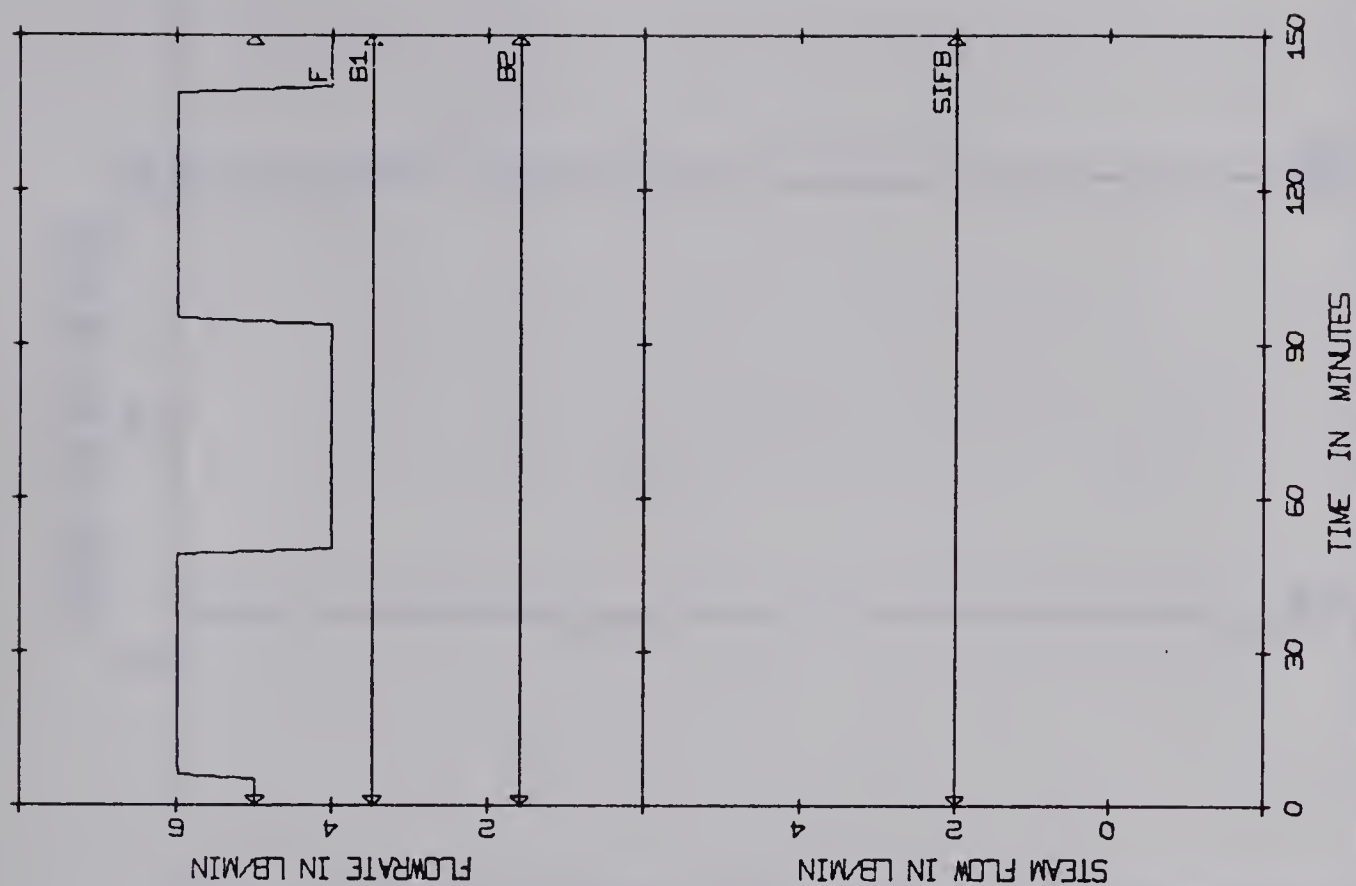


FIGURE 4.15 SIMULATED RESULTS OF THE EFFECT OF A CONTINUING DISTURBANCE ON MRAC, $\xi_{ij} = 10$, $t = 0$ TO 150 MINUTES (CONTROLS B1, B2, S NOT MONITORED)

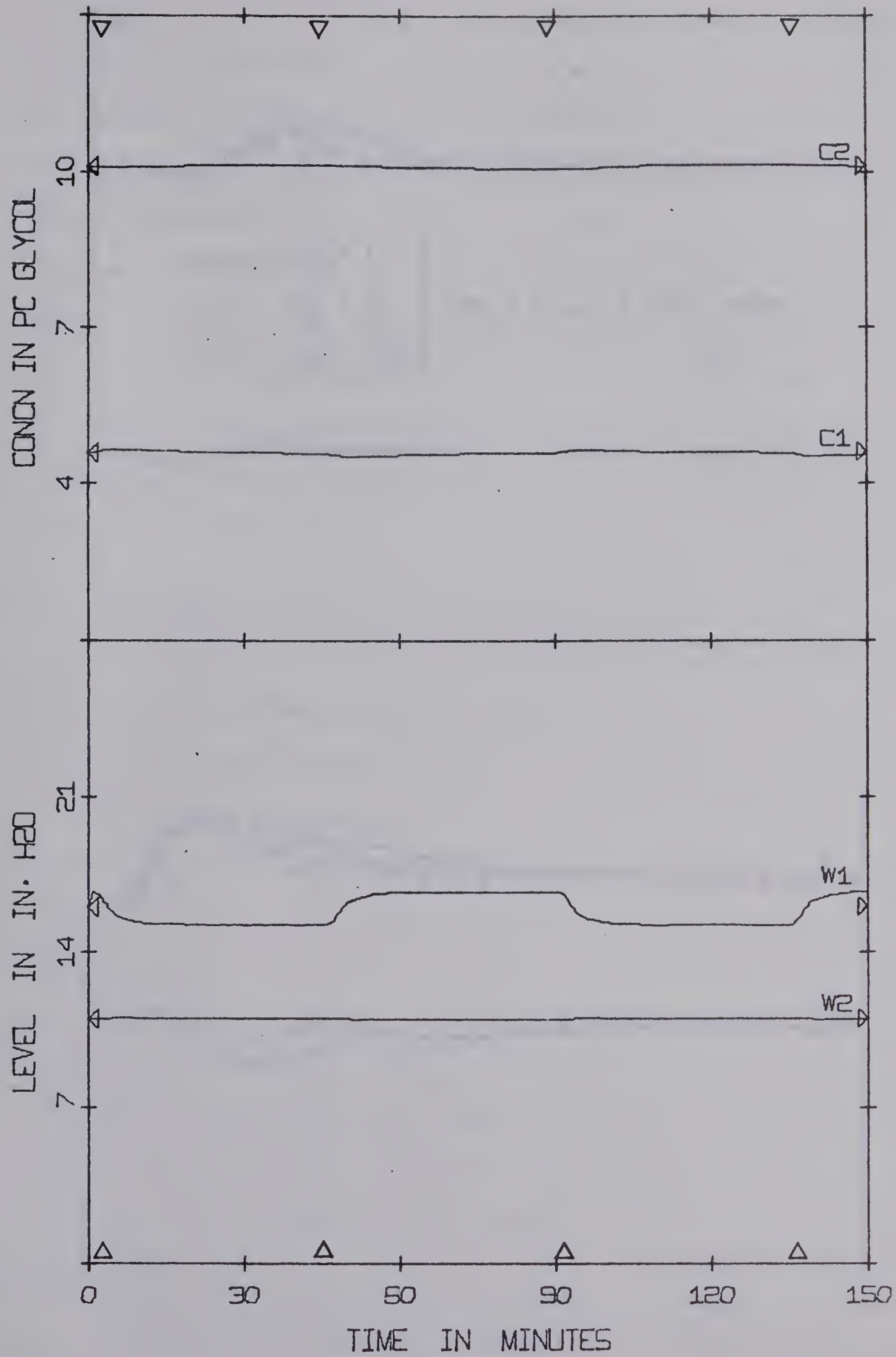


FIGURE 4.16 SIMULATED EFFECT OF A CONTINUOUS DISTURBANCE ON MRAC, $t \rightarrow \infty$

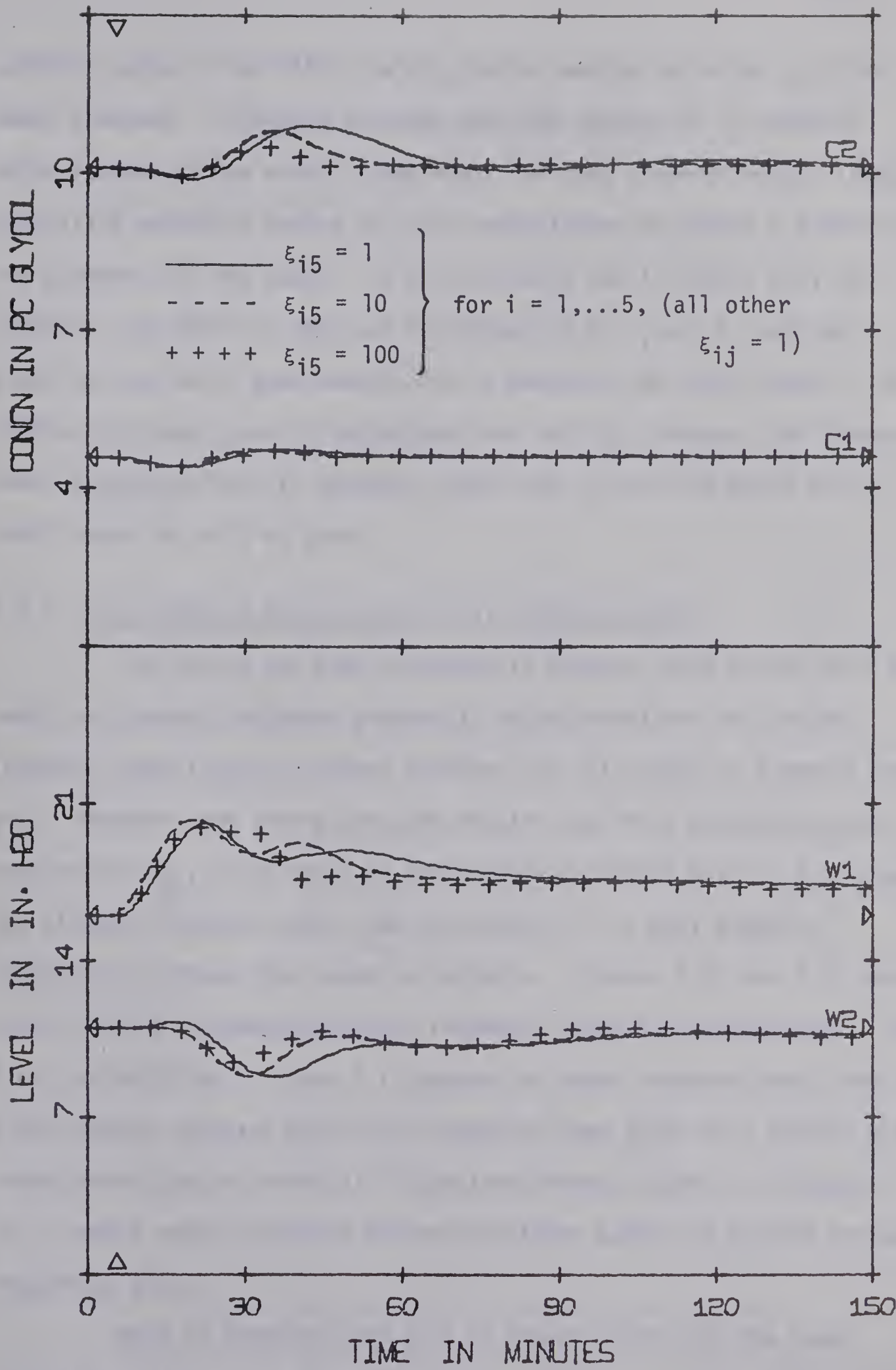


FIGURE 4.17 SIMULATED EFFECT OF STATE WEIGHTING WITH ADAPTIVE LOOP GAINS

adaptive gains in the fifth row of $\underline{\Xi}$ while keeping the other ξ_{ij} elements constant. It should be noted that the control of C_2 improves while control of the other states stays the same or deteriorates slightly. This state weighting method was also demonstrated in Figure 4.9 when all the elements did not adapt. In the simulated run in Figure 4.9, the adaptive loop gains in the rows corresponding to C_1 and h_1 were set equal to zero which gave essentially no weighting to these states. The control of these states deteriorated more notably; however, the improvement of the more heavily weighted states due to the high gains used in their loops can also be seen.

4.4.9 Final Process Response and Final Feedback Matrix

The theory for MRAC presented in Chapter Three stated that the model and process responses eventually become equal and the process feedback control matrix becomes constant for all values of adaptive loop gain. However, the theory does not require the final closed-loop process matrix, \underline{A}_p , to be equal to the closed-loop model matrix, \underline{A}_m , because the Liapunov function total time derivative, \dot{V} , is only negative-semidefinite rather than negative-definite. Figures 4.15 and 4.16 demonstrate that the process and model responses eventually become equal. The first two matrices in Table 4.1 compare the model feedback matrix and the final process feedback matrix (for adaptive loop gains of 1 and 10) and demonstrate that the eventual closed-loop process matrix is not equal to the model matrix although the error between model and process responses reduces to zero.

When an adaptive loop gain of 100 was used with the same initial conditions and repeated disturbance (i.e. open-loop initial conditions and a 40% step change in feedflow every 45 minutes), the third

TABLE 4.1
MODEL AND PROCESS FEEDBACK MATRICES

1) Optimal Model Feedback Matrix:

$$K_{=FBm} = \begin{bmatrix} 10.78 & -1.607 & -4.818 & 0.0 & -19.57 \\ 5.352 & .3598 & .5471 & 0.0 & 12.49 \\ 7.515 & 1.273 & .1833 & 24.61 & 32.69 \end{bmatrix}$$

2) Final¹ Process Feedback Matrix ($\xi_{ij} = 1$ or 10, Open-Loop Initial Control)

$$K_{=FBp} = \begin{bmatrix} 4.274 & -1.863 & .942 & .625 & -1.782 \\ 3.831 & - .4540 & .919 & -.018 & .225 \\ 7.477 & - .6290 & -.1703 & 2.217 & 1.394 \end{bmatrix}$$

3) Approximate² Final Process Feedback Matrix ($\xi_{ij} = 100$, Open-Loop Initial Control)

$$K_{=FBp} = \begin{bmatrix} 200,000 & -6000 & 150 & 30,000 & -9000 \\ 160,000 & -3000 & 150 & 30,000 & -4000 \\ 400,000 & 1000 & 150 & 90,000 & -8000 \end{bmatrix}$$

4) Final¹ Process Matrix ($\xi_{ij} = 100$, Multiloop Initial Control, Small Disturbances³)

$$K_{=FBp} = \begin{bmatrix} 7.214 & -6.274 & -2.656 & 2.118 & -14.60 \\ 7.543 & -.0192 & -1.564 & 2.182 & .6802 \\ 14.44 & 2.933 & -5.183 & 25.52 & 10.90 \end{bmatrix}$$

1. After 100 hours adapting (elements almost stationary).
2. Average of two values taken 20 hours apart after 200 hours adapting.
3. 4% disturbance in feed flow every 20 minutes.

feedback matrix in Table 4.1 was obtained after 200 hours of adapting. The large gains in this matrix produced oscillatory, stable control with a response similar to Figure 4.6 and the control variables exhibited "bang-bang" (i.e. open-shut) behavior. Therefore, the simulation results indicate that for certain conditions, the adaptive control law yields a nonstationary control matrix with large elements and the error between process and model states never reduces to zero. It was also discovered that the magnitude of the elements of the final process feedback matrix could be reduced and the ultimate control improved if the initial control policy was improved, the magnitude of the disturbances was reduced, or the adaptive loop gains were lowered. For example, a multiloop initial control policy and small disturbances (4% step change in feedflow every 20 minutes or 40% changes every 1000 minutes) produced the fourth matrix presented in Table 4.1. When the initial control was an optimal multivariable policy based on an inaccurate model (the first and second effect holdups used in the model were in error by 50% and 20%), an adaptive loop gain of 1000 produced a stationary \underline{K}_{FB} with elements similar to the optimal model feedback matrix and a reduction of the error to zero.

Several differences exist between the theory and the application of MRAC that could explain the large final feedback matrix obtained in some of the runs. The pseudo-inverse used to generate the process feedback matrix, \underline{K}_{FB} , from the adaptive control matrix, $\underline{\Gamma}$, (needed in all processes where the number of control variables is less than the number of state variables) provides only an approximate solution since the 15 elements of \underline{K}_{FB} are determined from the 25 elements of $\underline{\Gamma}$. This is one reason why there are several possible final control matrices depending on

the initial policy, adaptive loop gain, and type of disturbance. The pseudo-inverse approximation could be eliminated if a third-order reference model was used. A third-order model is available [5] and the future investigation of MRAC using this model should be considered in order to eliminate the pseudo-inverse problem.

A second difference between theory and application is that the theory does not make allowance for constrained control variables; however, the hybrid simulation restricted the controls to vary only about the values ± 1.0 in perturbed variables. Combinations of poor initial control policies, violent disturbances, and/or large adaptive loop gains violated these constraints and could cause the control matrices to become large as shown by the results presented in Table 4.1. Since all practical processes have constrained control variables, this is an important limitation of the theory.

Finally, the theory was developed for a continuous process and reference model; however, the application of the theory used a discrete model and sampled process states. The backward difference approximation used for the adaptive algorithm (i.e. Equation (3.48)) could result in large $\underline{\Gamma}$ matrices (and hence a large \underline{K}_{FB}) due to numerical instability problems. A large time increment (sampling interval), poor initial conditions (initial control policy), or large adaptive loop gains could cause the numerical stability problems. To test this hypothesis, the sampling interval of 64 seconds was doubled and then redoubled with an adaptive loop gain of 10, an open-loop initial control policy, and 40% step changes in feed flow every 45 minutes. When the sampling interval (and model calculations) were doubled, a constant \underline{K}_{FB} consisting of small elements resulted. However, when the sampling interval was doubled

again, the process feedback matrix blew up. This supports the conclusion that numerical problems were involved and is a potential problem in the discrete application of this MRAC technique. A higher order difference approximation for Equation (3.24) or a shorter sampling (adapting) period would correct this problem and allow higher loop gains; however, additional calculation time would be required.

4.5 CONCLUSIONS

The simulation results demonstrate the ability of model reference adaptive control to improve upon the initial control of a process. The rate of adapting is determined by the adaptive loop gains, ξ_{ij} , in a manner similar to that of the controller gains used in a conventional control scheme.

All elements of the Γ matrix need not adapt to provide improved control, but the guarantee of stability is then lost. For the evaporator application, higher individual loop gains are allowable when fewer elements adapt. Also, care must be taken when eliminating adapting loops or unstable control may result since the open-loop evaporator is unstable.

Adaptive control can recover from poor initial control policies such as positive feedback. Furthermore, the controller gains used in standard single variable control loops (i.e. multiloop control) provide a good starting point for adaptive multivariable control. This could make adaptive control an attractive method of transferring a process from multiloop control to multivariable control. The reference model does not have to be an exact dynamic model of the actual process but only defines the desired closed-loop process response; therefore, modelling errors are not as serious in adaptive control as they can be in other schemes. MRAC

can also be used for the on-line tuning of a multivariable scheme which is based on an inaccurate model. The results in Figures 4.13 and 4.14 demonstrating good control even though model inaccuracies were great (unseen disturbances and a physically impossible reference model) support this conclusion.

In the evaporator application under certain conditions, large nonstationary feedback control matrices resulted and these large matrices caused bang-bang control with the process and model responses never becoming equal. The conditions that caused the unstable results were large adaptive loop gains, poor initial control policies, and/or large disturbances. The discrete solution of the adaptive control differential equation was one reason for the large \underline{K}_{FB} matrix. Other differences between the theory and the application of MRAC, the pseudo-inverse approximation and the violation of control constraints, could also result in large feedback matrices.

State weighting can be accomplished by using large elements in the rows of the adaptive loop gain matrix $\underline{\Xi}$ corresponding to critical state variables. By varying the individual values of ξ_{ij} , it may be possible to use higher adaptive gains in certain loops than are possible when all loop gains are equal.

An important result is that control continues to adapt with every disturbance, even those which the reference model is not aware of. This would indicate that if a sufficiently low loop gain was chosen, adaptive control should be continued after it has improved the initial control, since later disturbances will tend to continually adjust and improve the control.

CHAPTER FIVE

MODEL REFERENCE ADAPTIVE CONTROL APPLIED TO A DOUBLE EFFECT EVAPORATOR: EXPERIMENTAL RESULTS

5.1 INTRODUCTION

This chapter presents an experimental application of model reference adaptive control (MRAC) based on Liapunov's direct method. The experimental apparatus consisted of a pilot plant double effect evaporator that is interfaced to an IBM 1800 data acquisition and control computer in the Department of Chemical and Petroleum Engineering of the University of Alberta. The theoretical background for this control method and simulation results for the evaporator have been presented in the previous two chapters. This chapter includes a description of the experimental control system and of the programming techniques used on the IBM 1800. The experimental results are then presented and compared to the simulation results. Finally, conclusions concerning the feasibility of model reference adaptive control for industrial applications are offered.

5.2 CONTROL SYSTEM

The steps required to implement model reference adaptive control are presented in block diagram form in Figure 5.1. An IBM 1800 data acquisition and control computer is interfaced to a pilot plant double effect evaporator through analog to digital converters, digital to analog converters, and required transducers. Figure 5.2 presents a schematic diagram of the evaporator. Further details concerning the evaporator equipment and instrumentation can be found in the theses of Newell [3], Fehr [4] and Andre [5].

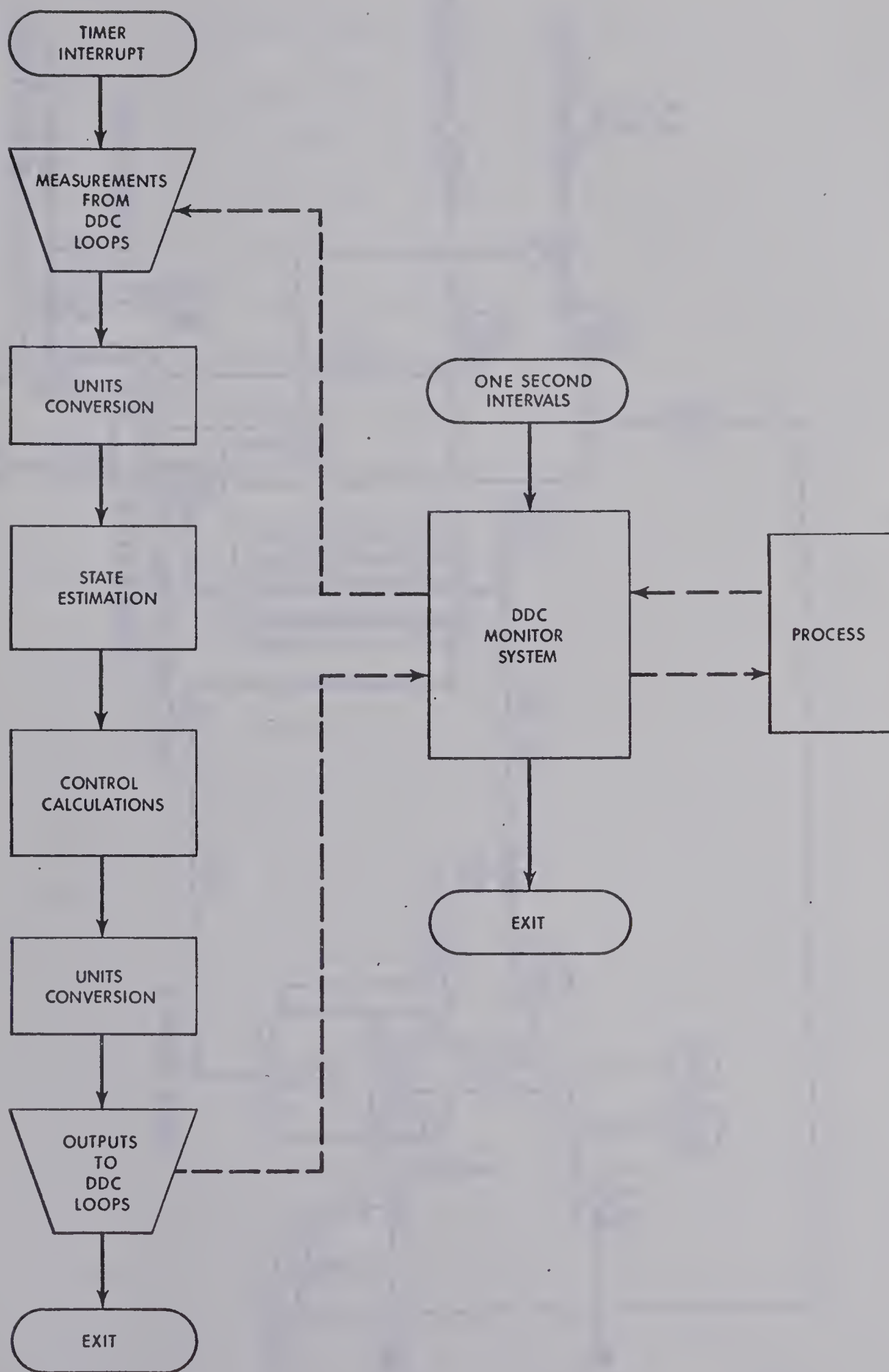


FIGURE 5.1 SCHEMATIC DIAGRAM OF MODEL REFERENCE ADAPTIVE CONTROL

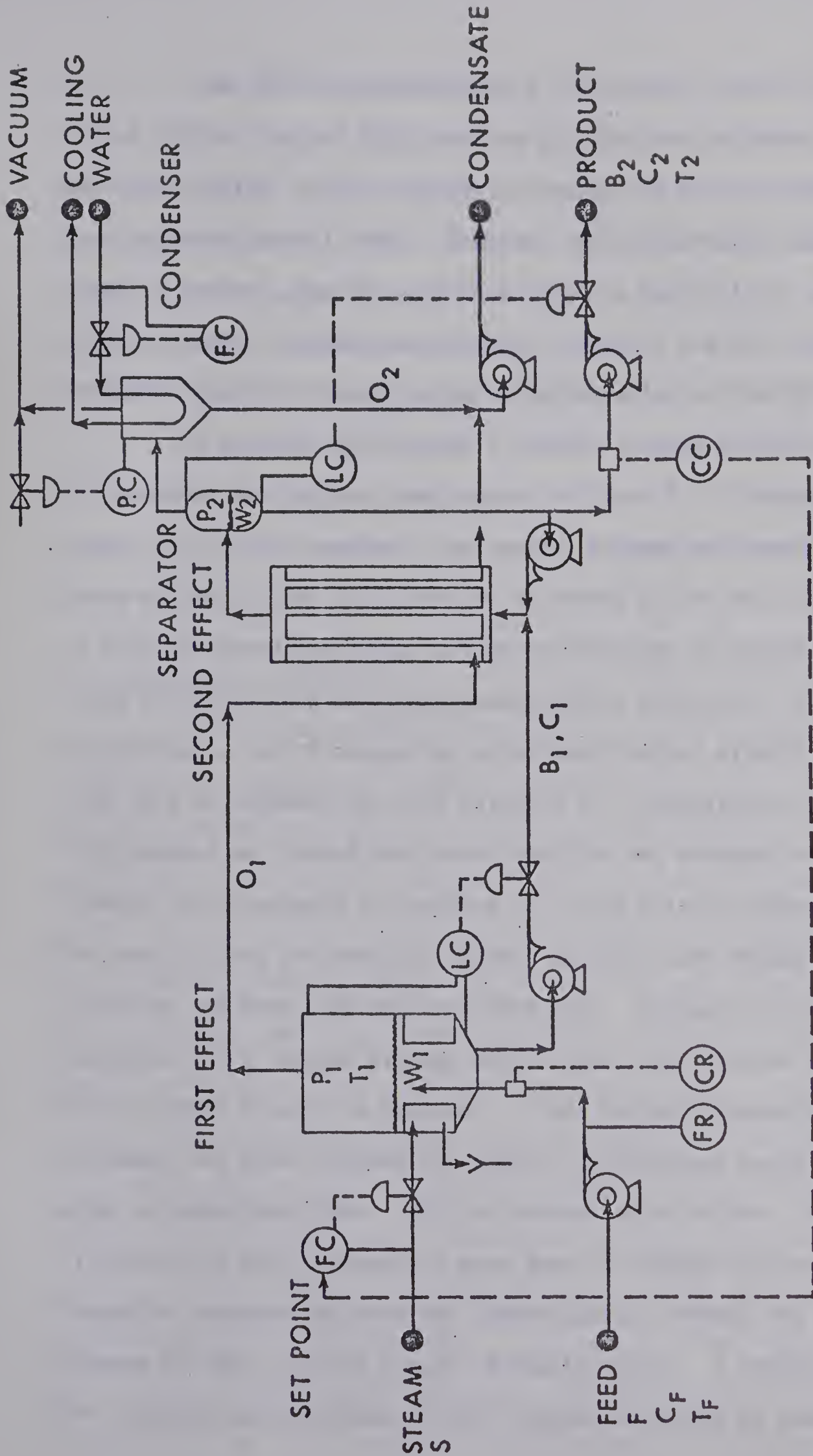


FIGURE 5.2 PILOT PLANT DOUBLE EFFECT EVAPORATOR WITH A CONVENTIONAL MULTILoop CONTROL SYSTEM

The IBM 1800 incorporates a time-shared version of an industrial Direct Digital Control (DDC) package [6] that can implement conventional multiloop control on the evaporator through six single control loops and four cascaded control loops. However, in multivariable model reference adaptive control, the DDC control package is used only to access the state variables (through measurements stored in the DDC loops) and to implement control (through setpoint manipulation in the DDC loops).

A standard multivariable control program developed by Newell [3] executed the various steps shown in Figure 5.1. Since one of the states, C_1 , is not measured, the control program performed the necessary state estimation and also provided filtering of the DDC measurements. It also performed the units conversion necessary to change the measured state variables into normalized perturbation form prior to the control calculations, and to change the calculated control signals from perturbation form to engineering units suitable for transmission to the process. This program was loaded into core from disk and executed at a standard interval of 64 seconds in response to a high priority timer interrupt. The results from the previous control interval were needed for the calculations and were also obtained from disk. Because of the slow disk operations (0.5 seconds average access time), the program required from four to seven seconds to execute. If the control program had been core resident, the time required for control calculations would have been an order of magnitude lower. All the control calculations, state estimation, filtering and units conversion were done in FORTRAN with only simple Assembler programs required for communications between the multivariable program and DDC (via the Process Variable Table). A complete listing of the standard multivariable control program developed by Newell is

available in another research report [3].

The computer program just described is modular in design and only the input and control sections of the standard multivariable program were changed to implement multivariable model reference adaptive control. The subroutines that calculated the model states and the adaptive control were identical to those used in the hybrid simulation studies. Thus, the time required to de-bug the real-time program was greatly reduced by using a hybrid computer in the simulation studies. More details of the programs, listings, logic flowsheets and execution for the adaptive control coreloads can be found in the adaptive control user's manual [7].

5.3 EXPERIMENTAL RESULTS

Fifteen experimental runs were made on the double effect evaporator to investigate the MRAC design parameters and to confirm the conclusions drawn from the simulation results of Chapter Four. The experimental runs investigated the effect of adaptive loop gain, initial control policy, state weighting, repeated disturbances, number of adapting elements, violation of control constraints, and the operation of the evaporator under MRAC at process conditions considerably different from those used to obtain the linear model.

The following figures show the response of the actual evaporator to feed disturbances of approximately 20%, and have an open-loop initial control policy unless otherwise specified. Figure 5.3 illustrates a typical evaporator experimental run. Three of the measured states (state C_1 is not measured) are presented on the left half of the plot with T_1 , first effect temperature, representing the first effect enthalpy, h_1 (i.e. x_{p3}), and the control variables and observable

disturbances given in the right half.

5.3.1 Improvement in Control

Figure 5.3 demonstrates that in spite of the unfavourable initial control policy, MRAC provides fairly rapid model-following and adequate control. Figure 5.4 compares another experimental run with different adaptive loop gains to the optimal feedback reference model, and demonstrates the improved control after a second 20% disturbance in feed flow.

Figure 5.5 compares the experimental run illustrated in Figure 5.3 with the simulation results for the same disturbance. As illustrated in this figure, the experimental results are in general agreement with the simulated results except for W_2 , the response of this variable being too oscillatory initially. This could be due to process noise as compared to the virtual absence of noise in the hybrid simulation. However, evaporator noise levels are quite small [8]. Modelling errors and the nonlinear nature of the evaporator are more likely the cause of these differences. Figure 5.6 also compared simulated and experimental results and a generalization seems possible; W_1 shows improved experimental control while the control of C_2 and W_2 is better in the simulation. This is also demonstrated in Figure 5.7 which compares experimental and simulated errors in W_1 . The experimental error reduces to zero more rapidly. Figure 5.8 demonstrates that the adapting parameter γ_{51} , the element of $\underline{\Gamma}$ that is affected most by W_1 , adapts more quickly in the experimental run. The modelling errors between the actual nonlinear evaporator and the linear open-loop model used in the simulation probably caused these differences.

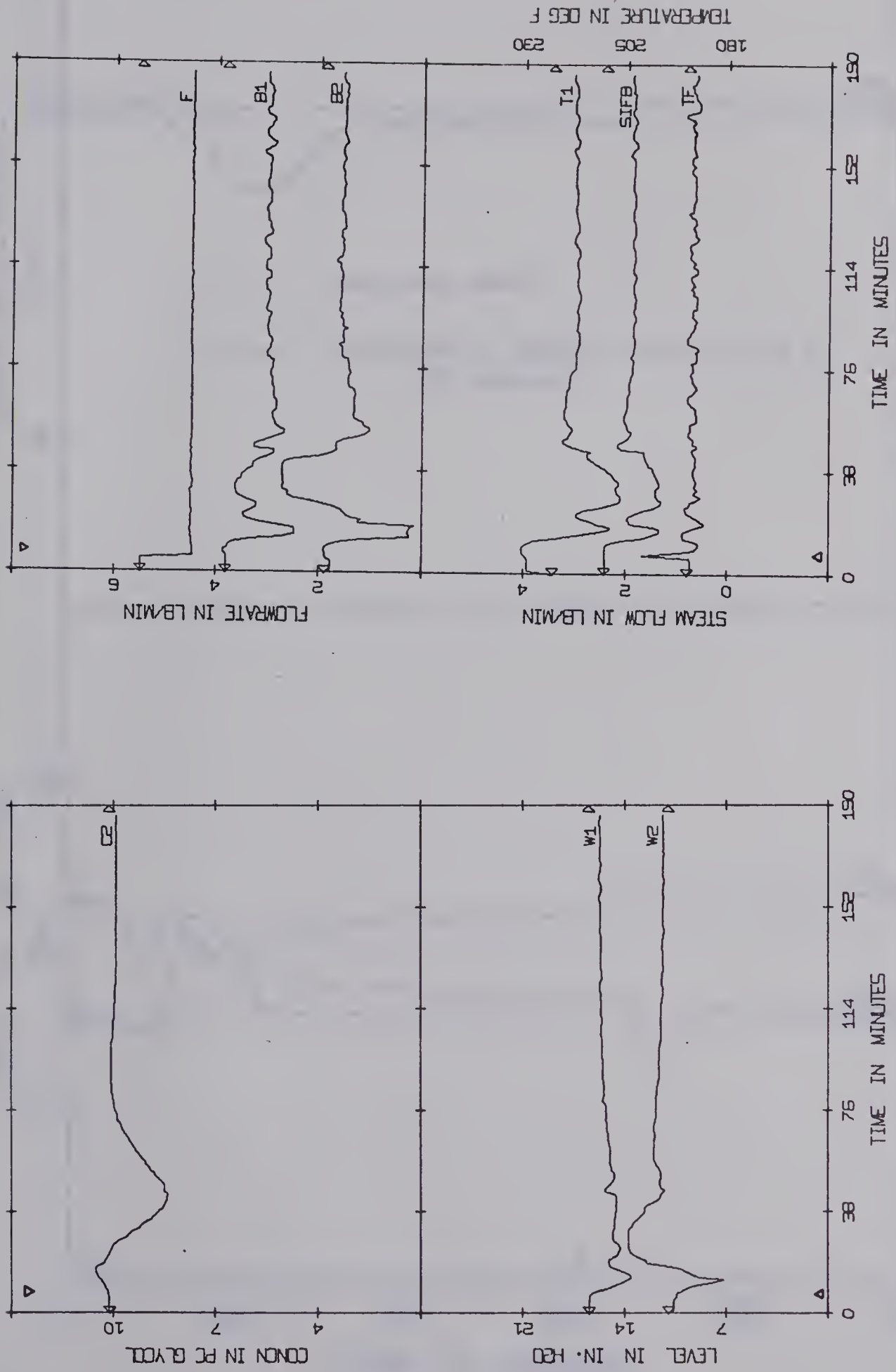


FIGURE 5.3. EXPERIMENTAL RESULTS OF MRAC, ADAPTIVE LOOP GAIN $\xi_{ij} = 1$

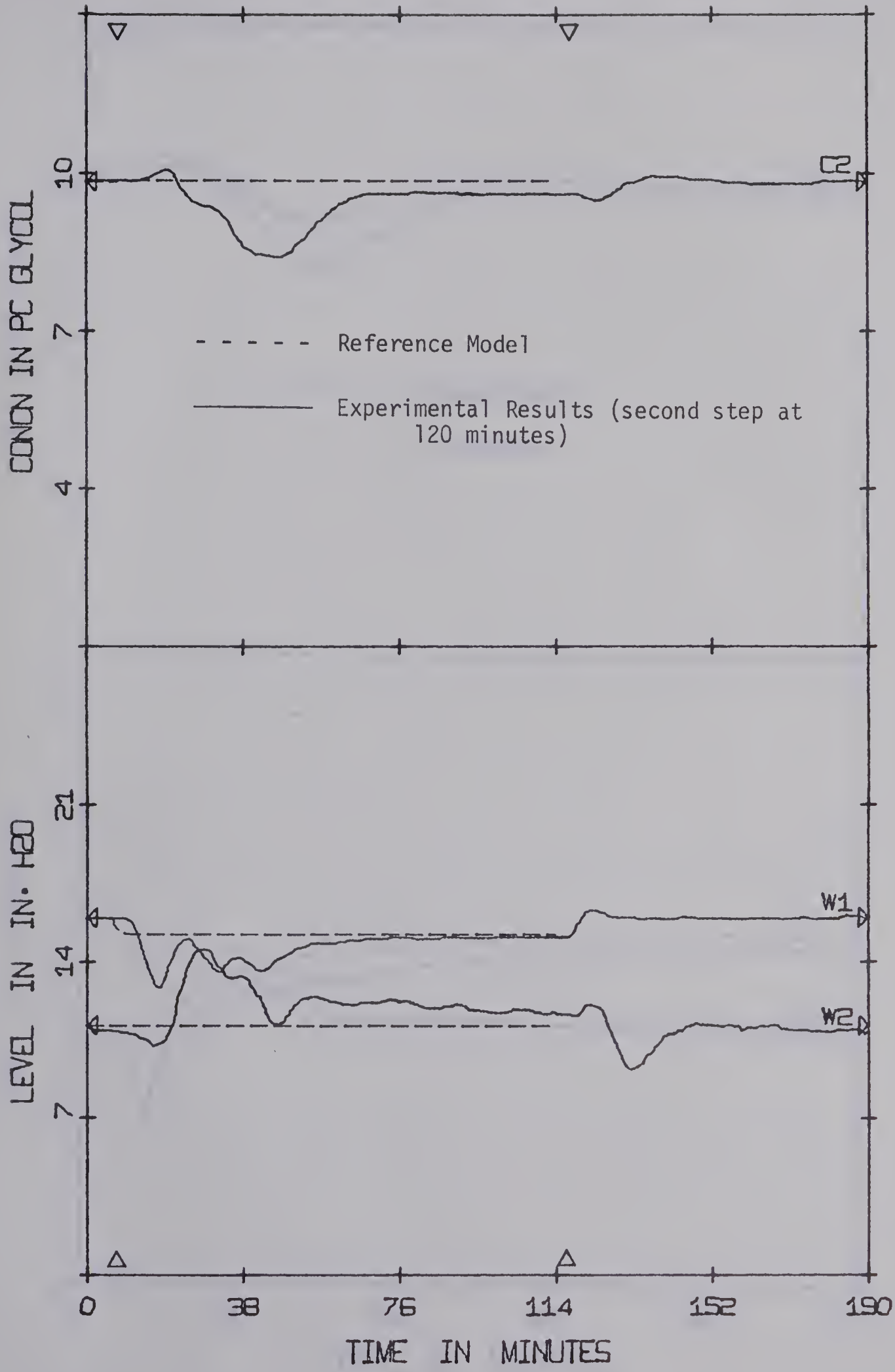


FIGURE 5.4 EXPERIMENTAL MRAC AND REFERENCE MODEL ($\xi_{i3} = 0.25$, $\xi_{i5} = 10$, $\xi_{ij} = 1$ for all other i, j)

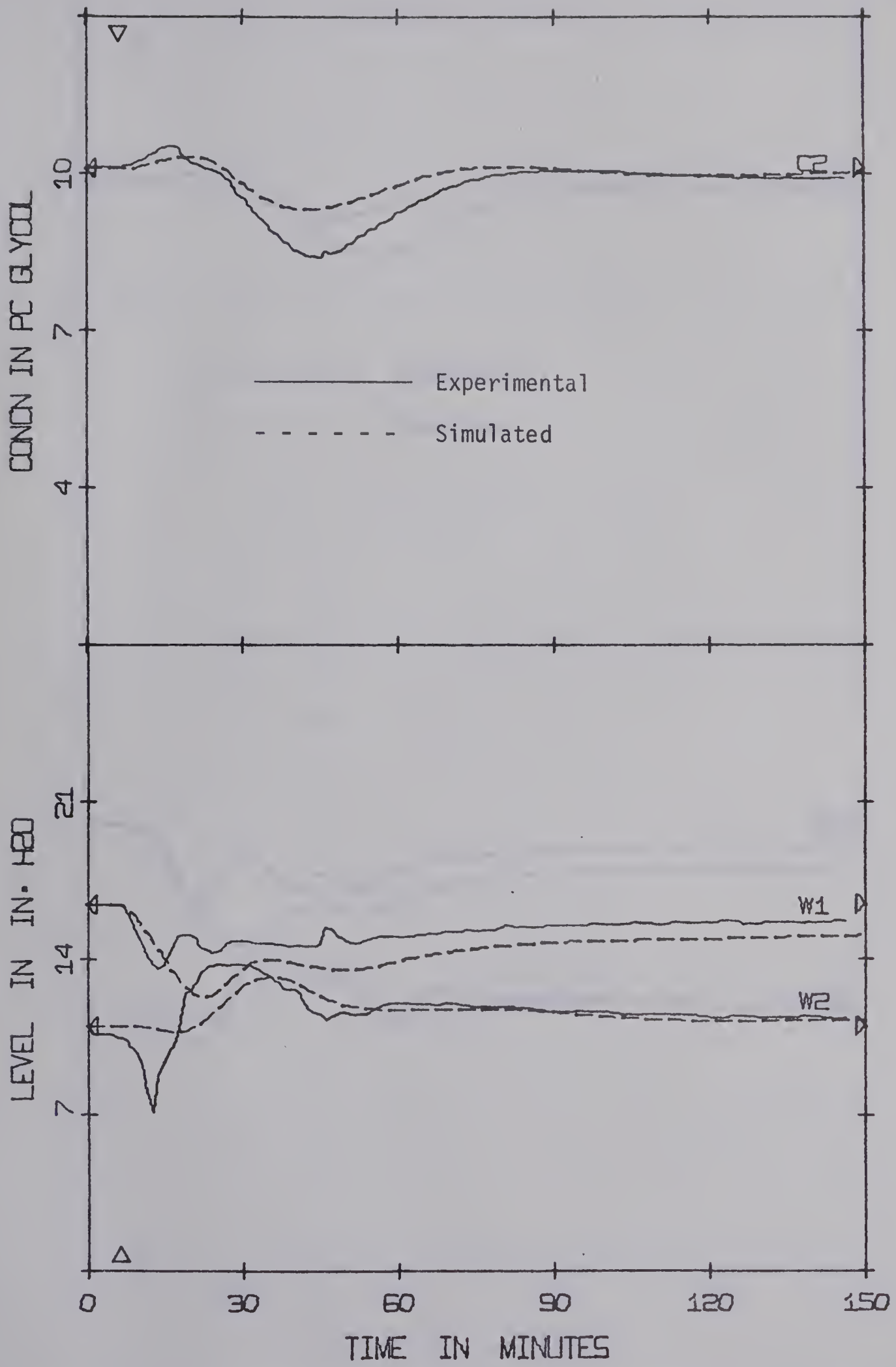


FIGURE 5.5 EXPERIMENTAL VS. HYBRID SIMULATION RESULTS, $\xi_{ij} = 1$

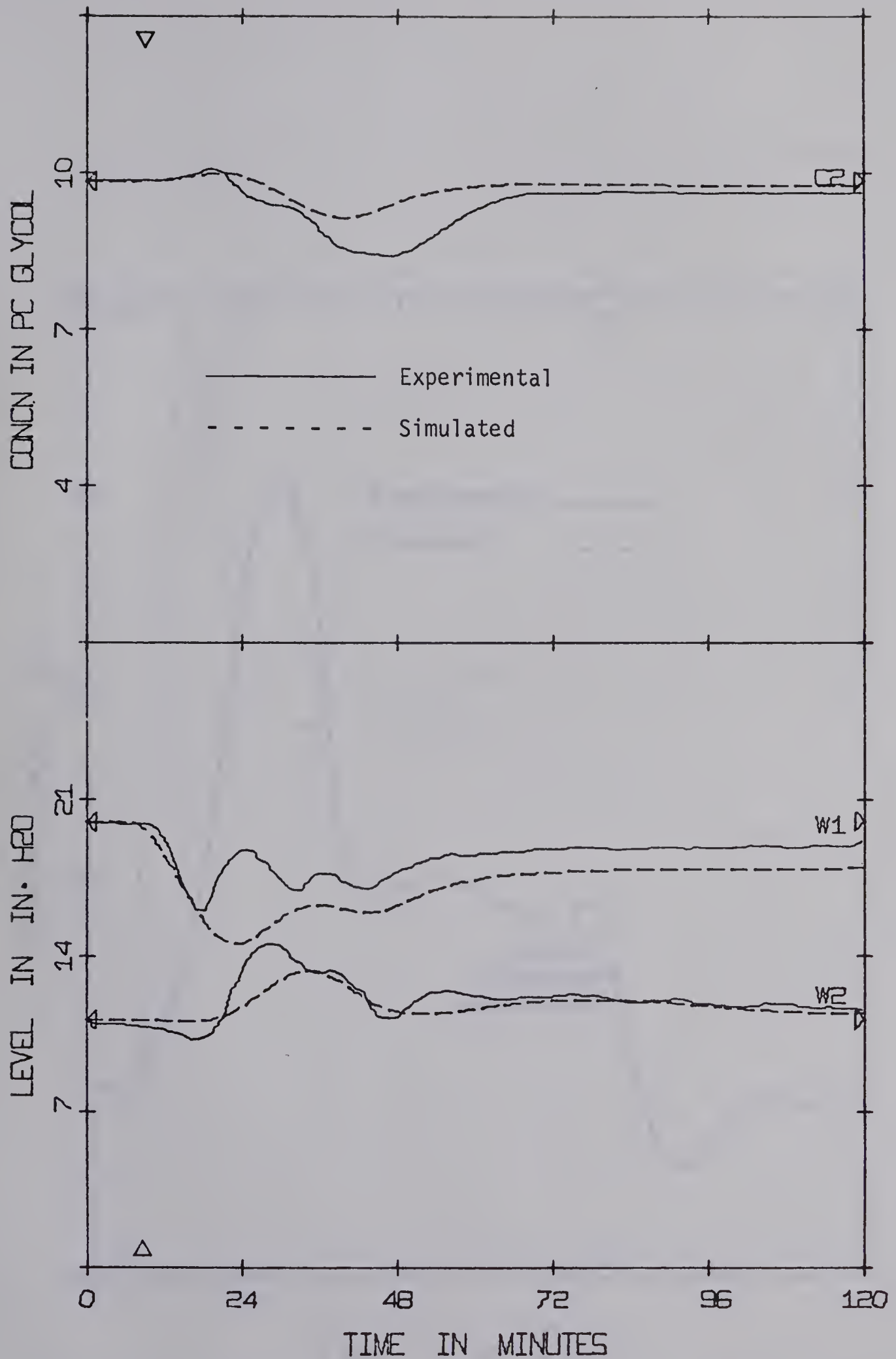


FIGURE 5.6 EXPERIMENTAL VS. HYBRID SIMULATION RESULTS ($\xi_{i3} = 0.25$, $\xi_{i5} = 10$, $\xi_{ij} = 1$, for all other i, j)

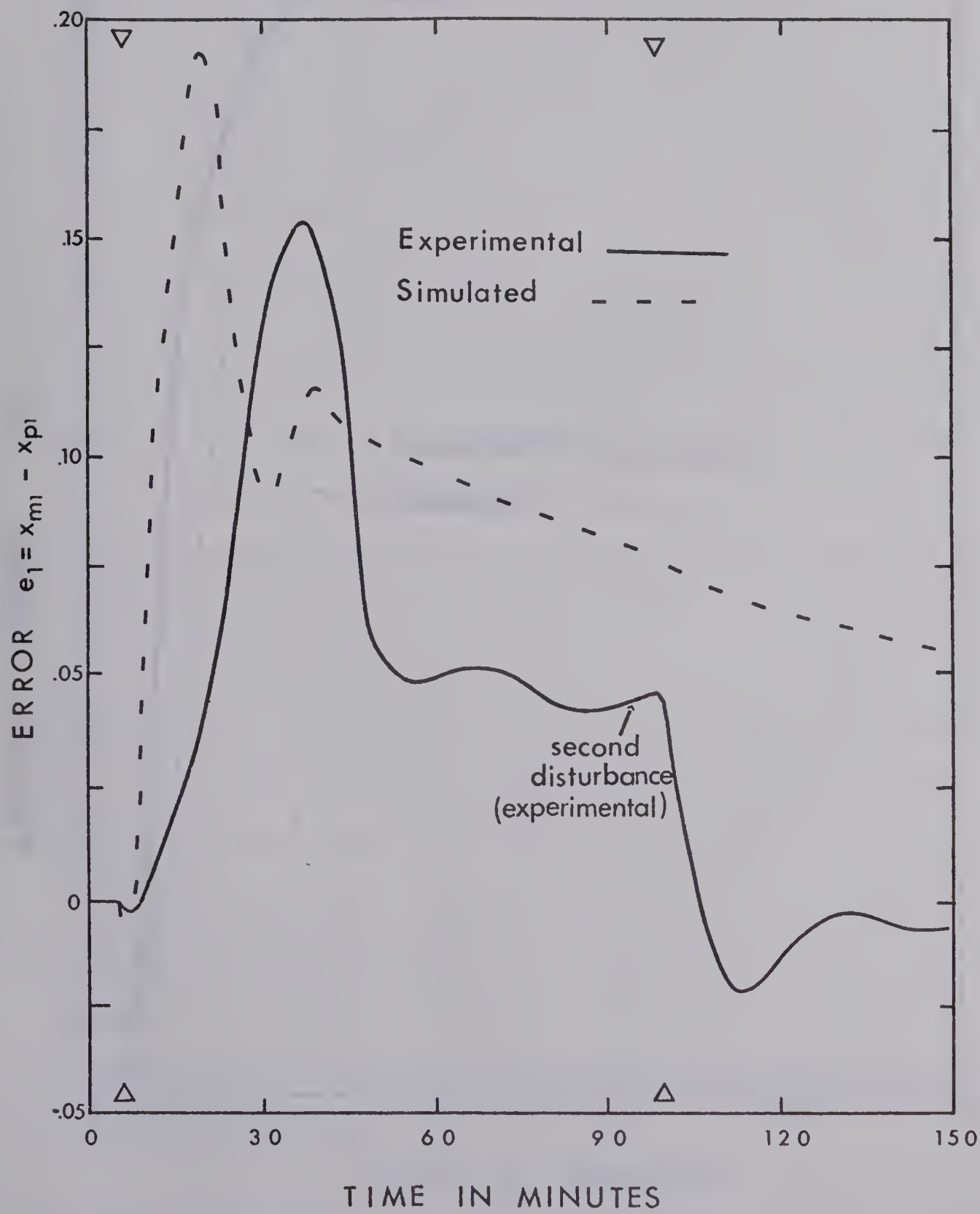


FIGURE 5.7 EXPERIMENTAL w_1 ERROR VS. SIMULATED w_1 ERROR ($\xi_{i3} = .25$, $\xi_{i5} = 10$, all other $\xi_{ij} = 1$)

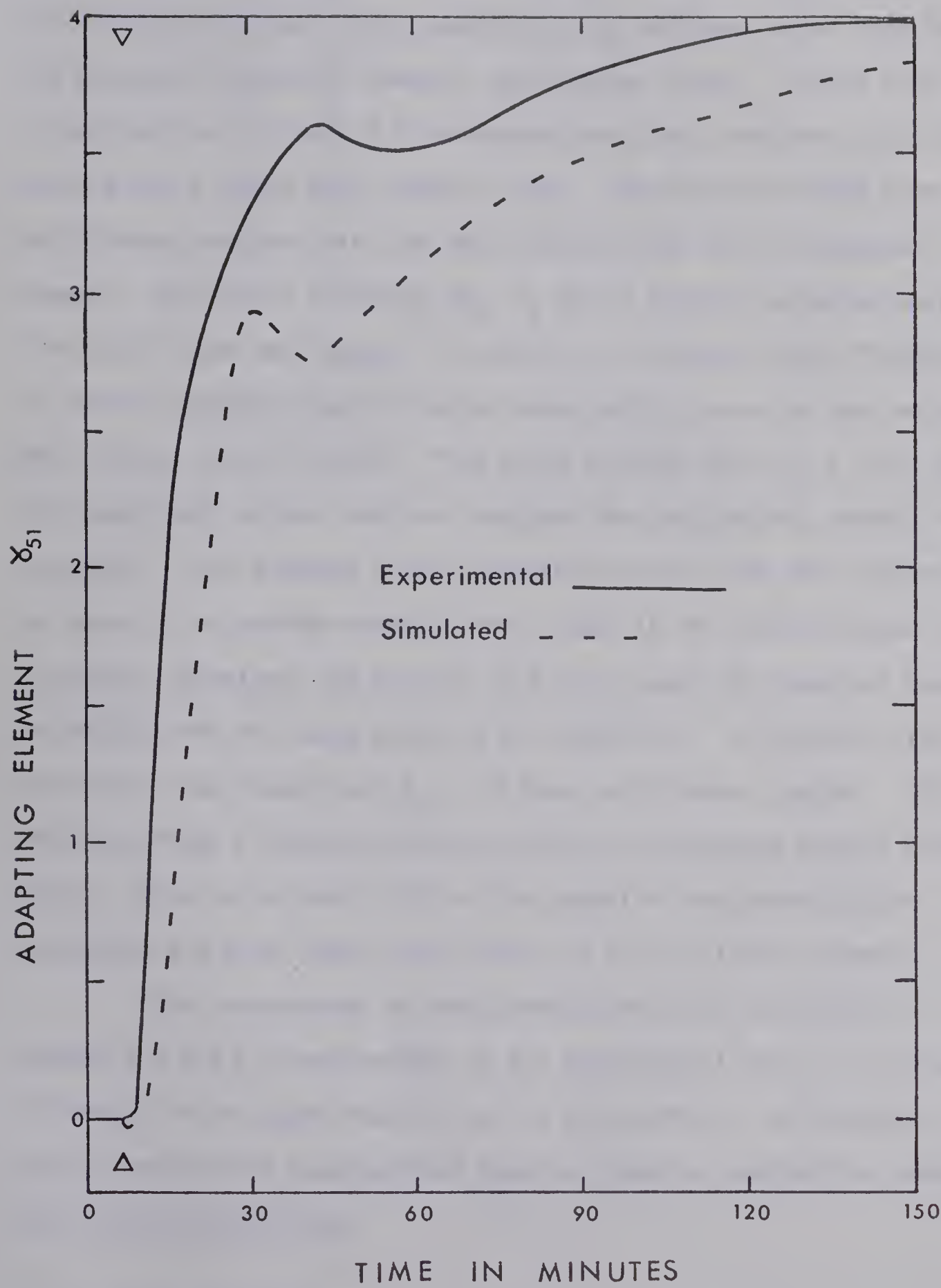


FIGURE 5.8 EXPERIMENTAL γ_{51} ELEMENT VS. SIMULATED γ_{51} ELEMENT
($\xi_{i3} = 0.25$, $\xi_{i5} = 10$, all other $\xi_{ij} = 1$)

5.3.2 Effect of Adaptive Loop Gain

Figure 5.9 illustrates adaptive control when $\xi_{ij} = 10$. This plot demonstrates more rapid adapting to the reference model than for the previous loop gains, however, oscillations result. Figure 5.10 is a continuation of Figure 5.9 and demonstrates that continued oscillations occur after a second step change in flow. The state variables have a satisfactory response with the oscillations being of low magnitude; however, the control variables (B_1 , B_2 and S) exhibit sustained oscillations with large amplitudes. In practical situations, these fluctuations in control variables would be undesirable due to excessive wear on equipment such as control valves. This would indicate that $\xi_{ij} = 10$ is above the upper limit of the adaptive loop gain for satisfactory control of the evaporator. The feedback control matrix resulting from this run was not as large as the optimal feedback matrix used in the reference model calculations; therefore, the gain of 10 did not cause the numerical problems associated with the large gains in the simulation. By contrast, the simulation runs showed that $\xi_{ij} = 10$ gave satisfactory control. This result confirms a conclusion derived from the simulation studies (Chapter Four): there is an upper limit on the adaptive loop gains for the evaporator and gains above this limit give an oscillatory response.

The disturbances in feed temperature, most noticeable in Figures 5.9 and 5.10 and present in all experimental runs, are a result of changes in the steam flow (S) to the first effect. An interaction results because the same manifold supplies steam to control the process and to pre-heat the feed.

5.3.3 State Weighting

Figure 5.11 demonstrates the effect of state weighting in

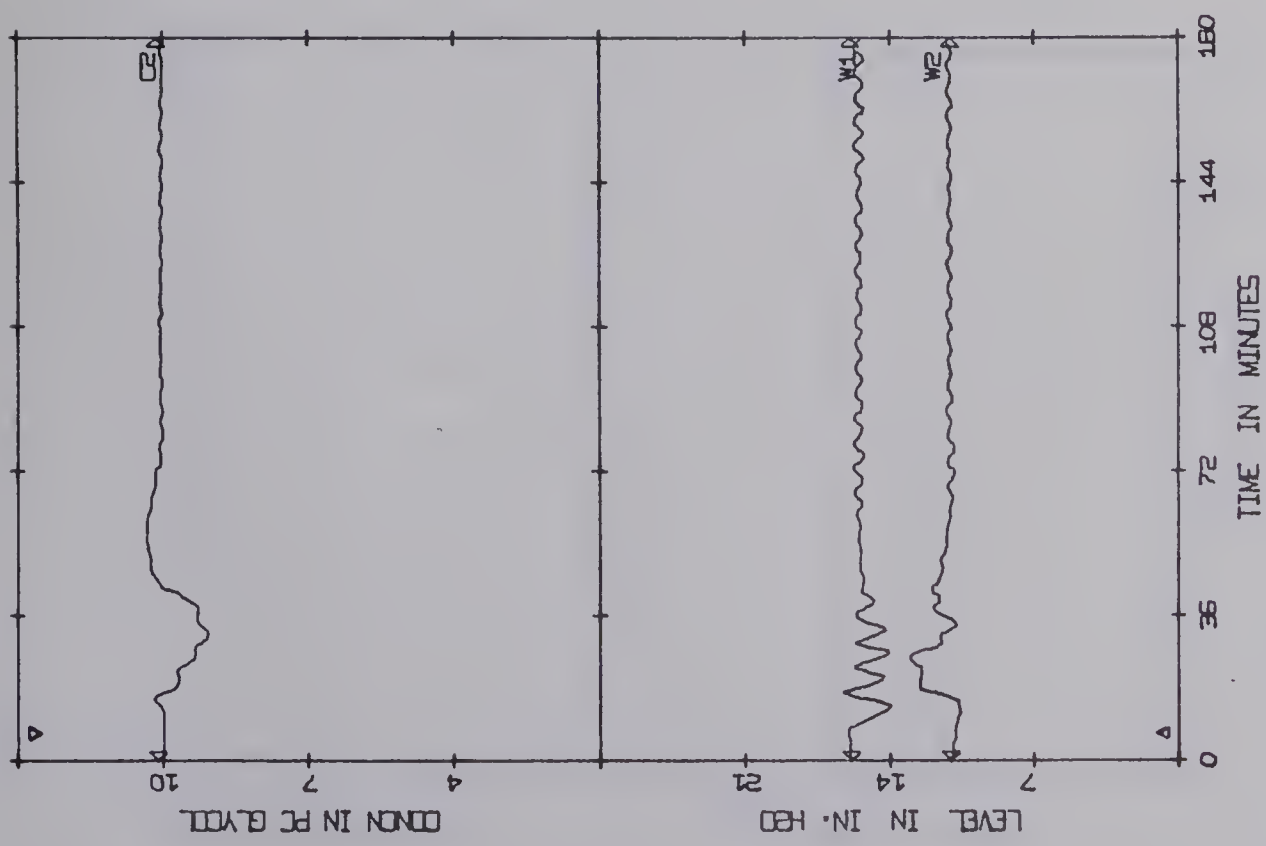
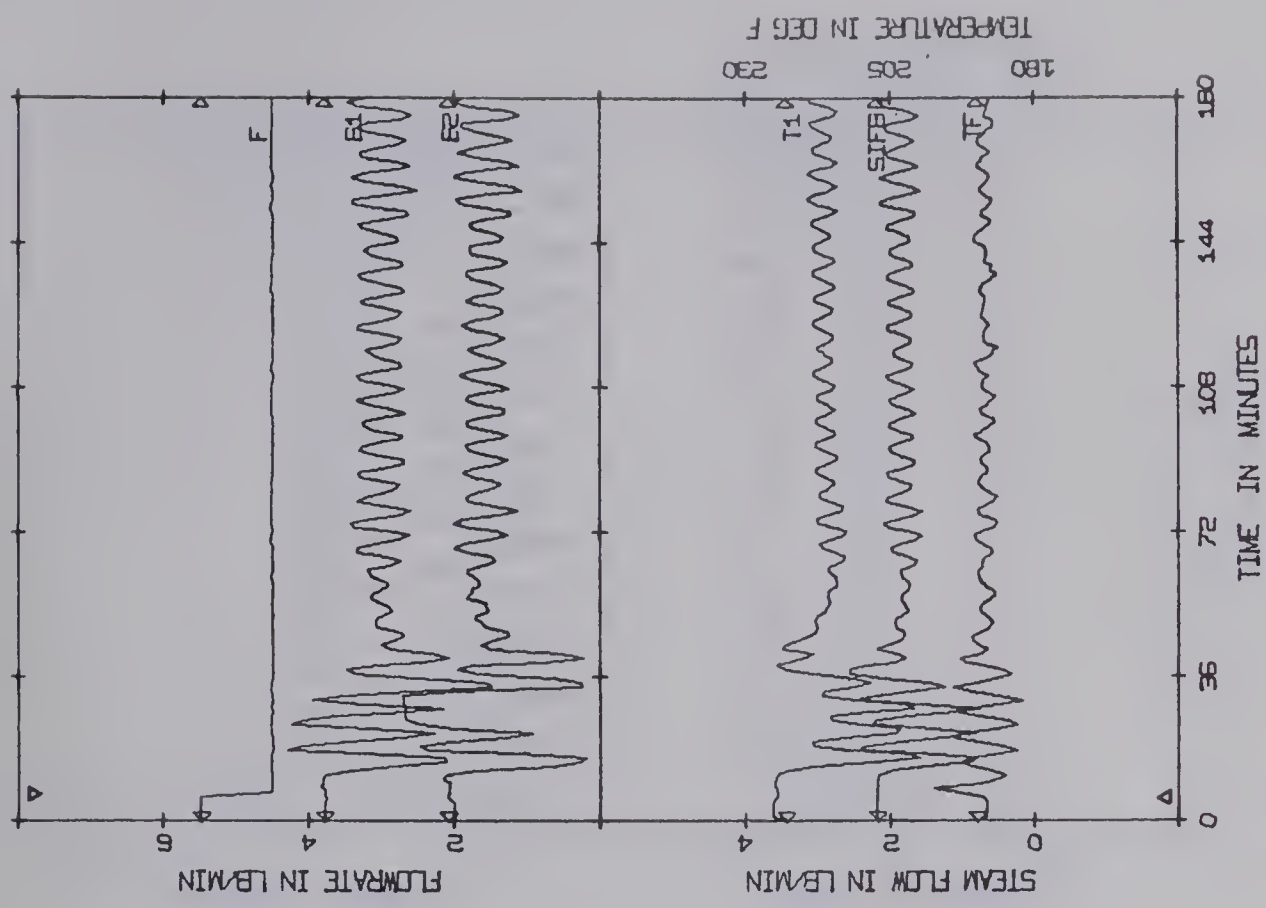
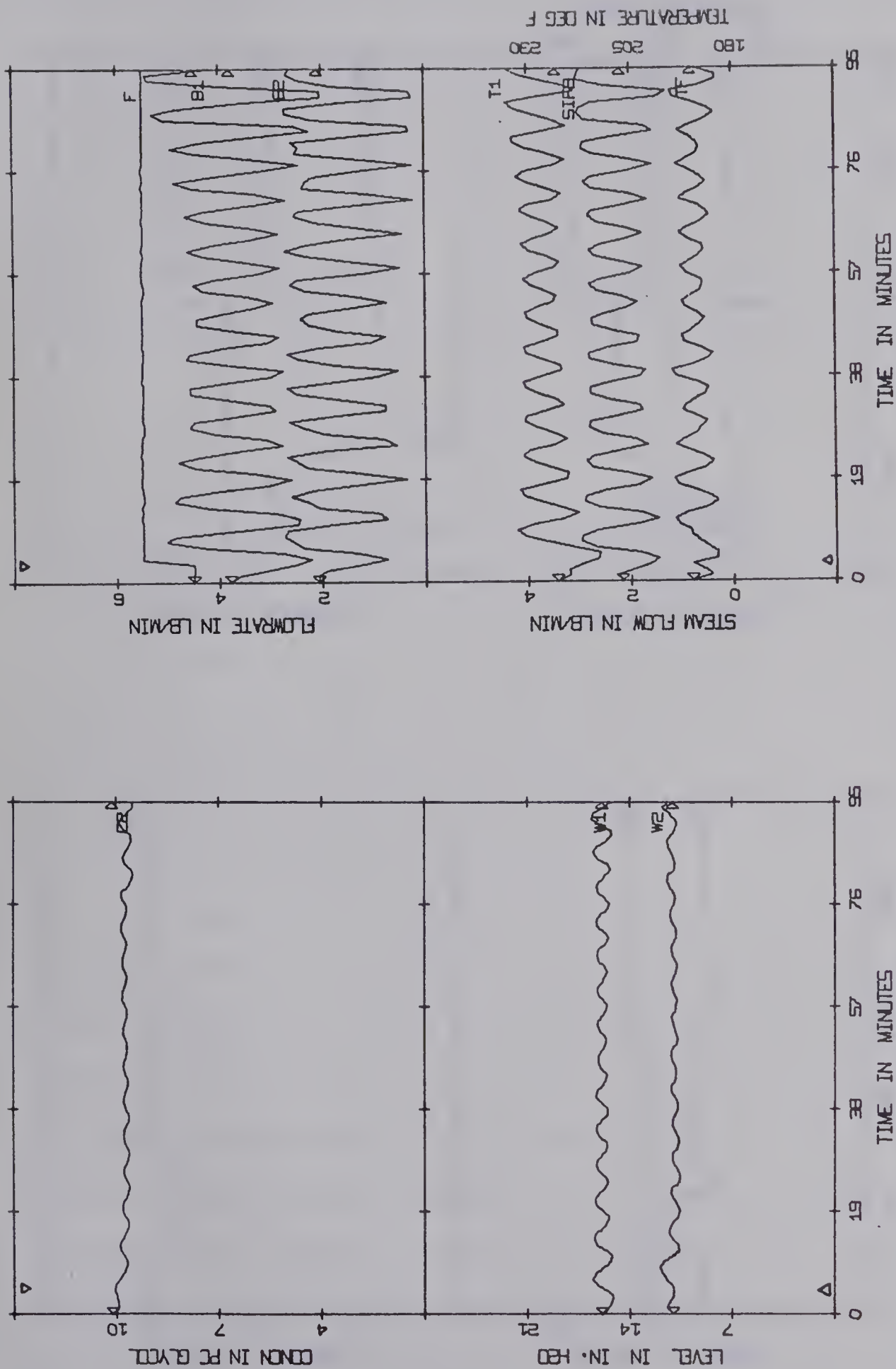


FIGURE 5.9 EXPERIMENTAL MRAC, $\epsilon_{ij} = 10$

FIGURE 5.10 EXPERIMENTAL MRAC: SECOND DISTURBANCE FOR $\xi_{ij} = 10$



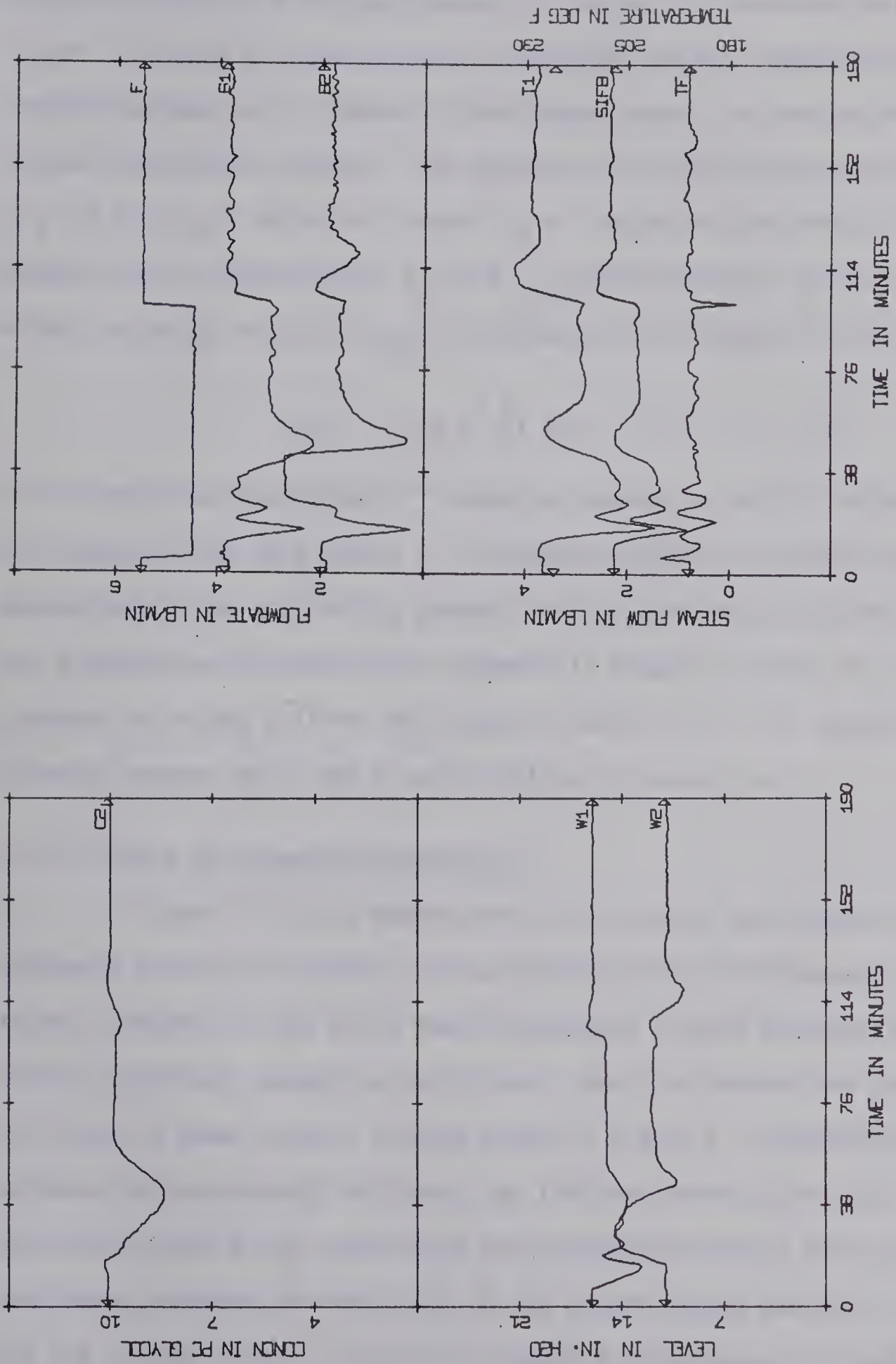


FIGURE 5.11 EXPERIMENTAL EFFECTS OF STATE WEIGHTING AND REPEATED DISTURBANCES ($\xi_{i3} = 0.25$, $\xi_{i5} = 10$, all other $\xi_{ij} = 1$)

adaptive control and the improvement in control for repeated disturbances. Figure 5.11 used the same adaptive loop gains and was subjected to the same disturbance as in Figure 5.4 and demonstrates the reproducibility of the experimental results. The adaptive loop gains were chosen as $\xi_{i3} = 0.25$, $\xi_{i5} = 10$ and all other $\xi_{ij} = 1$ to weight the errors in the second effect concentration, C_2 (i.e. x_{p5}), more strongly than the first effect enthalpy, h_1 (i.e. x_{p3}). The adapting law (Chapter Three)

$$\dot{\gamma}_{ij} = x_{pj} e^T p_{-i} \xi_{ij} \quad (i, j = 1, \dots, 5)$$

can be weighted towards the j^{th} state by increasing the j^{th} column of the adaptive loop gain matrix Ξ . Simulation studies in Chapter Four demonstrate that improved C_2 control results with this weighting method and a comparison of the initial response in Figure 5.3 with the initial response in Figure 5.11 for the states C_2 and T_1 (i.e. h_1) demonstrates improved control in C_2 and a deterioration of control in T_1 .

5.3.4 Effect of Repeated Disturbances

Figure 5.11 also demonstrates that control and adapting to the reference model will improve with continuing process disturbances. The initial response to the first feed disturbance is poor because of the initial open-loop control on the system. When the second step change in feed flow is made, control is much better. Figure 5.7 demonstrates the improved reference model following for the first effect level, W_1 . These runs confirm the theoretical and simulation results that demonstrated continuing adapting and reduction of the error between the model states and the process states to zero with repeated disturbances. Since the steam control causes continuing upsets in the feed enthalpy due to the common steam manifold, this result is important for this particular process.

5.3.5 Initial Control Policy

Figure 5.12 illustrates a good initial control policy, $\underline{r}(0)$, for MRAC, namely, well-tuned multiloop control values for the control loops illustrated in Figure 5.2. The initial multiloop control values are the same ones used in the simulation runs with multiloop initial control and are presented in the Appendix for Chapter Four. The initial response is much better than the corresponding run with initial open-loop control shown in Figure 5.11. The response does not show as much improvement over the multiloop control as the simulation results demonstrated. However, the control continued to adapt with MRAC and the second disturbance has less effect. Conventional multiloop control (without adapting) would give essentially the same type of response for the second disturbance as it did for the first disturbance.

5.3.6 Number of Adapting Elements of \underline{r}

All elements of \underline{r} need not adapt for adequate control to be maintained. In the run depicted in Figure 5.13, only 11 elements of the \underline{r} elements adapted, the same elements used in the simulation results of Figure 4.9 (Chapter Four). These loops were chosen such that adapting would be maintained for the largest elements in the optimal \underline{K}_{FB} matrix used in the reference model. The control here is exceptional because the loop gain chosen, $\xi_{ij} = 10$, is probably close to the best adaptive gain for this system. (Note that $\xi_{ij} = 10$ produced oscillatory results when all the gains adapted, Figure 5.9.) This phenomenon was also demonstrated in the simulation results.

5.3.7 Effect of Unseen Disturbances

The effect of unseen disturbances is important in the real

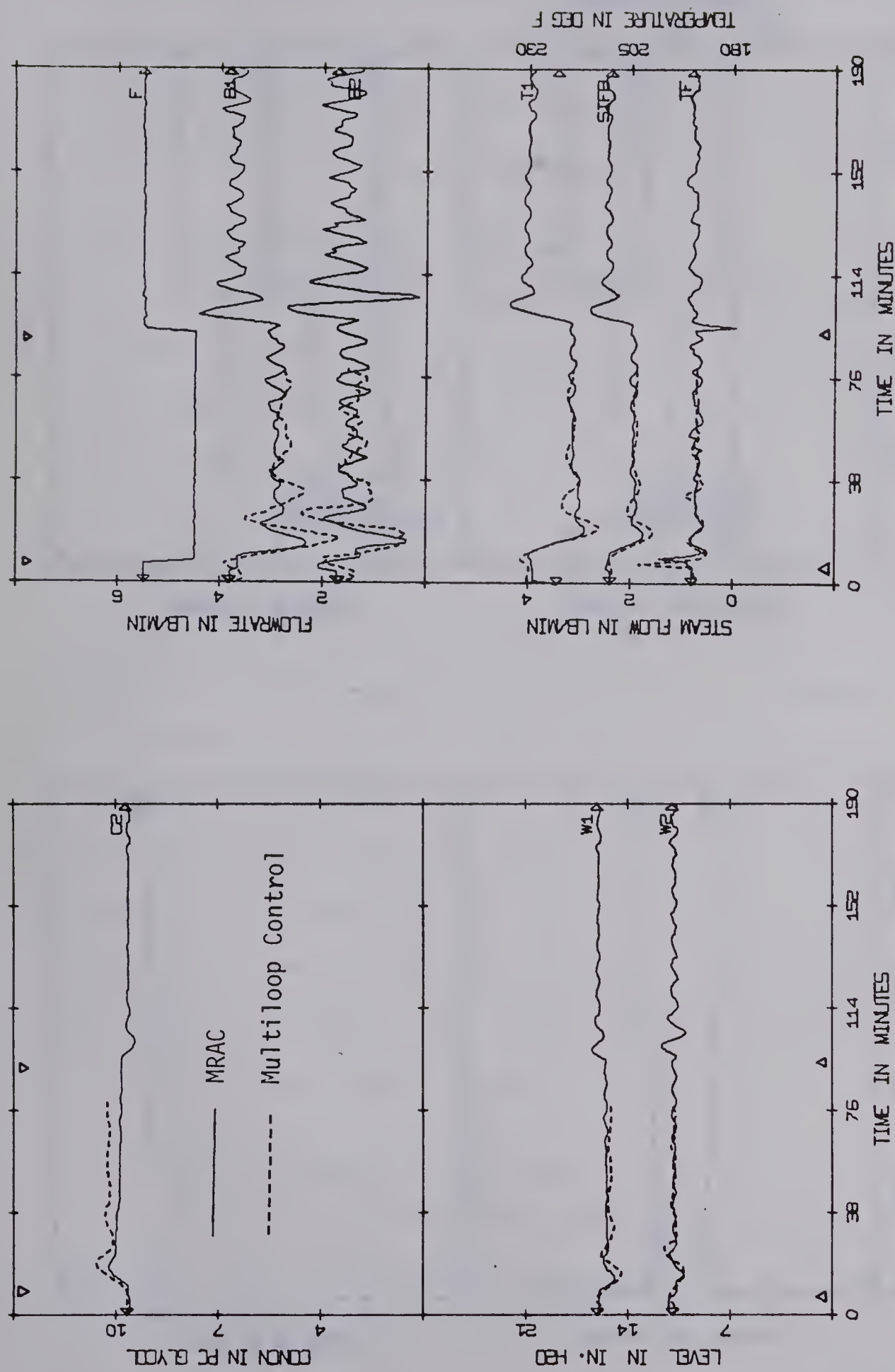


FIGURE 5.12 EXPERIMENTAL MRAC WITH MULTILoop INITIAL CONTROL VS. MULTILoop CONTROL ($\xi_{i3} = 0.25$, $\xi_{i5} = 10$, all other $\xi_{ij} = 1$)

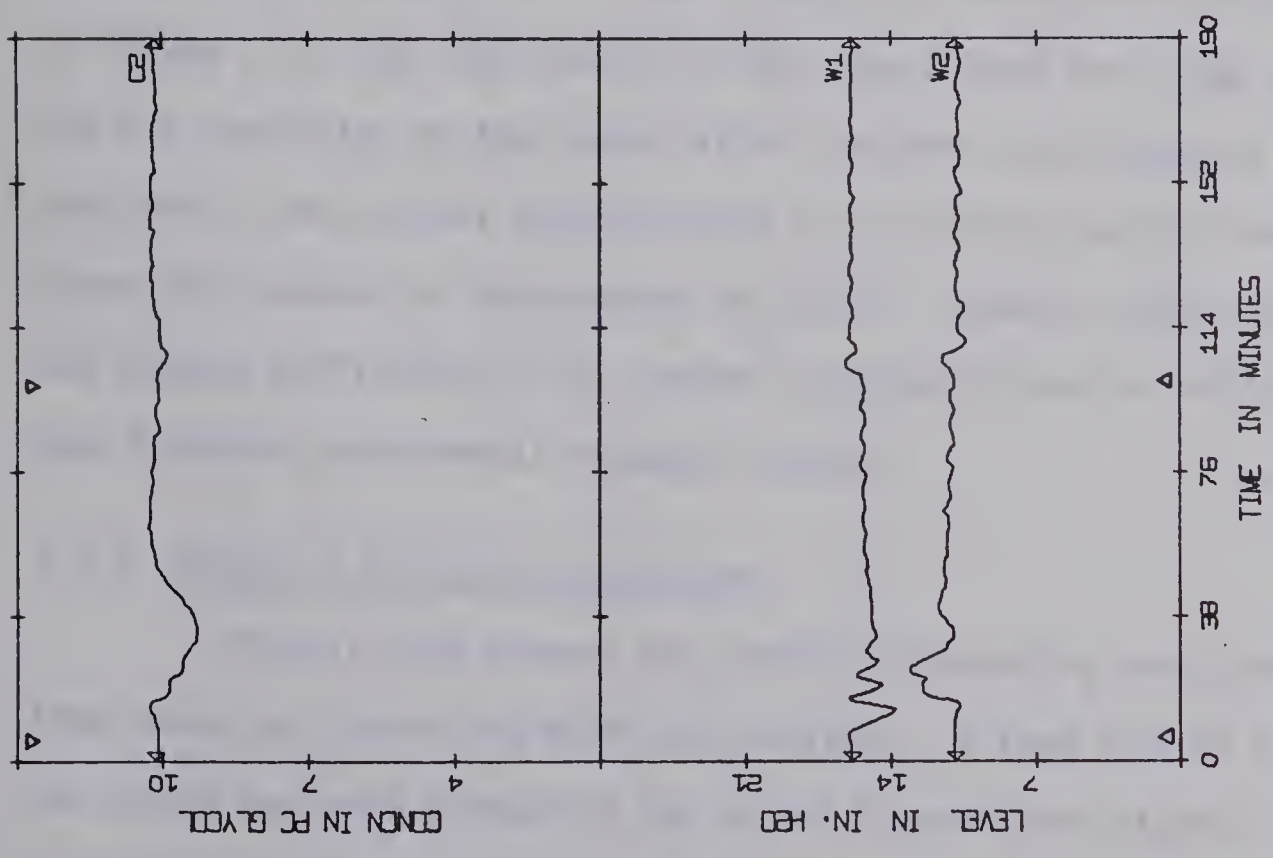
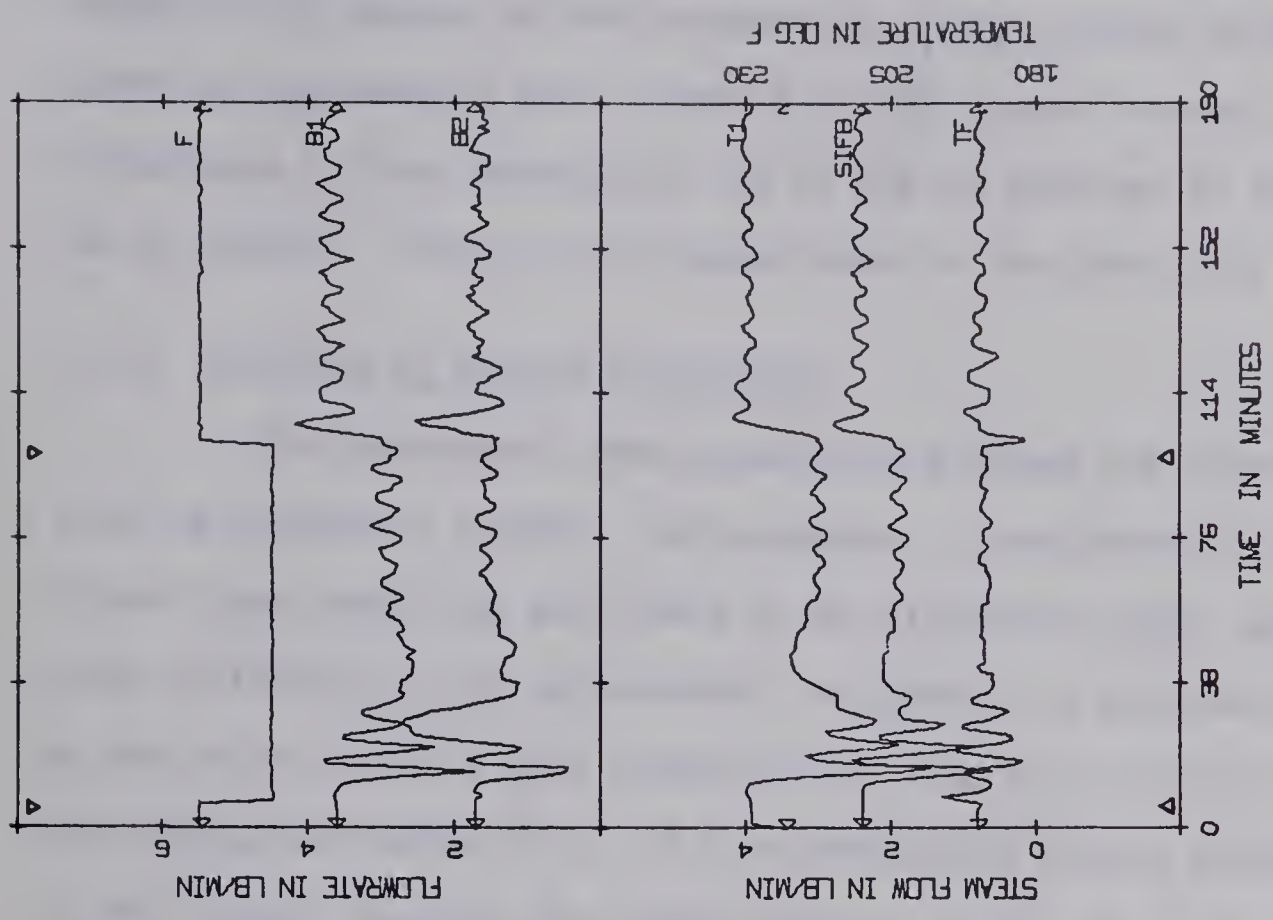


FIGURE 5.13 EXPERIMENTAL MRAC: 11 ELEMENTS ADAPTING, $\xi_{ij} = 10$

process since changes in feed composition, $C_F(d_2)$, cannot be detected during an experimental run. Figure 5.14 illustrates the small effect a disturbance in feed composition, C_F , of 10% not observed by the model has on control. This was also demonstrated in the simulation results.

5.3.8 Violation of Control Constraints

The experimental runs encountered problems not experienced with the simulation studies: the evaporator is nonlinear (as compared to the linear open-loop model used in the simulation runs), one of the state variables (C_1) is not measured, and there is a physical constraint on one of the controls that is more severe than the constraint used in the simulation studies (i.e. ± 1.0 in perturbed control variables). In this latter instance, the steam control variable, S , was not able to achieve a maximum flow rate of 4.0 lb/min that was assumed in the simulation study. In fact, a flow rate of only 3.0 lb/min could be achieved. In Figure 5.15, the +20% change in feed flow caused the steam constraint and the constraint on the second effect bottoms flow (negative flow was required by the control calculations) to be violated and in turn, caused the control to deteriorate initially. However, after the control has adapted sufficiently, the control constraints are not violated and a much improved experimental response results.

5.3.9 Change in Operating Conditions

Finally, the process was tested at operating conditions far from where the linearized model was obtained. A feed rate of 3.5 pounds per minute was used instead of the normal 5 pounds per minute. This caused a higher concentration in the second effect product than is normally produced since the steam flow rate was kept constant at the

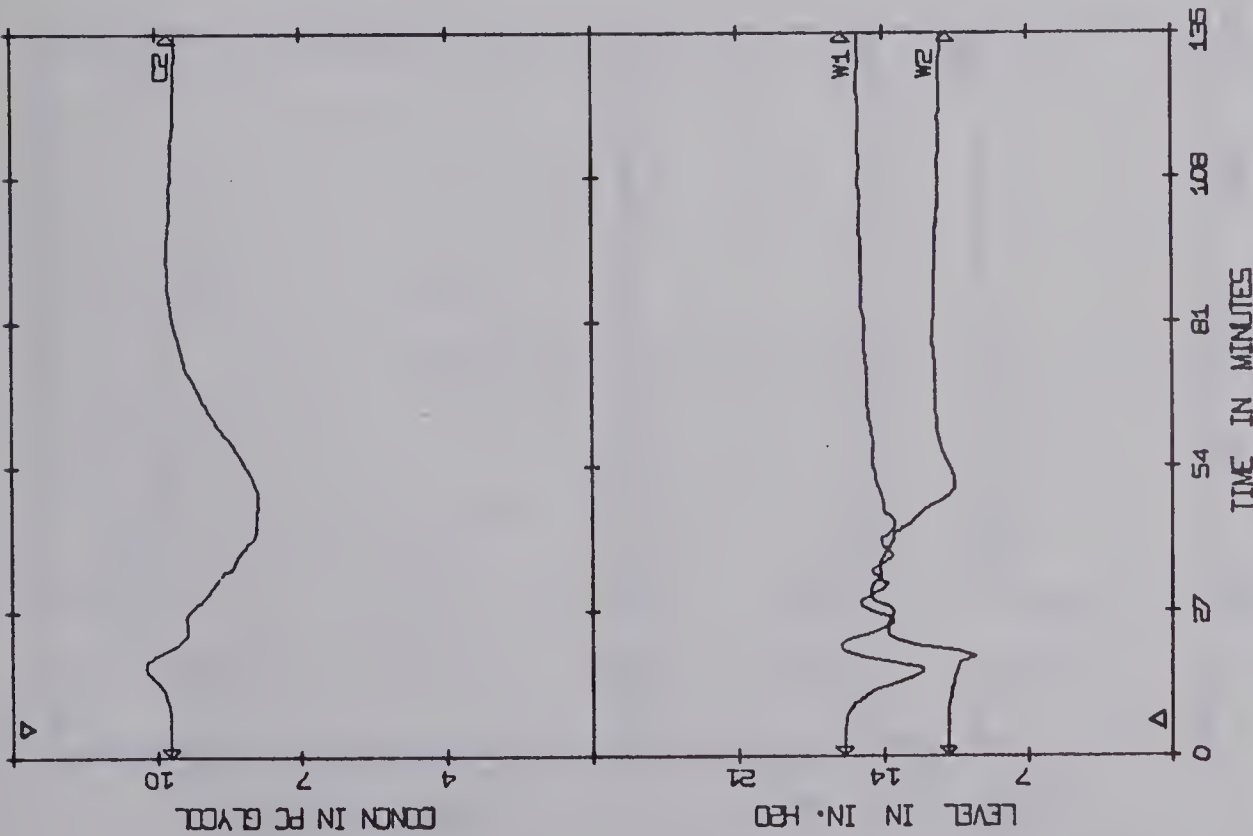
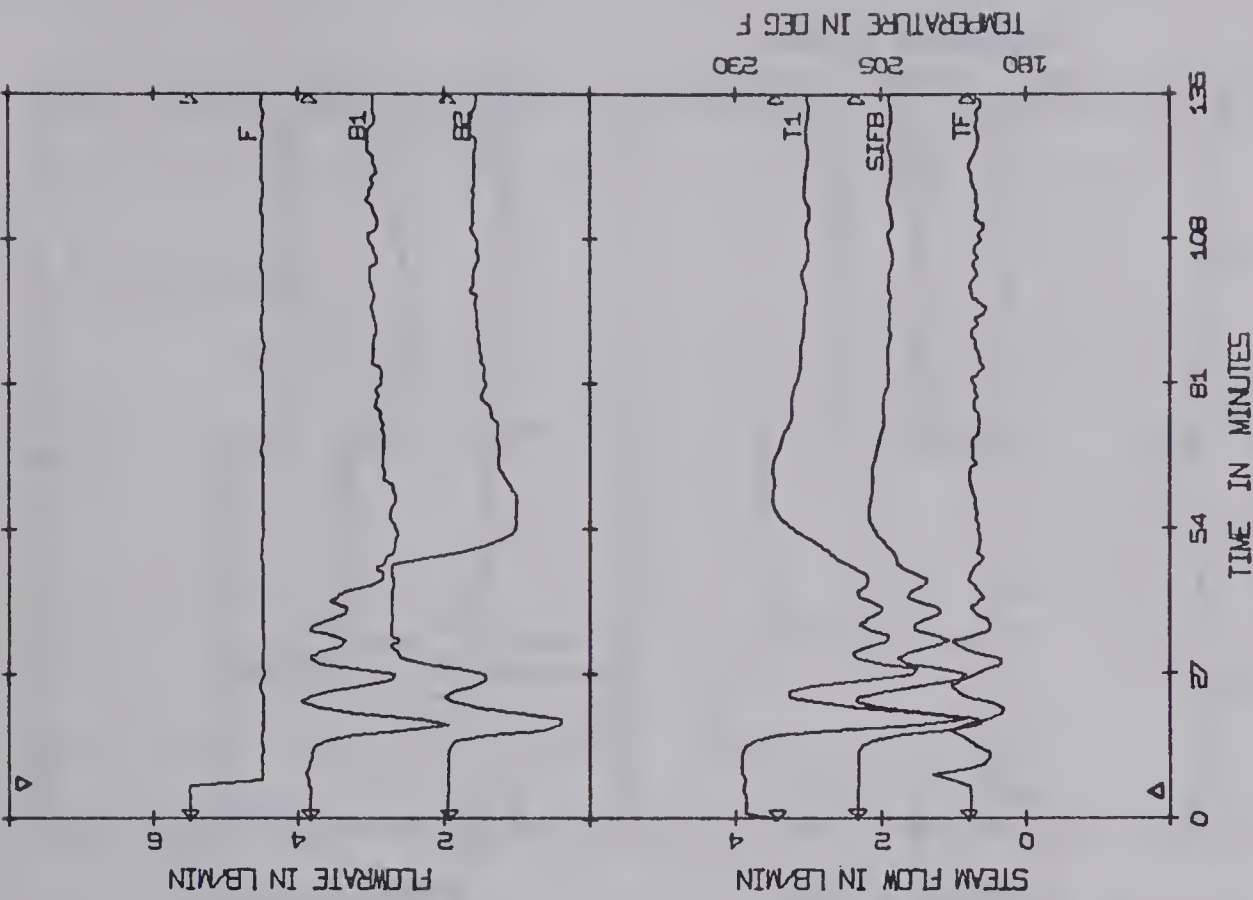


FIGURE 5.14 EXPERIMENTAL MRAC: EFFECT OF UNSEEN DISTURBANCE ($\xi_{ij} = 1$, -10% FEED COMPOSITION UNOBSERVED)

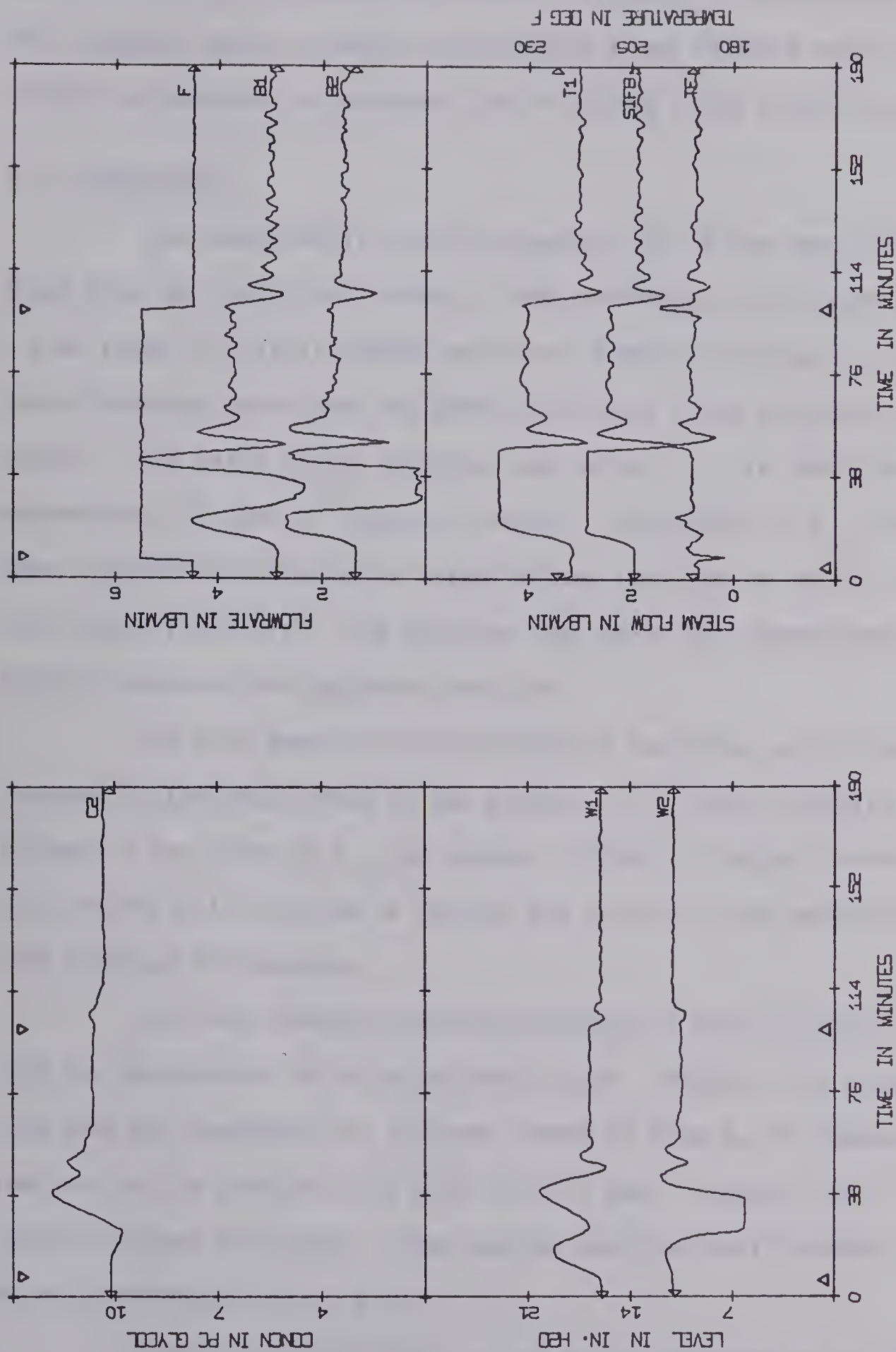


FIGURE 5.15 EXPERIMENTAL MRAC, VIOLATION OF STEAM CONSTRAINT ($\xi_{i3} = 0.25$, $\xi_{i5} = 10$, all other $\xi_{ij} = 1$)

nominal value of 2.0 pounds per minute. Figure 5.16 demonstrates that MRAC improves control greatly and produced a new feedback matrix to control the process at an unusual set of steady state conditions.

5.4 CONCLUSIONS

The experimental results supported all of the conclusions drawn from the simulation studies. MRAC performed satisfactorily for a wide range of initial control policies, adaptive loop gains, steady state operating conditions and modelling errors (such as unseen disturbances). The value of the adaptive loop gains, ξ_{ij} , is important in determining the type of response obtained. Low values of ξ_{ij} produced more sluggish responses while larger values resulted in faster, more oscillatory responses. Thus adaptive loop gains and conventional controller gains exhibit analogous behavior.

All runs demonstrated continuously improving control when repeated disturbances acted on the process. This would indicate that although a low value of ξ_{ij} can produce initially sluggish control, this control will continue to improve and provide closer model-following with repeated disturbances.

The large feedback matrices produced in the simulation results were not encountered in the experimental runs. However, the experimental runs were not conducted for the same length of time as the simulation runs nor was an adaptive loop gain above 10 used. However, with longer runs and higher loop gains, large control matrices would probably occur in the experimental runs, also.

A well-tuned multiloop control system provided an excellent initial control policy. The adaptive control scheme also provided adequate control for unseen disturbances which is an important evaporator

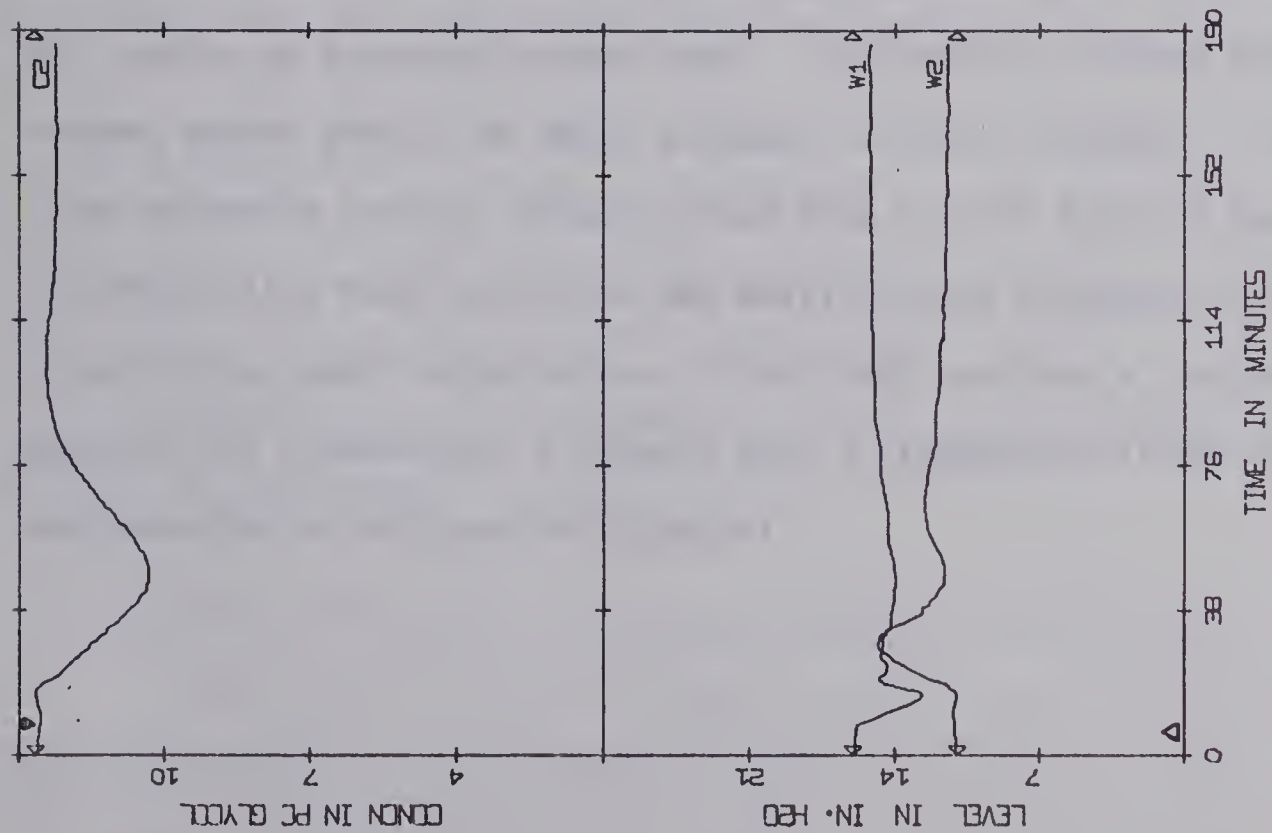
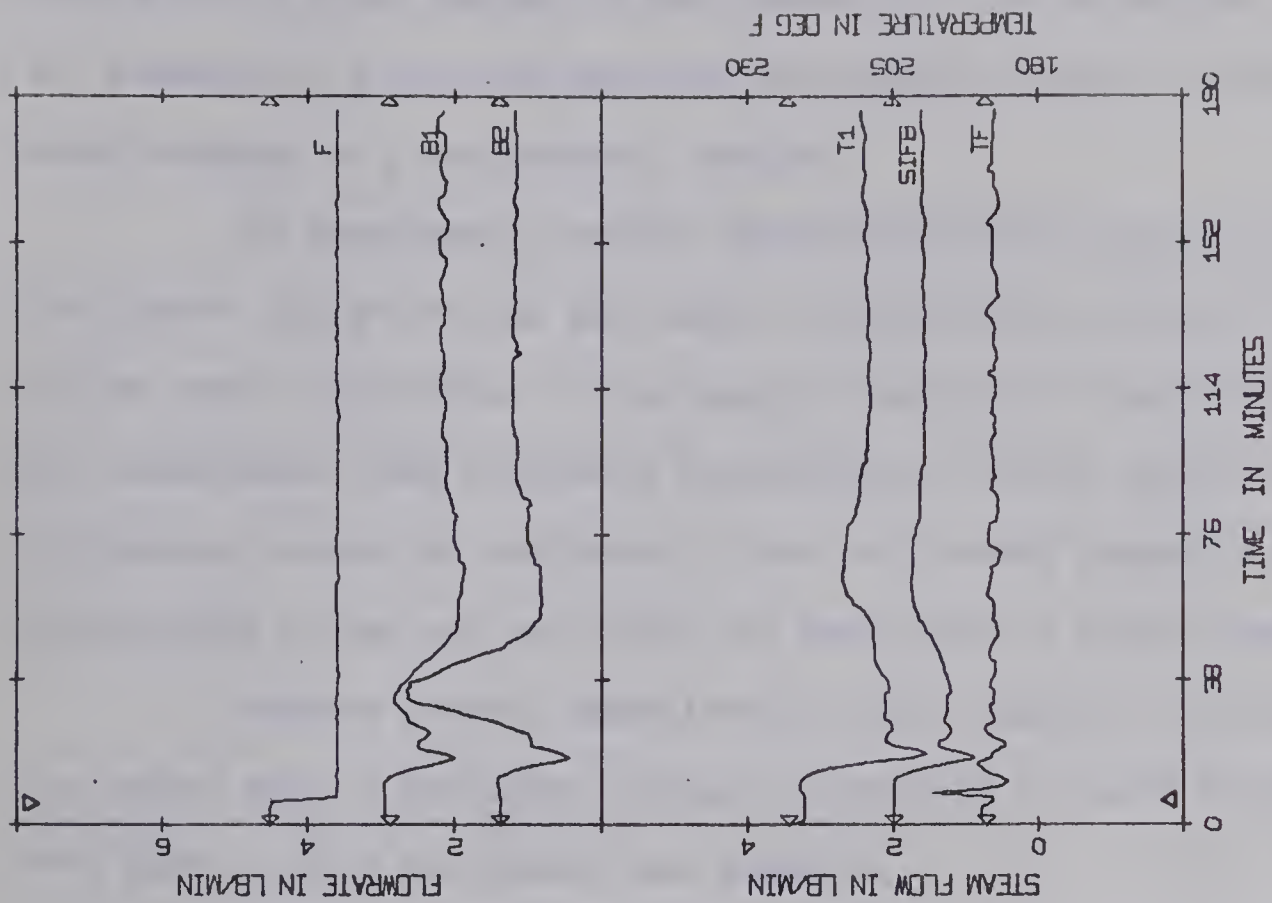


FIGURE 5.16 EXPERIMENTAL MRAC AT LOW FEED RATES, $\xi_{ij} = 1$

consideration since changes in feed composition are undetected. Also, all elements of $\underline{\Gamma}$ need not adapt for the process response to follow the model response in a satisfactory fashion.

The experimental results demonstrated that adaptive control can survive constraints on the control variables that are not included in the model calculations if the adaptive loop gain is small enough. The unsuspected steam constraint caused poorer initial control when a disturbance caused the violation of this constraint; however, later disturbances tended not to violate the constraint as control improved.

Adaptive control demonstrated further insensitivity to modelling errors when it maintained adequate control at a steady state far from that at which the process was modelled.

Two practical applications of model reference adaptive control designed by Liapunov's direct method may be postulated. This technique could prove useful in tuning multivariable control systems since it does not require an accurate process model. For example, optimal control schemes depend greatly on model accuracy for their success. If the fixed parameter control scheme derived from a model fails to perform satisfactorily, MRAC could tune the multivariable constants instead of requiring new model calculations. Also, MRAC provides a systematic approach for transferring a process from a standard multiloop control configuration to multivariable control.

CHAPTER SIX

CONCLUSIONS

The purpose of this work was to investigate a model reference adaptive control (MRAC) system designed by Liapunov's direct method of stability analysis. The theory for proportional feedback, feedforward model reference adaptive control as developed by Winsor and Roy [1] and Porter and Tatnall [2] was extended to include integral and setpoint control modes. Proportional feedback MRAC was then applied to a linear model of a double effect evaporator. The work included 44 simulation runs on an EAI 590 hybrid computer in order to test the various design parameters of the MRAC approach. The simulation runs investigated the effects of adaptive loop gain, initial control policy, unmeasured disturbances, state weighting, repeated disturbances, and the number of adapting elements. Fifteen experimental runs were then made on the evaporator/IBM 1800 control configuration to confirm the simulation results. Since the actual process was nonlinear and had an unexpected constraint on steam flow rate, the experimental runs also tested additional aspects of the control scheme. Table 6.1 presents a summary of the results and conclusions of the previous three chapters. The following two sections present recommendations for the industrial application of MRAC and suggestions for future work.

6.1 INDUSTRIAL APPLICATIONS OF MODEL REFERENCE ADAPTIVE CONTROL

Many types of processes could benefit from a MRAC system. Highly nonlinear processes that are subject to changing operating conditions can be difficult to control with a fixed parameter control scheme. Modern multivariable control schemes are usually based on a linear

TABLE 6.1

SUMMARY OF DESIGN CONSIDERATIONS IN MRAC BY LIAPUNOV'S DIRECT METHOD

DESIGN CONSIDERATION	THEORY EQUATION NUMBER	SIMULATION FIGURE NUMBER	EXPERIMENTAL FIGURE NUMBER	CONCLUSIONS
Adaptive Loop Gain, ξ_{ij}	3.24	4.3 4.4 4.5 4.6	5.5 5.9	Behavior analogous to conventional controller gain; high gains produce rapid, oscillatory responses, low gains produce slower adapting.
Initial Control Policy, $\Gamma(0)$	3.48	4.10 4.11 4.12	5.11 5.12	MRAC can recover from a poor initial control policy such as open-loop or positive feedback. Well-tuned multiloop control provides an excellent initial control policy.
Number of Elements of Γ that Adapt	3.14 3.17	4.7 4.8 4.9	5.13	Not all elements of Γ need adapt for control to be maintained; however, system stability is no longer guaranteed. Larger ξ_{ij} are possible with fewer adapting elements.
State Weighting	3.24	4.17	5.5 5.6	State weighting can be accomplished by using the adaptive loop gains to emphasize the columns of the Γ matrix corresponding to the important states.
Final Control Matrices	3.48	4.15 4.16		A combination of large adaptive loop gains, large control intervals, and poor initial control policies can cause large, non-stationary final control matrices. This is probably due to numerical instability problems associated with the discrete approximation of the adaptive control algorithm.

TABLE 6.1 (continued)

DESIGN CONSIDERATION	THEORY EQUATION NUMBER	SIMULATION FIGURE NUMBER	EXPERIMENTAL FIGURE NUMBER	CONCLUSIONS
Effect of Unseen Disturbances	Figure 3.2	4.13 4.14	5.14	Measurement of the disturbance improves control but is not essential to adapting with the feedback control configuration.
Violation of Control Constraints	3.2		5.15	Experimental results indicate low adaptive loop gains allow recovery if control constraints are violated, by contrast, theory does not allow for control constraints.

process model. MRAC could be used to tune the fixed parameter control scheme if process model inaccuracy or changing process conditions caused unsatisfactory results.

For application of model reference adaptive control to industrial processes, it is recommended that small adaptive loop gains and a good initial control policy be used. The MRAC system designed by Liapunov's direct method for linear systems is theoretically stable; however, process nonlinearities and numerical problems that arise with the discrete form of the adaptive control law can cause stability problems. To eliminate the numerical problems, smaller sampling (adapting) intervals or higher-order difference equations could be used to solve the adaptive control equations (3.24, 3.25), but a sacrifice in calculation time and computer storage would result.

The control matrices should be monitored if a poor initial control policy is used in order that a combination of severe disturbances or changing operating conditions does not result in large control matrices and "bang-bang" control. Intermittent application of MRAC, as opposed to continuous application, could be used on an industrial process in order to save computer time. After MRAC has improved the initial control and the process and model states have become almost equal, the MRAC algorithm calculations could be suspended until a set-point change is made that alters the process operating conditions. To demonstrate this application, MRAC was terminated on the simulated process after forty-five minutes and the resulting constant control matrix was used to control the process thereafter for a similar disturbance. Figure 6.1 demonstrates the performance of the fixed parameter control system that resulted with $\xi_{ij} = 10$ and open-loop initial control.

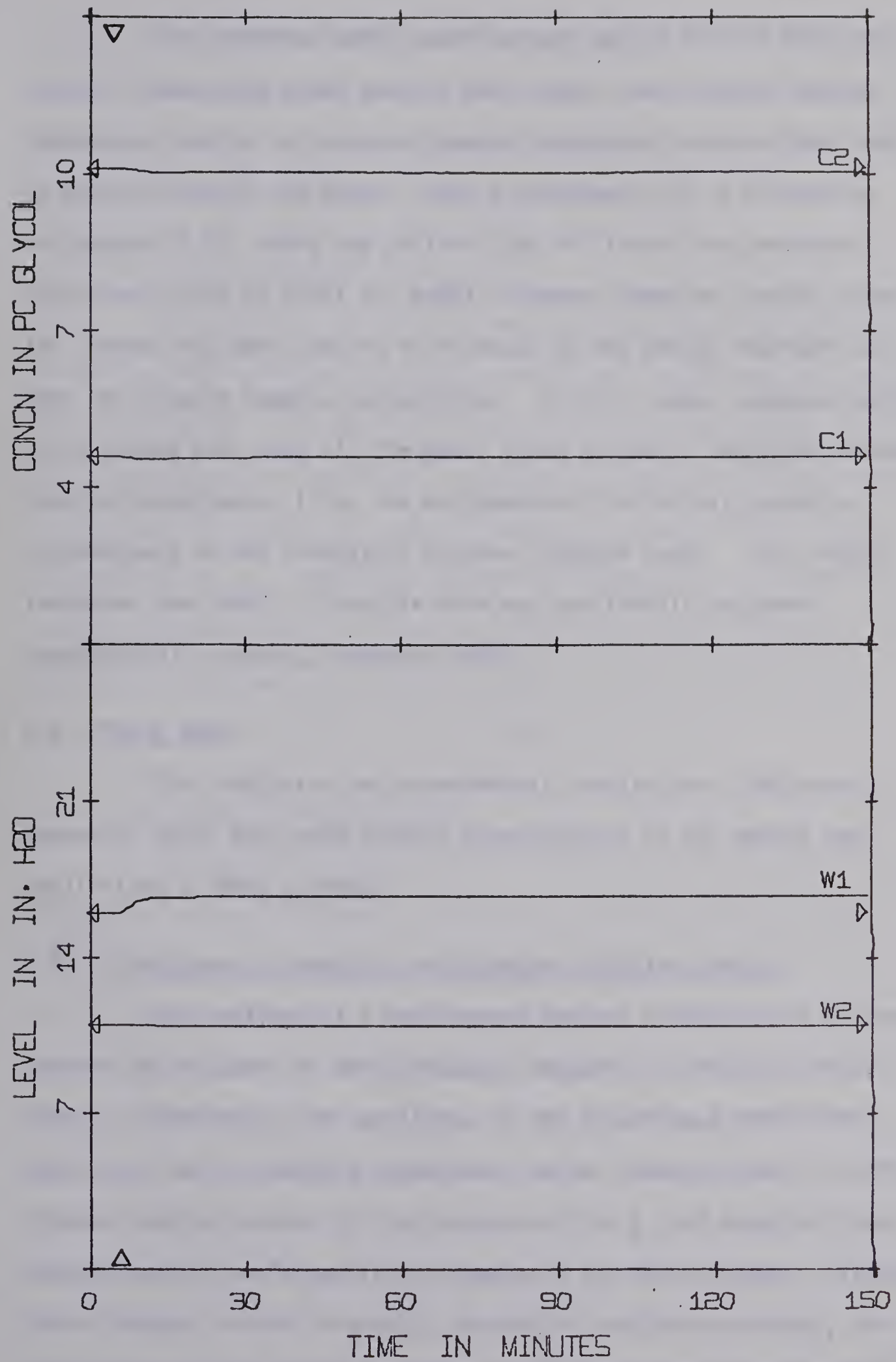


FIGURE 6.1 FIXED PARAMETER CONTROL DERIVED FROM MRAC
(MRAC FOR 45 MINUTES, $\xi_{ij} = 10$, OPEN-LOOP INITIAL CONTROL,
+ 20% FEED FLOW)

The reference model could be more easily derived than the optimal closed-loop model used in this study. Less complex design techniques that do not rely on dynamic programming calculations could be used to specify the model. Matrix assignment [3] or eigenvalue assignment [4,5], where the desired type of closed-loop response is specified, would be ideal for model reference adaptive control since the closed-loop model matrix is selected by the design engineer and does not require complex calculations. In this study, adequate control was achieved even when all the model state variables remained unchanged despite disturbances (i.e. the assignment of infinitely negative eigenvalues) in the simulation studies (Chapter Four). This result indicates that MRAC is feasible with any arbitrarily assigned, asymptotically stable, reference model.

6.2 FUTURE WORK

The simulation and experimental results have indicated a number of areas that need further investigation in the design and application of MRAC systems.

6.2.1 Feedforward, Integral, and Setpoint Adaptive Control

The addition of a feedforward control configuration can greatly improve the response of many processes compared to feedback control alone. Furthermore, the variations in the disturbance coefficient matrix, \underline{D} , due to changing disturbance vector steady-states, are often greater than variations in the process matrix, \underline{A} , and adaptive feedforward control could partially compensate for these changes. Similarly, since integral action is usually desirable to eliminate offset, the application of the theory developed in this work for integral adaptive

control could find extensive use. Setpoint control is essential in industrial processes and because setpoint changes vary process operating conditions and hence the linear process model, a further investigation of setpoint adaptive control should be conducted.

6.2.2 Selection of Adaptive Loop Gains

The adaptive loop gains were found to behave analogously to standard controller gains and had an appreciable effect on the adaptive control response. An a priori method of determining a good value of these gains would be desirable. Gromyko and Sankovskii [6] have also demonstrated the effect of adaptive loop gain in simulation studies and have developed a complicated method for determining the optimal value of adaptive loop gain from the model and process matrices if the variations in process parameter are known. Further investigation in the area of adaptive loop gains is needed.

6.2.3 Selection of Reference Model

Many possible asymptotically stable reference models could be chosen for a specific process. Because a reasonably accurate open-loop model was available for the evaporator, optimal feedback control was used in selecting the closed-loop reference model for this study. Other reference models can be chosen on the basis of eigenvalue assignment [5] and these reference models should also be tested. The evaporator is a nonlinear process and control of the evaporator using a fifth-order model essentially tested MRAC with a different order process than reference model. Loan [7,8] has recently investigated process identification by Liapunov's direct method for both lower-order and higher-order models. The theory he has developed could be investigated

on the evaporator by using reference models other than the fifth-order model used in this study and determining the effect of reference model order on control.

6.2.4 Constrained State and Control Variables

The MRAC theory outlined in this work does not consider constraints on the state or control variables. Gromyko and Sankovskii [6] have used constrained control variables in their paper on adaptive loop gains. They imply that stability is guaranteed only for a certain range of adaptive loop gains if there are constraints on the variables. The further implications of constrained variables should be investigated since all processes operate within certain limits.

6.2.5 Selection of the \underline{P} Matrix Used in the Adaptive Control Law

The rows of the Liapunov matrix \underline{P} appear in the adaptive control law

$$\dot{\gamma}_{ij} = x_{pj} e^T \underline{P}_i \xi_{ij}$$

and have a large effect on the adaptive control response. The \underline{P} matrix is obtained from the Liapunov equation

$$\underline{A}_m^T \underline{P} + \underline{P} \underline{A}_m = -\underline{Q}$$

and its value depends on an arbitrarily specified positive-definite matrix \underline{Q} and the closed-loop model matrix \underline{A}_m . Therefore, another design option is available when the \underline{Q} matrix is specified. The effect of this design parameter on control and its possible uses (e.g. state weighting) should be studied.

6.2.6 Discrete Approximation of the Adaptive Control Law

The numerical stability problems encountered in the evaporator application could be eliminated with higher-order difference approximations to solve the adaptive control algorithms. For example, the feasibility of doing a separate analysis on the adaptive algorithm

$$\dot{\gamma}_{ij} = x_{pj} e^T P_i \xi_{ij}$$

to determine the maximum adaptive loop gains for a specific \underline{P} matrix, difference equation, and control interval should be considered.

6.3 CONCLUSIONS

Model reference adaptive control designed from Liapunov stability considerations has been applied to a double effect evaporator. In both simulation and experimental studies, MRAC proved useful for changing from multiloop control to multivariable control. The scheme was able to recover from very poor initial control strategies. It was used to tune a multivariable control system based on an inaccurate model. Therefore, this MRAC scheme could be used in industrial situations where it is desired to change from multiloop to multivariable control or to tune existing multivariable control schemes. Feedback and setpoint control modes should be adequate for most multivariable MRAC systems; however, feedforward and integral adaptive control could be added to processes where offsets are not desirable.

The implementation of model reference adaptive control is straightforward, however, the nonlinear differential nature of the control law and the extensive matrix operations can cause calculation time and storage requirements to be an order of magnitude larger than for a similar fixed parameter control scheme. If calculation time

and/or storage requirements are limited, adapting only certain critical loops or the intermittent application of model reference adaptive control (e.g. with setpoint changes) could be considered.

NOMENCLATURE FOR CHAPTER TWO

Alphabetic

A	heat transfer area
\underline{A}	state coefficient matrix
\underline{B}	control coefficient matrix
C	concentration
C_p	heat capacity
e	error
E	activation energy
F	feed flow
h	level or local heat transfer coefficient
H	heat of reaction
J	performance criterion
k	frequency factor
K	controller gain
L	load or length
m	controller output
n	concentration
P	perimeter
q	flow
r	rate of reaction
R	setpoint, resistance to flow, or gas constant
s	Laplace variable
t	time
T	temperature, sampling period
U	overall heat transfer coefficient

NOMENCLATURE FOR CHAPTER TWO (continued)

\underline{u}	control vector
v	volume or river velocity
V	volume
x	composition or spacial coordinate
\underline{x}	state vector
z	Z-transform variable

Greek

α	constant of diffusion
β	time scaling factor
Δ	incremental quantity
ϵ	error
ρ	density
τ_I	integral time
τ	time delay or time constant
ω	frequency

Subscripts

c	coolant or controller
v	valve

Superscripts

\cdot	time derivative
---------	-----------------

NOMENCLATURE FOR CHAPTER THREE

Alphabetic

\underline{A}	state coefficient matrix
b	positive constant
\underline{B}	control coefficient matrix
B_1	first effect bottoms flow
B_2	second effect bottoms flow
C_1	first effect concentration
C_2	second effect concentration
C_F	feed concentration
\underline{C}	output coefficient matrix
\underline{d}	disturbance vector
\underline{D}	disturbance coefficient matrix
\underline{e}	error vector
F	feed flow
\underline{g}	controller parameters in M.I.T. MRAC technique
h_1	first effect enthalpy
h_F	feed enthalpy
\underline{I}	identity matrix
\underline{K}	control matrix
n	state dimension
p	disturbance dimension
\underline{P}	positive-definite symmetric matrix
\underline{Q}	positive-definite symmetric matrix
r	control dimension
S	steam flow
Δt	discrete time interval

NOMENCLATURE FOR CHAPTER THREE (continued)

\underline{u}	control vector
V	Liapunov function
w_1	first effect holdup
w_2	second effect holdup
\underline{x}	state vector
\underline{y}	output vector of integrated states
\underline{z}	"integral" state vector

Greek

$\underline{\underline{A}}$	state difference matrix, $\underline{\underline{A}}_m - \underline{\underline{A}}_p$
α_{ij}	elements of $\underline{\underline{A}}$
$\underline{\underline{\Gamma}}$	adaptive feedback control matrix
γ_{ij}	elements of $\underline{\underline{\Gamma}}$
$\underline{\underline{\Delta}}$	discrete control coefficient matrix
$\underline{\underline{\theta}}$	discrete disturbance coefficient matrix
$\underline{\underline{\Lambda}}$	disturbance difference matrix, $\underline{\underline{D}}_m - \underline{\underline{D}}_p$
λ_{ij}	elements of $\underline{\underline{\Lambda}}$
ν_{ij}	adaptive feedforward loop gains
ξ_{ij}	adaptive feedback loop gains
$\underline{\underline{\phi}}$	discrete state coefficient matrix
$\underline{\underline{\Omega}}$	adaptive feedforward control matrix
ω_{ij}	elements of $\underline{\underline{\Omega}}$

Subscripts

d	discrete
FB	feedback

NOMENCLATURE FOR CHAPTER THREE (continued)

FF	feedforward
I	integral
m	model
p	process
sp	setpoint
ss	steady state

Superscripts

k	control interval
T	transpose
'	perturbation variables or augmented vector
.	time derivative

NOMENCLATURE FOR CHAPTER FOUR

Alphabetic

\underline{A}	closed-loop state matrix
B_1	first effect bottoms flow
B_2	second effect bottoms flow
C_1	first effect concentration
C_2	second effect concentration
C_F	feed concentration
\underline{d}	disturbance vector
\underline{e}	error vector
F	feed flow
h_1	first effect enthalpy
\underline{K}_{FB}	feedback control matrix
\underline{P}	positive-definite matrix
S	steam flow
\underline{u}	control vector
V	Liapunov function
W_1	first effect holdup
W_2	second effect holdup
\underline{x}	state vector

Greek

α_{ij}	elements of $\underline{A} = \underline{A}_m - \underline{A}_p$
$\underline{\Gamma}$	adapting feedback matrix
γ_{ij}	elements of $\underline{\Gamma}$
$\underline{\Xi}$	adaptive loop gain matrix
ξ_{ij}	adaptive loop gains, elements of $\underline{\Xi}$

NOMENCLATURE FOR CHAPTER FOUR (continued)

Subscripts

- m model
- p process

Superscripts

- T transpose
- time derivative

NOMENCLATURE FOR CHAPTER FIVE

Alphabetic

B_1	first effect bottoms flow, lbs/min
B_2	second effect bottoms flow, lbs/min
C_1	first effect concentration, weight percent
C_2	second effect concentration, weight percent
\underline{d}	disturbance vector
\underline{e}	error vector
F	feed flow, lbs/min
h_F	feed enthalpy, BTU/min
h_1	first effect enthalpy, BTU/min
O_1	first effect overhead, lbs/min
O_2	second effect overhead, lbs/min
P_1	first effect pressure, psia
P_2	second effect pressure, psia
\underline{P}_j	column of Liapunov Matrix \underline{P}
SIFB	steam flow, lbs/min
S	steam flow
T_1	first effect temperature
T_F	feed temperature, °F
\underline{u}	control vector
\underline{x}	state vector

Greek

$\underline{\Gamma}$	adapting control matrix
$\underline{\Gamma}(s)$	adaptive loop gain matrix

NOMENCLATURE FOR CHAPTER FIVE (continued)

ξ_{ij} adaptive loop gains

Superscripts

T transpose

· time derivative

Subscripts

p process

NOMENCLATURE FOR CHAPTER SIX

Alphabetic

\underline{A}	state equation coefficient matrix
\underline{D}	state equation coefficient matrix
\underline{e}	error vector, model state - process state
\underline{P}	Liapunov matrix, positive-definite
\underline{Q}	arbitrary positive-definite matrix
\underline{x}	state vector

Greek

ξ_{ij}	adaptive loop gains
γ_{ij}	adapting control elements

Superscripts

\cdot	time derivative
T	transpose

Subscripts

p	process
m	model

REFERENCES FOR CHAPTER ONE

1. Andre, H., "A Mathematical Model for a Two Stage Concentrating Evaporator", Ph.D. Thesis, Department of Chemical and Petroleum Engineering, University of Alberta (1966).
2. Fehr, M., "Computer Control of an Evaporator", M.Sc. Thesis, Department of Chemical and Petroleum Engineering, University of Alberta (1969).
3. Jacobson, B.A., "Multiloop Computer Control of an Evaporator", M.Sc. Thesis, Department of Chemical and Petroleum Engineering, University of Alberta (1970).
4. Newell, R.B., "Multivariable Computer Control of an Evaporator", Ph.D. Thesis, Department of Chemical and Petroleum Engineering, University of Alberta (1970).
5. Nieman, R.E., "Application of Quasilinearization and Linear Programming to Control and Estimation Problems", Ph.D. Thesis, Department of Chemical and Petroleum Engineering, University of Alberta (1970).
6. Wilson, R.G., "Computer Control of Processes with Inaccessible State Variables", current Ph.D. research project, Department of Chemical and Petroleum Engineering, University of Alberta (1972).
7. Hamilton, J.C., "Experimental Evaluation of State Estimation in Multivariable Control Systems", current M.Sc. research project, Department of Chemical and Petroleum Engineering, University of Alberta (1972).
8. Alevisakis, G., "Control of Linear Systems Containing Time Delays", current M.Sc. research project, Department of Chemical and Petroleum Engineering, University of Alberta (1972).
9. McGinnis, R.G., "Multivariable Computer Control of a Distillation Column", current M.Sc. research project, Department of Chemical and Petroleum Engineering, University of Alberta (1971).
10. Porter, B., and Tatnall, M.L., "Performance Characteristics of Multi-Variable Model-Reference Adaptive Systems Synthesized by Liapunov's Direct Method", Int. J. Control, 10, 241 (1969).
11. Winsor, C.A., and Roy, R.J., "Design of Model Reference Adaptive Control Systems by Liapunov's Second Method", IEEE Trans., AC-13, 204 (1968).
12. Porter, B., and Tatnall, M.L., "Performance Characteristics of an Adaptive Hydraulic Servo-Mechanism", Int. J. Control, 11, 741 (1970).

REFERENCES FOR CHAPTER TWO

1. Distefano, G.P., Hybrid Computation in the Process Industries, EAI Bulletin No. 67471 (1968).
2. Greenberg, D.B., "Teaching Hybrid Computation in the Undergraduate Engineering Curricula", Analog/Hybrid Computer Educational Society Transactions, 3, 41 (1971).
3. Babushkin, F.M., Kogan, B.Ya., and Rybashov, M.V., "Automatic Setup of Problems on Analog Computers in Hybrid Systems (Review)", Automation and Remote Control, 32, 799 (1971).
4. Hambury, J.N., "Programming and Testing Hybrid Simulations", The Computer Bulletin, 13, 36 (1969).
5. _____, HOI Reference Handbook, EAI Pub. #00 827.00021-1 (1970).
6. Bekey, G.A., and Karplus, W.J., Hybrid Computation, John Wiley and Sons, Toronto (1968).
7. Kuo, B.J., Analysis and Synthesis of Sampled-Data Control Systems, Prentice-Hall Inc., Englewood Cliffs, N.J. (1963).
8. Vansteenkiste, G.C., "Study of the Dynamic Error Introduced by the Delay Inherent in Combined Analog-Digital Computation in Hybrid Systems", AICA Journal, 11, 226 (1969).
9. Hammond, J.L., and Alford, C.O., "Sampling Errors in Closed-Loop Hybrid Computer Programs", Simulation, 13, 307 (1969).
10. Deiters, R.M., and Nomura, T., "Circle Test Evaluation of a Method of Compensating Hybrid Computing Error by Predicted Integrals", Simulation, 12, 59 (1968).
11. Sharpe, E.B., "Hybrid Computers Aid Process Control", Control Eng., 15, 69 (1968).
12. Dahlin, F.B., and Nelson, J.M., "Simulation and Optimal Control of Chemical Processes", Chem. Eng. Progr., 60, 49 (1964).
13. Ruzskay, R., and Mitchell, E.E.L., "Hybrid Simulation of a Reacting Distillation Column", AFIPS Proc. SJCC, Boston, 389 (1966).
14. Fox, D.N., Parsons, J.R., and Dutcher, D.L., "Hybrid Simulation Spurs Control Studies", Control Eng., 13, 71 (1966).
15. Nilson, R.N., "Hybrid Simulation of a Variable Transport Lag", Simulation, 12, 65 (1968).
16. Kuo, B.J., Discrete-Data Control Systems, Prentice-Hall Inc., Englewood Cliffs, N.J. (1970).

REFERENCES FOR CHAPTER TWO (continued)

17. Kingma, Y.J., "Design Methods for Digital Dead Beat Controllers", AICA Journal, 10, 76 (1968).
18. Lawrence, B.R., Stebbing, J.D., Crate, G.F., Wright, E.J., and Gagne, R.E., "A Hybrid Simulation of Pickering Control", 1971 Summer Simulation Conference, Boston, 631 (1971).
19. Andrews, J.M., Moore, C.E., Jannasch, C.F. and Manson, J.K., "Process Optimization by Hybrid Computers", Chem. Eng. Progr., 60, 57 (1964).
20. Ung, M.T., "Sampling Optimization Hybrid Program", Simulation, 10, 21 (1968).
21. Bekey, G.A., "Optimization of Multiparameter Systems by Hybrid Computer Techniques", Parts I and II, Simulation 8, 19 and 21 (1964).
22. Gonzalez, R.S., "An Optimization Study on a Hybrid Computer", AICA Journal, 12, 138 (1970).
23. Sandoz, D.J., and Swanick, B.H., "Real-Time Hybrid Simulation of an Adaptive Control Technique", Proc. IEE, 117, 2165 (1970).
24. Godebole, S.S. and Smith, C.F., "Digital/Hybrid Simulation of a Novel Adaptive Control Scheme", Analog/Hybrid Computer Educational Society Transactions, 3, 197 (1971).
25. Mellichamp, D.A., "Model Predictive Time-Optimal Control of Second Order Processes", Ind. Eng. Chem. Process Des. Develop., 9, 494 (1970).
26. Mellichamp, D.A., "A Predictive Time Optimal Controller for Second-Order Systems with Time Delay", Simulation, 14, 27 (1970).
27. Carlson, A.M., "A Hybrid/Digital Software Package for the Solution of Chemical Kinetic Parameter Identification Problems", AFIPS Proc. FJCC, Las Vegas, 733 (1969).
28. Frank, A., and Lapidus, L., "Hybrid Simulation of Chemical Engineering Systems", Ch. Eng. Progr., 62, 67 (1966).
29. Carling, L.N., "Hybrid Computer Solution of Heat Exchanger Partial Differential Equations", AICA Journal, 10, 6 (1968).
30. Poulsen, N.J., "Distributed-Parameter Problem Solved on a Hybrid Computer by a Modified Function Storage Technique", Simulation, 13, 192 (1969).
31. Owen, A.T., and Kistler, R.W., "Application of Hybrid Computer Techniques to the Analysis of a Concentric Tube Heat Exchanger", Analog/Hybrid Computer Educational Society Transactions, 2, (1970).

REFERENCES FOR CHAPTER TWO (continued)

32. Vichnevetsky, R., and Tomalesky, A.W., "Incremental Method for the Hybrid Computer Simulation of a Tubular Heat Exchanger", Analog/Hybrid Computer Educational Society Transactions, 3, 41 (1971).
33. Eteson, D.C., and Zwiebel, I., "Hybrid Computer Solution of the Fixed Bed Adsorption Model", AIChE Journal, 15, 124 (1969).
34. Vichnevetsky, R., "A New Stable Computing Method for the Serial Hybrid Computer Integration of Partial Differential Equations", AFIPS Proc. SJCC, Boston, 143 (1969).
35. Hara, H.H., and Karplus, W.J., "Application of Functional Optimization Techniques for the Serial Hybrid Computer Solution of Partial Differential Equations", AFIPS Proc. FJCC, San Francisco, 565 (1968).
36. Dieters, R.M., and Nomura, T., "Improving the Analog Simulation of Partial Differential Equations by Hybrid Computation", Simulation, 12, 73 (1968).
37. Vichnevetsky, R., and Tomalesky, A.W., "A Hybrid Computer Method for the Analysis of Time Dependent River Pollution Problems", AFIPS Proc. SJCC, Atlantic City, 43 (1970).
38. Oliver, W.K., and Seborg, D.E., "Hybrid Computer Applications in Chemical Engineering: Illustrative Examples", Research Report 710611, Department of Chemical and Petroleum Engineering, University of Alberta (1971).
39. _____, "1130 Continuous Systems Modelling Program", IBM Application Program, #20-0282-1 (1968).
40. Farwell, R.A., "Control Systems Design and Analysis Program", Users Manual (1970).
41. Raven, F.H., Automatic Control Engineering, McGraw-Hill, Toronto (1968).
42. Bryant, L.T., Amiot, L.W., and Stein, R.P., "A Hybrid Computer Solution of the Co-Current Flow Heat Exchanger Sturm-Liouville Problem", AFIPS Proc. JFCC, San Francisco, 759 (1966).

REFERENCES FOR CHAPTER THREE

1. Eveleigh, V.W., Adaptive Control and Optimization Techniques, McGraw-Hill Book Company, Toronto (1967).
2. Bristol, E.H., "Adaptive Control Odyssey", ISA Silver Jubilee Conference, Philadelphia, 561 (1970).
3. Parks, P.C., "Liapunov Redesign of Model Reference Adaptive Control Systems", IEEE Trans., AC-11, 362 (1966).
4. Grayson, P.G., "The Status of Synthesis Using Liapunov's Method", Automatica, 3, 91 (1965).
5. Butchart, R.L., and Shackcloth, B., "Synthesis of Model Reference Adaptive System by Liapunov's Second Method", IFAC Conference on the Theory of Self Adaptive Control Systems, Teddington (1965).
6. Shackcloth, B., "Design of Model Reference Control Systems Using a Liapunov Synthesis Technique", Proc. IEE, 114, 299 (1967).
7. Winsor, C.A., and Roy, R.J., "Design of Model Reference Adaptive Control Systems by Liapunov's Second Method", IEEE Trans., AC-13, 204 (1968).
8. Porter, B., and Tatnall, M.L., "Performance Characteristics of Multi-variable Model Reference Adaptive Systems Synthesized by Liapunov's Direct Method", Int. J. of Control, 10, 241 (1969).
9. Rang, E.G., "Adaptive Controllers Derived by Stability Considerations", Minneapolis - Honeywell Regulator Co., Memorandum MR 7905 (1962).
10. Pazdera, J.S., and Pottinger, H.J., "Linear Systems Identification via Liapunov Design Techniques", Proc. of the 9th Joint Automatic Control Conference, Boulder, 795 (1969).
11. Porter, B., and Tatnall, M.L., "Stability Analysis of a Class of Multivariable Model-Reference Adaptive Systems having Time-Varying Process Parameters", Int. J. of Control, 11, 325 (1970).
12. Porter, B., and Tatnall, M.L., "Performance Characteristics of an Adaptive Hydraulic Servo-mechanism", Int. J. of Control, 11, 741 (1970).
13. Schooley, D.J., and Pazdera, J.S., "The Dynamic Response of Liapunov Designed Adaptive Model Reference Control Systems", Proc. of the Fourth Hawaii Conference on Systems Sciences, 1060 (1971).
14. Crandall, E.D., and Stevens, W.F., "An Application of Adaptive Control to a Continuous Stirred Tank Reactor", A.I.Ch.E. Journal, 11, 930 (1965).

REFERENCES FOR CHAPTER THREE (continued)

15. Casciano, R.M., and Staffin, K.H., "Model-Reference Adaptive Control System", A.I.Ch.E. Journal, 13, 485 (1967).
16. Ahlgren, T.D., and Stevens, W.F., "Adaptive Control of a Chemical Process System", A.I.Ch.E. Journal, 17, 428 (1971).
17. Newell, R.G., "Multivariable Computer Control of an Evaporator", Ph.D. Thesis, Department of Chemical and Petroleum Engineering, University of Alberta (1971).
18. Wilson, R.G., "Reduced Model Control Techniques", current Ph.D. research project, Department of Chemical and Petroleum Engineering, University of Alberta (1971).
19. Andre, H., and Ritter, R.A., "Dynamic Response of a Double Effect Evaporator", Can. J. Chem. Eng., 46, 259 (1968).
20. Greville, T.N.E., "The Pseudoinverse of a Rectangular or Singular Matrix and Its Application to the Solution of Systems of Linear Equations", SIAM Review, 1, 38 (1959).
21. Oliver, W.K., and Seborg, D.E., "Hybrid Simulation of a Model Reference Adaptive Control System", Research Report #711105, Department of Chemical and Petroleum Engineering, University of Alberta (1971).
22. Wilson, R.G., "GEMSCOPE User's Manual", Department of Chemical and Petroleum Engineering, University of Alberta (1971).
23. Whitaker, H.P., "The MIT Adaptive Autopilot", Proc. Self Adaptive Flight Controls Symp., Wright Air Development Center, Dayton, Ohio (1959).
24. Gromyko, V.D., and Sankovskii, E.A., "Adaptive System with Model and Combined Adjustment", Automation and Remote Control, 30, 1959 (1969).
25. Newell, R.B., and Fisher, D.G., "Implementation of Optimal, Multi-variable Setpoint Changes on a Pilot Plant Evaporator", 2nd IFAC Symposium on Multivariable Control Systems, Duesseldorf (1971).

REFERENCES FOR CHAPTER FOUR

1. Oliver, W.K., and Seborg, D.E., "Model Reference Adaptive Control by Liapunov's Direct Method: Literature Survey and Basic Equations", Research Report 711101, Department of Chemical and Petroleum Engineering, University of Alberta (1971).
2. Wilson, R.G., "Computer Control of Processes with Inaccessible State Variables", current Ph.D. research project, Department of Chemical and Petroleum Engineering, University of Alberta (1971).
3. Newell, R.B., and Fisher, D.G., "Evaporator Model Linearization", Research Report 690401, Department of Chemical and Petroleum Engineering, University of Alberta (1969).
4. Oliver, W.K., and Seborg, D.E., "Users Manual for Hybrid Simulation of the Double Effect Evaporator", Research Report 711022, Department of Chemical and Petroleum Engineering, University of Alberta (1971).
5. Newell, R.B., "Multivariable Computer Control of an Evaporator", Ph.D. Thesis, Department of Chemical and Petroleum Engineering, University of Alberta (1970).
6. Porter, B., and Tatnall, M.L., "Performance Characteristics of Multivariable Model Reference Adaptive Systems Synthesized by Liapunov's Direct Method", Int. J. of Control, 10, 241 (1969).
7. Newell, R.B., and Fisher, D.G., "Linear Evaporator Model Programmed for Solution on the EAI 580 Analog Computer", Research Report 701202, Department of Chemical and Petroleum Engineering, University of Alberta (1970).

REFERENCES FOR CHAPTER FIVE

1. Oliver, W.K., and Seborg, D.E., "Model Reference Adaptive Control by Liapunov's Direct Method: Literature Survey and Basic Equations" Research Report 711101, Department of Chemical and Petroleum Engineering, University of Alberta (1971).
2. Oliver, W.K., and Seborg, D.E., "Model Reference Adaptive Control of an Evaporator: Hybrid Simulation Results", Research Report 711105, Department of Chemical and Petroleum Engineering, University of Alberta (1971).
3. Newell, R.B., "Multivariable Computer Control of an Evaporator", Ph.D. Thesis, Department of Chemical and Petroleum Engineering, University of Alberta (1971).
4. Fehr, M., "Computer Control of an Evaporator", M.Sc. Thesis, Department of Chemical and Petroleum Engineering, University of Alberta (1969).
5. Andre, H., "A Mathematical Model for a Two Stage Concentrating Evaporator", Ph.D. Thesis, Department of Chemical and Petroleum Engineering, University of Alberta (1966).
6. _____, "DDC User's Manual", DACS Centre Publication, Department of Chemical and Petroleum Engineering, University of Alberta (1971).
7. Oliver, W.K., and Seborg, D.E., "User's Manual for Model Reference Adaptive Control Programs", Research Report 711025, Department of Chemical and Petroleum Engineering, University of Alberta (1971).
8. Hamilton, J.C., Current M.Sc. Research Project, Department of Chemical and Petroleum Engineering, University of Alberta (1971).
9. Oliver, W.K., and Seborg, D.E., "Experimental Results of Model Reference Adaptive Control Applied to a Double Effect Evaporator", Research Report 711115, Department of Chemical and Petroleum Engineering, University of Alberta (1971).

REFERENCES FOR CHAPTER SIX

1. Winsor, C.A., and Roy, R.J., "Design of Model Reference Adaptive Control Systems by Liapunov's Second Method", IEEE Trans., AC-13, 204 (1968).
2. Porter, B., and Tatnall, M.L., "Performance Characteristics of Multivariable Model Reference Adaptive Systems Synthesized by Liapunov's Direct Method", Int. J. of Control, 10, 241 (1969).
3. Porter, B., "Simple Method of Closed-Loop Matrix Assignment", Elect. Lett., 6, 79 (1970).
4. Porter, B., Synthesis of Dynamical Systems, Nelson and Sons Ltd., Don Mills, Ont. (1969).
5. Takahashi, Y., Rabins, M.J., and Auslander, D.M., Control and Dynamic Systems, Addison-Wesley, Don Mills, Ont. (1970).
6. Gromyko, V.D., and Sankovskii, E.A., "Adaptive System with Model and Combined Adjustment", Automation and Remote Control, 30, 1959 (1969).
7. Loan, N.J., "Design and Analysis of Nonscanning Adaptive Systems", Automation and Remote Control, 32, 912 (1971).
8. Loan, N.J., "Type of Nonscanning Adaptive Systems", Automation and Remote Control, 32, 584 (1971).

APPENDIX FOR CHAPTER THREE

NUMERICAL VALUES OF MATRICES USED FOR MRAC

- a) Optimal Continuous Feedback Matrix, \underline{K}_{FB} , for the Control Law $\underline{u}(t)$
 $= \underline{K}_{FB} \underline{x}_p(t)$

The optimal \underline{K}_{FB} was obtained from the IBM 360-67 program MARIC¹ with the state weighting matrix \underline{Q} = diagonal [10,1,1,10,100], the control weighing matrix $\underline{R} = \underline{0}$, in the performance index, $J = \int_0^\infty (\underline{x}^T \underline{Q} \underline{x} + \underline{u}^T \underline{R} \underline{u}) dt$.

$$\underline{K}_{FB} = \begin{bmatrix} 25.87 & -3.254 & -11.18 & -.1143 & -54.39 \\ 16.57 & .4828 & 1.200 & -12.48 & 74.99 \\ 7.218 & 1.169 & .0201 & 29.05 & 30.95 \end{bmatrix}$$

- b) Continuous Model Matrices

The \underline{K}_{FB} given above was substituted into $\dot{\underline{x}}_m = (\underline{A} + \underline{B} \underline{K}_{FB}) \underline{x}_m + \underline{D}_m \underline{d}$, (or $\underline{A}_m \equiv \underline{A} + \underline{B} \underline{K}_{FB}$) to yield

$$\underline{A}_m = \begin{bmatrix} -1.269 & -.0381 & -.2174 & .9558 & -5.744 \\ 0 & -.0755 & .1255 & 0.0 & 0.0 \\ 5.588 & -.7089 & -3.189 & -.0247 & -11.75 \\ 1.042 & -.0074 & -.0502 & -2.098 & 4.780 \\ -.6854 & .0119 & .0952 & .5162 & -3.139 \end{bmatrix}$$

$$\underline{D}_m = \begin{bmatrix} .1098 & 0 & 0 \\ -.0333 & .0766 & 0 \\ -.0188 & 0 & .0911 \\ 0 & 0 & 0 \\ 0 & 0 & 0 \end{bmatrix}$$

c) Discrete Model Matrices

The open-loop evaporator model, $\dot{\underline{x}}_p = \underline{A} \underline{x}_p + \underline{B} \underline{u} + \underline{D} \underline{d}$, can be written in discrete form as, $\underline{x}_p(k+1) = \underline{\phi} \underline{x}_p(k) + \underline{\Delta} \underline{u}(k) + \underline{\theta} \underline{d}(k)$, where

$$\underline{\phi} = \int_0^T e^{\underline{A}t} dt$$

$$\underline{\Delta} = \int_0^T e^{\underline{A}(T-t)} \underline{B} dt$$

$$\underline{\theta} = \int_0^T e^{\underline{A}(T-t)} \underline{D} dt$$

For $T = 64$ seconds, the matrices are

$$\underline{\phi} = \begin{bmatrix} 1.0 & -.0008 & -.0912 & 0 & 0 \\ 0 & .9223 & .0871 & 0 & 0 \\ 0 & -.0042 & .4396 & 0 & 0 \\ 0 & -.0009 & -.1052 & 1.0 & .0001 \\ 0 & .0391 & .1048 & 0 & .9603 \end{bmatrix}$$

$$\underline{\Delta} = \begin{bmatrix} -.0119 & -.0817 & 0 \\ .0116 & 0 & 0 \\ .1569 & 0 & 0 \\ -.0138 & .0848 & -.0406 \\ .0137 & -.0432 & 0 \end{bmatrix}$$

$$\underline{\theta} = \begin{bmatrix} .1182 & 0 & -.0050 \\ -.0351 & .0785 & .0049 \\ -.0136 & -.0002 & .0662 \\ .0012 & 0 & -.0058 \\ -.0019 & .0016 & .0058 \end{bmatrix}$$

The open-loop discrete evaporator model

$$\underline{x}_p(k+1) = \underline{\phi} \underline{x}_p(k) + \underline{\Delta} \underline{u}(k) + \underline{\theta} \underline{d}(k)$$

with feedback control

$$\underline{u}(k) = \underline{K}_{FBd} \underline{x}_p(k)$$

yields the closed-loop reference model used in the MRAC scheme.

$$\underline{x}_m(k+1) = (\underline{\phi} + \underline{\Delta} \underline{K}_{FBd}) \underline{x}_m(k) + \underline{\theta} \underline{d}(k)$$

$$\underline{x}_m(k+1) = \underline{\phi}_m \underline{x}_m(k) + \underline{\theta}_m \underline{d}(k)$$

The optimal discrete feedback matrix, \underline{K}_{FBd} , obtained from GEMSCOPE [22] with the same weighting matrices as in the continuous case and $T = 64$ seconds is:

$$\underline{K}_{FBd} = \begin{bmatrix} 10.78 & -1.607 & -4.818 & 0.0 & -19.57 \\ 5.352 & .3598 & .5471 & 0.0 & 12.49 \\ 7.515 & 1.273 & .1833 & 24.61 & 32.69 \end{bmatrix}$$

and the closed-loop matrices that result are

$$\underline{\phi}_m = \begin{bmatrix} .4341 & -.0110 & -.0785 & 0 & -.7874 \\ .1248 & .9037 & .0313 & 0 & -.2266 \\ 1.692 & -.2564 & -.3186 & 0 & -3.071 \\ 0 & 0 & 0 & -.0001 & -.0003 \\ -.0835 & .0015 & .0150 & 0 & .1515 \end{bmatrix}$$

$$\underline{\theta}_m = \begin{bmatrix} .1182 & 0 & -.0050 \\ -.0351 & .0785 & .0049 \\ -.0136 & -.0002 & .0662 \\ .0012 & 0 & -.0058 \\ -.0019 & .0016 & .0058 \end{bmatrix}$$

d) Solution² of $\underline{A}_m^T \underline{P} + \underline{P} \underline{A}_m = -\underline{Q}$ for \underline{P}

$$\underline{P} = \begin{bmatrix} 3.224 & 1.070 & -.0483 & .1258 & -5.444 \\ 1.070 & 5.367 & .0430 & .0038 & -1.968 \\ -.0483 & .0430 & .1629 & -.0103 & .0352 \\ .1258 & .0038 & -.0103 & .3529 & .2327 \\ -5.444 & -1.968 & .0352 & .2327 & 10.34 \end{bmatrix}$$

e) Results Using the Pseudo-Inverse of $\underline{\Gamma}$

Equation (3.4) gave $\underline{\Gamma}(t) = \underline{B} \underline{K}_{FB}(t)$ but $\underline{\Gamma}$ is solved from a backward difference equation using the discrete matrix $\underline{\Delta}$

$$\underline{\Gamma}(k) = \underline{\Delta} \underline{K}_{FBd}(k)$$

$$\underline{K}_{FBd}(k) = (\underline{\Delta}^T \underline{\Delta})^{-1} \underline{\Delta}^T \underline{\Gamma}(k)$$

$$(\underline{\Delta}^T \underline{\Delta})^{-1} \underline{\Delta}^T = \begin{bmatrix} -.3303 & .4618 & 6.258 & 0 & .6241 \\ -9.545 & -.0206 & -.2785 & 0 & -5.087 \\ -19.80 & -.1992 & -2.699 & -24.61 & -10.82 \end{bmatrix}$$

2. Solved by the method described by Chen, C.F. and Sheih, L.S., "A Note on Expanding $\underline{P} \underline{A} + \underline{A}^T \underline{P} = -\underline{Q}$ ", IEEE Trans. on Auto. Control, AC-13, 4, 448 (1968).

APPENDIX FOR CHAPTER FOUR

ADAPTING ELEMENTS FOR RUNS WITH A REDUCED NUMBER
OF ADAPTING ELEMENTS

FIGURE NUMBER	NUMBER OF ELEMENTS ADAPTING	ADAPTING ELEMENTS OF $\underline{\Gamma}$
4.7	21	All elements except $\gamma_{14}, \gamma_{24},$ γ_{34}, γ_{54}
4.7	11	First and fifth rows of $\underline{\Gamma}$ and γ_{44}
4.7	7	$\gamma_{11}, \gamma_{44}, \gamma_{15}, \gamma_{25}, \gamma_{35}, \gamma_{45}, \gamma_{55}$
4.8	4	$\gamma_{11}, \gamma_{44}, \gamma_{15}, \gamma_{55}$
4.9	7	$\gamma_{11}, \gamma_{44}, \gamma_{15}, \gamma_{25}, \gamma_{35}, \gamma_{45}, \gamma_{55}$

FEEDBACK CONTROL MATRIX FOR MULTILoop CONTROL

$$K_{=FB} = \begin{bmatrix} 0 & 0 & 0 & 0 & -4.89 \\ 3.52 & 0 & 0 & 0 & 0 \\ 0 & 0 & 0 & 15.8 & 0 \end{bmatrix}$$

PROCESS STEADY STATE OPERATING CONDITIONS

x - State Vector

W_1 - First effect holdup - 45.5 lb.
 C_1 - First effect concentration - 4.59 % glycol
 h_1 - First effect solution enthalpy-189.2 BTU/lb.
 W_2 - Second effect holdup - 41.5 lb.
 C_2 - Second effect concentration - 10.11 % glycol

u - Control Vector

S - Steam flowrate to the first effect - 2.0 lb/min
 B_1 - First effect bottoms flow - 3.48 lb/min
 B_2 - Second effect bottoms flow - 1.58 lb/min

d - Disturbance Vector

F - Feed flow - 5.0 lb/min
 C_F - Feed concentration-3.2 % glycol
 h_F - Feed enthalpy - 156.9 BTU/lb.

B30015